Papers presented to the

43rd ANNUAL METEORITICAL SOCIETY MEETING

La Jolla, California
2 - 6 September 1980

Co-sponsored by

University of California, San Diego

Lunar and Planetary Institute

California Space Institute

Hosted by the University of California, San Diego

UNIVERSITIES SPACE RESEARCH ASSOCIATION
Lunar and Planetary Institute

UCSD La Jolla
Central Library

La Jolla — 1980

FORTY - THIRD ANNUAL MEETING

of the

METEORITICAL SOCIETY

Sponsored by

UNIVERSITY OF CALIFORNIA, SAN DIEGO
LUNAR AND PLANETARY INSTITUTE
CALIFORNIA SPACE INSTITUTE

Hosted by

UNIVERSITY OF CALIFORNIA, SAN DIEGO
La Jolla, California
September 2 - 6, 1980

Compiled by
Lunar and Planetary Institute
3303 NASA Road 1
Houston, Texas 77058

LPI Contribution 412

Compiled in 1980

by

LUNAR AND PLANETARY INSTITUTE

PREFACE

This volume contains papers which have been accepted for publication by the Program Committee of the 43rd Annual Meteoritical Society Meeting. Papers were solicited to address the following major topics:

1. History of meteoritics
2. Stellar and cosmic elemental and isotopic abundances and anomalies
3. Meteorite chemistry and petrology
4. Lunar and planetary chemistry, petrology, and cratering
5. Planetary atmospheres
6. Solar flares and cosmic rays
7. Chronology

The Program Committee included Donald Burnett (*California Institute of Technology*); Pamela Jones (*Lunar and Planetary Institute*); John Kerridge (*University of California at Los Angeles*); Carleton Moore (*Arizona State University*); Robert O. Pepin (*University of Minnesota*); and Chairman, Hans Suess (*University of California at San Diego*).

The Organizing Committee for the meeting consisted of James Arnold, Gustaf Arrhenius, Gunter Lugmair, Douglas Macdougall, Kurt Marti (Chairman), M. Lea Rudee, Hans Suess, and Harold Urey, all of the University of California at San Diego. Social events were arranged by Florence Kirchner (Chairman), Louise Arnold, Jenny Arrhenius, Rose Marie Lugmair, Sheila Macdougall, Elisabeth Marti, Ruth Suess, Frieda Urey, and Norman Fong.

Logistic and administrative support for this meeting has been provided by Irene Spellman (*University of California at San Diego*) and by Pamela Jones (*Lunar and Planetary Institute*). This abstract volume has been prepared under the supervision of Paula Criswell (*Technical Editor, Lunar and Planetary Institute*).

The Lunar and Planetary Institute is operated by the Universities Space Research Association under contract No. NASW-3389 with the National Aeronautics and Space Administration.

MEETING CALENDAR

Tuesday, September 2, 1980

0800-1800	Geological Field Trip to Tourmaline Mines
0900-2100	Registration - First Floor, Tenaya Hall, Muir Campus Opening of Hospitality Room, Urey Room, 2102, Urey Hall Revelle Campus
1500	Council Meeting, 1101/1102, Tioga Hall, Muir Campus
1930-2130	SS I-USB-2622 Historical Perspective on the Collection of Meteorites
1930-2045	SS II-USB-2722 Terrestrial Signatures of the Influx of Interplanetary Matter

Wednesday, September 3, 1980

0800-1700	Registration, Outside Lecture Halls, Revelle Campus
0900-0915	Opening Ceremony, Mandeville Auditorium
0915-0945	Plenary Session, Mandeville Auditorium
1000-1200	W1-USB-2722 Origins of Early Solar System Components (IA) Rock-Forming Elements: Distribution and Isotopic Composition
1000-1215	W2-USB-2722 Iron Meteorites
1400-1700	W3-USB-2722 Origins of Early Solar System Components (IB) Rock-forming Elements; Distribution and Isotopic Composition
1330-1700	W4-USB-2622 Impacts and Related Phenomena
1730	Beach Party, Scripps Surfside - Adults and Children

Thursday, September 4, 1980

0900-1600	"People to People Tour of Tijuana"
0900-1145	T1-USB-2722 Origins of Early Solar System Components (IIA) Noble Gases and Light Elements; Isotopic Compositions and Host Phases
0900-1145	T2-USB-2622 Lunar Science
1330-1630	T3-USB 2722 Origins of Early Solar System Components (IIB) Noble Gases and Light Elements; Isotopic Compositions and Host Phases
1330-1615	T4-USB-2622 Breccias and Other Agglomerates
1830	Reception at University House - Adults Only Presentation of Leonard Medal to recipient, Dr. Heinrich Wänke Buffet

Friday, September 5, 1980

0900-1215	F1-USB-2722 Isotopes in Non-carbonaceous Meteorites: Anomalies and Ages
0900-1200	F2-USB-2622 Thermal History of Chondrites
1345-1645	F3-USB-2722 Origins of Chondrules and Chondrites
1345-1645	F4-USB-2622 Differentiated Meteorites and Asteroids
1830	Cocktails - Adults Only "Greentree Lane Party," at home of Dr. and Mrs. Hans Suess

Saturday, September 6, 1980

0900	Business Meeting of Meteoritical Society
0930-1215	S1-USB-2722 Parent Bodies of Enstatite Meteorites
0930-1230	S2-USB-2622 Galactic Cosmic Ray Interactions
1300	Farewell Reception

Sunday, September 7, 1980

0900-1800	Field trip to San Juan Mission/Palomar Observatory

43RD ANNUAL METEORITICAL SOCIETY MEETING

CONTENTS
(In Program Order)

Key to Symbols

* - Speaker
+ - Paper presented by title only
{ - Abstracts combined into one talk
USB-2622, 2722 - Lecture Halls, Revelle Campus,
Undergraduate Science Building
Letter/Numeral, e.g., "W1," - Wednesday, first session

Tuesday, September 2, 1980
Special Session II USB 2622

TERRESTRIAL SIGNATURES OF THE INFLUX OF INTERPLANETARY MATTER

Chairmen: J. R. Arnold and D. E. Brownlee

8 1930 Herr W. Englert P.* Herpers U. Watt E. Whittaker A. G.
A contribution to the riddle about the origin of certain glassy spherules

9 1945 Nishiizumi K.* Murrell M. T. Davis P. A.
Arnold J. R.
Cosmic ray produced 53Mn in deep sea spherules

10 2000 Brownlee D. E.*
A comparison of three sources of data on the composition of small meteoroids

11 2015 Kyte F. T.* Zhou Z.
Analyses of noble metals in the Cretaceous-Tertiary boundary

12 2030 Russell J. A.*
Spectral-height relations in Perseid meteors

Wednesday, September 3, 1980
W1 USB 2722

ORIGINS OF EARLY SOLAR SYSTEM COMPONENTS (1A) ROCK-FORMING ELEMENTS DISTRIBUTION AND ISOTOPIC COMPOSITIONS

Chairmen: A. El Goresy and G. W. Wetherill

13 1000 Kallemeyn G. W.*
Carbonaceous chondritic materials in the solar system

14 1015 Palme H. Rammensee W.*
Non-volatile siderophile elements in carbonaceous chondrites

15 1030 Fredriksson K.* Beauchamp R. Jarosewich E. Kerridge J. F.
Sulphate veins, carbonates, limonite and magnetite: Evidence on the late geochemistry of the C-1 regoliths

16 1045 Kerridge J. F.* Fredriksson K. Jarosewich E. Nelen J. Macdougall J. D.
Carbonates in CI chondrites

17 1100 Macdougall J. D.* Goswami J. N. Carlson J.
Refractory inclusions in CM meteorites: Petrographic studies

18 1115 Armstrong J.T.* Meeker G. P. Huneke J. C Wasserburg G. J.
The Murchison Blue Angel inclusion: Its mineralogy and petrology

19 1130 Papanastassiou D. A.* Wasserburg G. J.
Evidence of 26Mg excess in hibonite from Murchison

20 1145 Hutcheon I. D.* Bar Matthews M. Tanaka T. MacPherson G. J. Grossman L. Olsen E.
A Mg isotope study of hibonite-bearing Murchison inclusions

21 1200 Grossman L.* Bar Matthews M. Hutcheon I. D. MacPherson G. J. Tanaka T. Kawabe I.
A corundum-rich inclusion in Murchison

Wednesday, September 3, 1980
W2 USB 2622

IRON METEORITES

Chairmen: V. F. Buchwald and E. R. D. Scott

22 1000 Rammensee W.* Palme H. Wänke H.
Determination of activity coefficients for calculating condensation temperatures of metal alloys

23 1015 Albertsen J. F.* Roy-Poulsen N. O. Vistisen L.
Ordered FeNi and the cooling rate of iron meteorites below 320 degrees C.

24 1030 Narayan C.* Goldstein J. I.
Experimental model for chemical fractionation of iron meteorites

25 1045 Wasson J. T.* Willis J. Wai C. M. Kracher A.
Origin of iron meteorite groups IAB and IIICD

26 1100 Hoskuldsson A. Wold S. Esbensen K.*
Multivariate systematics of iron meteorite physico-chemistry

27 1115 Schorscher H. D. Wiedemann C. M. Danon J.*
Scorzelli R. B. Azevedo I. S.
Microprobe investigation of the Santa Catharina meteorite

28 1130 Novotny P. M. Goldstein J. I.* Williams D. B.
Analytical electron microscope study of four ataxites

29 1145 Buchwald V. F.*
The iron meteorites Jerslev, Puerta de Arauco and Winburg

30 1200 Clarke R. S. Jr.* Goldstein J. I. Jarosewich E.
Morgan J. W.
Antarctic iron meteorites from Allan Hills and Purgatory Peak

31 +Esbensen K. H. Wasson J. T. Buchwald V. F.
Detailed chemical investigation of sections through a large Cape York iron

Wednesday, September 3, 1980
W3 USB 2722

ORIGINS OF EARLY SOLAR SYSTEM COMPONENTS (1B) ROCK-FORMING ELEMENTS DISTRIBUTION AND ISOTOPIC COMPOSITIONS

Chairmen: J. C. Huneke and G. W. Lugmair

32 1400 Boynton W. V.* Frazier R. M. Macdougall J. D.
Trace element abundances in ultra-refractory condensates from the Murchison meteorite

33 1415 Bar Matthews M.* MacPherson G. J. Grossman L. Tanaka T.
Spinel-pyroxene aggregates in Murchison

34 1430 Rajan R. S.* Watters T. R. Kothari B. K.
Variation of fission tracks on the surfaces of olivines from Murchison: Time differences or heterogeneity of 244Pu on a microscale?

35 1445 Lorin J. C.* Havette A. Slodzian G.
High resolution ion microprobe isotopic determinations in primitive meteorites

36 1500 Niemeyer S.* Lugmair G. W.
Ti isotope anomalies in an "un-fun" Allende inclusion

37 1515 Niederer F. R.* Papanastassiou D. A. Wasserburg G. J.
Titanium isotope anomalies in Allende inclusions

38 1530 Davis A. M.* Allen J. M. Tanaka T. Grossman L. MacPherson G. J.
A sinuous inclusion from Allende: Trace element analysis of a rim

39 1545 Bunch T. E.* Chang S.
An alternative origin of Allende CAI inclusion rims, or a correlation between the early solar system and a British steel furnace

40 1600 Beckett J. R. MacPherson G. J.* Grossman L.
Major element compositions of coarse-grained Allende inclusions

41 1615 El Goresy A.* Ramdohr P. Nagel K.
A unique inclusion in Allende: A conglomerate of hundreds of various inclusions and fragments

42 1630 Arrhenius G.* Raub C. Schimmel C.
Experimental boundaries on thermal history of refractory minerals in carbonaceous meteorites

43 1645 Kracher A.* Kurat G.
Ordinary chondrites: The spinel puzzle

IMPACTS AND RELATED PHENOMENA

Chairmen: R. S. Deitz and D. Stöffler

44 1330 Huss G. R.*
Heterogeneous shock effects in type 3 ordinary chondrites

45 1345 Lambert P.*
Farmington meteorite: Shock effects in silicates and phosphates

46 1400 Storzer D.* Wagner G. A.
Two discrete tektite-forming events 140 thousand years apart in the Australian-southeast Asian area

47 +Lange M. A.
Impact induced dehydration of hydrous minerals and the accretion of volatile rich planets

48 1415 Newsom H. E.*
Post-impact hydrothermal circulation through impact melt sheets

49 1430 Roddy D. J.* Watson R. D. Theisen A. F.
Shock-induced luminescence at Meteor Crater, Arizona, measured by laboratory and airborne Fraunhofer Line discriminator systems

50 1445 von Engelhardt W.* Graup G.
Origin and transport of suevite, Ries Crater, Germany

51 1500 Stähle V.* Müller W.
Natural shock behavior of amphibolites and garnet-cordierite-gneisses from the Ries Crater, Germany

52 1515 Stöffler D.* Gault D. E. Reimold W. U.
Experimental hypervelocity impact into quartz sand: Pre-impact location of ejecta

53 1530 Schaal R. B.*
Disequilibrium features in experimentally shocked mixtures of olivine plus silica glass powders

54 1545 Thomsen J. M.* Austin M. G. Ruhl S. F.
Schultz P. H. Orphal D. L.
Dynamic cratering flows generated in laboratory-scale impact experiments

55 1600 Austin M. G.* Thomsen J. M. Ruhl S. F. Hawke B. R.
Cratering ejecta velocity and flow field velocity relationships

Impacts and Related Phenemona (continued)

56 1615 Dietz R. S.* Lambert P.
Shock metamorphism at Crooked Creek cryptoexplosion structure, Missouri

57 1630 Kelly A. O.*
Proposed astrobleme

58 1640 Cassidy W. A.* Lidiak E. G.
Amak crater: Probably meteoritic

59 1650 Milton D. J.* Ferguson J. Fudali R. F.
Goat Paddock impact crater, Western Australia

60 1700 McHone J. F. Jr. Lambert P.* Dietz R. S. Briedj M.
Impact structures in Algeria

61 +Lange M. A.
The evolution of a primary, impact generated atmosphere

62 +Kelly A. O.
Impact oceanic flood deposits in San Diego county

Thursday, September 4, 1980
T1 USB 2722

ORIGINS OF EARLY SOLAR SYSTEM COMPONENTS (IIA) NOBLE GASES AND LIGHT ELEMENTS ISOTOPIC COMPOSITIONS AND HOST PHASES

Chairmen: F. Begeman and D. A. Papanastassiou

63 0900 Nautiyal C. M. Padia J. T. Rao M. N.
Venkatesan T. R.* Englert P. Herpers U. Herr W.
Elemental and isotopic composition of noble gases in the Isna carbonaceous chondrite

64 0915 Fisher D. E.*
A search for primordial atmospheric-like argon in an iron meteorite

65 0930 Roskamp G.* Freundel M. Schultz L.
On the distribution of noble gases in archaean terrestrial rocks

66 0945 Mackinnon I. D. R.*
Analytical electron microscopy of matrix phases in Murchison and Mighei

67 1000 Matsuda J.-I. Lewis R. S.*
Murchison meteorite: Carrier phases of noble gases

68 1015 Smith P. P. K.* Buseck P. R.
High resolution transmission electron microscopy of an Allende acid residue

69 1030 Lewis R. S.* Matsuda J.-I.
Carrier phases of CCFXe and other noble gas components in the Allende meteorite

70 1045 Ott U.* Chang S. Bunch T.
Noble gases in Allende dark inclusions: Some implications

71 1100 Yang J.* Anders E.
Noble gases: Solubility in magnetite, graphite, and daubréelite

72 1115 Pepin R. O.* Frick U.
On the distribution of noble gases in Allende: A differential oxidation study

73 +Frick U. Pepin R. O.
Analysis of nitrogen isotopes by static mass spectrometry

LUNAR SCIENCE

Chairmen: M. J. Drake and U. Krähenbühl

74 0900 Jovanovic S. Reed G. W. Jr.*
Rare earth elements in acid leaches and residues from whole rock and mineral separates from lunar basalt 75055

75 0915 Laul J. C.*
Comparative chemistry of size fractions from the Apollo sites

76 0930 Bell J. F.* Hawke B. R.
A spectral reflectivity study of the Reiner Gamma formation

77 0945 Drake M. J.*
Formation of a lunar magma ocean by partial melting

78 1000 Warren P. H.*
Eccentric lunar anomalies: Geochemistry correlated with longitude

79 1015 Wänke H.* Dreibus G. Palme H. Rammensee W. Spettel B.
Laboratory experiments on the mobility of Au and other siderophile elements in lunar highland material

80 1030 Cirlin E. H.* Housley R. M.
Evolutionary history of volatiles during lunar regolith maturation

81 1045 Sörensen J. Wegmüller F. Krahenbühl U.* von Gunten H. R.
Surface deposits of trace elements on lunar samples investigated by heating techniques

82 1100 Thiemens M. H.* Lugmair G. W. Clayton R. N.
Nitrogen and samarium isotopes in ancient lunar microbreccias

83 1115 Yaniv A.* Marti K.
Long term average, 2 m.y., of He and Ne isotopic ratios in solar flares

84 1130 Thiel K.* Külzer H. Herr W.
Investigation of heavy ion induced sputtering: Implications for the solar wind erosion of extraterrestrial samples

Thursday, September 4, 1980
T3 USB 2722

ORIGINS OF EARLY SOLAR SYSTEM COMPONENTS (IIB) NOBLE GASES AND LIGHT ELEMENTS COMPOSITIONS AND HOST PHASES

Introduction - S. Epstein

Chairmen: T. K. Mayeda and J. H. Reynolds

85 1330 Kirschbaum C.* Bond J.K.
Xenon in magnetic separates of an Allende inclusion

86 1345 Hertogen J. Crabb J.*
Radiogenic 129Xe in mineral separates from the Allende meteorite

87 1400 Rison W.* Zaikowski A. Lumpkin G. R.
Search for 129Xe bearing phases in Allende by laser microprobe

88 1415 Jordan J. Jessberger E. K. Kirsten T. El Goresy A.
Alien xenon in Allende inclusions

89 1430 Frick U.*
Nucleosynthetic origin of anomalous krypton: Test of a simple model

90 1445 Cronin J. R.* Gandy W. E. Kjos K. M.
Pizzarello S.
Further studies of amino acids in the Murchison C2 chondrite

91 1500 Gibson E. K. Jr.* Chang S.
Carbon isotopic changes produced by thermal volatilization of the Murchison C2 chondrite

92 1515 Robert F. Epstein S.*
Carbon, hydrogen, and nitrogen isotopic composition of the Renazzo and Orgueil organic components

93 1530 Javoy M.* Halbout J.
Stellar or interstellar molecules in meteorites

94 1545 Clayton D. D.*
A cold-accumulation model for oxygen isotopes

95 1600 Wood J. A.*
Thoughts on CAI's, oxygen isotopes, and REE

96 1615 Corrigan M. J.* Fitzgerald R. W. Mendis A.
Arrhenius G.
Isotope fractionation in the protosolar medium

Thursday, September 4, 1980
T4 USB 2622

BRECCIAS AND OTHER AGGLOMERATES

Chairmen: M. Prinz and A. M. Reid

97 1330 Nelen J. Brenner P. Fredriksson K.*
Grier (b) a new "brecciated" chondrite

98 1345 Score R.*
Allan Hills 77216: A petrologic and mineralogic description

99 1400 Biswas S. McSween H. Y. Jr.* Lipschutz M. E.
Chemical and petrologic studies of the Leighton chondrite: A progress report

100 1415 Dreibus G.* Wänke H.
On the origin of the excess of volatile trace elements in the dark portion of gas-rich chondrites

101 1430 Kothari B. K.* Rajan R. S.
Fission tracks in Fayetteville and Weston phosphates: Metamorphic or brecciation ages?

102 1445 Ebihara M.* Wolf R.
Odd xenoliths in achondrites: A radiochemical study

103 1500 Smith M. R.* Schmitt R. A.
A chemical study of individual rock clasts found within the Kapoeta howardite

104 1515 Reid A. M.* Schwarz C. M.
Antarctic polymict eucrites

105 1530 Olsen E. J.* Grossman L. Davis A. M. Tanaka T.
The Antarctic achondrite ALHA 76005: A polymict eucrite

106 1545 Delaney J. S.* Bedell R. Frishman S. Klimentidis R. Harlow G. E. Prinz M.
Highly differentiated eucritic clasts in polymict breccias Allan Hills A78040 and A77302

107 1600 Reimold W. U.* Borchardt R. Ostertag R. Stöffler D.
Textural and modal analysis of Apollo 16 and 17 highland breccias

ISOTOPES IN NON-CARBONACEOUS METEORITES: ANOMALIES AND AGES

Chairmen: F. A. Podosek and P. J. Patchett

108 0900 Runcorn S. K.* Libby W. F. Libby L. M.
Lunar sample and crustal magnetization and early heat sources in the solar system

109 0915 Nozette S.* Boynton W. V.
An upper limit on the abundance of superheavy element Z=110 in the early solar system

110 0930 Kaiser T.* Kelly W. R. Wasserburg G. J.
Hoba and Tlacotepec: Two new meteorites with isotopically anomalous Ag

111 0945 Villa I. M.* Huneke J. C. Wasserburg G. J.
Spallogenic rare gases in iron meteorites with isotopically anomalous Ag

112 1000 Chen J. H.* Wasserburg G. J.
U and Pb isotopes in Allende inclusions and meteoritic whitlockite

113 1015 Tatsumoto M.* Nakamura N. Unruh D. M.
Pellas P.
U isotopic composition in meteoritic phosphate

114 1030 Morand Ph.* Audouze J. Allègre C. J.
Search for nickel isotopic anomaly of meteorites

115 Birck J. L. Ricard L. P. Allègre C. J.
Chromium isotopes in meteorites and terrestrial samples

116 1045 Patchett P. J.* Tatsumoto M.
Lu-Hf isotope systematics of the eucrite meteorites

117 1100 Hohenberg C. M.* Hudson B. Kennedy M. Podosek F. A.
Relative ages of chondrites by I-Xe and 40Ar-39Ar dating: A continuing story

118 1115 Minster J.-F. Allègre C. J.*
More data on 87Rb-87Sr dating of LL chondrites

119 1130 Jacobsen S. B.* Wasserburg G. J.
Sm-Nd isotopic systematics of chondrites and achondrites

120 1145 Unruh D. M.* Tatsumoto M.
A uniform U-Pb age for L chondrites and a method for correcting for terrestrial Pb contamination

121 1200 Luck J. M.* Allègre C. J.
187Re-187Os chronology of meteorites

THERMAL HISTORY OF CHONDRITES

Chairmen: E. R. Rambaldi and R. M. Walker

122 0900 Takeda H.* Yanai K.
Strongly recrystallized meteorites from Antarctica: Yamato-74160 and ALHA 77081

123 0915 Basu A.* Shaffer N. R. Hunt G.
Petrography of the Louisville meteorite (L6e)

124 0930 Wlotzka F.* Fredriksson K.
Morro do Rocio, an unequilibrated H5 chondrite

125 0945 Rubin A. E.* Keil K. Taylor G. J. Ma M.-S. Schmitt R. A. Bogard D. D.
A heterogeneous lithic fragment in the Bovedy L3 chondrite: Origin by impact melting of porphyritic chrondrules

126 1000 Melcher C. L.* Ross L. Mills A. A. Grossman J. N. Sears D. W.
A new measure of the metamorphic history of ordinary chondrites

127 1015 Pellas P.*
Confirmation of differing cooling histories of chondritic asteroids

128 1030 Scott E. R. D.*
Thermal history of chondrites containing rapidly solidified metal-troilite inclusions

129 1045 Clarke R. S. Jr.* Scott E. R. D.
Occurrence and origin of tetrataenite, ordered FeNi, in meteorites

130 1100 Heuser W. R.* Burnett D. S. Larimer J. W.
K-U studies of silica-rich inclusions in the Shaw chondrite

131 1115 Sears D. W.* Marshall C.
Some studies on the metal of unequilibrated ordinary chondrites

132 1130 Bogard D. D.*
Ar diffusion properties and 40Ar-39Ar dating of meteorites

133 1145 Nakamura N.* Tatsumoto M.
A 4.0 b.y. impact metamorphism age of the Modoc L6 chondrite determined by the Sm-Nd method

ORIGINS OF CHONDRULES AND CHONDRITES

Chairmen: T. J. Ahrens and B. H. Mason

134 1345 Gooding J. L.* Keil K. Mayeda T. K.
Clayton R. N. Fukuoka T. Schmitt R. A.
Oxygen isotopic compositions of petrologically characterized chondrules from unequilibrated chondrites

135 1400 Mayeda T. K. Olsen E. J. Clayton R. N.*
Oxygen isotopic anomalies in an ordinary chondrite

136 1415 Grossman J. N.*
Interrelationships of petrography, mineralogy, and chemistry in Chainpur chondrules

137 1430 Rambaldi E. R.* Wasson J. T.
The origin of chondrule rims in the Bishunpur (L3) chondrite

138 1445 King E. A.*
Multi-zoned chondrules: A newly recognized particle type from ordinary chondrites

139 1500 Noonan A. F.* Rajan S. Fredriksson K. Nelen J.
Chondrules in the Kapoeta and Bununu howardites

140 1515 Hewins R. H.* Klein L. C.
Cooling histories of chondrules in the Manych (L-3) chondrite

141 1530 Hartmann W. K. Wilkening L. L.*
Chrondule-sized spherules from an explosion crater

142 1545 Kluger F. Weinke H. H.*
Chondrule formation by impact: The cooling rate

143 1600 Zook H. A.*
A new impact model for the generation of ordinary chondrites

144 1615 Curtis D. B.*
Boron abundances in meteorites: A new perspective

145 1630 Tarter J. G.* Evans K. L. Moore C. B.
Chlorine in chondrites

Friday, September 5, 1980
F4 USB 2622

DIFFERENTIATED METEORITES AND ASTEROIDS

Chairmen: R. Brett and E. F. Helin

146 1345 Moore C. B.* Lewis C. F. Evans K. L. Tarter J. G.
Sulfur and chlorine contents of achondrites

147 1400 Ma M.-S.* Laul J. C. Schmitt R. A.
Genetic relationship between Allan Hills (ALHA) 77005 and shergottites--a geochemical study

148 1415 Manhes G.* Allègre C. J.
U-Th-Pb systematics of the Juvinas achondrite

149 1430 Michel-Lévy M. C.* Palme H. Spettel B. Wänke H.
The Bouvante eucrite

150 1445 Nehru C. E.* Delaney J. S. Harlow G. E. Prinz M.
Mesosiderite basalts and the eucrites

151 1500 Crozaz G.* Tasker D. R.
Thermal history of mesosiderites

152 1515 Harlow G. E.* Delaney J. S. Nehru C. E. Prinz M.
The troubles with tridymite and phosphate in mesosiderites: Feasibility of possible reactions

153 1530 Berkley J. L.* Keil K.
Ureilites revisited: Petrologic evidence for a cumulate origin

154 1545 Keil K.* Berkley J. L. Fuchs L. H.
Suessite, Fe3Si, a new mineral in the North Haig ureilite

155 1600 McFadden L. A.*
A new look at the near-earth asteroid population and its relation to meteorites: A reexamination of their surface characteristics as determined from existing and new spectral reflectance (0.33-1.0 micrometers) measurements

156 1615 Helin E. F.* Gaffey M. J.
1979 VA, A possible carbonaceous asteroid

157 1630 Hostetler C. J.* Hostetler A. E. B.
Asteroid taxonomy using Kiviat figures

PARENT BODIES OF ENSTATITE METEORITES

Chairmen: K. Keil and H. Wänke

158 0930 Larimer J. W.* Ganapathy R. Trivedi B. M. P. Baker J. T.
Unusual minerals and other materials in enstatite chondrites

0945 K. Marti
Introduction: The Abee Consortium

159 0950 Rubin A. E.* Keil K.
Mineralogy and Petrology of the Abee enstatite chondrite

160 1000 Kallemeyn G. W.* Sears D. W. Wasson J. T.
A chemical study of the Abee Consortium slice

161 1010 Frazier R. M.* Boynton W. V.
Rare-earth element abundances in separates from the enstatite chondrite Abee

162 1020 Tatsumoto M. Unruh D. M.*
U-Pb study of Abee Consortium samples

163 1030 Bogard D. D.*
40Ar-39Ar ages of Abee clasts

164 1040 Goswami J. N.* Lal D. Sinha N.
Nuclear track records in the Abee chondrite

165 1055 Wacker J. F.* Marti K.
Noble gases in Abee

166 1110 Thiemens M. H.* Clayton R. N.
Nitrogen isotopes in Abee clasts

167 1120 Rudee M. L.* Herndon J. M.
The thermal history of Abee

168 1130 Leitch C. A.* Smith J. V.
Mechanical aggregation of enstatite chondrites from an inhomogeneous debris cloud

169 1145 Crabb J.*
Primordial noble gases in E-chondrites

170 1200 Okada A.* Keil K. Taylor G. J.
The Norton County enstatite achondrite: A brecciated, plutonic igneous rock

171 1215 Watters T. R.* Prinz M. Rambaldi E. R. Wasson J. T.
ALHA 78113, Mt. Egerton and the aubrite parent body

GALACTIC COSMIC RAY INTERACTIONS

Chairmen: R. C. Reedy and P. Signer

172 0930 Englert P.* Herr W.
Cosmogenic 53Mn and 26Al: Depth and size effects on the production rates in St. Severin, Keyes, Kirin and other chondrites

173 0945 Kirsten T.* Englert P. Herr W. Ries D.
Cosmogenic nuclides in 13 chondrite finds: Implications for exposure age systematics

174 1000 Honda M.* Horie K. Imamura M. Nishiizumi K. Takaoka N. Komura K.
Irradiation history of Kirin meteorite

175 1015 Goswami J. N. Lal D. Nautiyal C. M. Padia J. T. Rao M. N. Venkatesan T. R.* Wasson J. T.
Determination of preatmospheric masses of meteorites using particle tracks and neon isotopic ratios

176 1030 Wetherill G. W.*
Multiple cosmic-ray exposure ages of meteorites

177 1045 Libby L. M.* Libby W. F.
Dating the initiation of cosmic rays in our galaxy

178 1100 Trivedi B. M. P.* Larimer J. W.
Meteorites as probes of galactic structure

179 1115 Reedy R. C.*
Systematics of nuclear reactions in meteorites

180 1130 Spergel M. S.* Reedy R. C. Lazareth O. W. Levy P. W.
Depth dependence of cosmogenic nuclides in spherical meteoroids

181 1145 Birck J.-L.* Morand Ph. Allègre C. J.
Magnesium-calcium-potassium isotopic variations in iron meteorites: A method for studying cosmic rays

182 Birck J.-L. Zanda B. Allègre C. J.
L16/L17 variations in meteorites

183 1200 Evans J. C. Jr.* Reeves J. H.
Aluminum-26 survey of Antarctic meteorites

184 1215 Nitoh O. Nishiizumi K. Imamura M. Honda M.* Arnold J. R.
Cosmogenic 40K and 53Mn in Antarctic meteorites

185 +Durrani S. A.
Use of thermoluminescence for meteorite dating

PETROGRAPHY, MINERALOGY AND CHEMICAL COMPOSITION ON THE CHONDRITE, NŌGATA, NŌGATA-SHI, FUKUOKA-KEN, JAPAN, OLDEST OBSERVED FALL IN THE WORLD.

Shima, Masako*, Yabuki, H.**, Murayama, S.*, and Okada, A.**
* The National Science Museum, Ueno-Park, Taito-ku, Tokyo, Japan. and
**The Institute of Physical and Chemical Research, Wakō-shi, Saitama, Japan

At the end of October, 1979, we are informed that the Suga Jinja, a Sinto Shrine, Nōgata-shi, Fukuoka-ken, Japan, kept a stone which weighs 472g, and is stored in an old wooden box, on the lid of which is written the date, April 7, Jōgan 3 (May 19, 861 Julian Calendar). The appearance of the stone has the typical features of a chondrite.

According to the description of M. Iwakura, a Shinto Priest, and N. Shitama, a local historian, Suga Jinja was founded in the 7th century. On the night of May 19, 861, a great detonation accompanied by a brilliant flash occurred in the precinct of the shrine. Early next morning, villagers found a heavy stone at the bottom of a hole, which it had made in the ground. It appears to us that the observation of this meteorite fall has exactly been handed down by word of mouth. If the date is correct, this chondrite must be the oldest "observed fall" in the world. At present, the oldest chondrite fall is recorded at Ensisheim, Alsace, France, on November 16, 1492. Unfortunately, the box and writing script appear to belong to a later period; so far no other evidence on the date has been found.

The place of fall of the Nōgata chondrite is approximately 130°45.0' E., 33°43.5' N.

A thin section and a polished thin section were prepared for microscopic investigation and electron probe microanalysis. Petrographically, Nōgata is an olivine-hypersthene chondrite with well-recrystallized structure. Transparent minerals are principally olivine and orthopyroxene and minor amount of feldspar, calcic pyroxene and apatite. Opaque minerals are metallic Ni-Fe, troilite, chromite and trace of native copper. This meteorite has been oxidized into interior by terrestrial weathering due to exposure to the atmosphere for many years. Each grain is surrounded by or entirely covered with brownish thin film of iron oxide. Chondrules are few and scarcely identified in thin sections even with an aid of polarized light, because of extreme obliteration of the primary texture. Only three barred olivine chondrules, 0.5, 0.8 and 0.9 mm in size, are recognized in the total area of about 200 mm^2 of thin sections.

Microscopic analyses indicate that olivine in Nōgata has the optical axial angle $2V = -84°$, average refractive indesis are $\alpha = 1.681$ and $\gamma = 1.722$ and the molar composition is Fa_{25-26}. For orthopyroxene, these are; $2V = -70°$, $\alpha = 1.681$ and $\gamma = 1.696$ in average and $En_{74}Fs_{26}$, and for plagioclase, $2V = -53°$, $\alpha = 1.533$, $\gamma = 1.542$ in average and $Ab_{89}An_{11}$. Unit cell parameters of olivine are $a = 4.777$, $b = 10.278$ and $c = 6.015$ Å and of orthopyroxene are $a = 18.278$, $b = 8.872$ and $c = 5.209$ Å. On the other hand, electron probe microanalysis data give the molar compositions Fa_{27} for olivine, $Wo_2En_{76}Fs_{22}$ for orthopyroxene, $Wo_{48}En_{44}Fs_8$ for clinopyroxene and $Or_6Ab_{83}An_{11}$ for plagioclase. In phosphate minerals, probably chlor apatite, characterized by its low birefringence and optical axial angle of nearly zero, Ca, Cl, P and small amount of Fe were detected by electron probe microanalyses.

The preliminary results of wet chemical analyses are as follows: MgO 24.60%, Na_2O 0.91%, K_2O 0.11%, MnO 0.34%, total Fe 19.01%, Ni 1.52%, and Co 0.062% and $Fe/SiO_2 = 0.49$, $SiO_2/MgO = 1.59$. These numbers as well as the data obtained by electron probe microanalyses indicate that the chondrite Nōgata belongs to LL group chondrite.

#2

OVER 4,000 NEW ANTARCTIC METEORITES COLLECTED 1979-80 SEASON

Yanai K.
National Institute of Polar Research, Tokyo

Japanese party collected over 4,000 pieces on bare ice area near the Yamato Mountains. These specimens are chondrites in majority as previous cases, but the finds include under 10 irons, over 20 type II carbonaceous chondrites, over 100 achondrites(eucrites and diogenites in majority) and many possibly unique specimens.

A few specimen have been recovered by same party on bare ice area nea the Belgica Mountains, East Queen Maud Land.

THE METEORITE CONCENTRATION MECHANISM AT ALLAN HILLS, ANTARCTICA

JOHN O. ANNEXSTAD

CURATOR'S OFFICE, NASA, JOHNSON SPACE CENTER, HOUSTON, TEXAS

During the 1978-79 austral summer season a 15 kilometer long triangulation survey network was established at the Allan Hills for the study of ice ablation and movement as related to meteorite finds. The triangulation chain is composed of 20 stations extending from the Allan Hills westward. This network was resurveyed the following Antarctic summer and preliminary ablation measurements indicate that the ice surface is wearing away at an average rate of 5 centimeters per year. The yearly vertical movement (upwelling) of the ice in the area of highest meteorite concentration approximately balances this yearly erosion rate. The horizontal vectors show dissimilar directional movement at three different locations along the network, which suggests that the region of stagnant ice where meteorites have been found is a localized effect. The crevasse patterns and the horizontal vectors at the westernmost stations of the network show that the surface flow of the ice sheet is generally toward the northeast. The ice surface flow direction becomes more easterly at the stations situated closer to the Allan Hills where the surface exhibits a step-like topography. The yearly movement of the ice surface ranges along the network from over 2 meters on the west to less than 20 centimeters on the east. Although the mechanism of meteorite transport and concentration is imperfectly understood, it appears that the Allan Hills ice field serves as a small but effective collection basin for a limited part of the East Antarctic ice sheet.

#4

SUMMARY STATISTICS OF 1977 AND 1978 ANTARCTIC METEORITE COLLECTIONS AND A GLIMPSE OF THE 1979 COLLECTION

King, T.V.V., R. Score, C.M. Schwarz, and B.H. Mason
Lunar Curatorial Laboratory, Northrop Services, Inc., Houston, Texas and Div. Mineral Sciences, Smithsonian Institution, Washington, D.C. 20560

During the past year meteorites with masses greater than 150 grams collected by the joint Japanese-American Antarctic expeditions for the field seasons of 1977-78 and 1978-79 have been classified at the Johnson Space Center and the Smithsonian Institution. The complete classified collection of the '77-'78 season consists of 103 meteorites: 7 irons, 2 carbonaceous chondrites, 5 achondrites, 48 H group chondrites, and 40 L or LL group chondrites. Achondrites represent five individual classifications: mesosiderite, ureilite, diogenite, eucrite, and winonaite. One petrologic type 2 and one petrologic type 3 carbonaceous chondrites are present.

The '78-'79 collection of 66 specimens has been classified as follows: 31 L or LL group chondrites, 16 H group chondrites, 10 irons, 8 achondrites, and 1 carbonaceous chondrite. Achondrites are represented by 5 polymict eucrites, 1 aubrite, and 2 ureilites. The carbonaceous chondrite is petrologic type 2. The following histogram shows the distribution of the ordinary chondrites in the '77 and '78 collections by chemical group and petrologic type.

The distribution of chemical groups within each petrologic type of ordinary chondrites is similar for both the '77-'78 and '78-'79 collections. The petrologic type 6 specimens are dominated by the L group chondrites, and the petrologic types 4 and 5 meteorites are overwhelmingly represented by the H group chondrites. Due to the distinct groupings and similarities between intra and inter specimen comparisons, it is believed that the samples represent a limited number of falls.

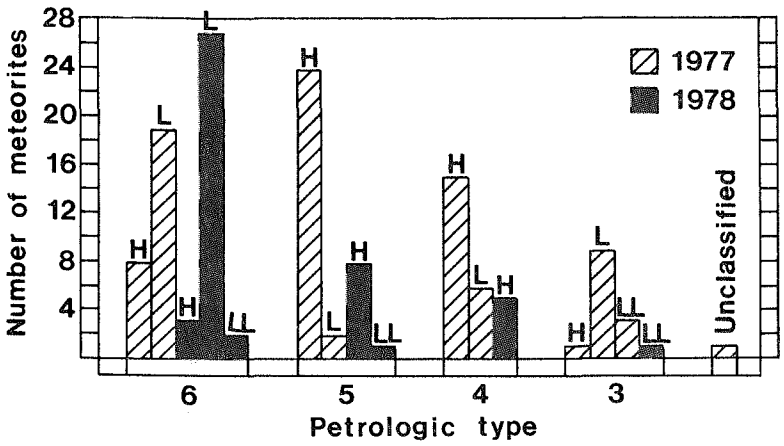

Distribution of collections

The 1979-80 collection is comprised of 83 meteorites, which will not be divided with Japan. Preliminary classification and weights are based on field notes, observations of the collection when it was repacked in California for shipment to J.S.C., and previously noted relations between meteorite mass and container size. The more unique samples from the collection will be classified by September. The 83 samples in the collection consist of: 1 iron, 77 ordinary chondrites, and 5 achondrites (estimated to range in weight from 500 grams to nearly 3 kg). It is estimated that 36 ordinary chondrites have a mass less than 20 gms, 29 of approximately 150 gms, 10 specimens less than 500 gms, and 2 specimens have masses of more than 3 kg.

SEARCHING FOR METEORITES: THE PRESS RELEASE STRATEGY. Sipiera, Paul, P., Harper College, Palatine, IL 60067, Olsen, Edward J., Field Museum, Chicago, IL 60605

In April 1976 the Field Museum and Harper College initiated a program of meteorite recovery similar to the very successful program conducted by UCLA in 1974. As reported by Scott et al, 1977, the UCLA effort produced six new meteorites and one previously known meteorite from a total of approximately 350 specimens that were sent in for identification. Since that initial period, an additional four meteorites have been received (J.N. Grossman, pers. comm.). In both programs the approach was similar: to distribute press releases to the communications media offering a $100 reward for the discovery of any new meteorite. This type of approach is very effective in that it generates considerable public interest in meteorites, and develops an awareness of their scientific importance.

In the present study we report a result quite different from that of the UCLA effort. During the period from April 1, 1976 to March 31, 1980 our program received a total of 1453 inquiries about meteorites, with approximately half of these including specimens for identification. Statistically, public response came from 44 states and 6 countries, with the bulk being from Illinois and its adjacent states. We are of the opinion that our efforts were geographically far-reaching in that we received a specimen from Hawaii and information requests from two South American countries. As a result of these efforts, one fragment of Canyon Diablo was brought in during the first two weeks of the program and two years later a small fragment of the Nakla, Egypt fall was sent in from England. No new meteorite specimens resulted from this indirect approach.

It is our conclusion that the success or failure of a meteorite recovery program such as this depends primarily on the source region where the press releases are made. This indirect approach cannot operate productively just anywhere, but should be centered in high probability areas which favor the recovery of meteorites: areas of low rainfall, unglaciated, and a low density of heavy industries that produce slags.

#6

CAVITATION AND HEAT CONDUCTIVITY IN THE ATMOSPHERIC DISRUPTION OF LARGE METEORITES

Huss, Glenn I
American Meteorite Laboratory, P.O. Box 2098, Denver, Colorado 80201

The disruption of large meteorites by atmospheric forces has been studied mathematically and conjecturally; directly, through the use of radar and photography; and indirectly, through observation of the shapes and the distribution patterns of the meteorites spawned by these disruptions. However, it is still becoming more and more common for researchers to speak of "thermal disruption" of incoming meteorites, and a recent paper (Nozette, 1979) attributed to atmospheric heating a glassy vein which penetrated deeply into a stony meteorite. It is difficult to find a basis for either of these hypotheses.

Historically, evidence of internal heating from ablation has been notably lacking in meteorites. Heat conduction in stones is too slow to appreciably affect the meteoritic body during ablation and heat penetrates only a few millimeters at best. Melted crustal material has been found to penetrate to a maximum depth of only 6 mm into open fissures during ablation. Rather than filling fissures and cracks with molten material from the exterior of the meteorite, ablation tends to produce cavitation, which assists the disruption of the meteorite.

It is suggested that the lack of a highly oxidized external crustal layer on Collescipoli resulted from the disruption of the Collescipoli parent mass as it progressed below the area of retardation during atmospheric flight. Visual evidence of flow in shock melts is presented.

Nozette, Stewart, 1979. Meteoritics 14, 273-281.

Dod, Bruce D., Wayland College, Plainview, TX 79072 and
Sipiera, Paul P., Harper College, Palatine, IL 60067

A REVIEW OF THE STREWNFIELD DISTRIBUTION PATTERNS OF THE PLAINVIEW, TEXAS METEORITE FINDS WITH ADDITIONAL DATA IN CONFIRMATION.

The area around Plainview, Texas has long been recognized as the site of a massive meteorite shower. Hundreds of meteorites have been collected (with over 700 kg recorded) since they were first recognized in the late 1800s. Recovery of this shower's material is still ongoing today. One of these specimens was determined, in 1950, to be unrelated to those reported earlier in the United States National Museum Reports of 1917, and was thus described as a new find. This brings to light an important question: How many of the early finds were not related to each other that were described in the 1917 report? Up to the present, all assumptions were made that the finds in and around Plainview, Texas were from one fall. This is not an unreasonable assumption since these meteorites are very similar in their appearence to each other, their relative rarity, and prohibitive expense for a determinative analysis.

In the present study, an attempt has been made to investigate the petrology and mineralogy of recent Plainview finds and to compare this data to the National Museum's 1917 report to ascertain possible relations or distinctions. Recent finds of "thumbnail" specimens has also been made which lends credence to the concept that the actual trend of the strewn-field is from east to west, passing just south of the present city limits of Plainview. With this data in hand, the several meteorites found to the northeast of Plainview are unrelated and should be considered distinct.

#8

A CONTRIBUTION TO THE RIDDLE ABOUT THE ORIGIN OF CERTAIN GLASSY SPHERULES.

Herr, W.[1], Englert, P.[1] and Herpers, U.[1],
Watt, E.[2] and Whittaker, A.G.[2]
1) Institute of Nuclear Chemistry, University of Cologne, D 5 Koeln-1, Federal Republic of Germany,
2) The Aerospace Corporation, Los Angeles, Calif., U.S.A.

Polar ice caps and ice fields of high altitude glaciers are promising for collecting meteoritic and cosmic dust. From 700 kg of ice (the age of which was ~ 300 years) taken from a well-known glacier of the Swiss Alps, approximately 0.5 g of organic and inorganic residue was recovered. A careful microscopic examination revealed therein about 100 glassy microspheres with diameters ranging from 30 to 150 μm. Neutron activation analysis of individual transparent objects (each 0.9 - 2.3 x 10^{-6} g of weight) showed the presence of K, Sc, Cr, Fe, La, Eu, Au etc. in varying concentrations. In many cases a detection limit of 10^{-14} g/g was achieved. The results were compared with those of spherules taken from the lunar surface and from different terrestrial sources, e.g. Pele's Tears", Hawaii, etc. A systematic study by mass spectrometry (of positive and negative ions) as well as by electron diffraction disclosed that some of the glacier spheres consisted mainly of elemental carbon. The question is still open, whether these objects consisting of "carbyne"-modifications are due to ablation processes of C-chondrites or whether there is a possible connection to the influx of cometary matter.

COSMIC RAY PRODUCED ^{53}Mn IN DEEP SEA SPHERULES.

K. Nishiizumi, M. T. Murrell, P. A. Davis and J. R. Arnold
Dept. of Chemistry, Univ. of Calif., San Diego, La Jolla, CA 92093

Cosmic ray produced ^{53}Mn ($t_{1/2}$ = 3.7x10^6 y) was measured in a group of deep sea stony spherules and in individual metallic spherules using highly sensitive neutron activation analysis. This study represents an extension of a previous paper [1].

In addition to meteorites and lunar samples, deep sea spherules are most probably a third type of extraterrestrial material available for study. Although recent investigation strongly suggests that such spherules are extraterrestrial, perhaps the strongest case for space exposure of these objects would be in the detection of cosmic ray produced nuclides. It is not yet known if deep sea spherules are melted cosmic dust particles or merely ablation debris from larger objects. The measurement of cosmic ray produced nuclides in these spherules should help to answer such questions by providing information on their origin and cosmic ray exposure history. For this present study a group of stony spherules (65 particles) and individual metallic spherules were selected from the Millard collection [2, 3]. This collection of spherules was isolated from Pacific Ocean red clay which was collected from a depth of 4280 m [2]. The chemically separated Mn samples were irradiated in an especially well-thermalized reactor (EL-3 at Saclay, France). The ^{54}Mn activities in the irradiated samples were determined using a highly sensitive intrinsic Ge well-detector. The chemical composition, preliminary ^{53}Mn data, as well as ^{53}Mn data previously reported for metallic spherules [1] are presented in Table 1. The activity level of the stony spherules is slightly lower than the average saturated ^{53}Mn activity level of chondrites. The simplest interpretation of this result is that these spherules are merely ablation debris from stony meteorites. This ^{53}Mn content might also be due to undersaturation. The low or nearly zero ^{53}Mn activity in the metallic spherules can be explained by Mn loss due to atmospheric heating [1].

We are grateful to Dr. Y. Yokoyama for making the EL-3 reactor available to us.

References:

[1] Nishiizumi, K. and Brownlee, D. E. (1979) 16th Int'l. Cosmic Ray Conf., OG 12-17 (Kyoto).
[2] Millard, H. T. and Finkelman, R. B. (1970) J. Geophys. Res. 75, 2125-2134.
[3] Murrell, M. T. et al., (1980) Geochim. Cosmochim. Acta (submitted)

Table 1

	Weight (μg)	Mn (ppm)	Fe (%)	Co (%)	Ni (%)	dpm ^{53}Mn /kg Fe
Stony spherules	4477	2100	27.2	0.05	0.62	247±22
Metallic spherule LJ#5	702	2400	80.4	0.04	0.23	83±47
Metallic spherules A	459	<100	66.9	0.32	4.7	10±9 [1]
B	476	<100	65.6	0.42	3.9	16±10 [1]
H-chondrite (average)		2300	28	0.08	1.7	414±50

#10

A COMPARISON OF THREE SOURCES OF DATA ON THE COMPOSITION OF SMALL METEOROIDS.

Brownlee, D. E., Lunatic Asylum, Calif. Inst. of Tech., Pasadena, CA 91125 and Univ. of Washington, Astronomy Dept., Seattle, WA 98195

There are now three somewhat independent sources of laboratory data relating to the properties of small meteoroids. The data has been obtained by analysis of small micrometeorites collected from the stratosphere and by analysis of much larger meteor ablation spherules and rare unmelted cosmic materials recovered from the sea floor. The micrometeorite investigations have shown that typical 10 μm interplanetary particles are volatile-rich fine-grained aggregates whose closest meteorite analogs are CI's and the matrix of CM's. However, close examination of the morphology and elemental composition of submicron constituents clearly shows that the dust material is significantly different from the fine-grained portions of carbonaceous chondrites. It appears that typical small dust particles are composed of a material which, probably due to friability, does not produce conventional meteorites. The obvious possibilities are either that the parent materials of dust and meteorites are totally unrelated or that carbonaceous chondrites are samples of the dust material which has been altered by parentbody processes to produce strong rocks that are capable of surviving atmospheric entry.

A shortcoming of the stratospheric particles is that they are small and their properties are difficult to directly compare with existing meteorite data. Less pristine but much larger (0.1-1.0 mm) particles have been collected from the sea floor. Presumably most of these extraterrestrial particles are products of partial and total melting of millimeter and smaller samples of the "dust material." The sea floor data has been obtained by two independent approaches. One is analysis of relic grains in rare irregular particles which underwent only partial melting and the other is bulk elemental analysis of the more common once-molten spherules. Microprobe and SEM study of relic grains in nearly a hundred only partially melted particles indicate the parent materials are fairly similar to CM meteorites and that only a small fraction of the particles could come from CI, CV, H, L or E chondrites. Some of the particles actually contain features unique to CM's such as forsterite grains enclosing Cr-rich FeNi metal beads and diopside rimmed spinel-perovskite inclusions. The bulk composition of once molten spheres indicates a correlation with CM or CI composition. The majority of the 0.1-1 mm spheres have chondritic elemental compositions indicating that the precusors were fine grained and that the analyses of spherules are probably indicative of the bulk compositions of the parents. The Mg/Si ratios show very small dispersion around the CM/CI value indicating compatability with these meteorites and a general lack of volatile loss of elements less volatile than Si. Of the elements measured Al, Ca, Mg, and Ti are the most straightforward to interpret because they are demonstrably not effected by volatile fractionation (during entry) and because they are strong discriminators for classifying chondrite groups. Abundance measurements for several hundred spherules show obvious clustering near CM/CI meteorites but with some points in the H, L, and CV fields. The abundance histograms may represent a fairly unbiased characterization of the elemental composition meteoroid complex near 1 AU. It is significant that the three sample materials studied indicate that typical small meteoroids are made out of a material similar to CM meteorites, the major difference being in the nature of the fine-grained constituents.

This work was supported by NASA grants NSG 9052 and NGL 05-002-188. Div. Contrib. No. 3469 (362).

ANALYSES OF NOBLE METALS AT THE CRETACEOUS-TERTIARY BOUNDARY

Kyte, F.T., and Zhou Z.
Institute of Geophisics and Planetary Physics, U.C.L.A.
Los Angeles, California CA 90024

The objective of this study is to examine the hypothesis that the Ir anomaly at the Cretaceous Tertiary boundary is of meteoritic origin. It is believed that a thorough study of siderophile elements, in particular the noble metals at this boundary, can establish the validity of this hypothesis. Certainly the presence of Ir at levels greater than 10% of CI concentrations requires an unambiguous explanation. An impacting asteroid should leave a clear meteoritic signal which should even permit identification of its compositional group.

A 3.5cm section of the Fish Clay from Stevens Klint, Denmark has been analyzed by instrumental and radiochemical neutron activation analysis. The entire sample was from within the boundary and it was cut into 9 samples parallel to the bedding. Preliminary data indicate that Fe, Ni, Co, Ge, Ir, Re, Pt, Au, and Os all show significant enrichment at the base of the boundary.

#12

SPECTRAL-HEIGHT RELATIONS IN PERSEID METEORS

Russell, J.A.
University of Southern California, Los Angeles, Cal. 90007

One of the first relationships noted in meteor spectra was that those showing the H and K lines of ionized calcium were of meteors that appeared above a height of 80 km, whereas those without the H and K lines appeared below that altitude.

It has been known since 1961 that the strength of the H and K lines varies inversely as the strength of the forbidden oxygen line at λ5577.

Studies of the 1977 and 1978 Perseid showers have indicated that meteors with strong forbidden oxygen radiation at λ5577 appear and disappear about 9 km higher than meteors with little or no radiation at that wavelength.

If the last two variations involving the λ5577 radiation are valid, the full cycle of relationships requires that H and K line strength should vary inversely with height. The data of 1977 and 1978 indicate that Perseid meteors with H and K lines do indeed appear and disappear about 6 km lower than those without H and K lines. This inversion of the earlier height versus H and K relationship can be credited to the changing nature of the meteoroid sample as the power of available instrumentation has increased over the years.

The question as to the relative importance of differences in structure and differences in the conditions of radiation in producing these spectral-height relationships is still not completely answered. That differences in structure do exist is supported by the observation that the heights of appearance of meteors tend to cluster about two or three values. Also, Perseid spectra with and without λ5577 radiation have been recorded on the same film a few minutes apart. We may add that although the cometary meteoroids producing the 1978 shower appear to have been randomly distributed, in 1974 a concentration of meteoroids with distinctive spectral features occurred with a large probability of being non-random. We may be observing here evidence that all cometary fragments in a given shower are not chemically and/or structurally the same.

CARBONACEOUS CHONDRITIC MATERIALS IN THE SOLAR SYSTEM

Kallemeyn, G.W.
Institute of Geophysics and Planetary Physics, University of California, Los Angeles, CA 90024 USA

Carbonaceous chondrites are generally thought to represent some of the most compositionally primitive materials in the solar system. Abundances in the CI group and the Sun are indistinguishable for most elements. Carbonaceous chondrite-like clasts are found in a variety of meteorite groups. These carbonaceous chondritic materials consist of collections of grains formed in or initially present in the primitive solar nebula.

The known carbonaceous chondrite groups form rather discrete compositional clusters in terms of parameters such as refractory and volatile element abundances and oxygen isotopes. Chondrite groups having certain common properties may be linked together into clans. The various compositional clusters probably either resulted from components forming under differing nebular conditions, or initial inhomogenieties in the nebula including the possibility of presolar materials. An important question also arises as to whether the hiatuses between these clusters were present in the spectrum of materials formed some 4.5 Gy ago, or whether they are artifacts due to the incomplete sampling of a continuous spectrum. The thrust of this study was to determine a wide range of elemental abundances (refractories through volatiles) in carbonaceous chondrites. Using this as a base to build upon, nebular models pertaining to the formational processes carbonaceous chondrites and carbonaceous chondrite-like clasts were included in the study as potential "missing links" between clusters.

Twenty "grouped" and four "anomalous" carbonaceous chondrites, along with five carbonaceous chondrite-like clasts, were analyzed by INAA and RNAA for some thirty elements. Refractory element abundances link the four carbonaceous chondrite groups into three clans: CI, CM-CO, and CV. These clans probably indicate formation at different heliocentric distances. Refractory abundances relate to the earliest physical processes in the solar nebula and the possible existence of presolar materials (i.e., Ca,Al-rich inclusions). Volatile element abundances are rather distinct among all four groups and serve to distinguish CM from CO chondrites which are placed in the same clan, on the basis of nonvolatile element abundances. Volatile abundances also relate to nebular processes. They give clues to the spatial and time distribution, efficiency, and extent of the condensation processes taking place in the various formation regions.

#14

NON-VOLATILE SIDEROPHILE ELEMENTS IN CARBONACEOUS CHONDRITES.

Palme H. and Rammensee W.

Max-Planck-Institut für Chemie, 6500 Mainz, W.-Germany

We have used a new analytical technique to determine simultaneously the abundances of non-volatile metals in carbonaceous chondrites. In the liquid metal extraction method (1), a neutron irradiated sample is equilibrated with metal at high temperatures (around 1300°C for 20 minutes) and a fixed oxygen fugacity. Subsequent heating to 1580°C for a very short time allows the molten metal containing all siderophile elements to coagulate and segregate. After cooling the metal is physically separated, dissolved and counted on a Ge(Li)-detector. Since similar amounts of silicate and metal are used, and since all elements of interest have metal/silicate partition coefficients much higher than 100, no chemical yield determinations are necessary.

The precisions of the analyses of refractory siderophile elements are better than 5 % for Ir, Re, Os, W, and Mo, between 5 % and 10 % for Pt and between 10 % and 20 % for Ru. The abundances of the more volatile elements Co, Ni, Cu, As, and Au can be determined with a precision much better than 5 %. Copper, As, and Au have been carefully checked for possible volatilization losses. These losses were in all cases smaller than 5 %. Significant volatilization losses have only been observed for Ga and Se. The oxygen fugacity has to be low to prevent formation of volatile Os, Re, W, and Mo oxides.

Preliminary data on Orgueil, Murchison, and Allende have been obtained. All three meteorites have a Mo/Ir ratio of around 1.85, the corresponding Mo concentration of Orgueil is 900 ppb, compared to the previously used C1 abundance of 1.4 (2). With this Mo value the cosmic abundance of Mo would decrease from 4 atoms Mo/10^6 atoms Si to 2.5, a value which has been estimated by Suess and Zeh (3) from semi-empirical nuclear abundance rules. The Ir/Re ratios of Orgueil, Murchison, and Allende are identical within 5 % (12.5); variations in Ir/W ratio may slightly exceed analytical uncertainties, the mean ratio is 5.0. Orgueil and Murchison have a Pt/Ir ratio of 2, while an Allende sample is somewhat lower. From the observed Cu abundance in Orgueil (139 ppm) a cosmic abundance of 575 atoms Cu/10^6 atoms Si is derived compared to 540 ± 60 (4). The Cu/As ratios are similar in three types of meteorites analysed, indicating the same depletion factors for Cu and As in type 2 and 3 carbonaceous chondrites.

1.) Rammensee W. and Palme H. (1980) in preparation.
2.) Lipschutz M. (1971) in Handbook of Elemental Abundances in Meteorites (ed. B. Mason), p. 323.
3.) Suess H.E. and Zeh D. (1973) Astrophys. and Space Sci. 23, 173.
4.) Goles G.G. (1971) in Handbook of Elemental Abundances in Meteorites (ed. B. Mason), p. 229.

SULPHATE VEINS, CARBONATES, LIMONITE AND MAGNETITE: EVIDENCE ON THE LATE GEOCHEMISTRY OF THE C-1 REGOLITHS

Fredriksson, K.*, R. Beauchamp**, E. Jarosewich* and J. Kerridge***
*Smithsonian Inst., Washington, DC 20560, **Battelle NW Laboratories, Richland, WA 99352, ***UCLA, Los Angeles, CA 90024

The light colored, mostly water soluble, veins in three C-1 chondrites have been studied in polished ultrathin sections, PUTS (1), prepared without water. It has been possible to obtain electronprobe analyses of the scarce and delicate phases in these veins, previously believed to be mostly epsomite with some bloedite (2,3). The new analyses show that most veins consist of sulphates of Na, Mg and Ni in variable proportions, while a few are pure (<1% Fe, Mg, Na) Ca-sulphate. In agreement with (2) but contrary to (3) no proper veins of carbonates were observed, although a great variety of carbonates are omnipresent in these meteorites, usually associated with magnetite. This will be discussed in a companion paper by Kerridge et al. (4). While the complex sulphates have NiO contents varying from a few to ~14 wt%, they are, remarkably, almost free of iron and manganese in contrast to the carbonates. These iron-free sulphates are reminiscent of the recently described mineral, nickel-bloedite (5), occurring as surface efflorescence on Ni-rich sulfide ores. Apparently oxidation during weathering causes iron to precipitate (as Fe^{3+}) while Na, Mg and Ni remain in solution until water is removed and the sulphates crystallize. We suggest that similar processes occurred within the C-1 regoliths. This is supported by previous (2) and current observations (in PUTS) of extensive corrosion of most Fe(Ni)S crystals, even to complete conversion to Ni-free limonitic pseudomorphs, which seem to be the source for some of the Ni-free magnetites, especially spherulitic forms as well as other types mostly in the veins. Apparently earlier magnetites, i.e. the famous platelets and the framboidal types associated with carbonates (4), may have had a similar origin but probably in a higher temperature regime.

A new bulk chemical analysis shows that essentially all Na, nearly half the Ca and 1/10 of Mg (but <0.01% Fe) is soluble in hot water; this portion has a Ni/Fe ratio of >1/2 compared to the bulk with ~1/20. A mass balance calculation will be presented and compared to the modal composition given in (2).

(1) Beauchamp, R. & Fredriksson, K. (1979). Meteoritics 14, 344.
(2) Bostrom, K. & Fredriksson, K. (1966). Smithsonian Misc. Contr. 151, #3.
(3) Richardson, S. M. (1978). Meteoritics 13, 141-159.
(4) Kerridge, J. et al. These abstracts.
(5) Nickel, E. H. & Bridge, P. J. (1977. Mineral. Mag. 41, 37-41.

#16

CARBONATES IN CI CHONDRITES

Kerridge, J.F.
Institute of Geophysics, UCLA, Los Angeles, California 90024
Fredriksson, K., Jarosewich, E., Nelen, J.
Smithsonian Institution, Washington, D.C. 20560
Macdougall, J.D.
Scripps Institution of Oceanography, La Jolla, California 92093

In addition to reduced carbon in the form of organic matter, most carbonaceous chondrites contain oxidised carbon as inorganic carbonates. In CI chondrites these carbonates consist of subequal amounts of dolomite and a ferroan magnesite, traditionally termed breunnerite, with minor Ca-carbonate, probably vaterite. Dolomite contains up to 8 mole% $FeCO_3$ and up to 13 mole% $MnCO_3$, equivalent in some cases, therefore, to ankerite. Breunnerites range from 15 to 40 mole% $FeCO_3$, with up to 17 mole% $MnCO_3$ and invariably less than 1 mole% $CaCO_3$. In neither dolomite nor breunnerite do Fe and Mn contents exhibit any systematic interrelationship. Ca-carbonate is essentially pure $CaCO_3$. Breunnerite grain sizes are systematically larger than those of dolomites and Ca-carbonates, ranging up to a few millimeters in diameter.

Most dolomites and breunnerites have irregular morphologies, frequently appearing to be clastic fragments, although euhedral grains are fairly common. Some dolomites and probably all Ca-carbonates occur as rounded amoeboid particles apparently formed by spherulitic crystallisation. Magnetite is commonly associated with dolomite and Ca-carbonate, either as inclusions or within aggregates. Magnetite can also be associated with sulfate veins, which apparently formed later than the carbonates and under conditions which were somewhat more oxidising (see Abstract by Fredriksson et al.).

Carbonates similar to those described here may be found in a variety of terrestrial environments, so the meteoritic occurrences are unlikely to be uniquely diagnostic of formation conditions of the CI chondrites. However, an origin by crystallisation during a period of aqueous activity and mineralisation already inferred for the CI parent body on other grounds, seems quite consistent with the present observations. There appear to be no grounds for postulating a nebular, i.e. "condensation", origin for the carbonates or, indeed, any other major mineral constituent of CI chondrites.

REFRACTORY INCLUSIONS IN CM METEORITES: PETROGRAPHIC STUDIES

Macdougall, J. D., Goswami, J. N. and Carlson, J.
Geological Res. Division, Scripps Inst. of Oceanography, La Jolla, CA.

The refractory inclusions contained in the CM meteorites are an important but as yet relatively little studied source of data on early solar system processes. Their mineralogical and chemical properties (1), anomalous Mg isotope compositions (2), and rare earth element compositions (3) all suggest that at least some of these are very early condensates. Here we present further data based on extensive optical, SEM and electron microprobe studies of polished sections of Murchison, Murray, Nogoya, Cold Bokkeveldand Mighei. These studies reveal the following major points: (1) All CM meteorites examined contain similar and characteristic suites of inclusions which vary primarily in their degree of alteration. (2) Two refractory inclusion types dominate. The more abundant is composed mostly of pure Mg spinel rimmed by a very thin (few μm) diopside layer and containing variable amounts of perovskite, usually within the spinel. About 5-50 spinel inclusions >20μm occur per cm^2 of CM section. Hibonite bearing inclusions ("SH" of ref. 1) are rarer, <0.1 x the abundance of the spinel inclusions. In all other respects except presence of hibonite, these are similar to the spinel inclusions. Hibonite does not show a reaction relationship with spinel although the two phases are frequently intergrown. Rarely perovskite occurs within hibonite. (3) Both refractory inclusion types occur in two textural varieties: as irregular, often convoluted, fluffy-textured assemblages, and as compact spherules with igneous-like textures. Both types usually are rimmed with diopside. (4) A common feature of all inclusion types is a hydrous (?) Fe-rich silicate band several microns wide which occurs just inside the diopside rim. It is not yet clear from our work whether this iron-rich band marks the position of a pre-existing layer or whether it is simply an alteration product of the spinel. (5) Although most of the inclusions observed in sections are intact, some have been fragmented before incorporation into the meteorite. Optical examination of the fragmented inclusions shows that the iron-rich band referred to above occurs in some fragments, but not all, paralleling the broken edge. This suggests that this feature was produced prior to incorporation of the refractory inclusions into the meteorite. (6) The degree of alteration of the inclusions, although variable on a mm scale within individual meteorites, shows a general correlation with the overall alteration state of the host meteorite. A common replacement phase in the interiors of altered inclusions is calcite. The diopside rims are usually the least altered component, persisting even when much of the inclusion interior has been replaced by secondary phases.

References. (1) Macdougall, E.P.S.L. 42, 1 (1979). (2) Macdougall and Phinney, G.R.L. 6, 215 (1979); Tanaka et al., Lunar Planet. Sci. 11, 1122 (1980). (3) Boynton et al., Lunar Planet. Sci. 11, 103 (1980).

#18

THE MURCHISON BLUE ANGEL INCLUSION: ITS MINERALOGY AND PETROLOGY

Armstrong, J. T., G. P. Meeker, J. C. Huneke, and G. J. Wasserburg, Lunatic Asylum, Div. Geological and Planetary Sciences, California Inst. of Technology, Pasadena, CA 91125

Hibonite-bearing inclusions found in CV and CM chondrites are thought to contain some of the earliest phases condensed from the solar nebula. A well preserved inclusion of this type, found by R. Becker, has been isolated from the Murchison CM chondrite for extensive analysis. This inclusion, dubbed "Blue Angel" for its light blue color, is ~1 mm in diameter. It is comprised of four crudely concentric zones: (1) a dark gray inner core of large subhedral to euhedral hexagonal plates of hibonite with trace poikilitic perovskites and occasional large pore spaces; (2) an intermediate very porous blue zone composed of finely crystalline, euhedral, hexagonal plates and prismatic needles of hibonite with trace perovskite and very minor traces of spinel (calcite appears between many of the hibonite crystals as a cement); (3) an outer white zone composed primarily of calcite which is cross-cut with numerous very fine (<1μm) veins of silicates and which contains randomly oriented, fine-grained assemblages of subhedral to euhedral spinel, perovskite, hibonite, and minor diopside; and (4) a discontinuous rim zone containing an inner rim of massive anhedral to subhedral spinel with poikilitic perovskite and rare hibonite, and a very thin (<5μm) outer rim of aluminous pyroxene.

Vanadium is present in substantial abundance in the core and blue zone hibonites which have virtually identical chemistry (Table, #1). Vanadium is present in significantly lesser amounts in the white zone and rim hibonites and spinels (Table 1, #2-3). Iron and chromium are in low concentration, but clearly present in both hibonites and spinels in this inclusion.

The white zone and rim hibonites are chemically distinct from those found in the blue zone and core. The average Al/Mg atomic ratio is 33.4±4.7 (1σ) for blue zone and core hibonites and 22.4±4.8 for the white zone and rim. The average Mg/Ti ratio is 1 for blue zone and core hibonites and somewhat greater than 1 for the white zone and rim, reflecting coupled substitution of Mg and Ti for Al. The hibonites in all zones are very stoichiometric, closely corresponding to the formula $Ca(Al, V, Cr, Fe, Mg, Ti, Si)_{12}O_{19}$.

There is evidence of fracturing of a portion of the rim during incorporation of the inclusion into the meteorite. In one portion, there is a sharp contact between the matrix and calcite from the white zone. Textural arguments indicate that calcite thoroughly impregnated the outside portions of the inclusion and penetrated even into the core. This penetration appears to have taken place after the inclusion was formed, but prior to its incorporation into the meteorite in its current position. Some of the silicate veining in the outer zone is inferred to have occurred after emplacement. This inclusion's mineralogy shows that the complex mineral alteration and crystallization typical of carbonaceous chondrites must be considered even in studying the meteorites' earliest high temperature inclusions.

Table 1. Average (±1σ) analyses of Blue Angel hibonites and spinels

#	MgO	CaO	FeO	Al_2O_3	Cr_2O_3	V_2O_3	SiO_2	TiO_2
1	2.01±.26	8.40±.18	.01±.03	83.87±1.54	.06±.05	1.08±.19	.19±.09	4.11±.62
2	3.02±.53	8.31±.33	.16±.24	82.87±2.09	.03±.04	.24±.21	.33±.16	5.11±.86
3	28.52±.41	.07±.11	.24±.13	71.19±1.14	.14±.12	.17±.10	.07±.06	.17±.07

(1. hibonite from zones 1 & 2, n=49; 2. hibonites from zones 3 & 4, n=18; 3. spinels from zones 3 & 4, n=20.)

Div. Contrib. No. 3467(360).

EVIDENCE OF ^{26}Mg EXCESS IN HIBONITE FROM MURCHISON

Papanastassiou, D. A. and G. J. Wasserburg, The Lunatic Asylum, Division of Geological and Planetary Sciences, Caltech, Pasadena, CA 91125

We report Mg isotopic analyses on a hibonite inclusion from Murchison (CM), named the Blue Angel for its distinct color, and discovered by R. H. Becker. Petrographic, mineralogic, and chemical information is provided in a companion abstract [1]. Hibonite is important as it has the highest estimated condensation temperature for major element oxides [2], may have a high Al/Mg ratio, and may be chemically resistant to alteration. The Mg measurements reported here extend to Murchison the application of high precision mass spectrometric analyses. We list in the Table analyses by direct loading of three ~50μm crystals from the core of the inclusion and the results on a fourth crystal which was fused and the Mg chemically separated. The techniques were described [3,4]. Two of the crystals were rinsed in 1N HCl to remove soluble phases (e.g., $CaCO_3$) possibly rich in Mg, so as to enhance effects from hibonite. All crystals yield a uniform, raw $^{25}Mg/^{24}Mg$ corresponding to unfractionated Mg isotopes relative to terrestrial Mg to within 1‰ per amu. All directly loaded crystals show a uniform, distinct excess $\delta(^{26}Mg/^{24}Mg) = 13.6$ ‰. This excess is resolved without the need to normalize for instrumental fractionation and demonstrates the presence of excess ^{26}Mg in this inclusion. The fused sample yields a lower ^{26}Mg excess due to contamination during fusion but which confirms the existence of the effect. If we assume that the observed excess is due to ^{26}Al decay and with an average Al/Mg from Armstrong et al. [1], and if we assume a normal initial $^{26}Mg/^{24}Mg$, we obtain $^{26}Al/^{27}Al = 5\times10^{-5}$ at the time of formation of the Blue Angel. This ratio is similar to that for Allende inclusions BG2-6, WA, Egg-1, Egg-2, and Egg-3 [5,6,7], but contrasts with $^{26}Al/^{27}Al < 2\times10^{-7}$ in the HAL hibonite from Allende [8] and with reports of $^{26}Al/^{27}Al \sim 10^{-3}$ in hibonite from Leoville using an ion-probe [9]. Using an ion-probe, Macdougall and Phinney [10] found for Murchison that the hibonite crystals (100-500μm) they analyzed were normal within their lower precision of 5-10‰ except for a hint of excess ^{26}Mg in one hibonite inclusion. They also observed highly fractionated Mg isotopes in another crystal. Tanaka et al. [11] reported excess ^{26}Mg in melilite from Murchison, but the absence of ^{26}Mg excess in hibonite. We conclude that there is now clear evidence for significant excess of ^{26}Mg in hibonite in Murchison. The inferred $^{26}Al/^{27}Al$ for the Blue Angel hibonite (high temperature) does not differ significantly from that commonly found in the anorthite (lower temperature).

Murchison: Blue Angel Hibonite

Mean Crystal Dimension	Fractionation[a] $\delta(^{25}Mg/^{24}Mg)$ ‰ per amu	$\delta\,^{26}Mg$[b] ‰
1. 70 μm (blue)	-1±1	13.6±1.2
2. 50 μm (grey)[c]	+0.5±1	13.7±0.8
3. 40 μm (blue)[c]	-0.5±1	13.6±0.3
4. Fused hibonite	+1±1	6.3±2.0

With $^{27}Al/^{24}Mg = 42$, $(^{26}Al/^{27}Al)_o = 5\times10^{-5}$

[a]Fractional deviation of the raw measured ratio from $^{25}Mg/^{24}Mg = 0.12475$ for normal Mg. $\delta(^{25}Mg/^{24}Mg)$ is the Mg isotope fractionation. [b]Excess ^{26}Mg relative to normal $(^{26}Mg/^{24}Mg)$ after correction for fractionation. Errors are $2\sigma_m$. [c]HCl rinse.

Div. Contrib. No. 3466(359).

Ref.: [1] Armstrong, Meeker, Huneke & Wasserburg (1980) this vol.; [2] Blander & Fuchs, GCA 38(1975)1605; [3] Lee, Papanastassiou & Wasserburg [LPW], GCA 41(1977)1473; [4] Esat, Brownlee, Papanastassiou & Wasserburg, Science 206(1979)190; [5] LPW, GRL 3(1976)109; [6] LPW, Ap. J. Lett. 211(1977)L107; [7] Esat, Papanastassiou & Wasserburg LPS X(1979) 361; [8] Lee, Russell & Wasserburg, Ap. J. Lett. 228(1979)L93; [9] Lorin & Christophe Michel-Levy, Proc. 4th ICGCIG(1978)257; [10] Macdougall & Phinney, GRL 6(1979)215; [11] Tanaka, Davis, Hutcheon, Matthews, Olsen, MacPherson & Grossman, LPS XI(1980)1122.

#20

A Mg ISOTOPE STUDY OF HIBONITE-BEARING MURCHISON INCLUSIONS

Hutcheon, I.D.[1], Bar Matthews, M.[1], Tanaka, T.[1], MacPherson, G.J.[1]
Grossman, L.[1], and Olsen, E.[2]
[1]University of Chicago, Chicago, IL 60637
[2]Field Museum of Natural History, Chicago, IL 60605

The Mg isotopic composition of four hibonite-bearing inclusions and three hibonite single crystals from the Murchison C2 chondrite has been measured with an ion microprobe. Two of the inclusions, BB-1 and BB-4, and all of the hibonite fragments were recovered using a freeze-thaw technique described earlier (1), while two other inclusions, MUCH-1 and SH-4, were discovered by optical microscope examination of broken surfaces. All analyses were performed with a primary beam current of ~2nA and a beam diameter <5μm to ensure that the beam did not overlap the characteristically intergrown phases; isotopic data are summarized in the table below. BB-1 and BB-4 are blue, spheroidal objects (~100μm diameter) comprised mostly of intergrown spinel and lath-shaped hibonite, as described in (1). Single hibonite crystals DJ-5,6 and 9 are similar to DJ-1 described in (1) and are of similar compositions with only a factor of two range in Mg. MUCH-1 is composed of bladed hibonite crystals (typically ~130μm x 20μm) radiating outwards from the inclusion center, surrounded by loosely compacted perovskite and calcite. Unlike other refractory Murchison inclusions, no spinel was observed. MUCH-1 hibonite resembles the DJ fragments in appearance and composition; all are characterized by low Mg (0.5-1.2% MgO) and uniform Sc (0.06-0.10% Sc_2O_3). SH-4 is a fine-grained aggregate, ~1mm in diameter, containing diopside, fassaite, spinel, olivine, perovskite, hibonite, calcite, and a blocky, hydrated feldspathoid.

Excess ^{26}Mg was detected only in the hibonites from BB-1 and BB-4. No evidence for mass fractionated Mg like that reported in (3) was observed. The ^{26}Mg excesses in three hibonites exhibit the linear correlation with the Al/Mg ratio characteristic of most Allende refractory inclusions and, together with data from spinel, define an Al-Mg isochron of slope $(^{26}Al/^{27}Al)_0 \sim 5x10^{-5}$. These data are the first unambiguous evidence of ^{26}Mg excesses in hibonite which are correlated with the Al/Mg ratio. The slope of the hibonite isochron is identical to that defined by data from melilite in Murchison inclusions MUM-1 and MUM-2 (2) and to the slope of the standard Allende isochron (4), suggesting that Murchison BB and MUM inclusions are both contemporaneous with Allende Type B1 inclusions. In contrast, the DJ, MUCH-1, and SH-4 hibonites contain no excess ^{26}Mg with $^{27}Al/^{24}Mg$ up to ~200. $^{26}Al/^{27}Al$ was $<2x10^{-6}$ when these hibonites formed. If the lack of ^{26}Al is due to decay, then these hibonites formed ≳3 My after Murchison BB hibonites. The similarity in physical appearance and chemical and isotopic composition of the DJ hibonites and those in MUCH-1 suggests that of the inclusions thus far observed, MUCH's are the most likely source of DJ hibonite fragments.

Sample	$\delta^{26}Mg$ (‰)	$^{27}Al/^{24}Mg$
BB-1 spinel	0±2	2.5
hibonite	6±2	25
BB-4 spinel	-1±2	2.5
hibonite #1	15±2	30
hibonite #2	25±3	75
MUCH-1 hibonite	-1±3	196
DJ-5 #2	1±2	190
#3	0±2	181
DJ-6	0±3	113
DJ-9	0±2	123
SH-4 hibonite	-1±2	14

References:
(1) G.J. MacPherson *et al.* (1980) *Lunar Planet. Sci. XI*, pp. 660-662.
(2) T. Tanaka *et al.* (1980) *Lunar Planet. Sci. XI*, pp. 1122-1124.
(3) Macdougall, I.D. and Phinney, D. (1979), *Geophys. Res. Lett.* 6, 215-218.
(4) Lee, T. (1979) *Rev. Geophys. Sp. Phys.* 17, 1591-1611.

A CORUNDUM-RICH INCLUSION IN MURCHISON

Grossman, L., Bar Matthews, M., Hutcheon, I.D., MacPherson, G.J., Tanaka, T. and Kawabe, I.
University of Chicago, Chicago, IL 60637.

An inclusion in which corundum is a major phase has been discovered in the Murchison C2 chondrite. It is a deep blue spheroid, ~250μm in diameter, that was recovered from the $\rho>3.5$ fraction upon heavy liquid separation of the products of freeze-thaw disaggregation of the meteorite. After an 8μg fragment was removed for trace element analysis, the rest was made into a polished thin section for petrographic and electron and ion microprobe investigations.

The inclusion, labeled BB-5, consists of only three phases: hibonite-80% by area, corundum - 20% and traces of perovskite. Corundum occurs in masses ~50μm in size surrounded by blue pleochroic hibonite blades, 30-70μm in length and 10-20μm in width. Perovskite grains are interstitial to the hibonite blades and elongated parallel to their length. The corundum is virtually pure Al_2O_3, the only impurity being 0.32% TiO_2, and the hibonite is noteworthy for its low MgO and TiO_2 contents, 0.65 and 2.0 wt %, respectively.

If this inclusion is a direct vapor-to-solid condensate from a gas of solar composition, equilibrium temperatures on the order of 1740°K at 10^{-3} atm. total pressure are implied by the presence of corundum which, from the textures, would have had to condense prior to hibonite. If, on the other hand, BB-5 crystallized from a liquid, its bulk chemical composition, ~93.5% Al_2O_3 and 6.5% CaO, would have required temperatures between 2100 and 2250°K for melting. In this case, the bulk composition and extreme temperature pose stringent constraints on possible melting processes. Whether the inclusion was melted or not, the major element composition indicates that it or its precursor was isolated from the nebular gas at a higher temperature than most refractory inclusions in Murchison. This is also indicated by preliminary data on refractory trace element fractionation patterns.

The Mg isotopic compositions of hibonite and corundum were measured with the ion microprobe. Both phases show small excesses of ^{26}Mg: $\delta^{26}Mg=7\pm2^{o}/oo$ ($\pm2\sigma_{mean}$) with $^{27}Al/^{24}Mg=138\pm5$ for hibonite and $\delta^{26}Mg=3\pm8^{o}/oo$ with $^{27}Al/^{24}Mg=(1.4\pm0.2)\times10^{4}$ for corundum. The large error in the corundum data is due to low count rates arising from the exceptionally low Mg content and the reduced primary beam current (~2nA) used to ensure that individual phases were spatially resolved during analysis. These data suggest that BB-5 is uniformly enriched in ^{26}Mg and show unmistakably the absence of the linear correlation between ^{26}Mg excesses and $^{27}Al/^{24}Mg$ ratios common to most Allende refractory inclusions. An isochron extending from normal Mg at $^{27}Al/^{24}Mg=0$ through the BB-5 hibonite datum would predict $\delta^{26}Mg\sim700^{o}/oo$ at an $^{27}Al/^{24}Mg$ ratio corresponding to the corundum. The uniform enrichment in ^{26}Mg independent of the $^{27}Al/^{24}Mg$ ratio suggests that BB-5 either formed from a reservoir containing ~7°/oo excess ^{26}Mg but no live ^{26}Al or that hibonite and corundum were isotopically re-equilibrated after decay of ^{26}Al.

#22

DETERMINATION OF ACTIVITY COEFFICIENTS FOR CALCULATING CONDENSATION TEMPERATURES OF METAL ALLOYS.

Rammensee W., Palme H. and Wänke H.
Max-Planck-Institut für Chemie, 65 Mainz, W.-Germany

Since metals in the solar nebula condense in alloys, a knowledge of the activity coefficients of each metal in this alloy is a prerequisite to calculate precise condensation temperatures. Wai and Wasson (1) and Palme and Wlotzka (2) have shown that slight changes of activity coefficients cause large variations in condensation temperatures. Since activity coefficients in alloys are generally only known for binary systems, it is necessary to measure these activity coefficients in cosmochemically relevant systems.

A Knudsen effusion cell combined with a quadrupole mass-spectrometer was used to determine the activities of the components of metal alloys by continuously measuring the vapour pressures of the different species of the gas phase at temperatures between 1040°C and 1490°C. The experimental equipment is characterized by a very short molecular beam path between the Knudsen effusion hole and the ionisation chamber of the quadrupole filter, in order to determine vapour pressures of elements with very low concentrations.

Preliminary results in FeNiCo alloys indicate that this system deviates from ideality. Therefore the calculation of condensation temperatures of Fe, Co, and Ni assuming ideal solution is only a first approximation. Especially the Ni/Co ratio of the first condensing alloys depends sensitively on the activity coefficients of Ni and Co in the condensed alloy. The experiments will be extended to include most of the cosmochemically relevant siderophile trace elements, such as e.g. Ga and Ge.

1.) Wai C.M. and Wasson J.T. (1977) Earth Planet. Sci. Lett. 36, 1-36.
2.) Palme H. and Wlotzka F. (1976) Earth Planet. Sci. Lett. 33, 45-60.

ORDERED FeNi AND THE COOLING RATE OF IRON METEORITES BELOW 320°C.

Albertsen, J.F., Roy-Poulsen, N.O. and Vistisen, L.

Physics Laboratory I, H.C. Ørsted Institute and Niels Bohr Institute
University of Copenhagen, Universitetsparken 5, Copenhagen, Denmark.

Mössbauer spectroscopy and X-ray diffractometry of taenite fields of several iron meteorites, mesosiderites, pallasites and chondrites have demonstrated that an ordered alloy FeNi (tetrataenite) is present in the majority of the meteorites.

In the composition range 25-45% Ni within the taenite fields the ordering makes the taenite decompose into domains of ordered FeNi and a low-Ni (disordered) taenite, which fill out the space between the domains of the ordered FeNi. When the polished cross section of a taenite field is etched with Nital, this duplex structure becomes visible as a brownish Zone inside the taenite field. The widespread occurrence of this cloudy zone among meteorites indicate that most meteorites cooled slowly enough to allow the taenite to become ordered and even to allow domains of ordered FeNi in the cloudy zone to reach linear dimensions of generally several hundred Angstroms. The size of the domains as well as the degree of order obtained within them evidently depend on the cooling history of the meteorite below the ordering temperature 320°C. The degree of order in FeNi has been measured by Mössbauer spectroscopy. Taenite fields from iron meteorites belonging to the chemical groups: IA, IIC, IID,IIIA, IIIB, IIIC, IIID, IVA, IVB have been investigated.

As might be expected the degree of order of FeNi in different taenite fields from the same meteorite show very little variation, but taken together the meteorites display an almost complete range of order of FeNi from virtually zero in the IIC meteorite Cratheus 1950 to nearly perfect order in the IA meteorites. The majority of the other meteorites, e.g. the IID, IIIA, IIIB, IIIC, IIID and IVB meteorites of this study contain a slightly less ordered FeNi than found in the IA meteorites. The IVA meteorites show a considerable range in degree of order at a distintly lower level than in the IA and IIIA-D meteorites.

The state of order of FeNi depend on the cooling and shock histories of the meteorites at temperatures below 320°C. Together with the available cooling rates at 650-450°C, the study of the FeNi in taenite fields provide us with detailed cooling histories of the meteorites and their parent bodies.

#24

ABSTRACT

EXPERIMENTAL MODEL FOR CHEMICAL FRACTIONATION OF IRON METEORITES

Narayan, C. and Goldstein, J. I.
Dept. of Metallurgy & Materials Engrg., Lehigh University, Bethlehem,PA 18015

The purpose of this research was to understand how the compositional trends of trace elements in Fe-Ni meteorites develop using experimental techniques and computer modeling. The current Scott-Wasson theory predicts that plane front solidification is responsible for the fractionation. However plane front and dendritic growth experiments accomplished in the laboratory together with thermal modeling of parent meteorite bodies indicate that these parent bodies would solidify dendritically rather than with a plane front. Fe-Ni-X alloys, where X is a third element, were grown dendritically and the composition data from the bulk alloy and dendrite cores were used to calculate the partition coefficients K_D^X of the ternary elements. These K_D^X values were corrected for solid state diffusion effects using the model developed by Flemings, et al. (1970). The corrected equilibrium partition coefficients are 0.43 for Au, 0.58 for Ge, 0.2 for P, 0.88 for Ni, 1.35 for Pt and 1.73 for Ir. Further experimentation also indicated that K_D^X values can be influenced significantly by elements that depress the melting point of Fe-Ni. Because group IIIAB meteorites have increasing amounts of P, an element that depresses the melting point of Fe-Ni, and because Ge shows peculiar trends in this group, the effect of P on K_D^{Ge} was studied. The results show K_D^{Ge} increasing sharply from 0.58 to more than 1.0 for just 0.5 wt% P in the solid. This increase is shown in Fig. 1. This functional dependence was incorporated into the Flemings, et al. model and the variation of Ge and Ni across the dendrite was plotted on a log Ge vs. log Ni plot. Figure 2 shows the Ge-Ni plot for different initial bulk compositions. The (+) sign indicates the starting composition in each case. Figure 3 shows the chemical grouping of meteorites based on Ge and Ni contents. Preliminary experiments with S and high P contents indicate $K_D^{Ge} >> 1$. The K_D^{Ge} can be used to explain the negative slope of groups I, IIAB and IIICD.

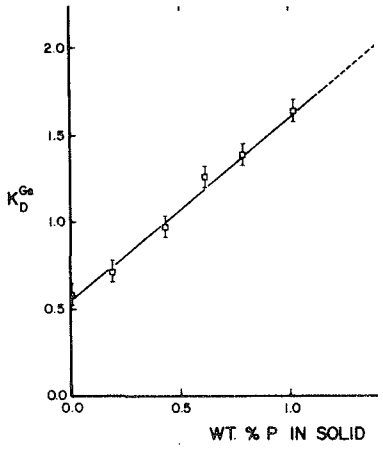

Fig. 1

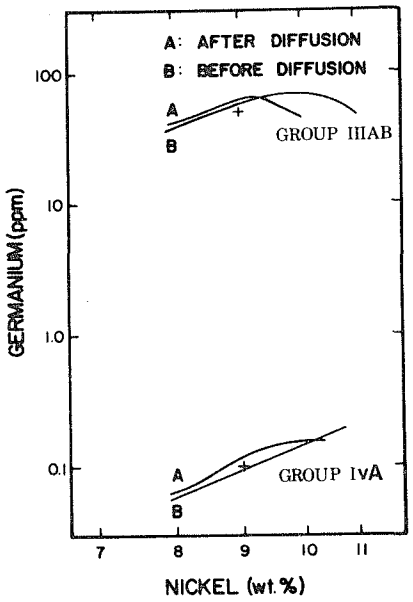

Fig. 2

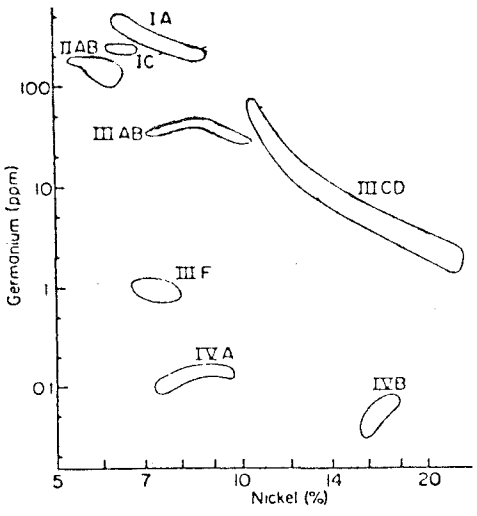

Fig. 3

ORIGIN OF IRON METEORITE GROUPS IAB AND IIICD

Wasson, J.T., Willis, J., Wai, C.M.[+], and Kracher, A.[≠]
Institute of Geophysics and Planetary Physics, University of California, Los Angeles, CA 90024

Several low-Ni iron meteorites previously assigned to group IAB have been reclassified IIICD. The resulting fractionation patterns in the two groups are similar. It is generally agreed that the fractionation patterns in the metal and the presence of chondritic silicates indicate that IAB and IIICD did not form by fractional crystallization of a metallic magma. Other models have been proposed, but all have serious flaws. We offer a new model involving the formation of each iron in a pool of impact melt on a chondritic parent body consisting of material similar to the chondritic inclusions, but initially unequilibrated. These impact melts ranged in temperatures from ∿1190 K to ∿1350 K. The degree of equilibration between melt and unmelted solids ranged from minimal at the lowest temperature to moderate at the highest temperature. The lowest temperature melts, produced by melting Ni-rich sulfides and metal in the unequilibrated chondritic parent, were near the cotectic in the Fe-Ni-S system and had Ni contents of ∿12 atom %. Upon cooling, these precipitated metal having ∿600 mg/g Ni (i.e., as in Oktibbeha County) by equilibrium crystallization. Low-Ni irons formed in high temperature melts having compositions near the FeS-Fe eutectic or somewhat more metal rich. We suggest that the decreasing Ge, Ga and refractory abundances with increasing Ni concentration reflect the trapping of these elements in oxide phases in the unequilibrated chondritic material, and that very little entered the Ni-rich melt parental to the Oktibbeha County iron. The remaining elements tended to have element/Ni ratios in the melts that were more or less independent of temperature. Niemeyer discovered a remarkable inverse correlation between I-Xe age of the chondritic inclusions and Ni content of the host metal, which can be understood in terms of our model by considering the detailed evolution of the (mega)-regolith in which these groups originated. The most Ni-rich melts could only be generated from an unequilibrated chondrite parent; as the continuing deposition of impact energy produced increasingly higher grades of metamorphism, the maximum Ni contents of the impact melts (and their subsequently precipiated metal) gradually decreased. Thus high Ni contents can only be found in irons produced during early impacts. Although the converse is not true, the mean ages of low-Ni irons should be substantially younger than those of high-Ni irons.

+ present address: Department of Chemistry, University of Idaho, Moscow, ID 83843 USA
≠ present address: Mineralogische Abteilung, Naturhistorisches Museum, A-1014, Wien, Austria

#26

MULTIVARIATE SYSTEMATICS OF IRON METEORITE PHYSICO-CHEMISTRY

Höskuldsson, A., Wold, S.[1] & Esbensen, K.[2]
Technical University of Denmark, DK-2800 Lyngby, Denmark

Using the "IRON METEORITE DATA BASE", Esbensen & Buchwald (1979) we have carried out a multivariate study of the systematics of iron meteorites using a factor analytical approach. Incorporation of missing values presents problems specific to the available data matrix. The largest consistent subset of data with no missing values has been treated by Sears (1979) who analyzed 37 (66) meteorites for 16 (13) chemical elements primarily interested in information regarding the processing of the total iron meteorite population. This represent a modest information retrieval relative to the "IRON METEORITE DATA BASE" (532 objects/35 physical and chemical variables). Using a multiple regression approach as well as multivariate linear models (principal components) we estimate missing values for each individual major iron meteorite group (IAB, IIAB, IIIAB (IIIA, IIIB), IVA and IVB) totalling 355 objects; in this way we are able to utilize a significantly higher fraction of the total information present.

We present the resultant systematics of iron meteorite physico-chemistry, e.g., a 14 variable comparable synopsis of these major groups viz. detailed analysis of group IIIA including the newest data available. Using pattern recognition techniques (SIMCA), Wold (1976) we are able to divide group IAB into two compositionally defined subgroups matching cosmic-age subgroups as defined by Voshage & Feldmann (1979). We also present tentative compositional subdivision of group IVA partly substantiating earlier indications of Wood (1978) based primarily on cooling rate considerations; we cannot substantiate an analogous proposal for group IIIA, however.

1) Research group for Chemometrics. Institute of Chemistry, University of Umeaa, S-90187, Sweden.
2) Presently at Institute of Geophysics and Planetary Physics, University of California, Los Angeles, CA 90024 USA

Esbensen, K.H. & V.F. Buchwald (1979): Meteoritics, 14, 2. p.573-576.
Sears, D.W. (1979): Meteoritics, 14, 3. p. 297-306.
Voshage, H. & H. Feldmann (1979): EPSL,
Wold, S. (1976): Pattern Recognition, 8, p. 127-139.
Wood, J.A. (1978): NASA Conference Pub. 2053, Morrison and Wells (Eds.) p. 45-56.

MICROPROBE INVESTIGATION OF THE SANTA CATHARINA METEORITE

Schorscher, H.D. and Wiedemann, C.M.
Instituto de Geociências, UFRJ, Rio de Janeiro, Brasil
Danon, J., Scorzelli, R.B. and Azevedo, I.S.
Centro Brasileiro de Pesquisas Físicas, Rio de Janeiro, Brasil

Two different Fe-Ni phases are the main constituents of the Santa Catharina meteorite. A darker coloured Ni-rich phase is present 35-42% by vol. and the Fe-richer, brighter coloured phase 63-56%. Schreibersite, troilite and fracture fillings are minor constituents. The two Fe-Ni phases form domains of oriented overgrowths, (100) and (111) being predominant. Both phases are inhomogeneous; the Ni-poorer one showed variations of 26-31% Ni and 74-69% Fe (by weight) with Co < 1%. No oxigen was detected in this phase. The Ni-rich is present as an ordered superstructure (Llo) as demonstrated by Mössbauer spectroscopy and X-ray diffraction (Danon, J., Scorzelli, R.B., Souza Azevedo, I.,Laugier, J., Chamberod, A., Nature 284, 537-538 (1980)). The microchemical composition shows Ni values of 51.3 - 48.6% (average - 50.1% Ni) and Fe of 48.9 - 46.7% (average 47.5% Fe). O, S and Co are present as minor elements totalling up to 2.5% by weight. S and O show synchronous variations in zoned individuals and are believed to belong to the early cosmic history of the meteorite. Much higher oxigen contents occur along cracks as a consequence of weathering. In this conditions the S-contents drop sharply.

#28

ANALYTICAL ELECTRON MICROSCOPE STUDY OF FOUR ATAXITES

Novotny, P. M., Goldstein, J. I. and Williams, D. B.
Dept. of Metallurgy & Materials Engrg., Lehigh University, Bethlehem, PA 18015

A Philips EM400T Analytical TEM/STEM was used to obtain x-ray and microstructural data from the plessite structure in the ataxites Arltunga, Nordheim, Tawallah Valley and Hoba. Examination of Arltunga and Nordheim disclosed that each meteorite had a plessite structure which was a result of the Widmanstatten transformation $\gamma \rightarrow \alpha + \gamma$. STEM x-ray microanalysis revealed that the thin (~ 1 μm) taenite in each meteorite had composition profiles indicative of fast cooling ($> 500^{\circ}C/10^{6}$ yrs.). A typical STEM profile from an $\alpha/\gamma/\alpha$ region in Arltunga is shown in Fig. 1. The center of the γ phase has a Ni content less than 25% Ni and has transformed to martensite (M). Martensite has formed within most of the taenite in Arltunga and Nordheim. The highest Ni content found in the taenite at the α/γ boundary was 43.5% in Arltunga and 45.6% in Nordheim.

SEM and TEM examination of Tawallah Valley and Hoba indicated that the microstructure was predominantly plessite which had formed by the reaction $\gamma \rightarrow \alpha_2 \rightarrow \alpha + \gamma$ where α_2 (martensite, M) decomposes to $\alpha + \gamma$. A few Widmanstatten α platelets formed by the reaction $\gamma \rightarrow \alpha + \gamma$ were also present. A STEM profile across a Widmanstatten α platelet into the γ taenite region in Tawallah Valley is shown in Fig. 2. Duplex $\alpha + \gamma$ regions containing decomposed α_2 in Tawallah Valley and Hoba were also examined by STEM x-ray microanalyses. The highest Ni content found in the taenite at the α/γ boundary was 50.9% in Hoba and 51.7% Ni in Tawallah Valley.

Electron and light optical examination of the four ataxites failed to reveal the presence of ordered taenite or cloudy zone in any of the meteorites. The lack of cloudy zone could indicate that the meteorites had been reheated or that a critical cooling rate is necessary for the formation of cloudy zone.

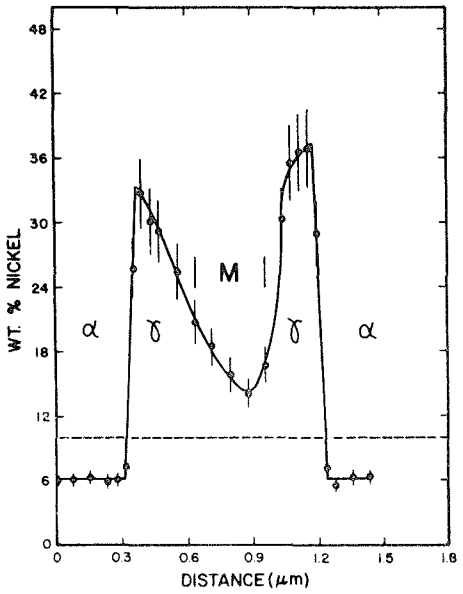

Figure 1 - Arltunga

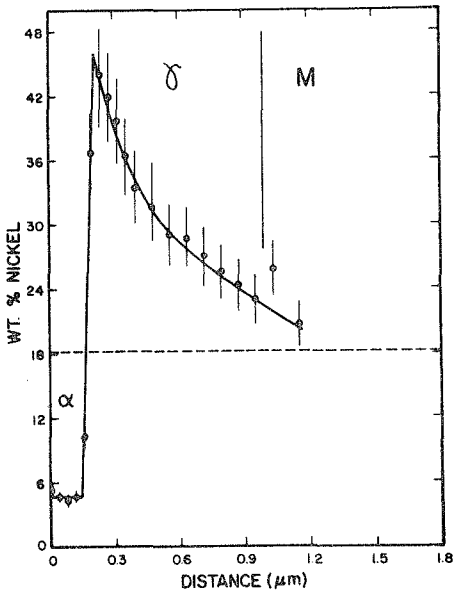

Figure 2 - Tawallah Valley

THE IRON METEORITES JERSLEV,PUERTA DE ARAUCO AND WINBURG

Vagn Fabritius Buchwald
Dept. of Metallurgy,Technical University,2800 Lyngby, Danmark.

Jerslev is a 41 kg iron meteorite, found in 1977 on the island of Sjælland, 80 km West of Copenhagen. It is a coarsest octahedrite, Ogg, of group II B, related to Sikhote-Alin and Old Woman.

Puerta de Arauco is a 1.5 kg iron meteorite, found in 1904 in a pass crossing the Andes Mountains; it is now in the La Plata Museum, Argentina. It is a fine octahedrite, Of, probably of group IV A, related to Duchesne and Chinautla. It is pear-shaped, and the well-preserved specimen exhibits steep temperature gradients from the atmospheric flight.

Winburg was found in South Africa about 100 years ago, but is practically undescribed. The main mass of about 40 kg is presently in the National Museum, Bloemfontein. It is an anomalous octahedrite with ill-defined Widmanstätten structure, and it is not a member of the resolved chemical groups.

The meteorites have been examined by classical metallography, microprobe work, microhardness testing and, to a limited extent, by transmission electron microscopy, and some of the more interesting results will be reported.

#30

ANTARCTIC IRON METEORITES FROM ALLAN HILLS AND PURGATORY PEAK

Clarke, R. S., Jr.,* J. I. Goldstein,** E. Jarosewich,* and J. W. Morgan***
*Department of Mineral Sciences, Smithsonian Institution, Washington, D.C. 20560. **Department of Metallurgy and Materials Engineering, Lehigh University, Bethlehem, PA 18015. ***U.S. Geological Survey, Reston, VA 22092

Eight iron meteorites have been recovered by joint US-Japanese expeditions in the Allan Hills, Antarctica, during the 1976 through 1978 field seasons. A separate geologic party found the Purgatory Peak iron in the Victoria Valley during the 1977 season. Only ALHA 76002 has been previously studied. It has been classified as a coarsest octahedrite or group IIAB meteorite on the basis of its structure and bulk composition, and as a group IA iron on the basis of its trace element chemistry (Olsen et al. 1978).

Macroetched surfaces have been prepared for the specimens recovered during the 1977 and 1978 seasons. The assignment of tentative classifications based solely on visual inspection of these surfaces has been possible for all but one of the meteorites. The following specimens are all coarse octahedrites of chemical group IA: PGPA 77006, ALHA 77250, -77263, -77283, -77289, and -77290. ALHA 78252 is a medium octahedrite apparently of chemical group IIIA. ALHA 77255 is a fine structured meteorite containing a spherical silicate(?) inclusion. It requires further study before classification.

Specimen ALHA 77283 is of particular interest. It is the only obviously carbon-rich specimen among the coarse octahedrites. Behavior while being cut on the saw combined with the presence of small black knobby protrusions in carbon-rich areas indicates that this is a diamond bearing meteorite similar to Canyon Diablo. This appears to be the first evidence for a meteorite fall of crater forming intensity in Antarctica.

Detailed bulk chemical, trace element, electron microprobe, and metallographic analyses are in progress for all nine of these specimens. A summary of the results of these studies will be presented.

Olsen, E. J., A. Noonan, K. Fredriksson, E. Jarosewich, and G. Moreland. Meteoritics 13, 209-225 (1978).

DETAILED CHEMICAL INVESTIGATION OF SECTIONS THROUGH A LARGE CAPE YORK IRON

Esbensen, K.H.[1], Wasson, J.T. and Buchwald, V.F.[2]
Institute of Geophysics and Planetary Physics, University of California, Los Angeles, CA 90024 USA

Cape York is probably the largest iron meteorite and belongs to the largest group (IIIA). The elemental fractionations in group IIIAB are widely held to indicate formation by fractional crystallization. Large sulfide nodules in Cape York are prolately ellipsoidal and oriented with their long axes parallel (Y-Y' axis in Fig.). Metallurgical experience indicates that these axes parallel the growth direction during solidification; the troilite nodules may be interdendritic melt residues. We are studying by neutron activation 12 samples along a 170 cm section of a single taenite crystal (the Agpalilik mass) parallel to the troilite long axes and another 18 samples along perpendicular sections. Our precision should allow us to detect systematic variations in Ga, As, Ir and Au as small as 4% or less. Resolvable fractionation trends will have important implications regarding fractional crystallization and/or fractionation during solid-state growth of large taenite grains. The sampling of Agpalilik will allow a hitherto unmatched characterization of the chemical variability of a single-crystal meteorite and will provide a reference study as to the representativeness of analysis-sampling of iron meteorites.

1 Presently at Institute of Geophysics and Planetary Physics, University of California, Los Angeles, CA 90024
2 Technical University of Denmark, DK-2800 Lyngby, Denmark

Full slice of the Cape York iron meteorite (Agpalilik mass).

12 samples along Y-Y'.
13+3 samples along Z-Z'.
2 samples along O-X.

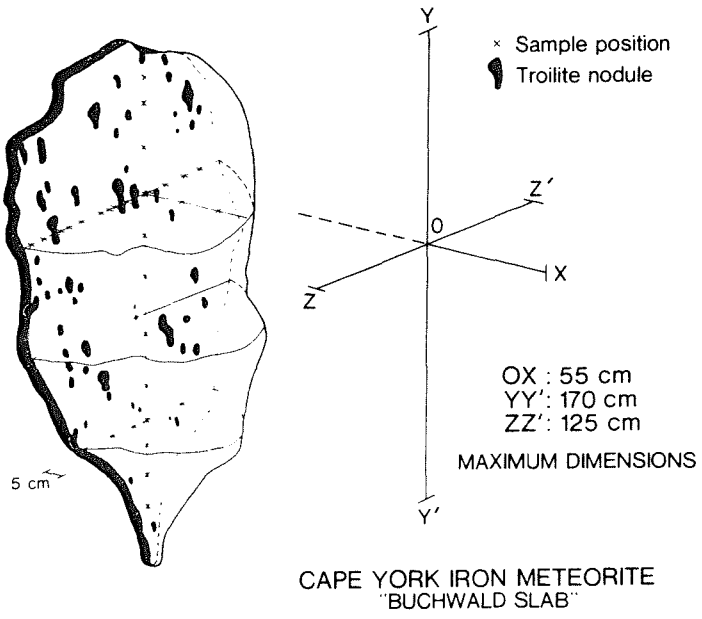

CAPE YORK IRON METEORITE
"BUCHWALD SLAB"

#32

TRACE ELEMENT ABUNDANCES IN ULTRA-REFRACTORY CONDENSATES FROM THE MURCHISON METEORITE

Boynton, W. V., Frazier, R. M., Department of Planetary Sciences and Lunar and Planetary Laboratory, University of Arizona, Tucson, Az 85721, and Macdougall, J. D., Scripps Institute of Oceanography, La Jolla, Ca 92093

Several hibonite, spinel-bearing inclusions in the Murchison meteorite have been analyzed for trace element abundances by neutron activation analysis. The inclusions have abundances of highly refractory trace elements on the order of 100 times chondrites, suggesting that they may be the highest temperature nebular condensates yet found. In fact, one of the inclusions, MH-115, has a rare-earth element (REE) pattern essentially identical to that predicted for the earliest REE containing condensate (1). The enrichment of the REE ranges from about 4 times chondrites (4x) for the most volatile REE, Eu and Yb, to about 100x for the most refractory REE, Dy, Ho and Lu. This REE pattern is complementary to the group II REE patterns observed in the Allende Ca, Al-rich inclusions which are deficient in highly refractory trace elements. It appears, however, that the Murchison inclusions are not precisely complementary to the group II Allende inclusions. The Allende inclusions are deficient in Hf, suggesting Hf is a highly refractory trace element. The Murchison inclusion MH-115, however, is not highly enriched in Hf as expected for the complementary material. The large amounts of Sc and Ir make determination of Hf in the small sample (~1μg) by INAA rather difficult, so this result must be regarded as tentative. If real, the result may indicate a difference in conditions between the Murchison inclusion and the Allende inclusion formation zones. For example, if the oxygen fugacity in the two zones were different, the volatility of Hf would change relative to the REE.

It is hoped that these inclusions will significantly increase our understanding of early chemical processes that may have occurred in the nebula. The group II inclusions in Allende provided much information about refractory element fractionation processes. Unfortunately, the trace element pattern in the group II inclusions is determined, not so much by the properties of the inclusion itself, but by the properties of the hypothetical earlier condensate which removed the missing refractory REE. Now, however, we have a sample of this earlier condensate and can determine which phase or phases contain the REE. If the phases did not form simultaneously, the REE patterns in separated phases should permit the determination of the order in which the phases condensed.

References

1. Boynton, W. V. Geochim. Cosmochim. Acta 39, 569 (1975).

SPINEL-PYROXENE AGGREGATES IN MURCHISON

Bar Matthews, M., MacPherson, G.J., Grossman, L. and Tanaka, T.
University of Chicago, Chicago, IL 60637

Spinel-pyroxene aggregates were discovered in the Murchison C2 chondrite by Fuchs *et al.* (1). Here we present petrographic and mineralogical data from a large number of these inclusions collected by freeze-thaw disaggregation and heavy liquid separation. These objects have a botryoidal to irregular external morphology, are creamy-white and have a sugary-textured outer surface. Two textural variants have been observed, distinguished by their internal structures: nodular and banded. The nodular variety consists of several clumps of Fe-free spinel grains, each mantled by Fe-free clinopyroxene that grades outward from fassaite (15-22% Al_2O_3, 5-10% TiO_2) near the spinel to diopside ($Al_2O_3 \leq 2.5\%$). Also present in these mantles are minor amounts of a greenish Fe-bearing silicate phase whose composition is similar to the "spinach" phase of Fuchs *et al.* (1) and occasional troilite. The group of spinel-pyroxene clumps in each inclusion is rimmed as a whole by Fe-free forsterite grains (<1 to 10μm) and, on the outermost part of the rim, by much rarer grains of Fe-free aluminous enstatite (Al_2O_3 1-1.5%; grain size <1 to 10μm). Perovskite and rare noble-metal nuggets can be present, usually as inclusions within spinel or fassaite. Melilite and hibonite have not been found. The banded variety of these inclusions contains the same phases as above, but spinel forms folded sheets that are mantled on both sides by fassaitic to diopsidic pyroxene. Cavities are common in both varieties, and, in the banded type, the sheets wrap around them. This suggests that either the cavities are real or that they were originally filled by some unknown material that has been completely removed during thin section preparation. No alkali- or halogen-bearing phases have been found in either variety of inclusions.

We propose that the perovskite and spinel condensed from the solar nebular gas at high temperature. Apparently, some of the spinels had grown or accreted into sheet-like bodies while others had formed more nearly spherical ones prior to condensation of their mantling clinopyroxenes. Accretion of the spherical bodies into the observed botryoidal objects was followed by condensation of forsterite and then enstatite at temperatures still high enough to prevent FeO from entering their structures. In fact, the absence of FeO from these outermost rim phases argues against *in situ* low-temperature alteration of the materials in C2 chondrites.

No counterpart to this type of inclusion has yet been found in the Allende C3 chondrite. These objects do bear a striking resemblance, however, to some of the micrometeorites recovered from deep sea sediments by Brownlee *et al.* (2). This similarity lends additional support to the idea that the micrometeorite population contains particles that were derived from the same source as inclusions in C2 chondrites.

(1) Fuchs, L.H., Olsen, E. and Jensen, K.J. (1973) *Smithson. Contrib. Earth Sci.* 10.
(2) Brownlee, D.E., Bates, B.A., Pilachowski, L.B., Olszewski, E. and Siegmund, W.A. (1980) *Lunar Planet. Sci. XI*, pp. 109-111.

#34

VARIATION OF FISSION TRACKS ON THE SURFACES OF OLIVINES FROM MURCHISON: TIME DIFFERENCES OR HETEROGENEITY OF ^{244}Pu ON A MICROSCALE?

R.S. Rajan, T.R. Watters and B.K. Kothari
Department of Terrestrial Magnetism, Carnegie Institution of Washington, 5241 Broad Branch Road, N.W. Washington, D.C. 20015

In a recent study, Macdougall and Kothari (1976) found evidence for ^{244}Pu fission tracks on the surfaces of olivine crystals. They interpreted the mean of the observed track densities as compaction ages, assuming a mean $(\frac{Pu}{U})_o$ ratio = 0.015. It is the purpose of the present work to understand the huge scatter in the observed fission track densities within a single meteorite, and what the deduced 'compaction ages' really mean. We have studied about 200 crystals from gently disaggregated Murchison samples for both surface tracks and side tracks.

Our surface track density measurements on 31 crystals show a range from $1.4 \cdot 10^4/cm^2$ to $1 \cdot 10^6/cm^2$ with a mean of $\sim 1 \cdot 10^5/cm^2$. The side tracks are observed only up to a distance of R($\sim$9 microns), where R is half the mean range of fission tracks due to ^{244}Pu spontaneous fission. It is interesting to note that side track measurements of comparable quality were possible on 67 crystals (about twice as many) and are reported here. The track densities derived from side tracks range from $2.2 \cdot 10^4/cm^2$ to $1.2 \cdot 10^6/cm^2$, and have a mean of $3.4 \cdot 10^5/cm^2$, corresponding to $\rho_{Pu}/\rho_u = 22$. By studying the side tracks on different sides of a single crystal, we have established that the fission track densities vary by up to a factor of 20 on the different sides of a single crystal. In fact, of the fourteen crystals which had observable tracks on 3 sides or more, six had side track densities that varied by at least a factor of ten.

There are three possible explanations for our results that need to be considered: i) It is possible that C_U (and by inference C_{Pu}) varies by as much as a factor of ten or more, on a ten micron scale. Very high fluence neutron irradiations ($\sim 5 \cdot 10^{18} n/cm^2$) are needed to check this point. ii) It is unlikely that geometric factors relating to the contact of the matrix and olivine can produce such large variations, though it cannot be rigorously excluded. Again, study of the olivine crystals themselves, after the high irradiation mentioned above, will resolve this problem. iii) If uranium is indeed homogeneous, then the typical variation of track densities on single crystal surfaces from $\sim 5 \cdot 10^5/cm^2$ to $5 \cdot 10^4/cm^2$ (which correspond to ρ_{Pu}/ρ_u = 34 and 2.7 resp.) must refer to actual time differences of up to $\sim$270 Myr. Using the nominal $(Pu/U)_o = 0.015$, our results suggest that some of the matrix material that was in contact with the olivine was as old as 4.55 Gyr, while some other matrix material came into contact with the same crystal as much as 270 Myr later.

The present data strongly support the possibility that bulk of the olivines were previously part of inclusions or aggregates which were subsequently broken. Studies on selected euhedral olivines are in progress, to better understand their origin.

Ref: Macdougall, J.D. and B.K. Kothari, EPSL, 33, 36 (1976).

HIGH RESOLUTION ION MICROPROBE ISOTOPIC DETERMINATIONS IN PRIMITIVE METEORITES

Lorin[+], J.C., Havette[++], A. and Slodzian[+++], G.
+ Laboratoire de Minéralogie-Cristallographie. Université Paris VI. Paris.
++ Laboratoire de Pétrographie-Volcanologie. Université Paris-Sud. Orsay.
+++ Laboratoire de Physique des Solides. Université Paris-Sud. Orsay.

The feasibility of making successful isotopic determinations in secondary ion mass spectrometry critically depends upon the ability to resolve or reduce interferences due to molecular or multicharged ions without incurring drastic losses in sensitivity. Since energy spectra of polyatomic ions are generally narrower than the atomic ion spectra, discrimination in favour of high energy secondary ions has been used as a means to suppress interfering ion species. The fact that this procedure has no effect on certain types of interferences, such as those caused by hydrides, consitutes a major stumbling block to its actual applicability, not to mention the fact that this method also entails a dramatic drop in sensitivity. Therefore, a procedure of isotope determination at high mass resolutions (up to 5000) has been developped (to be published elsewhere), which takes advantage of the fact that the *transfer optics* (Slodzian and Figueras, 1977) makes it possible to achieve high mass resolutions without prohibitive losses in sensitivity. This procedure has been successfully tested on a number of elements (Li, K, Mg, Si, Ca, Ti, Zr, U) and in a variety of matrices (silicates, oxides). Coupled with the quantitative elemental analysis developped by Havette and Slodzian (1980) it allows, in the course of the same run, to establish a direct correlation of the isotopic data with the compositionnal data on spot samples, typically 20 µm in diameter.

Application of this procedure of isotope measurement to the problem of the 26-Al distribution in the early solar system is presently in progress. Large variations in initial 26-Al abundances are observed among different types of objects. $(26\text{-Al}/27\text{-Al})_i$ in Leoville L1 (type B) inclusion is found to be $5\pm1\times10^{-5}$, undistinguishable from that observed in Allende WA inclusion by Lee et al. (1977). On the other hand, a markedly lower abundance, $<2\times10^{-5}$, is observed in Allende ophitic inclusion IAM2, which singles it out as a possible candidate to FUN type anomalies, although there is no evidence, at least in the feldspar phase, of mass-dependent fractionation larger than 1% per m.u. in the isotopes of Mg and Si. Silicon has, within ±1%, a normal isotopic composition also in L1. No 26-Al effects have been detected so far in the Mezo-Madaras unequilibrated chondrite. An aluminum-rich glassy chondrule of this meteorite, described by Kurat (1967), shows normal, within error limits, magnesium composition, thereby setting an upper limit of 1.4×10^{-5} to the initial (26-Al/27-Al) ratio in this object. If we believe that 26-Al was evenly distributed throughout the primitive solar nebula, the latter observation implies that more than one million years after condensation of Allende WA and Leoville L1 refractory inclusions chondrule formation was still an on-going process in the early solar system.

Havette, A. and Slodzian, 1980, *J. Physique* 41, L427.
Kurat, G., 1967, *Geochim. Cosmochim. Acta* 31, 1843.
Lee, T., D. Papanastassiou and G.J. Wasserburg, 1977, *Astrophys. J.* 211, L107.
Slodzian, G. and A. Figueras, in *Proc. 8° Int. Conf. X Ray Optics and Micro-Analysis*, 1977.

#36

Ti ISOTOPE ANOMALIES IN AN "UN-FUN" ALLENDE INCLUSION.

S. Niemeyer and G. W. Lugmair
Chemistry Department, B-017, University of California, San Diego
La Jolla, California 92093

We report the first results in our study of titanium isotopic compositions which we initiated about one year ago. Titanium was of interest because it is an iron-group element, a group for which little isotopic work had been reported previously, and in addition Ti's status as a major element, especially in the refractory-rich Allende inclusions, facilitates comparison among different mineral phases. Although further refinements of our experimental procedures are still being carried out, we have obtained reliable data for several terrestrial rocks and meteorite samples. Currently, the total procedural blank is about 10^{-8}g and the chemical separation and loading technique yield a stable TiO^+ signal. No corrections for isobaric interferences are required. Isotopic compositions of Ti from rock samples are compared to the grand average of individual analyses of our terrestrial standard made up from high purity (99.96%) Ti metal. Ti isotopic compositions determined for several terrestrial basaltic rocks are all indistinguishable from the terrestrial standard within experimental uncertainties which are on the order of 2×10^{-4} ($2\sigma_{mean}$).

We then analyzed Ti separated from a coarse-grained Allende inclusion. This sample (CW2) consists of 70-80% melilite, 5-10% pyroxene, 5-10% spinel, 1-3% anorthite and traces of awaruite(Ni_3Fe) and hibonite (W. L. Mansker, priv. comm.). Mineral separates have been prepared and an extensive Sm-Nd study of these samples yielded a well-defined internal isochron corresponding to an age of 4.51 $\pm$ 0.06 AE. (1). All non-radiogenic isotopes of Sm and Nd were found to be normal, indicating that this inclusion does not belong to the "FUN" family. However, the results for Ti show a clear excess of 1.1 $\pm$ 0.3‰ at mass 50 for the bulk sample with all other isotopes normal within uncertainties. Ti from a pyroxene separate shows an excess at mass 50 slightly, but not significantly, lower than the bulk rock. Work on other mineral separates is in progress in order to test whether isotopic equilibrium exists between different phases.

Niederer et al. (2) have clearly demonstrated the existence of large Ti isotopic anomalies in FUN inclusions such as EK-1-4-1. However, as mentioned above, the normal Nd and Sm in CW2 indicates it does not belong to the FUN family. Thus the clear evidence for a Ti isotopic anomaly in CW2 suggests that Ti anomalies may be more widespread, or more easily observable, than for many other elements previously studied in Allende inclusions.

(1) Scheinin N. B. and Lugmair G. W., Unpublished results.

(2) Niederer F. R., Papanastassiou D. A. and Wasserburg G. J. (1980), Lunar and Planet. Science XI, 809.

TITANIUM ISOTOPE ANOMALIES IN ALLENDE INCLUSIONS

Niederer, F. R., D. A. Papanastassiou, and G. J. Wasserburg, The Lunatic Asylum, Div. of Geological and Planetary Sciences, Caltech, Pasadena, CA 91125

We report on Ti isotope abundances in Ca-Al-rich inclusions from Allende. Data are obtained using a TiO^+ beam. The data on oxides of isotopes 46-49 are insensitive to the correction for isobaric interferences among the TiO^+ species. We have ascertained that the ^{50}Ti data which are sensitive to $^{18}O/^{16}O$ show no complexities due to independent oxygen fractionation. FUN samples EK-1-4-1 and C-1 were shown to have large effects for all Ti isotopes not used for normalization for mass fractionation (Niederer, Papanastassiou, and Wasserburg, 1980a,b). These results are confirmed here with new analyses. The Ti effects for the FUN samples correlate directly with Ca effects (Lee, Papanastassiou, and Wasserburg, 1978). The extension of these measurements to many common, coarse-grained inclusions and to fine-grained aggregates has been carried out (see Table). The results show the presence of smaller but distinct anomalies in all samples investigated for all Ti isotopes not used for normalization. Isotope anomalies for Ti are common in Ca-Al rich inclusions in Allende and are present in samples which show no nuclear isotope effects for Ca or other refractory elements. The Ti data require the presence of at least three distinct nucleosynthetic components, represented one each by EK-1-4-1 and C-1 and the third by deficits in ^{47}Ti and ^{49}Ti and excess ^{50}Ti. The deficits in ^{47}Ti and ^{49}Ti appear to scale only approximately, so that four independent components may be present. Based on normalization to $^{46}Ti/^{48}Ti$, the Ti isotope patterns include: a) excess in ^{47}Ti, ^{49}Ti, and ^{50}Ti; b) excess in ^{47}Ti, coupled with deficits in ^{49}Ti and ^{50}Ti; c) deficits in ^{47}Ti and ^{49}Ti, in variable ratio, coupled with ^{50}Ti excesses. The endemic isotopic anomalies in Ti are in marked contrast to rare effects in the neighboring Ca. It is especially noteworthy that ^{46}Ca does not show any anomalies at the level of 1% despite its very low abundance which results in high sensitivity for the detection of addition at this species. The absence of effects at ^{46}Ca and the presence of a variety of effects at ^{47}Ti, ^{48}Ca, ^{49}Ti, and ^{50}Ti strongly indicate a blend of quasi-equilibrium nuclear processes near the Fe peak.

Titanium Isotope Abundances in Allende[a]

Sample	ε (47,48)	ε (49/48)	ε (50,48)
FUN Inclusions			
EK-1-4-1	12.7±1.6[b]	18.8±2.2	36.9±2.4
	12.6±0.9[c]	16.8±1.9	37.8±1.6
C-1	5.2±0.8[b]	-7.0±1.0	-51.2±1.1
	6.0±2.0[c]	-8.4±3.0	-53.2±3.0
Egg-3	-3.5±0.8[b]	-5.8±0.8	6.7±1.0
Coarse-Grained Inclusions			
Egg-1	-2.9±0.9[b]	-4.6±1.2	6.4±0.9
	-2.2±1.9[d]	-3.6±2.0	7.0±2.0
Egg-4	0.4±2.0	0.2±2.0	9.1±2.8
	-1.3±0.8[d]	-1.2±0.9	9.0±0.9
Egg-6	-1.0±0.7	-4.7±1.1	4.2±1.2
D-7 pyx[e]	-2.2±1.1	-2.9±1.3	11.4±2.0
WA pyx	0.0±0.9	-4.7±2.9	-2.2±1.9
Fine-Grained Aggregates			
B-30[e]	-0.5±0.9	-2.6±1.6	7.2±1.6
B-29[e]	-0.5±2.0	-3.3±2.0	5.0±2.3
B-32[e]	-0.3±1.2	-1.7±1.2	8.4±2.1

Ref.:Gray,Papanastassiou & Wasserburg,Icarus 20 (1973)213;Lee,Papanastassiou & Wasserburg,Ap.J. Lett.211(1977)L107; Niederer,Papanastassiou & Wasserburg,LPS XI(1980a) 809;Ap.J.Lett.(1980b) in press.Cont.No.3468(360).

[a] $\varepsilon(i,j)=[(^iTi/^jTi)_{CORR}/(^iTi/^jTi)_N-1]\times10^4$; N=normal;CORR=measured ratio (M) corrected to a standard state for an effective fractionation α from $(^{46}Ti/^{48}Ti)_M/(^{46}Ti/^{48}Ti)_N=(1+\alpha)^2$.Errors are $2\sigma_m$.

[b] Mean from NPW (1980b).

[c] New dissolution.

[d] Repeat analysis.

[e] Described by by Gray et al.(1973).

#38

A SINUOUS INCLUSION FROM ALLENDE: TRACE ELEMENT ANALYSIS OF A RIM

Davis, A.M., Allen, J.M.*, Tanaka, T., Grossman, L. and MacPherson, G.J.
University of Chicago, Chicago, Illinois 60637, U.S.A.
*University of Toronto, Toronto, Ontario, Canada M5S 1A1

Wark and Lovering (1) published the first detailed description of narrow, multi-layered rims that surround most coarse-grained Allende inclusions. They also found fine-grained inclusions to be aggregates of tiny spheres, each of which has the same sequence of layers as the rims. Those interested in the chemistry of primitive objects in carbonaceous chondrites have dreamed of extracting rim material from a coarse-grained inclusion for trace element analysis, but sampling techniques have not yet achieved the required sophistication. We describe here a sample of rim that nature has "extracted" for us.

It was the shape of this so-called sinuous inclusion on two facing slabs of Allende that first attracted our attention. A thin section was prepared from the portion of the inclusion in one slab and a sample was extracted with a tungsten needle from the other slab for trace element analysis. The inclusion consists of a ribbon of spinel within whose center is a chain of perovskites and on either side of which is a sequence of mineralogically distinct layers. On one side is a sequence identical to that around Type A inclusions: AI, a zone 18-30μm thick with voids and fine-grained anorthite, nepheline and an unknown Ca-Al-silicate; AII, a zone 4-18μm thick of diopside, with 5% Al_2O_3 and 1% TiO_2 where it abuts AI and decreasing amounts of these elements outwards; and AIII, a zone 0-15μm thick of pure hedenbergite outside of which are porous masses of andradite, nepheline and diopsidic to hedenbergitic pyroxene. On the other side of the spinel ribbon is a single layer that bears a resemblance to rims found around Type B inclusions. It consists of porous nepheline and sodalite within which are embedded clinopyroxene and olivine.

Two samples were taken for chemical analysis by INAA: a bulk sample (#1) and dark grains from an aliquot of the bulk (#2). The major element composition of the sinuous inclusion resembles that of fine-grained Group II inclusions, except that it has a higher TiO_2 content, like that of coarse-grained Groups I and II inclusions. This is in accord with the small amount of perovskite in fine-grained inclusions and the prominent perovskite chain in the sinuous inclusion. The samples have typical Group II REE patterns and, when modelled according to Davis and Grossman (2), give perovskite removal temperatures of 1670.3 and 1670.6 K. These temperatures are at the low end of the range for fine-grained inclusions. Sample #1 contains a larger amount of the component with the flat REE pattern than sample #2. The sinuous inclusion differs from fine-grained inclusions in its relatively high refractory siderophile content, ~2 times Cl chondrite levels. All volatile elements determined in the sinuous inclusion fall within the concentration ranges for fine-grained inclusions.

If it is assumed on the basis of mineralogy and texture that the sinuous inclusion is indeed a rim, then rims must have Group II REE patterns. Since rims have different REE patterns from interiors of coarse-grained inclusions, the former did not form by simple reaction of volatiles with the latter. Furthermore, because the interiors do not have a complementary pattern to that of rims, the rims did not condense from the gas remaining after formation of the interiors. Rather, our work indicates that rims formed by introduction of volatiles *and* refractories from a reservoir that was chemically distinct from that which gave rise to the interiors.

(1) Wark, D.A. and Lovering, J.F. (1977) *Proc. Lunar Sci. Conf. 8th*, 95-112.
(2) Davis, A.M. and Grossman, L. (1979) *GCA* 43, 1611-1632.

An Alternative Origin for Allende CAI Inclusion Rims, or a Correlation Between the Early Solar System and a British Steel Furnace

Bunch, T.E. and Chang, S.
NASA-Ames Research Center, Moffett Field, CA 94035

Of the 76 complete and fragmented Type A and B CAI coarse-grained inclusions in Allende that we have examined, all but two show some evidence of deformation or melting. Eight Type A and six Type B inclusions were completely melted. The remaining inclusions show varying proportions of melt zones, mechanically deformed phases, glassy and devitrified veins, recrystallization, solid state transformations (diaplectic) and fine-grained cryptocrystalline zones. Most inclusions possess textures that imply crystallization from liquids, complicated by autometamorphism, partial to complete recrystallizations, and late stage shock effects.

Petrographic and SEM observations of rim-interior interfaces clearly have melt relationships in most cases. Rim hibonite shows acicular, dendritic or spherulitic growth habits in glass or divitrified zones immediately adjacent to the unmelted interiors. These growth habits, particularly in a glass matrix, are consistent with rapid growth (quenching) from a liquid. The globular shape of rim perovskite and anhedral rim spinel also imply rapid crystallization. Rim phases described by Wark and Lovering (1977) could form as melt products or from subsolidus crystallization from melted interior phases. Our microprobe analyses indicate small bulk compositional differences between rims and interiors, with the exceptions of Fe which is increased in the bulk rims by factors of up to 60, and depletion of (Na+K) in the rims by factors typically <6.

Alumina and mullite ($Al_6Si_2O_{13}$) bricks in electric arc steel furnaces breakdown in the hot face surfaces to form dendritic hibonite in glass, anorthite, and hercynite; CaO and FeO are added from furnace slag (Buist 1968). Whereas these refractory bricks are simpler in composition than CAI inclusions, the thermal alteration textures are very similar to CAI rims.

We conclude from the above observations and data, that CAI inclusions crystallized from liquids and were involved in at least one shock episode. A later reheating event partially melted the margins of these inclusions to form devitrified or layered rims. Partial melting of CAI inclusions may have resulted from ablation with an Fe-rich nebular gas cloud or impact-derived dust cloud. All events pre-dated allende matrix implacement.

References: (1) Wark, D.A. and J.F. Lovering, 1977. Proc. Lunar Planet, Sci., Conf. 8th, 95-112. Pergamon. (2) Buist, D.S., 1968. Min. Mag. 36, 676-683.

#40

MAJOR ELEMENT COMPOSITIONS OF COARSE-GRAINED ALLENDE INCLUSIONS

Beckett, J.R., MacPherson, G.J. and Grossman, L.
University of Chicago, Chicago, IL 60637

An accurate knowledge of the pre-alteration major element compositions of coarse-grained inclusions is necessary to answer the following questions: a) Do Type A and Type B inclusions (1) differ in major element composition? b) Do the major element compositions of coarse-grained inclusions plot along or near predicted vapor-solid condensate trajectories? c) In those inclusions interpreted to have been molten, can textural differences be explained by phase relationships on appropriate phase equilibrium diagrams?

Previously published data do not suffice, either because the analysed aliquots are non-representative of inhomogeneous objects, because the compositions include alteration components such as FeO or Na_2O or because modes were visually estimated rather than calculated from point counts. We have calculated the major element compositions of the primary phase assemblages in two fluffy Type A (2), two compact Type A (2), two Type B1 and four Type B2 inclusions by combining detailed point count modes of thin sections of them with electron microprobe analyses of their constituent phases.

Our results from this limited data base suggest that CaO is higher in Type A's than Type B's (33-36% *vs* 18-30%) and MgO and SiO_2 are lower in Type A's than Type B's (3-10% and 20-25% *vs* 8.5-14% and 23-35%, respectively). Type A and Type B inclusions have completely overlapping Al_2O_3 contents. Fluffy Type A's appear to be slightly richer in SiO_2 and poorer in MgO than compact Type A's. Type B1 inclusions are richer in CaO and poorer in MgO than B2's. Fluffy Type A inclusions plot quite close to calculated condensate composition trajectories, while many Type B's are significantly displaced from them, usually having low MgO contents for their CaO contents. On one atmosphere liquidus diagrams for the system $CaO-MgO-Al_2O_3-SiO_2$, Type B1 inclusions plot in the primary phase field for melilite and B2's plot in the primary phase field for spinel. These results are in accord with textural evidence that melilite was the first-crystallizing phase in B1's (2) and spinel the first in B2's.

(1) Grossman, L. (1975) *G.C.A.* 39, 433-454.
(2) MacPherson, G.J. and Grossman, L. (1979) *Meteoritics* 14, 479-480.

A UNIQUE INCLUSION IN ALLENDE: A CONGLOMERATE OF HUNDREDS OF VARIOUS INCLUSIONS AND FRAGMENTS

El Goresy, A.[1], Ramdohr, P.[1], and Nagel, K.[2]
[1]Max-Planck-Institut f.Kernphysik, Heidelberg, F.R. Germany; [2]Institut f. Datenverarbeitung in der Technik, Karlsruhe, F.R. Germany.

The structure of inclusion 10 I/15 became obvious during an inspection of a freshly cut slab from Allende at low magnification. The inclusion (6 mm in diameter) clearly showed distinct zoning features with 1) a dark grey, apparently fine-grained core, surrounded by 2) a light grey thick belt consisting of coarse melilite lathes. A well developed and, in part, convoluting rim separates the melilite-rich belt from the meteorite groundmass.

(1) Core: In reflected light and SEM the apparently opaque fine-grained but friable core was found to consist of hundreds of various ragged fragments several hundred microns in size and spherical inclusions all held together by the surrounding melilite belt. The spaces between the spherical objects and the fragments are filled with non-compacted single idiomorphic crystals of hibonite, melilite, diopside, andradite, sodalite, and metals. At least three distinct types of microclasts and spherical inclusions were encountered: a. very refractory ragged clasts of various shapes and size (100-600 microns) consisting of gehlenitic melilite, hibonite, spinel and perovskite. The texture is indicative of a distinct sequence with perovskite as the earliest mineral. These microclasts display a concentric spiral texture with rhythmic alternating zones of small grains if gehlenite (Geh_{93}-Geh_{100}, average Geh_{96}) and zones of an intimate intergrowth of hibonite+spinel. The hibonite-spinel intergrowth is unique and is indicative if epitaxial overgrowth of hibonite along (111) of the spinel. Compositional characteristics of minerals in these microclasts are consistent from clast to clast: on one hand, the very narrow compositional variation of melilite, on the other hand, the sharp variation of the hibonite chemistry even among lathes enclosed in the same spinel grain. Hibonite compositions vary between 88.2-79.0% Al_2O_3, 8.98-8.01% CaO, 6.88-1.28% TiO_2, 3.63-0.52% MgO, and 3.26-0.21% V_2O_3. The host spinel contains 1.19% V_2O_3, 0.2% TiO_2, and 1.75% FeO. Hibonite and melilite are iron-free. The FeO-content of spinel indicates that oxidizing conditions must have prevailed for some time during the formation of these clasts. b. Spherical objects consisting of gehlenitic melilite (Geh_{96}-Geh_{98}), Ti, Al fassaite (10.8% TiO_2, 19.8% Al_2O_3) perovskite (cores), diopside, and andradite (rims). Single crystals of pure andradite occur on the surface of the spheres. c. Spherical objects consisting of titaniferous Cpx occupying the cores surrounded by diopside, hedenbergite, and at last, pure andradite.

The core contains both fremdlinge and homogeneous Mo-rich Pt metal grains. Fremdlinge consist of Pt metal grains (Os-Ir-Pt-Ru) embedded in molybdenite. Pt metal grains and FeNi alloys occur also in the non-compacted material between the clast along with andradite, sodalite, and hibonite, thus indicating accretion under chemical disequilibrium, presumably at very low temperatures.

(2) Melilite belt: This zone consists almost conclusively of large (up to 1 mm) deformed and heavily shocked melilite crystals (Geh_{94}-Geh_{86}, average Geh_{90}) with very few spinel inclusions. The present investigations indicate that the core assembled together by low temperature accretion of broken fragments of very refractory material along with less refractory and volatile objects, FeNi and Pt metal grains prior to deposition of the refractory melilite belt. In order to preserve the observed features no melting could have taken place during deposition of the melilite belt around the core.

#42

EXPERIMENTAL BOUNDARIES ON THERMAL HISTORY OF REFRACTORY MINERALS IN CARBONACEOUS METEORITES; G. Arrhenius*, C. Raub** and C. Schimmel*;
*Scripps Institution of Oceanography, La Jolla, CA. 92037;
**Forschunginstitut für Edelmetalle und Metallchemie, 707 Schwäbisch Gmünd,FRG

Speculation about the thermal evolution of primordial condensates including "condensation temperatures" has been based on observed phase relationships in meteorites coupled with hypotheses about the thermal state of the source cloud from which the solids formed. Since the outcome of such considerations is critically dependent on assumptions concerning temperature and pressure, and since these are a priori unknown, the conclusions remain hypothetical. Interdiffusion between coexisting solids provides a basis for realistic evaluation of thermal exposure and is particularly sensitive in the temperature region down to about one half of the melting temperature. Simple diffusion couples such as pure platinum in nickel iron, discovered and measured by [1] have been selected by [2] for consideration of thermal exposure during and after formation. This choice avoids the uncertainties associated with the interpretation of more complex platinum metal alloy couples also found in carbonaceous meteorites [3].

The well-known phase relationships and diffusion kinetics in the systems Fe-Pt and Ni-Pt can be applied to the system Pt-($Fe_{0.4}Ni_{0.6}$), observed in carbonaceous meteorites. However [6] has proposed that unknown phases may occur in the ternary system, which would extensively slow down intermetallic diffusion so as to invalidate the conclusions from the experimental data quoted above. Although there is no evident basis for such an assumption, an experimental study was undertaken of the diffusion of Pt into $Fe_{0.4}Ni_{0.6}$ at a series of temperatures, and the diffusion coefficient determined as a function of composition in the diffusion path. The diffusion coefficients thus measured in this ternary system at 1100°K range from $4.6 \cdot 10^{-6}$ cm^2/day at 5% Pt to $7 \cdot 10^{-6}$ at 10% Pt, in concord with earlier published data for the binary system at the same temperature.

Oxide diffusion barriers, which have also been invoked as retardants are thermodynamically excluded in this system at temperatures as high as 1600°K and at the gas compositions generally assumed. Measurement of diffusion of metals through iron oxide films [7] demonstrated them to be ineffective as diffusion barriers at the thickness involved (unobservable by EMX and SEM).

Diffusion measurements in platinum-nickel iron couples overgrown with refractory silicates in carbonaceous meteorites appear at the present time to provide the only existing observational evidence for the actual upper limits of formation temperatures for these refractory minerals. The temperature at growth of the melilite and spinel crystals containing the metal couples could accordingly not have exceeded 1000K; however, the kinetic temperature of the source medium could, in radiation equilibrium with such grains, be an order of magnitude higher [5].

References: [1] El Goresy, Nagel and Ramdohr, (1978) Lunar Planet. Sci. IX, 282; [2] Arrhenius and Raub, (1978) J. Less Common Metals 62, 417; [3] Wark, (1979) Astrophys. Space Sci. 65, 351; Arrhenius, (1978) in Dermott, ed., Origin of the Solar System, Wiley, N. Y.; [4] Grossman, (1972) Geochim. Cosmochim. Acta, 36, 597; [5] De and Arrhenius, (1978) Adv. Colloid Interface Sci., 253; [6] Larimer, (1979) Astrophys. Space Sci. 65, 351; [7] Cabrera, (1980) Thesis, Univ. of Calif., San Diego.

ORDINARY CHONDRITES : THE SPINEL PUZZLE

Kracher, A. and Kurat G.
Mineralogische Abteilung, Naturhistorisches Museum
A-1014 Wien, Austria

The spinel-group mineral in equilibrium with ordinary chondritic silicates ("equilibrium spinel" (3) below) is a chromite characterized by c$\sim$0.87 and f$\sim$0.90 (c=Cr/(Cr+Al), f=Fe/(Fe+Mg)). Spinel (s.s.) is stable in ultramafic rocks only at high pressures (spinel lherzolites).In some ordinary chondrites, e.g. MezöMadaras (MM,L3), Tieschitz (Tie,H3), Gobabeb (Go,H4), Dubrovnik (Du, a L3-L6 breccia), several different types of spinel group minerals are present, covering almost the entire range from very-low-Cr compositions to almost pure chromite (in MM: c=0.006-0.98, f=0.39-0.95; HOINKES and KURAT, 1974):

(1) Spinel (Tie: f=0.048; KURAT,1971) to ceylonite (MM,Du: f=0.3 to 0.4) with very low Cr (0.5-3.0%). There may be more than one source for these,since spinels from MM and Du, which are otherwise compositionally very similar, have 2.03% and $<$ 0.1% ZnO, respectively. Alternatively, this difference could simply reflect high mobility of Zn. Compositionally, there are similarities to some spinels in carbonaceous chondrites,e.g. the high Fe/Mn ratios ($>$200). V2O3 seems to be much higher in MM and Du spinels, V/Al typically 2-3X cosmic, but few data are available for comparison.

(2) Suite of intermediate compositions, c$\sim$0.2-0.87, f$\sim$0.4-0.9, with strong correlations between c,f,MnO,V2O3, and with the exception of MM also TiO2. ZnO varies rather erratically, also suggesting Zn mobility. The Fe/Mn ratio decreases from 120-150 at low c to the value typical for equilibrium spinel (see below). FUDALI and NOONAN (1975) regard this suite as a "primary crystallization sequence", but do not discuss the parental material involved, which would have to have very high Al,low Si and a low (Ca+alkali)/Al ratio. There is some evidence for the existence of melts of the appropriate composition on chondrite parent bodies (MM: KURAT,1967; Lancé: KURAT and KRACHER, 1980).

(3) "Equilibrium chromite" - its abundance and compositional uniformity are related to the "equilibrated" character of the coexisting silicates. Its composition varies slightly through the H-L-LL sequence, e.g.,its Fe/Mn ratio is comparable to that of coexisting olivine (H:31, L:46, LL:51), as it is in terrestrial spinel from lherzolites. A major part of the bulk V and Zn is contained in chromite; V/Al is about 24X cosmic.

(4) Chromite with still higher c, and occassionally higher f, than chromite (3) is also found in MM.Minor element contents,particularly TiO2, do not lie on an extension of the trend observed in the intermediate suite (2). Their composition is reminiscent of spinels from IAB silicate inclusions,except that the latter have lower f reflecting the more reduced nature of the silicates. There is some evidence (unpublished data) of enrichment of chalcophile elements in chromites from IAB silicate inclusions (ZnO up to 2%, Fe/Mn ratio ca. 5.5, 3x lower than in "coexisting" olivine), suggesting reaction with sulfides, and a similar origin could be envisaged in MM.

Conclusions : Fe-and Cr-poor spinel group minerals in ordinary chondrites come from several different sources. As resistant minerals they may represent the only surviving evidence for some of the rock types predating the formation of ordinary chondrites.

FUDALI and NOONAN (1975) Meteoritics 10, 31-39; HOINKES and KURAT (1974) in : Analyse extraterr.Mat., Springer; KURAT (1967) GCA 31, 491-502; KURAT (1971) Chem.Erde 30, 235-249; KURAT and KRACHER (1980) Z.Naturwiss.35a, 180-190.

#44

HETEROGENEOUS SHOCK EFFECTS IN TYPE 3 ORDINARY CHONDRITES

Huss, Gary R.
Texaco Inc., P.O. Box 3109, Midland, Texas 79702

Petrographic examination of fourteen type 3 ordinary chondrites extends the finding of Dodd and Jarosewich (1979) that the vast majority of types 4-6 ordinary chondrites have experienced some degree of shock metamorphism. Ten of the fourteen meteorites examined show, in the thin sections studied, presently accepted evidence of shock metamorphism, from fracturing and undulose extinction of olivine to pockets of shock melt and veining. Huss et al. (1980) suggest that heterogeneous recrystallization of fine-grained opaque matrix in type 3 ordinary chondrites may also be a result of shock. This recrystallization exists in close proximity to other evidence of shock in many type 3 chondrites and is also found in the four chondrites showing no other shock evidence.

The intensity of the shock effects can change dramatically within a few centimeters. One thin section of the Sharps chondrite appears to have experienced moderate shock, placing it in facies d of Dodd and Jarosewich (1979), while another section from no more than ten centimeters away exhibits characteristics of facies b, relatively mild shock. Because of the heterogeneity of shock effects, caution is recommended in assigning a meteorite to a particular shock facies.

REFERENCES

Dodd, R. T., and E. Jarosewich (1979) Earth Planet. Sci. Lett. 44 335-340.

Huss, G. R., K. Keil and G. J. Taylor (1980) Geochim. Cosmochim. Acta 44 (In Press).

FARMINGTON METEORITE: SHOCK EFFECTS IN SILICATES AND PHOSPHATES

Philippe Lambert
Arizona State University, Tempe, AZ 85281

Farmington is a black L-5 chondrite (1-6). High shock effects in metals have been described earlier (4-6). Farmington also displays a remarkable series of high shock metamorphism in its transparent minerals. The main mass of the meteorite is characterized by highly deformed silicates and by a complex network of thin black breccia veins running randomly throughout the entire body. In the breccia fragment (4) subrounded monocrystalline and polycrystalline silicate grains are dispersed in a dark cryptocrystalline matrix. Silicates are entirely recrystallised. The contact with the main mass is underlined by a metal rich black breccia vein which locally intrudes the wall. All observed plagioclases have melted, widely flowed and recrystallised. They still display a highly vesicular texture. In the main body of the meteorite pyroxenes and olivines present irregular fractures, deformation bands, crystallographically controled planar features and pronounced undulose extinction. Fractures are partially filled by metal veinlets and metal emulsions. With black veining this is responsible for the black color of the meteorite. Some olivines are entirely opaque and all intermediates exist in between. Few pyroxenes have melted and recrystallised "in situ". The black veins contain numerous small metal droplets and enclose clasts of non-modified minerals as well as isotropic and nearly isotropic small fragments of olivine and pyroxene compositions which are colorless to light brown. All olivines and pyroxenes in the silicate clasts of the breccia fragment have melted and recrystallised without flowing or melting. Often underlined by alignment of metal droplets, traces of original mineral fractures are sometimes visible in recrystallised olivines. Fine metal droplets are also randomly distributed in the mass of the recrystallised olivines and pyroxenes. Apatite and chlorapatite have melted,with evidence of flowing, and recrystallised. The breccia fragment is likely a large breccia vein. Significance of all these features will be discussed.

References: (1) Snow (1890) - Science 16, 38; (2) Kunz and Weinschenk (1892) - Tschermaks Min. Petr. Mitt. 12, 177; (3) De Felice et al., (1963), Science 142, 673; (4) Buseck et al., (1965), Geochem. Cosmochim Acta, 30, 1; (5) Wood (1967) Icarus, 6, 1; (6) Heymann (1967) Icarus 6, 189.

#46

TWO DISCRETE TEKTITE-FORMING EVENTS 140 THOUSAND YEARS APART IN THE AUSTRALIAN-SOUTHEAST ASIAN AREA

Storzer D.[α] and Wagner G.A.[β]
Laboratoire de Minéralogie du Muséum, 75005 Paris, France.[α]
Max-Planck-Institut für Kernphysik, 69 Heidelberg, Germany.[β]

The 'Australasian' tektite strewnfield is the largest among the known tektite occurrences. Together with its deep-sea microtektites it covers about 5% of the Earth's surface. The concept of a single origin of this wide-spread 'Australasian' tektite strewnfield stems from K-Ar and subsequent fission track dating on numerous southeast Asian and Australian tektites suggesting their simultaneous formation about 0.7 Ma ago (1-3). However, a few years ago refined fission track dating, using the plateau-correction technique to account for thermal track fading, indicated that Australian tektites might be systematically older than southeast Asian tektites (4). Since at that time the age difference between both tektite groups could not be resolved unequivocally, two Australites, two Indochinites and one Philippinite were selected for a new fission track plateau-dating study.

The accuracy of a fission track age is composed of the precision of track counting statistics and the systematic errors of neutron dosimetry and the decay constant. By irradiating all samples simultaneously the systematic errors can be eliminated and any age difference precisely measured.

Although the apparent, thermally lowered, fission track ages of all five tektites cluster around 0.7 Ma the plateau-ages define two groups: 0.830 ± 0.028 (2σ) Ma for Australites and 0.693 ± 0.025 (2σ) Ma for Indochinites and the Philippinite. These two age groups do not overlap within their 2σ-errors and, therefore, are clearly distinct.

From these results we conclude that instead of one 'Australasian' tektite strewnfield there exist two discrete strewnfields, namely an Australian and a southeast Asian one. The two events of tektite formation are separated by an age gap of 140 thousand years. Of course, this does not exclude the possibility of a geographical overlap of both fields.
The existence of two smaller strewnfields instead of one very large field has important implications, for instance, it may explain the absence of a giant parental impact crater. With the exception of the tiny Darwin crater (0.81 ± 0.04 (1σ) Ma) there are, so far, no impact craters known which have the same age as any of the two tektite strewnfields (5).

1) Gentner W. and Zähringer J. (1959), Z. Naturforsch., 14a, 686
2) Fleischer R.L. and Price P.B. (1964), Geochim. Cosmochim. Acta, 28, 755
3) Gentner W., Storzer D. and Wagner G.A. (1969), Geochim. Cosmochim. Acta, 33, 1075
4) Storzer D. (1973), Abstracts of Geochronology and Isotope Geology, Tervuren, No 9
5) Storzer D. and Wagner G.A. (1979), Meteoritics, 14, 541

IMPACT INDUCED DEHYDRATION OF HYDROUS MINERALS AND THE ACCRETION OF VOLATILE RICH PLANETS

Lange, M. A.
Inst. für Mineralogie, Universität Münster, 4400 Münster, W. Germany

It has long been noted that certain types of carboneceous chondrites include copious amounts of structural water (1; up to 20 vol.%). The water is usually bound in layer silicates like e.g. serpentine (= Se; $Mg_3Si_2O_5(OH)_4$) (2). Arrhenius et al. (3) noted that there seems to be a strong genetic relationship between chondrites and the planetesimals (or aggregates) which formed the terrestrial planets. Hence, in the course of their accretion, collisions of volatile (water) bearing aggregates may have played a major role and may have influenced the formation of these planets.

In this paper, an attempt is made to quantify two processes related to the accretion of volatile bearing aggregates. For the calculations presented here, it is assumed that water is primarily bound in Se in either, the aggregates or the surface layer of a growing planet; hence, only processes related to the dehydration of Se are considered. The basis for the model studies are analytically determined minimum velocities and -pressures which are required for the dehydration of Se as a function of porosity upon impact (4).

Hartung (5) notes that accumulation and fragmentation of planetesimals may have competed in the early planetary accretion. The modes of fragmentation or accumulation of aggregates during mutual collision depend on material properties, impact velocities and the relative sizes of the impacting bodies (6). It is proposed that the compressional strength of a planetesimal is greatly reduced due to the effects of sudden release of volatiles (e.g. water) throughout its interior upon impact. Since impact release of water generally requires lower impact velocities than mechanical fragmentation of silicate bodies, fragmentation would occur at much lower impact velocities in water bearing aggregates as compared to water free planetesimals. The model studies presented here provide data on the critical amount of water in a planetesimal which leads to its fragmentation as a function of impact velocity and the size ratios of the colliding bodies.

The second process considered in this study is the disruption of surface layers on a growing planet due to the explosive release of water which was previously accumulated. Since the release of water upon impact requires certain threshold velocities (as specified in (4)), accretion of water bearing aggregates below this threshold allows collection of structurally bound water on the surface of the proto-planet. Once the impact velocities exceed the critical velocities, this water will be released catastrophically. This might give rise to negative accretion rates depending on the size and the impact velocity of the planetesimal. Model studies regarding this are presented and critical parameters governing these processes are specified.

References: (1)Wijk, H.B.(1956) Geochim. Cosmochim. Acta. 9, 279-289. (2)Kaula, W.(1968)Introduction to Planetary Physics, Wiley, N.Y. (3) Arrhenius, G. et al.(1974)in The Sea, Wiley Interscs., 839-861. (4)Lange, M.A. et al.(1980)in Lunar and Planetary Science XI, 596-598. (5)Hartung, J.B.(1975)in Lunar Science VIII, 337-339. (6) Matsui, T. et al.(1977) Nature 270, 506-507.

#48

POST- IMPACT HYDROTHERMAL CIRCULATION THROUGH IMPACT MELT SHEETS

Newsom, Horton E.
Lunar and Planetary Laboratory, (also Department of Geosciences)
University of Arizona, Tucson, Arizona 85721

A model of the post-impact interaction of water with an impact melt sheet is constructed to explain the presence of hydrothermal alteration fluid-flow channels, and the redistribution of volatile elements in terrestrial melt sheets. Beneath a newly formed melt sheet the water table begins to boil forming a water-steam interface, which then descends below the sheet to a depth of about one half the thickness of the sheet. Porosity and permeability are enhanced in the fractured basement rocks, which can extend laterally to twice a crater's diameter, and below a crater to a depth of several kilometers. The amount of water vaporized beneath a melt sheet is calculated by using the amount of thermal energy available from crystallization and cooling of the melt sheet (1), with corrections for heat lost from the top of the melt sheet, super-heating of steam, and heating of basement rocks below the boiling temperature. Dividing the corrected energy by the heat of vaporization results in a maximum total steam/melt-sheet ratio of 0.24 by weight. As the melt crystallizes, fractures occur rapidly in the outer crystalline rind allowing steam to penetrate the crystallized portion of the melt sheet. A two-phase zone near the surface of the sheet consists of ascending steam and descending condensed water. Liquid water circulates through the center of the melt sheet only if the water table is above the base of the sheet and when temperatures drop below the boiling point. Clays form by hydrothermal alteration below and within the melt sheet, while volatile elements are transported to the upper portions of the sheet where fluid flow channels also form.

The model can be applied to terrestrial and martian impact melt sheets. A terrestrial example is the 200 m thick melt sheet within the 65 km diameter Manicouagan Crater, Quebec. The discharge of water as steam through this melt sheet was $\simeq$ 700,000 m^3/day, averaged over a crystallization time of 1,600 years. Flow net solutions indicate that this rate of flow is consistent with regional geologic constraints. In comparison, this flow rate is equal to the groundwater volume pumped daily by the city of Tucson, Arizona. Fluid circulation also redistributes volatile elements in melt sheets, as illustrated by data from the melt sheet at East Clearwater, Quebec (2). The movement of volatile elements seriously complicates the use of trace elements to fingerprint the type of meteorite responsible for a crater. The model also applies to martian melt sheets, since only a relatively small increase in permeability offsets the effect of the lower gravity. The lower atmospheric pressure on Mars is not a problem because the steam pressure confined under an impermeable melt sheet is greater than the surface pressure, and since the atmospheric pressure was greater prior to 3.9 AE ago, during formation of most of the impact melt sheets. Martian impact melt sheets probably contain both iron-rich alteration clays and near-surface accumulations of salts due to post-impact hydrothermal circulation. Erosion of the impact melts may have, therefore, produced a major fraction of the martian soil analyzed by Viking.

References: (1) Onorato, P.I.K., Uhlmann, D.R., and Simonds, C.H. (1978) J. Geophys. Res. 83, 2789. (2) Palme, H., Goble, E., & Grieve, R.A.F. (1979) Proc. Lunar Planet. Sci. Conf. 10th, 2465-2492.
Note: supported by NASA grant NSG 7576.

SHOCK-INDUCED LUMINESCENCE AT METEOR CRATER, ARIZONA, MEASURED BY LABORATORY AND AIRBORNE FRAUNHOFER LINE DISCRIMINATOR SYSTEMS

David J. Roddy, Robert D. Watson, and Arnold F. Theisen
U.S. Geological Survey, Flagstaff, Arizona, 86001

A series of laboratory measurements using the Fraunhofer Line-Depth (FLD) Method, have been completed on shocked sandstone and dolomite at Meteor Crater, Arizona (Barringer Meteorite Crater) and show: (a) solar-excited luminescence in the shocked rocks, and (b) a correlation between luminescent intensity and level of shock metamorphism. Aerial measurements were also made at Meteor Crater with the FLD method, and indicate the airborne system is also capable of detecting direct solar-excited luminescence in the most highly shocked rocks. Luminescence, both solar- and thermal-excited, in shocked rocks appears related to certain types of shock-produced internal defects that are sensitive to activation by electromagnetic energy. For example, studies at Meteor Crater and other impact sites (Roach, 1962, Roddy, 1968) have shown shocked sandstone, limestone and dolomite respond to thermal excitation with release of thermo-luminescent energy. Luminescence excited by direct solar radiation has now been found in the same shocked rocks at Meteor Crater with the FLD Method. Using this method, ratios of intensities of 3 different Fraunhofer Lines with respect to their adjacent solar continuums are measured, and then compared with identical FLD wavelength ratios reflected from both shocked and unshocked rock specimens. If luminescence excited by solar (or artificial solar in laboratory) radiation is present, then the reflected ratio is less than the incident ratio because of the contribution from a luminescence component in the shocked test specimen. Differences in reflectivity between the central intensity of a Fraunhofer line and adjacent continuum can be ignored usually because variation of reflectivity with wavelength is negligible for most material over a few nanometers wavelength. The instrumentation used for the aerial measurements, assembled for other programs of Hemphill and Watson, consists of a Perkin-Elmer engineered model FLD designed for NASA's Advanced Application Flight Experiments (AAFE) Program. This airborne FLD instrument had a ground resolution of 45 m at a flight altitude of $\sim$ 2500 m AGL and 90 k/hr ground speed.

The laboratory measurements used a variety of samples from each different rock type, soil surfaces, vegetation, and caliche-coated rocks at Meteor Crater. Without exception, the most highly shocked Coconino sandstones from the southern ejecta blanket exhibit artificial solar-excited luminescence, by factors of 10 to 65 times as great as unshocked Coconino. The aerial measurements showed comparable results, i.e, the most highly shocked Coconino sandstone from the excavated pits in the southern ejecta blanket, excavated shaft debris of Coconino fragments on the crater floor, and excavated Coconino ejecta on the north rim exhibit significant luminescence.

Determination of solar-excited luminescence from the air using the FLD method appears feasible within limits of spatial resolution of this equipment flown over exposed areas of shocked rocks. Since this airborne FLD system is capable of detecting luminescent distributions in the ppb range, we suggest it has a potential as a remote sensing technique in detecting isolated areas of exposed shocked rocks in remote and poorly accessible areas known to be impact sites.

#50

ORIGIN AND TRANSPORT OF SUEVITE, RIES CRATER, GERMANY

Engelhardt,W.v. and GRAUP,G.

Mineralogical Institute University Tuebingen,Fed.Rep.Germany

From microscopical investigations of 1350 rock inclusions in suevites and 140 samples of suevite matrix, and chemical analyses the following conclusions were derived:

I.Cratering mechanics: The Ries event can not be simulated by a "shallow depth burst" impact. The point at which the kinetic energy was delivered to the ground and from which the shock wave started was situated well below the boundary between the sediments and the crystalline basement,i.e. at least 1000 m below the surface so that only crystalline rocks were shocked at pressures above about 100 kbar (shock effects are absent,or extremely rare and weak in sedimentary rocks of the "Bunte Breccia"). The primary transient crater consisted of a larger crater within the sedimentary cover and a crater of smaller diameter in the basement. The primary crater was considerably modified by later movements, resulting in the present flat-bottomed central crater, the inner ring and the circular depression between the inner ring and the morphological "rim".

II.Transport mechanisms: Sedimentary material and weakly shocked rocks from the basement were ejected from the growing crater in ballistic trajectories and landed at velocities approximately equal to ejection velocities(extensive mixing of "Bunte Breccia" with local material, Hörz et al.1977). Highly shocked fragments, molten material and vapors from the basement were ejected as an ascending plume spreading out into high altitudes, as observed by Piekutowski (1977) at experimental explosion craters in layered targets. Solid particles fell down from the plume and landed outside the crater at relatively low veolocities, forming patches of ejected suevite. The "soft" landing of ejected suevite is indicated by sharp boundaries to the substratum and lack of mixing. Suevite matrix consisted ,probably,mainly of finely divided glass particles from fused crystalline rocks (not of fused sediments as suggested by Kieffer and Simonds,1980)which later converted to montmorillonite. Suevite within the crater consists of brecciated crystalline rocks of relatively low shock grade, intermixed with some shocked and molten material which did not leave the crater cavity. Suevite dikes were formed during the compression stage by intrusion of radially outward moving highly shocked material into fissures of crater bottom and walls.

References: Hörz,F.,Hüttner R. and Oberbeck,V.R: Roddy,D.J. et al. Impact and Explosion Cratering 1977,p.425-448.- Kieffer,S.W. and Simonds,Ch.H. Rev.Geophys.Space Phys. 18 (1980), p.143-181.- Piekutowski,A.J: Roddy,D.J. et al. Impact and Explosion Cratering 1977,p.67-102.

NATURAL SHOCK BEHAVIOR OF AMPHIBOLITES AND GARNET-CORDIERITE-GNEISSES FROM THE RIES CRATER, GERMANY.

Stähle, V. and Müller, W.
Mineralogisch-Petrographisches Institut der Universität, Heidelberg

The study of amphibolites and garnet-cordierite-gneisses in transmitted and reflected light produced the complete rock sequence of natural shock metamorphism. The investigated metamorphic rocks come from the Bunte Breccia and others from Suevite localities, which are distributed around the Ries crater.

Based on petrographic criteria the shocked metamorphic rocks could be classified into 7 classes ranging from weakly shocked samples to rocks containing pseudotachylite veins and finally to totally fused slag-like rocks. The presently used shock scale, mainly developed from CHAO (1968) and STÖFFLER (1971), represents a finer and more precise division. The highest shocked amphibolites for example show that all hornblendes are broken down to pyroxene+spinel+glass surrounded by bubbly melt glasses of plagioclase and partly fused magnetites and ilmenites.

With increasing shock pressure the strongly shocked garnet-cordierite-gneisses contain, besides quartz and feldspar glasses, solid state and liquid state glasses of a cordierite composition. The diaplectic cordierite glasses are completely isotropic within their original grain boungaries. Refractive index measurements on single grains yielded the mean value of n=1.540. On the average the fused cordierite glasses show a somewhat lower refractive index of n=1.535. Contrary to the colorless diaplectic cordierite glasses the bubbly melt glasses are stained. Their intense light green to dark green shade is probably caused by iron in the second valence state. Both kind of glasses have identical chemical composition.

The observation of cordierite at lower shock states has not been succesful so far, because such cordierite grains are secondarily altered into pinite products. Suitable experimental shock data may close this gap. On the other hand vesicular melt glasses of pinite products were found in medium shocked gneisses, which is significant for the low melting point of these clayey alteration products.

Further some of the rarer country rocks within the Ries crater are described in respect to their unusual shock mineralogy.

Chao, E.C.T. (1968) Mono Book. Stöffler, D. (1971) J. Geophys. Res. 76.

#52

EXPERIMENTAL HYPERVELOCITY IMPACT INTO QUARTZ SAND: PRE-IMPACT LOCATION OF EJECTA, Stöffler, D. (1-3), Gault, D.E. (2), Reimold, W.U. (3)

(1) Lunar and Planetary Institute, Houston, TX 77058
(2) Murphys Center of Planetology, Murphys, CA 95247
(3) Institute of Minerology, University of Münster, Germany

EXPERIMENTS. Aluminum projectiles (radius 3.18mm; mass 0.376g) were fired into loose, dry quartz sand at 5.9-6.5km/s at the NASA Ames Research Center's vertical gun facility. Targets contained a 9mm thick layer of sand of concentric annuli with different colors. The depth of the layer was at 0, 9, 18, and 27mm in two series for the four depths (see Figure). Crater diameters were 32-34cm with depths of 5.3-6.5cm. Ejecta were collected around the craters within at least two 45° sectors on the reference ground plane and in vertical catchers at a radial distance of about 7 crater radii following previous procedures (1). Mass; color of sand grains; grain size-distribution; mass, types, and color of shock-metamorphosed grains; and presence of projectile material on grains were determined for each sample.

RESULTS. With reference to the figure, a summary of main results is:
(1) The boundary line (dashed line) above which sand was excavated and ejected beyond the crater rim is rather shallow. It deviates from a simple bowl-shaped cavity, having a shoulder at about 0.3 crater radius. A larger volume of the final crater is produced by downward, lateral, and oblique upward flow and compaction of sand.
(2) The type, color, and distribution of melt and shock-lithified breccia particles in the ejecta permit defining corresponding zones of shock pressure produced by the impact. Peak pressures at point of impact range from 47-51GPa. Assuming a lower limit of 3-5GPa produces lithified breccia (1,2), pressures attenuated an order of magnitude within the two shock zones shown in the figure. The mass distribution of melt has two distinct maxima, one inside the crater and a second at 33-41° in the vertical ejecta catchers as observed in the previous experiments (1).
(3) Shock-fused projectile aluminum forms a thin crust on the glassy side of melt agglutinates with only minor mixing between the metal and the adjacent vesiculated silica glass.

These results will allow calculation of velocity vectors of the particle motions within the target during the crater formation. Calculations are currently in progress.

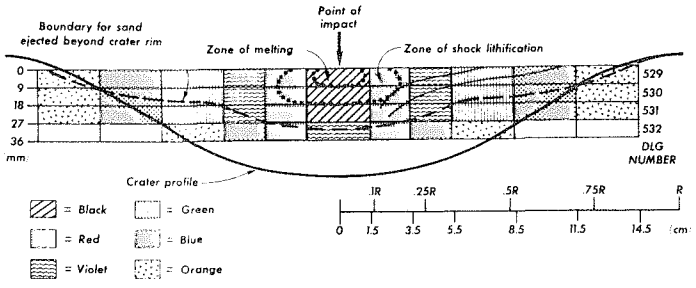

REFERENCES. (1) Stöffler, D., Gault, D.E., Wedekind, J.A., and Polkowski, G., J. Geophys. Res. 80, 4062 (1975); Kieffer, S.W., The Moon, 13, 301 (1975)

DISEQUILIBRIUM FEATURES IN EXPERIMENTALLY SHOCKED MIXTURES OF OLIVINE PLUS SILICA GLASS POWDERS

Rand B. Schaal
LOCKHEED, Houston, TX 77058

Introduction. Metamorphism caused by the passage of shock waves through minerals and rocks is controlled by the following factors: 1) high peak pressures (10^1-10^4 kbar); 2) short time duration (10^{-6}-10^2 sec); 3) high temperature (10^2-10^4 °C); 4) high strain-rate; and 5) high stress. These factors result in mineralogical and chemical disequilibrium. The purpose of this study is to petrographically and chemically characterize features in experimentally shocked mixtures of olivine plus silica glass powders (chemically reactive components) in order to monitor the extent of disequilibrium with changes in pressure. 17 samples were shocked to pressures between 62 and 642 kbar using a 20 mm powder gun which causes a peak pressure pulse of 1 msec duration. St. Johns olivine (Fo_{92}) and amersil (vitreous SiO_2) were ground and sieved. The <45 μm grain size fraction of each were mixed in a ratio of one part Fo_{92} to two parts SiO_2, by weight. 18 mg of loose powder was packed in a metal target for each shot, creating an initial sample density of ∿1.6 g/cm^3.

Petrography. In thin section each of the 17 samples appears as a well-compacted, granular aggregate with all initial pore spaces collapsed. Ten samples shocked between 62 and 359 kbar display comminution, forming a fine-grained matrix. Overall birefringence caused by Fo_{92} crystals reduces with increasing comminution as grains become fragmented into smaller pieces. Seven samples shocked between 393 and 642 kbar contain flowed, vesicular melt separating relict crystalline grains rounded by edge melting. Relict Fo_{92} grains are fractured and strained; relict SiO_2 grains are deformed by flow. Colorless and green schlieren accent the flow in the melt.

Glass Chemistry. Electron microprobe analyses of shock glass in 4 samples (562, 580, 610, and 642 kbar) indicate that these glasses have narrow composition ranges which overlap and, combined, span between 48 and 64% SiO_2. For comparison, the SiO_2 content in Fo_{92} is 40%, in enstatite (En) it is 58%, in the calculated bulk composition of the Fo_{92} + SiO_2 starting material it is 80%, and in amersil it is 100%. Thus, the composition of the shock glasses is different from that of the starting material.

Disequilibrium. Fracturing, comminution, and strain in relict crystals indicate that strong pressure anisotropy developed in these samples accompanying rapid collapse of pore spaces and collision and shear of grains. Intergranular melting attests to drastic heating on grain boundaries. Quenching preserved this heterogeneous temperature distribution.

High pressure equilibrium experiments in the system Mg_2SiO_4-SiO_2 up to 25 kbar (Chen and Presnell, 1975, Am. Min. 60, 398-406) indicate that the composition of the eutectic between En and quartz (qtz) remains constant at all pressures (at 63% SiO_2), and a second eutectic forms between Fo and En above 1.3 kbar, but its composition (54% SiO_2 @ 25 kbar) moves progressively toward Fo as pressure increases. The melt created in shocked samples spans a composition range between the qtz- and the Fo-normative eutectics, straddling the En-composition barrier. These shock-induced melts are atypical; they do not represent eutectic equilibrium fusion nor congruent whole-rock fusion; they appear to be unequilibrated products of fusion in the wide thermal trough which spans across the En-composition at high pressures in the Fo-qtz system (Chen and Presnell, 1975).

#54

DYNAMIC CRATERING FLOWS GENERATED IN LABORATORY-SCALE IMPACT EXPERIMENTS

Thomsen, J. M., Austin, M. G. and Ruhl, S. F., Physics International Co., San Leandro, CA. 94577; Schultz, P. H., The Lunar and Planetary Institute, Houston, TX 77058, and Orphal, D. L., California Research and Technology, Inc., Livermore, CA 94550.

The fundamental dynamics of impact cratering are being investigated in laboratory experiments of, and calculations simulating, the normal impact of aluminum projectiles into plasticene clay targets at a nominal impact velocity of 6 km/sec. Following the impact both the projectile and the target near the impact point are severely deformed, and material is ejected from the growing transient crater in the neighborhood of the crater lip. The cratering flow field is defined as the velocity flow field in the target which remains after the passage of the primary shock wave. Using the calculated results, the dynamic paths of Lagrangian zones within the cratering flow field are followed. It is found that the overall motion is very orderly, but that individual "particle" paths do not agree exactly with the paths predicted by the steady state Maxwell Z-Model. The calculated results are also compared with the experimental post-impact deformation of horizontal layers of colored clay emplaced within the target.

CRATERING EJECTA VELOCITY AND FLOW FIELD VELOCITY RELATIONSHIPS

Austin, M. G., Thomsen, J. M., and Ruhl, S. F., Physics International Co., San Leandro, Calif. 94577 and Hawke, B. R., Hawaii Institute of Geophysics, University of Hawaii, Honolulu, HI 96822

A two-dimensional finite difference calculation of a laboratory-scale hypervelocity (6 km/sec) impact of a 0.3 g spherical 2024 aluminum projectile into a homogeneous plasticene clay half-space has been analyzed to quantify the relationships between peak shock induced particle velocity u_p, the cratering flow field velocity u_c, and the ejection velocity u_e. The shape and magnitude of the outgoing shock wave determine u_c. Subsequent rarefactions u_r due to free surfaces add to u_c to get u_e. It appears possible to say $u_e \leq 2\ u_p$ for an individual particle.

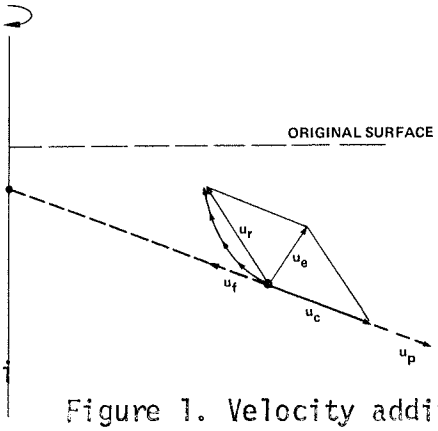

Figure 1. Velocity addition.

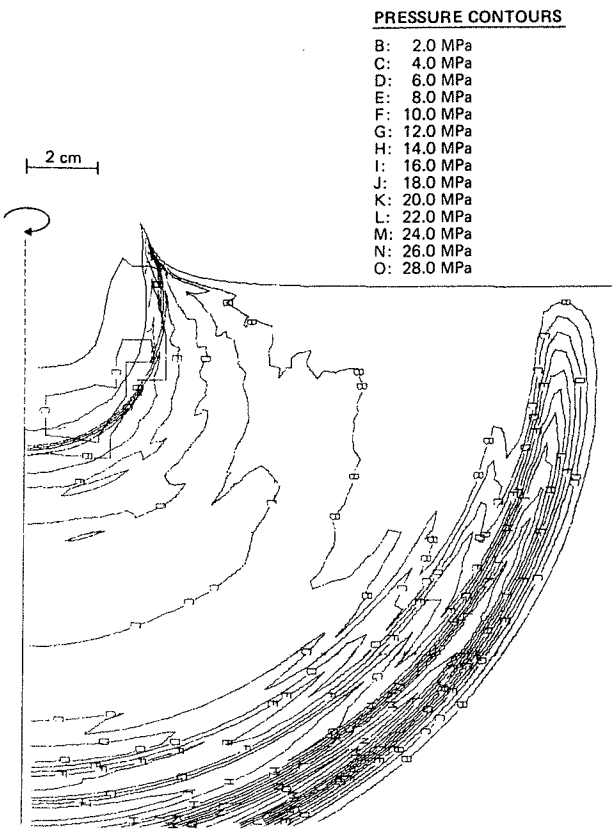

Figure 2. Pressure contours at 99 μs after impact.

#56

SHOCK METAMORPHISM AT CROOKED CREEK CRYPTOEXPLOSION STRUCTURE, MO.

Robert S. Dietz and Philippe Lambert
Arizona State University, Tempe, AZ 85281

The 7-km-diameter and circular Crooked Creek cryptoexplosion structure in Crawford County, Missouri, has a damped wave style with a central highly disturbed (brecciated and shattered) dome surrounded by a ring graben. The structure was first mapped by Hendriks (1954 , Missouri Geol. Survey Report) who also found shatter-coned Potosi dolomite and interpreted it an ancient eroded impact site or astrobleme. This interpretation has been contested most notably by Snyder and Gerdemann (1965, Amer. J. Sci.) who regarded it as cryptovolcanic and supposedly related to a linear series of endogenic structures from Illinois to Kansas. The disturbance affects Ordovician and Cambrian and is in places probably overlain by undisturbed Pennsylvanian strata so that it was a mid-Paleozoic deformation event (Hendriks, oral comm. in Snyder and Gerdemann, 1965). The Bonneterre formation (Upper Cambrian) has been uplifted about 1000 feet above its normal stratigraphic position while the Jefferson City formation (Lower Ordovician) has been depressed about 250 feet in the ring graben.

In a reconnaissance of this disturbance, one of us (RSD) collected, in the central domal uplift, float fragments of what are apparently rare detached pieces of Lamotte(?) sandstone (an identification concurred in by Missouri stratigrapher Bruce Stinchcomb) although this formation is not exposed as a mappable unit. At Crooked Creek the stratigrahically lowest formation mapped is the Bonneterre dolomite (Upper Cambrian). Immediately underlying is the Lamotte sandstone (Upper Cambrian) which is a transgressive clastic unit which overlies the Precambrian basement complex. These fragments were subjected to thin section examination as sandstones, which might reveal shock metamorphism, are virtually absent in the carbonate sequence at Crooked Creek.

The shocked sandstone is very coarse-grained (mm-sized) and porous. Mineralogically it is composed almost purely of sub-rounded quartz granules (some of which display crystallographic faces) although some feldspar and lithic sandstone fragments are present. All grains reveal a strong undulose extinction and are highly fractured--the fractures often radiating from contact points. Some grains are broken and collapsed into former voids presenting a breccia texture. Definite decorated planar elements in quartz are locally present, but only among those which are in point-point contact. The planar elements show one to four different orientation sets. The most abundant are parallel to the $(10\bar{1}3)$ and the $(1\bar{0}12)$ crystallographic planes of quartz. Rather remarkably, the quartz grains with planar elements are unfractured possibly due to the low porosity of the immediate environment.

The planar element orientations observed are those commonly associated with impact shock metamorphism. Supplementing the damped-wave structural style and the presence of bona fide shatter cones, this finding adds further support to the astrobleme interpretation of the Crooked Creek disturbance -- i.e., origin by meteorite impact in the mid-Paleozoic.

PROPOSED ASTROBLEME
Allan O. Kelly
None

A three mile in diameter granite dome, top elevation 570 feet above sea level, three miles east of Carlsbad, Ca. and 30 miles north of University of California at San Diego.

Has trench around dome and a basaltic plug coming out of trench on north side. Rock outside of trench in rim is of several different materials including marine clays and silica deposits. Twentyeight natural springs on dome and in trench and few if any springs beyond trench rim. Shatter cone striations in hard marine clay in Creataceous outcrop just beyond southwest rim. Dome is faulted across center from north to south and from east to west. Old Eocene rocks tilted upward toward dome on west side. A few big granite boulders of cone shape ten to fifteen feet high but no striations found in these boulders.

#58

AMAK CRATER: PROBABLY METEORITIC

Cassidy, W.A., and Lidiak, E.G.
University of Pittsburgh, Pittsburgh, PA 15260

Amak Crater (C.N. = 55°44'N;163°09'W) is a probable meteorite impact crater with rim-rim diameter of 160 m and greatest depth 21.3 m. The crater is emplaced on a bench or terrace of unsorted sediments ranging from boulders to sand-size grains. This terrace ends at a wave-cut cliff which actually sections part of the crater. Thin volcanic ash beds in the cliff face show stratigraphic relationships; from these it is seen that the SE rim is raised. It is not obvious that the SW rim is correspondingly raised, but the section observed in that quadrant is almost tangential to the structure. Topographically, the crater has prominent raised rims except in the SW quadrant and at the south side, where erosion has removed the outer rim flank and the rim crest. The crater surface and surroundings are completely covered with a well-developed soil and extremely dense vegetation which made visual search for meteorite fragments or impact products impossible. Suspected iron-shale particles were collected along the base of the cliff at places where they would accumulate if they had weathered out of the near-surface sediments at the top of the cliff. These specimens were found only in the vicinity of the crater. No impactites were noted. Topographic and magnetic maps were constructed in order to better understand the form and structure of the crater.

GOAT PADDOCK IMPACT CRATER, WESTERN AUSTRALIA

Milton, D.J., Ferguson, John and Fudali, R.F.
U.S. Geological Survey, MS928, Reston, Virginia 22092
Bureau of Mineral Resources, Box 378, Canberra, A.C.T., Australia
Smithsonian Institution, Washington, D.C. 20560

Goat Paddock Crater, in the Kimberley District, W. A., is slightly over 5 km in diameter, excavated in Proterozoic sandstone and siltstone. Drill holes in the floor penetrate 211 m of lacustrine sediments containing Eocene microflora and enter shatter-coned sandstone below. The crater wall rises as steep cliffs as much as 150 m above the level of the crater fill. Brief reconnaissance in 1979 showed complex patterns of overturning, folding, and faulting in the walls and rim, extensive brecciation and microscopic shock features, and a patch of melt rock at the base of the crater wall.

More thorough field study will take place this August, allowing a report to the Society meeting.

#60

IMPACT STRUCTURES IN ALGERIA

McHone, J.F., Jr. (1); Lambert, P. (2); Dietz, R.S. (2); Briedj,M(3)
(1) University of Illinois, Urbana, IL 61801; (2) Arizona State University, Tempe, AZ 85281; (3) Direction des Mines et de la Geologie, Algiers, ALGERIA

From orbital, aviation and geologic documents, several circular structures on the Sahara sedimentary platform were selected for field investigation. Three present definite evidence of shock metamorphism and are considered of impact origin.

AMGUID CRATER (26°05'N; 004°23.5'E; 450 m diameter, 30 m deep) is perfectly circular, with a steep wall, a raised rim and an ejecta blanket. The strata are uplifted, outward dipping, dislocated and locally overturned at the rim crest. Large blocks are scattered around the rim. There is petrological evidence of shock by planar elements in quartz. AMGUID is a well preserved impact crater probably no older than one hundred thousand years. TALEMZANE (33°19'N; 004°02'E; 1.7 km diameter, 70 m deep) is also perfectly circular and displays a raised rim. The strata are uplifted, outward dipping, and locally highly fractured. Numerous breccia veins are clearly exposed in the crater wall. Consolidated debris form a continuous blanket more than 500 m outward from the rim. Reworked mixed breccias are exposed at the base of the crater wall. Planar elements are observed in quartz clasts in the mixed breccia. Talemzane is an impact crater on the order of 0.5 to 3 million years old. TIN BIDER (27°36'N; 005°07'E) is a multiple concentric ring structure about 6 km in diameter. Subhorizontal Upper Cretaceous sedimentary beds outside the structure dip inward a few degrees at the periphery and become extremely folded nearer the center, yet a general circular symmetry is always retained. A clearly exposed contact between upper deformed beds and underlying non-deformed beds is remarkably flat, dipping less than 10° inward. The upper beds display strong centrifugal folding. In the center of the structure vertically disposed Lower Cretaceous sandstones at least 500 m above their normal stratigraphic position are exposed. Although no shatter cones (but wind striations) were observed and no intensive brecciation or fracturing, there is definite evidence of planar elements in the quartz grains of the central sandstones. Among known astroblemes and impact craters Tin Bider is rather unique because of the remarkable prominence of soft deformation. Its age may be early Tertiary. Other structures examined, including Aflou and Foum Tequentour, both previously reported as probable impact sites (1) and (2), are not astroblemes.

References: (1) Marks et al., 1972, Proc. kkl. Nederl. Akad. Wetenseh. 75, 348-355. (2) McHone and Dietz. 1978. Meteoritics, 13, 557-560.

THE EVOLUTION OF A PRIMARY, IMPACT GENERATED ATMOSPHERE

Lange, M. A.

Inst. für Mineralogie, Universität Münster, 4400 Münster, W. Germany

Most models for the evolution of the terrestrial atmosphere and hydrosphere propose a secondary degassing of the Earth as the most likely mechanism (e.g. 1). In contrast, (2) and (3) propose the generation of a primary atmosphere due to the release of volatiles during accretion via impact vaporization of planetesimals. Such a model is supported by the observed similarity of rare gas pattern in the Earth's atmosphere and carboneceous chondrites (4).

The purpose of this paper is a reeveluation of the models by (2) and (3) by means of improved model studies. The present calculations deal only with water, the most abundant terrestrial volatile. It is assumed that water is primarily bound in serpentine (=Se; $Mg_3Si_2O_5(OH)_4$) in either, the planetesimals or the surface layers of the growing Earth. The basis for the model studies are analytically determined minimum velocities and -pressures which are required for the dehydration of Se as afunction of porosity upon impact (5).

The major processes considered in the model calculations are the dehydration of either the planetesimals or the surface layers and the formation of Se due to the hydration of forsterite (=Fo) and enstatite (=En) during the accretion of the Earth. It can be shown that the fate of an impact generated atmosphere is primarily goverened by two parameters, the hydration rate of Fo and En HR, and the dehydration efficiency DE. HR was experimentally determined by (6) and was adjusted to the appropriate pressures and temperatures in the present model. DE is defined as the ratio of initially released water from each lattice site upon impact to the amount of water finally leaving the target; DE was used as a free parameter in the calculations. A model for the homogeneous accretion of the Earth (7) was used to determine the number of planetesimals hitting the surface of the proto Earth per unit of time. For each time step, impact dehydration is balanced with the amount of water used for the hydration of En and Fo.

The results of this study show that for dehydration efficiencies $DE < 0.3$ most of the available water resides within the Earth at the end of accretion. For $DE \geq 0.35$, the bulk of the available water forms a primary atmosphere/hydrosphere regardless of the size of HR. Since most of the target material undergoing dehydration is comprised by the highly comminuted ejecta material, dehydration efficiencies $\geq 35\%$ seem to be most likely. Hence, it is proposed that a primary atmosphere/hydrosphere was formed according to the models of (2) and (3) in the course of the Earth's accretion.

References: (1) Rubey, W.W.(1951)Bull. Geol. Soc. Amer. 62, 1111-1148. (2) Arrhenius, G. et al.(1974)in The Sea, Goldberg ed., Wiley Intersc., 839-861. (3) Benlou, A. et al.(1977)Astrophysics and Space Sc. 46, 293-300. (4) Signer, P.(1964)in The Origin and Evolution of Atmospheres and Oceans, Wiley, N.Y., 183-190. (5) Lange, M.A. et al.(1980) in Lunar and Planetary Science XI, 595-598. (6) Martin, B. et al.(1970)Chemical Geology 6, 185-202. (7) Weidenschilling, S.J.(1976) Icarus 27, 161-170.

#62

Impact Oceanic Flood Deposits in San Diego County.
Allan O. Kelly
None

About twenty color slides to show anamalous gravel deposits in San Diego County extending from Point Loma on the coast, south to the border, and inland over the mountains to the Borrego Valley desert. Thence through Warners Valley back through the north County to the coast and south to U.C.S.D. These separate and distinct deposits contain many different kinds of rock and range in size from huge traveled boulders down through beach cobblestones to fine sands and clay. All are late Pleistocene in age and none can be attributed to present day transportation and deposition in the locations where found.

ELEMENTAL AND ISOTOPIC COMPOSITION OF NOBLE GASES IN THE ISNA CARBONACEOUS CHONDRITE. Nautiyal, C.M., Padia, J.T., Rao, M.N., Venkatesan, T.R.,Physical Research Laboratory, Ahmedabad 380009,India AND Englert, P., Herpers,U., and Herr, W., Inst. für Kernchemie, Köln (West Germany)

Here we report the step wise heating data of a C3(O) carbonaceous chondrite which showed petrographic features intermediate between C2 and C3 meteorites according to Methot et al(1). A five step temperature run was performed on this sample and the total values of all the temperature fractions are given in table 1. The Ne-21/Ar-36 and Ar-36/Xe-132 ratios are 0.0046 and 323.45 respectively. According to Mazor et al(2), the C3(O) meteorites have these ratios 0.03 and 242 respectively. The Ar-36/Xe-132 values agree within 30% variations whereas the Ne-20/Ar-36 values show large differences. The reason for this difference is partly due to the fact that this meteorite is a find and heavy neon losses might have occurred in this sample during its terrestrial residence time. However, the He-4/Ne-20 values for Isna is $\sim$1250 which is much higher than the generally found value of $\sim$200-400 for other C3 chondrites. The He-4/Ne-20 ratio is anomalously high.

Even though the total Ne shows heavy diffusion losses, the isotopic ratios have not changed so much. The 600°C,1000°C,1200°C and 1500°C temperature points in the three-isotope Ne diagram plot are close to the mixing line joining the "planetary" and GCR end points,showing that the trapped neon is of "planetary" type. This is also borne out by theHe-3/He-4 ratio of 1.4×10^{-4} which is representative of "planetary" type. In order to look for other solar effects we carefully checked nearly 50 olivine crystals for solar flare irradiation records but without any success.

The cosmogenic Ne-21 is very small (similarly $^{3}He_{c}$) yielding a cosmic ray exposure age of about 0.1 my. This is considered to be very low when compared to the other C3(O) meteorites which have cosmic ray exposure ages of about 5-10 my. This low Ne-21 age may be due to heavy diffusion losses. We find it difficult to calculate the Ar-38 exposure age because of the large excess of Ar-36 due to probably $^{35}Cl(n,\gamma)\ ^{36}Ar$ production.

Effects of secondary neutron irradiation can be seen in the Ar-38/Ar-36 ratio (0.165) and the Xe-128/Xe-132 ratio of 0.083. The Xe-129/Xe-132 value of 1.207 indicates large excess of radiogenic xenon. Fission xenon seems to be marginally present. Elemental abundances in this sample and further detailed studies of xenon are in progress and will be reported elsewhere.

REFERENCES: 1. Methot, R.L. et al,(1975),Meteoritics 10, 121-131.

2. Mazor et al. (1970), Geochim. Cosmochim. Acta 34, 781-824.

Table-1

He		Ne			Ar	
3/4	(4)*	20/22	21/22	(22)*	40/36	(36)*
0.00014	930.4	5.224	0.300	0.142	13.617	160.14

* Gas contents are in 10^{-8} cc STP/g.

#64

A SEARCH FOR PRIMORDIAL ATMOSPHERIC-LIKE ARGON IN AN IRON METEORITE

Fisher, D. E.
University of Miami, Miami, Florida 33149

Interpretation of planetary argon data is generally based on the assumptions that there existed a unique primordial argon with $^{40}Ar/^{36}Ar \sim 10^{-4}$, and that measured planetary ratios greater than this value reflect the growth of radiogenic ^{40}Ar from ^{40}K decay. In particular, the terrestrial atmospheric value of 295.5 is ascribed to this process coupled with degassing of the solid earth. Hennecke and Manuel (1977) have suggested instead that the value of $^{40}Ar/^{36}Ar$ in the atmosphere is primordial, and that terrestrial argon is a remnant of a solar system-wide component which they have observed in iron meteorites. The present experiment describes the release of argon from an iron meteorite in six heating extractions, with a molybdenum crucible protected from fluxing with the sample by an inner lining of well-degassed silicate glass, in a search for this proposed primordial component.

Eighty-six percent of the ^{40}Ar was removed in the first extraction, as opposed to only 8% of the ^{38}Ar and 21% of the ^{36}Ar. The bulk of the ^{36}Ar and ^{38}Ar came off in the third extraction, after 90% of the ^{40}Ar had already been removed. A plot of the ratios $^{40}Ar/^{36}Ar$ vs. $^{38}Ar/^{36}Ar$ at each heating step show the data beginning near the atmospheric point and then sauntering steadily down the line joining the atmospheric to the cosmogenic component. This clearly indicates a loosely-bound atmospheric component coming off first, decreasing as the more tightly-bound cosmogenic component increases. The final extraction shows nothing left but a pure cosmogenic component (with less than 0.1% of the total abundances).

There is no indication in the data for a tightly-bound indigenous component with atmospheric-like isotopic ratios; i.e., no indication that there exists in this iron meteorite a primordial argon with $^{40}Ar/^{36}Ar \sim 295$.

ON THE DISTRIBUTION OF NOBLE GASES IN ARCHAEAN TERRESTRIAL ROCKS

G. Roskamp, M. Freundel and L. Schultz

Max-Planck-Institut für Chemie, D - 6500 Mainz, Westgermany

Recent work has shown that carbon seems to be the major host phase of planetary type noble gases in meteorites (e.g. Lewis et al., 1975; Frick and Chang, 1978; Göbel et al., 1978). To study primordial gases of the earth as well as possibly trapped gases from an ancient atmosphere carbon phases from archaean rocks are again good candidates (Frick and Chang. 1977). We report preliminary results of noble gas analyses on 14 samples from the 3.7 AE old Isua supracrustals (SW - Greenland) and from the 3.0 AE old Pongola series in South Africa.

The carbonaceous matter was enriched by an HCL - H_2SO_4 treatment of the samples and by magnetic as well as density separation techniques. In those cases where no clean carbon-separates could be prepared by this method, the samples were treated with HF - H_2SO_4 in a Teflon bomb for 2 hours at 160°C. In all residu es only graphite lines are visible in the X-ray diffraction pattern.

A typical result is given in table 1. It is striking that a considerable part of the primordial gases as well as of the radiogenic 40-Ar is residing in the carbon phase. With an upper limit for the potassium content of 18 ppm a K-Ar age of 17 AE is calculated indicating that the 40-Ar is not the product of an in-situ decay from 40-Ar.

Stepwise heating experiments to separate the excess 40-Ar from the primordial component show that most of the gas is released between 800 and 1200°C and that the release pattern of 36-Ar and 40-Ar is quite similar. The excess 40-Ar in carbon phases of the archaean samples indicates that this material (not yet well determined) is able to trap noble gases in relatively large quantities. It is conceivable that during a metamorphic event Ar released from K-bearing phases can be captured in the same rock by this carbonaceous material. It also indicates that the trapped noble gases in meteorites might be redistributed by thermal events between the original carriers and that the carbon-containing phases can act as catchers for these gases.

Sample 2780	^{36}Ar	^{84}Kr	^{132}Xe	$^{40}Ar/^{36}Ar$
	in 10^{-10} ccSTP / g			
Bulk	25	2.1	.98	4840
C-separate	980	36	10	11600

Table 1: Noble gas content of a bulk sample and of a carbon-separate of Isua supracrustal 2780

REFERNECES

Lewis, R.S., Srinivasan, B. and Anders, E. (1975), Science, 190, 1251
Frick, U. and Chang, S. (1978), Meteoritiecs, 13, 465
Frick, U. and Chang, S. (1977), Geochim.Cosmochim.Acta, Suppl. 8, 273
Göbel, R., Ott, U. and Begemann, F. (1978), J.Geophys.Res., 83, 855

#66

ANALYTICAL ELECTRON MICROSCOPY OF MATRIX PHASES IN MURCHISON AND MIGHEI

Ian D. R. Mackinnon
LOCKHEED, 1830 NASA Road 1, Houston, TX 77058

X-ray microanalysis and focused probe microdiffraction techniques (using a JEOL 100CX Scanning Transmission Electron Microscope (STEM) have been used to study thin foils of matrix material from the Murchison and Mighei CM carbonaceous chondrites. These techniques are invaluable for the study of fine-grained material as the electron beam can be focused to a small probe to obtain information from extremely small areas at the specimen surface (typically <20nm). In addition, with a high accelerating voltage (100kV) and a thin specimen, only minimal spreading of the electron beam occurs. Therefore, the X-ray source size in STEM microanalysis can almost equal the size of the beam at the specimen.

Qualitative energy dispersive analyses of individual matrix grains confirm previous work that some of the matrix phyllosilicates are iron-rich (e.g., cronstedtite, Muller et al., 1979; Barber, 1980) though many are Fe-Mg phyllosilicates of the type described by Bunch and Chang (1980). Qualitative analyses of discrete grains of SBB-type mixed layer material (Mackinnon and Buseck, 1979) also confirm the presence of Fe in these structures (McKee and Moore, 1980). In addition, EDS spectra from the SBB-type structures show small amounts of aluminum and sulfur. In Murchison, Ni also occurs in some spectra from SBB-type structures.

SBB-type structures also occur as fine-scale intergrowths (~500A wide) with planar serpentine-type minerals. Qualitative microanalysis of the intergrowths in Mighei show that there are regions with high or low amounts of sulfur, in addition to regions of Fe-rich silicate without sulfur. Microdiffraction patterns from SBB-type and S-type intergrowths show that c* for both phases are parallel, suggesting that the two phases formed simultaneously. In addition, very weak diffraction spots corresponding to an ~14.5A basal spacing occur. This periodicity may be due to the presence of chlorite or a two-layer serpentine-type mineral. Cylindrical chrysotile and planar-roll serpentine (Mackinnon, 1980) occur in close association with grains of SBB-type and S-type intergrowths. Electron beam damage of the intergrowth material is substantially less rapid than discrete SBB-type or chrysotile grains.

The occurrence of sulfur (and Ni) in the spectra of SBB-type material suggests either: (a) the SBB-type material may be the phyllosilicates, described by Bunch and Chang (1980), intimately mixed with poorly-characterized-phases (PCP's) or (b) SBB-type material may be a PCP. It is interesting to note that the X-ray diffraction pattern from a fibrous PCP in Murchison (Fuchs et al., 1973) shows one sharp line at 5.4A and a weak line at 2.7A. Electron diffraction patterns from SBB-type material show d_{003} ~5.9A (strong) and d_{200} (inferred) ~2.7A.

References:

Barber, 1980: Contrib. Min. and Pet., in press.
Bunch and Chang, 1980: Geochim. Cosmochim. Acta, in press.
Fuchs et al., 1973: Smith. Contrib. Earth Sci., No. 10.
Mackinnon, 1980: Proc. Lunar and Planet. Sci. Conf. 11th, in press.
Mackinnon and Buseck, 1979: Nature 280, 219-220.
McKee and Moore, 1980: In Lunar and Planetary Science XI, 703-704.
Muller et al., 1979: Tscher. Min. Petr. Mitt. 26, 392-394.

MURCHISON METEORITE: CARRIER PHASES OF NOBLE GASES

Jun-ichi Matsuda and Roy S. Lewis

Enrico Fermi Institute and Department of Chemistry, University of Chicago
Chicago, IL 60637

One of the more interesting samples isolated from Murchison is 2C10m, the 1-3 μm fraction of a severely etched residue, containing substantial amounts of three presolar components: Ne-E (*H* and *L*) and s-process Xe (Alaerts *et al.*, 1980). The carriers of these components are, respectively, spinel and two apparently carbonaceous phases, Cα and Cβ, of release temperatures ~800 and ~1400°C (probably carbynes; Whittaker *et al.*, 1980). In an attempt to characterize these carriers, we separated 2C10m into 3 density fractions, after removing 4% fine-grained (<1 μm) material. SEM examination showed that the separation had been poor. All fractions consisted mainly of spinel + chromite (~2:1 ratio), with progressively higher amounts of adhering carbonaceous matter in the lower-density fractions.

Sample	Weight %	Ne_E^{22} 10^{-8} cc/g	Xe^{132} 10^{-10} cc/g	$\frac{Xe^{130}}{Xe^{132}}$	Xe_s^{130} 10^{-10} cc/g	Xe_s^{130} %
2C10m	≡100	50 ±3	19.3	0.182	0.4	≡100
<2.8 g/cm³	4	*<400*	*740*	0.167	5 ±3*	45 ±30
2.8-3.33 g/cm³	15	74 ±28	31	0.194	1.0 ±0.3	38 ±12
>3.33 g/cm³	77	21 ±8	10	0.189	0.3 ±0.1	52 ±20

*The true weight of this 0.01 mg sample may have been higher, in which case all gas concentrations would be correspondingly lower.

Noble gas concentrations decrease at higher densities, consistent with earlier indications ($HClO_4$ treatment, etc.) that the gases are located mainly in low-density, carbonaceous phases. But there is no separation of Cα and Cβ: the ratio of Ne_E^{22}/Xe_s^{130} is constant in all 3 density fractions, as well as in two T-fractions (1100° and 1600°) of the >3.33 g/cm³ fraction. Of course, most carbynes have closely similar densities, and so a better separation would require smaller density steps and better disaggregation.

In another experiment, we tried to see whether chromite and carbynes were important carriers of CCFXe, as in Allende (Lewis and Matsuda, this volume). We therefore treated an HNO_3-etched residue, CB, with H_3PO_4 and H_2SO_4, to dissolve chromite and spinel, while leaving mainly the organic polymer and carbynes. The remaining material was separated into non-colloidal and colloidal fractions, CE and CG.

Sample	Treatment	Weight %	Ne_E^{22} %	$\frac{Xe^{130}}{Xe^{132}}$	Xe_f^{136} %
CB		≡100	≡100	0.161	≡100
CE	H_3PO_4+	<10	<33	0.174	<28
CG	H_2SO_4	11	<7	0.161	<7

Evidently removal of chromite, spinel, and some polymer has caused loss of >60% of the Ne-E and >65% of the CCFXe, while allowing an s-Xe component to show in sample CE. Apparently chromite is a major carrier of CCFXe, as in Allende (Lewis *et al.*, 1977; Srinivasan *et al.*, 1977).

#68

HIGH RESOLUTION TRANSMISSION ELECTRON MICROSCOPY OF AN ALLENDE ACID RESIDUE

Smith, P.P.K. and Buseck, P.R.
Department of Geology, Arizona State University, Tempe, AZ 85281.

Characterisation of the host phases of noble gases in carbonaceous chondrites has been hindered by their fine-grained nature. High resolution transmission electron microscopy (HRTEM) has previously been used successfully to identify submicron silicate grains in stony meteorites (1); we report here the application of HRTEM to the acid-insoluble residue that carries the bulk of the noble gas content of carbonaceous chondrites. Density-separated Allende residue samples were provided by S.Chang.

Chromite and minor spinel in the size range 2 - 0.2 μm were identified by electron diffraction. High resolution lattice fringe imaging reveals many more chromites, with diameters as small as 5 nm and thus too small to give recognizable diffraction patterns. Grains that show a lattice fringe spacing of 0.58 nm may be pentlandite or daubreelite, both of which have a (111) d-spacing of this value. Mineral identification by HRTEM has been supported by energy-dispersive X-ray analysis on a STEM instrument, which provides semi-quantitative analyses from areas as small as 10 nm in diameter. Most analyses correspond to chromite, with one spinel and one chromiferous pentlandite also observed. Small chromite and pentlandite particles are present in a density fraction with S.G.<2.25; clearly such density separates do not provide complete separation of heavy minerals from the lighter carbonaceous component of the residue.

The bulk of the acid residue consists of a tangled aggregate of crystallites that have a prominent lattice fringe spacing of 0.34-0.38 nm. Individual crystallites are up to 20 fringes in thickness, with lengths of up to 30 nm. The microstructure of this carbonaceous material appears strikingly similar in HRTEM images to that previously described for glassy polymeric carbon formed by heat treatment of polyvinylidene chloride, and interpreted as interwoven ribbon-shaped packets of graphitic layer planes (2). In the case of carbonised PVDC this structure is known to contain a high density of closed micropores, in contrast to the very low internal surface area of graphitizing carbons (3). The carbonaceous matter thus provides a plausible site for the retention of gases.

Our results differ significantly from those of Whittaker et al. (4) who report that $\geq$90% of the Allende residue carbon is in the form of carbynes. Extremely thin hexagonal flakes observed in one of our samples give hexagonal diffraction patterns with a d-spacing of 0.444$\pm$0.002 nm, which may correspond to «carbyne or chaoite (d_{110} = 0.446 and 0.447 respectively), but these grains only comprise a few percent of the sample. We regard this identification as tentative, since it is based on diffraction information from a single zone axis.

1. Mackinnon,I.D.R., Buseck,P.R. (1979) Proc.Lun.Sci.Conf.10th, 937-949.
2. Ban,L.L., Crawford,D., Marsh,H. (1975) J.Appl.Cryst. 8, 415-420.
3. Jenkins,G.M., Kawamura,K. (1976) "Polymeric Carbons - Carbon fibre, glass and char", Cambridge University Press.
4. Whittaker,A.G., Watts,E.J., Lewis,R.S., Anders,E. (1980) Submitted to Science.

CARRIER PHASES OF CCFXe AND OTHER NOBLE GAS COMPONENTS IN THE ALLENDE METEORITE

Roy S. Lewis and Jun-ichi Matsuda

Enrico Fermi Institute and Department of Chemistry, University of Chicago
Chicago, IL 60637

Continuing our efforts to ascertain the host phases of meteoritic noble gases, we have examined 5 chemical separates, all derived from the same parent sample (Allende BB, the colloidal fraction of an HCl,HF-insoluble residue, depleted in spinel and coarse chromite). Phase Q, the carrier of normal planetary gases, was largely removed from BB with HNO_3, yielding sample BG (carbon, chromite, spinel). Portions of BG were treated with selective solvents for the main phases. The composition of the samples was checked by SEM, XRD, and INAA.

Sample	Treatment	Weight	Phases Left				Cr	$\frac{Xe^{136}}{Xe^{132}}$	Xe_f^{136}	Xe_f^{136}
		% Left	C	Chr	Sp	Q	%		10^{-10}cc/g	%
BG	---	100	++	++	+	++	8.7	0.46	150	≡100
BK	H_3PO_4+H_2SO_4	78	++			+	0.3	0.52	90	48 ±17
BT	$HClO_4$	21	+	++	+		21	0.64	640	88 ±32
Bβ	$Cr_2O_7^=$+H_2SO_4	17	?	++	+			0.64	850	93 ±33

The distribution of anomalous Xe_f^{136} (= CCFXe) is given in the last two columns. The errors come mainly from a 25% variation in spectrometer sensitivity. The two chromite-rich samples, BT and Bβ, are enriched 4- to 6-fold over the parent sample, BG, and account for ~90% of the total CCFXe. The carbon sample BK (>80% carbynes; Whittaker *et al.*, 1980) actually is depleted relative to the parent sample BG, and accounts for only ~50% of the total CCFXe; it cannot be the sole carrier of CCFXe. Two alternatives remain. (1) Chromite and carbon (actually, some subfractions of these phases) are the principal carriers of CCFXe and associated anomalous gases, as proposed by Lewis *et al.* (1977, 1979). (2) The main carrier of CCFXe and associated gases is a new, minor phase, resistant to oxidizing reagents that destroy carbon ($HClO_4$, $Cr_2O_7^=$) but less resistant to reagents that destroy chromite (H_3PO_4).

REFERENCES

Lewis R.S., Gros J., and Anders E. (1977) *J. Geophys. Res. 82*, 779-792.

Lewis R.S., Alaerts L., and Anders E. (1979) *Lunar and Planetary Science X*, 725-727.

Whittaker A.G., Watts E.J., Lewis R.S., and Anders E. (1980) *Science*, in press.

#70

NOBLE GASES IN ALLENDE DARK INCLUSIONS: SOME IMPLICATIONS

Ott, U.,*† Chang, S.,** and Bunch, T.**
*Department of Physics, University of California, Berkeley, CA 94720
**NASA-Ames Research Center, Moffett Field, CA 94035

We have reported an apparent deficiency of the trapped noble gases of the "anomalous" type relative to the "normal" type in the Allende Dark Inclusion DI #5 (1) when compared to bulk Allende (1) or another Dark Inclusion, DI #2 (2). Because min-pet observations showed DI #5 to be the most thermally altered of all Dark Inclusions studied, partial loss of the anomalous noble gas component during alteration was suggested as an explanation.

In order to test this hypothesis we have performed a stepwise heating analysis of DI #5. Trapped noble gases were released below the supposed temperature of alteration (700°C). This result does not exclude a thermal metamorphic effect, however, because, unlike in I-Xe dating (3,4), the effect of preheating on the thermal release pattern of trapped gases has not been investigated in detail. If the "chemical erosion model" for the release (5) is correct, gas release below the preheating temperature can be expected.

Alternative explanations for the observed relative deficiency of the "anomalous" gas can be based on processes occurring during formation of noble gas carriers and concomitant gas trapping (location unknown) or during accretion of noble gas carriers on the Allende parent body, or both. The alternatives have implications for either the hypothetical presence of a superheavy element as progenitor of CCF-Xe (6) or the nature of the carrier formation and the noble gas trapping processes and their possible temperature dependence (7).

References: (1) Lun. Plan. Sci. XI (1980), 119. (2) Lun. Plan. Sci. X (1979), 952. (3) JGR 74 (1969), 6679. (4) Lun. Plan. Sci. XI (1980), 932. (5) GCA 42 (1978), 1775. (6) Science 190 (1975), 1251. (7) Science 198 (1977), 927.

†Present address: Max-Planck-Institut für Chemie, 6500 Mainz, W. Germany.

NOBLE GASES: SOLUBILITY IN MAGNETITE, GRAPHITE, AND DAUBRÉELITE

Jongmann Yang and Edward Anders

Enrico Fermi Institute and Department of Chemistry, University of Chicago

To simulate trapping of noble gases from the solar nebula, various solids were grown from a noble-gas atmosphere at 440-720 K. Gas contents were measured either by mass spectrometry or, in experiments where 36 d Xe^{127} tracer had been added, by γ-counting.

Fe_3O_4 and C. $Fe(CO)_5$ was treated in a noble-gas atmosphere at 520-720 K for 5 to 44 days. The initial products, Fe and CO, reacted further to yield Fe_3O_4, C, and iron carbide(s), which were separated or selectively dissolved by chemical treatments. A correction for adsorbed gas was assessed either by stepped heating or, in tracer experiments, by exchange with inactive Xe at 400°C. The principal results are: (1) When grown simultaneously, all three solids have gas contents identical within a factor of 3. (2) Henry's Law for Xe is obeyed at least between 10^{-8} and 10^{-5} atm. (3) The distribution coefficient for Xe in Fe_3O_4, ~0.2 cm^3 STP g^{-1} atm^{-1}, is similar to the Lancet and Anders (*1*) value at 600 K. (4) No clear temperature dependence could be established yet, as the reproducibility is poor (mean ratio of replicates = 3 x), and the reaction is very incomplete at T $\lesssim$600 K, causing large errors in the analysis, especially for phases inferred by difference.

Chromite and C. Vacuum-deposited films of stainless steel (440c; 17% Cr) or mixtures of $Cr(CO)_6$ and $Fe(CO)_5$ were heated as above, yielding Fe^{3+}-rich ferrichromite and carbon. Gas concentrations of the chromite and carbon were identical within a factor of 3, as predicted by Lewis *et al.* (*2*). Solubilities are somewhat higher than for Fe_3O_4, but the reproducibility is poor.

Daubréelite ($FeCr_2S_4$) was made at 440-720 K by reaction of stainless steel films with an H_2S-H_2 atmosphere containing noble gases (Ne 7×10^{-6} atm, Ar 3×10^{-6} atm, Kr + Xe 2×10^{-9} atm). Solubilities for the 3 heavy gases decrease by about 3 x from Ar to Xe, and are about 0.6 x those for magnetite at 500 K: the solubility of Ne is about 0.1 x the magnetite value (*1*). Heats of solution are 2-3 x smaller than for Fe_3O_4: $-\Delta H_s \simeq 5$ kcal/mole for Ar, Kr, Xe and <1 kcal/mole for Ne.

These data confirm earlier work (*1*), showing that minerals grown at the low temperatures of the solar nebula trap large amounts of noble gases, though thus far failing to reproduce either the elemental or the isotopic patterns of planetary noble gases. Our data do not confirm the 10^{-5} x lower solubilities for Fe_3O_4 reported by Honda *et al.* (*3*) for condensation of Fe_3O_4 from quenched vapor--a process that does not seem relevant to the solar nebula.

REFERENCES

1. Lancet M.S. and Anders E., *Geochim. Cosmochim. Acta 37*, 1371 (1973).
2. Lewis R.S., Gros J. and Anders E., *J. Geophys. Res. 82*, 779 (1977).
3. Honda M., Ozima M., Nakada, Y. and Onaka T., *Earth Planet. Sci. Lett 43*, 197 (1979).

☆☆☆☆☆☆☆☆

#72

ON THE DISTRIBUTION OF NOBLE GASES IN ALLENDE : A DIFFERENTIAL OXIDATION STUDY

R. O. Pepin and Urs Frick
School of Physics and Astronomy, U.of Minnesota, Minneapolis MN 55455

In the Allende C3V meteorite there are strong indications that more than 50% of the heavy noble gases (Ar,Kr,Xe), with a variety of isotopic components, reside in acid-insoluble carbonaceous matter *[1]*. The latter comprises about 0.2 - 0.4% by weight of this stone and has been recently shown to exhibit structural features of carbynes *[2]*. Earlier we have reported on closed-system combustion of a gas-rich Allende residue in 20 torr oxygen *[3]*; the gas release is primarily due to chemical attack rather than thermal activation, and relative enhancement of "anomalous" low-level components is as large as in any open-system oxidation method with H_2O_2, HNO_3, $HClO_4$, or atomic oxygen. Since this method effectively mobilizes *all the noble gases of the residue* below 600°C, we expect it to offer the opportunity to determine the elemental and isotopic signature of "carbon-free" Allende matter, which is then simply represented by integrating the release from a bulk sample above 600°C. Therefore we have progressively heated a fine-grained matrix sample (<4 μm) in an oxygen atmosphere. A small fraction (2 - 20%) of the released gases has been utilized to successfully perform simultaneous microanalyses of nitrogen isotopes in the static mass spectrometer *[4]*.

Noble gas elemental data reveal a variety of interesting facts. We can establish three distinct outgassing peaks, characterized by activation below 600°C (carbonaceous matter), gas mobilization between ~550°C and 900°C (probably sulfides), and the high temperature diffusive release tentatively assigned to silicates; these phases contain about 53%, 7%, and 40% of the total heavy gases, respectively. Although a very different protocol has been followed, the temperature release pattern of the combustibles (<600°C) perfectly matches the pattern obtained from the residue; the amounts are consistent with the expected carbon content of the matrix (~0.3%).

Isotopic data confirm the presence of "normal" Xe, somewhat lighter than average carbonaceous chondritic AVCC, and "anomalous" Xe in the phases combustible below 600°C; the "sulfides" exhibit a small fission-like component, while the Xe in the "silicates" is uniform and of roughly AVCC composition. Most of the large quantities of "excess" (radiogenic) $^{129}Xe^*$ are tied up in incombustible phases ("silicates"). Comparatively, the combustibles of the matrix contain lower amounts of $^{129}Xe^*$ than the residue, perhaps indicating the redistribution of ~5% of $^{129}Xe^*$ from "silicates" into carbonaceous structures during acid treatment.

The integrated elemental composition of combustibles and "silicates" are virtually identical with Ar:Kr:Xe equal 110:1.15:1. Thus we have to conclude that the mechanism of planetary gas entrapment in various substances results in similar fractionation in spite of the different nature of the potential carrier phases. While natural and artificial processes with carbonaceous matter are known to mimic "planetary fractionation" almost perfectly *[5]*, it seems now that such fractionation is by no means an exclusive feature of "organics".

References : [1] Frick and Chang (1978) Meteoritics 13, p.465
[2] Lewis et al.(1980) Lunar and Planetary Science XI, p.624
[3] Frick and Pepin (1980) ibidem, p.303
[4] Frick and Pepin, this volume
[5] Frick et al.(1979) Proc.Lun.Planet.Sci.Conf.10th, p.1961

ANALYSIS OF NITROGEN ISOTOPES BY STATIC MASS SPECTROMETRY

Frick, U. and R. O. Pepin

Department of Physics, University of Minnesota, Minneapolis MN 55455

Noble gas abundances in lunar and meteoritic matter are usually in the range $\sim 10^{-2}$ to 10^{-11}ccSTP/g. Sample masses of 10-100mg, containing anywhere from $\sim 10^{-7}$g of ^{4}He to $\sim 10^{-15}$g of ^{132}Xe, are typical for isotopic analysis by static mass spectrometry. Nitrogen would be an important element to add to the roster of noble gases measured simultaneously in these samples. Work by the Kerridge and Clayton groups has revealed large (>30%) $^{15}N/^{14}N$ differences in solar wind N trapped in lunar soils and breccias, with progressively greater ^{15}N depletion in older samples. Apart from the general question of any tendency for isotopic co-variation in N and the rare gases, there is the specific question of whether the Xe signature in breccias with ancient gas components -excess heavy isotopes from ^{244}Pu fission in the lunar interior- correlates with ^{15}N depletion. Certain carbonaceous chondrites, such as Allende, that show abundant evidence for the presence of unmixed nucleogenetic products, may also contain minor N components from nuclear processing -for example, near-pure ^{14}N. Experimental isolation of small anomalous N components will probably require chemical or physical separates of minor mineral phases and high resolution in stepwise heating. But current dynamic spectrometry techniques need several μg of N -i.e., grams of bulk Allende for a stepwise heating experiment- and cannot detect the noble gases except for qualitative measures of He and Ar in favorable cases.

We have developed techniques for isotopic analysis of very small amounts of N in gas fractions in which all noble gases are also measured. Volumetric splits of ∿2-20% of the gases evolved from a sample heated in pure O_2 are cooled at LN_2 temperature in glass capillaries to condense CO_2, SO_2, and H_2O, exposed on TiZr getter to remove H_2 added by metal valve manipulations in the processing line (which if present tends to generate a mass 29 interference by formation of the hydride HN_2), and analyzed statically in the rare gas spectrometer. Isotopic compositions have been measured on N amounts in the spectrometer ranging from 100ng to 30pg, abundances with one-third these amounts. Standard deviations of individual isotopic ratios are ∿±0.5‰ on 100ng, ∿±2-3% on 30pg, and are determined chiefly by electrometer noise. Typical accuracy in δ^{15}N, including uncertainties in ratio extrapolation and in comparison with standard N, is ∿2‰.

Applied to a 30-step combustion heating experiment on a <4μm grain-sized fraction of bulk Allende, measurements by this technique reveal a complex isotopic structure in N from carbon, sulfide, and silicate phases of the meteorite, but no δ^{15}N value as low as the -90‰ found by Thiemens and Clayton in one step of a similar (pyrolysis) Allende heating. Noble gas release from combustion of the carbonaceous carrier phases is complete by ∿600C; minumim δ^{15}N of N released by oxidation up to this temperature, ∿25% of the total in the sample, is -53‰, and coincides with release of the major fraction of H-Xe(CCF-Xe). Mobilization of N from sulfides and silicates begins at ∿580C (and at progressively higher temperatures for Ar, Kr, and Xe). Rather heavy N (-10‰) is evolved at this temperature, from either the carbon or sulfide phases. With increasing temperature, δ^{15}N drops sharply to a second minimum of -54‰ at 700C for N from sulfides or silicates, then rises monotonically to +15‰ at 1100C as ∿60% of the total N in the sample outgases from the silicates. In comparison, ∿45% of the total Xe is contained in the silicates, and 136/132 is virtually constant at ∿0.330. Integrated values are N = 42.4ppm, a factor ∿2 higher than bulk Allende concentration (probably due to carrier enrichment in this fine-grained separate), and δ^{15}N = -29‰, within the range of previous measurements on bulk Allende.

Nitrogen analyses of an Allende acid residue, and of samples containing recent and ancient solar wind nitrogen, are in progress.

#74

Rare Earth Elements in Acid Leaches and Residues from Whole Rock and Mineral Separates from Lunar Basalt 75055.

S. Jovanovic and G. W. Reed, Jr.
Chemistry Division, Argonne National Laboratory, Argonne, IL 60439

Mineral separates from basalt 75055 were leached for ∿10 minutes with hot H_2O and then for the same time with 0.1 N HNO_3 to remove in the first case H_2O-soluble phases, in particular, and in the second to determine Cl and P_2O_5 association with the minerals. The 0.1 N acid leach dissolved ∿40% of the non-H_2O soluble fractions of these elements. The Cl/P_2O_5 ratio was close to that of the residue after the 0.1 N HNO_3 leach suggesting the same mineral, apatite, as the source of these elements. This result prompted us to extend the experiment to examine the REE since in lunar material REE and P are associated with the phase designated as KREEP. U, also KREEP related, was already being measured.

Five samples were measured: a whole rock aliquant, a residue from the mineral separation, 95-99% pure pyroxene and plagioclase phases and an ilmenite-rich phase. Significant fractions of REE were leached with 0.1 N acid, but there appears to be no consistent relationship between REE and P_2O_5. Relative to W.R., the acid leaches and residues from mineral separates appear depleted in HREE. Relative to W.R., an enriched HREE component is found in the residue from the mineral separation after it was leached with 0.1 N acid. These observations and a number of others will be elaborated on; they indicate a complex association of REE with basalt components. Although pyroxene is the main major mineral repository for REE in the basalt, about 1/3 of the REE were leached in 10 minutes with 0.1 N acid, a treatment which would not be expected to attack the pyroxene.

Comparative Chemistry of Size Fractions From the Apollo Sites

Laul, J. C.
Battelle Northwest Laboratories, Richland, Washington 99352

Eleven surface-matured soils (10084, 12001, 12033, 14163, 15221, 15271, 64501, 67461, 72501, 76501 and 78221) from six Apollo sites (Apollo 11, 12, 14, 15, 16 and 17) were sieved into four size fractions (>90μm, 20-90μm, 10-20μm and <10μm). The chemical study for 31 major, minor and trace elements in 55 bulk and size fractions was done by INAA at Battelle Northwest, whereas, the petrologic study of >90μm, 20-90μm and 10-20μm size fractions of the same soils was carried out by Papike's group at Stony Brook, New York.

To first approximation, the chemistry of coarse >90μm, 20-90μm and even 10-20μm fractions is nearly identical but quite different from the <10μm fine fractions. This observation is one of the major findings which indicates that the cutoff for change in chemistry is probably below the <10μm size. The <10μm fine fractions comprise about 10-15% of the bulk soil and are consistently more feldspathic and enriched in highland (anorthositic + KREEP) material especially KREEP relative to the coarse fractions in all soils. The chemical compositions of the bulk and four size fractions are matched by petrologically constrained multicomponent mixing model. In each soil there is a general trend of decrease in mare material and increase in highland material from the coarse to the fine fractions. However, the relative proportions of anorthositic and KREEP components varies widely both in the coarse and fine fractions depending on the soil. The KREEP enrichment observed in the fines at the six Apollo sites strongly suggests that KREEP is distributed in the soil on a moonwide basis. However, the nature of KREEP type is different from site to site. The origin of different KREEP type enrichment in the fines at each site is largely derived locally or from nearby sources; which implies that any lateral transport of fines over large distances of several km is rather inefficient. Lateral transport at short distances and vertical mixing of the regolith appear to be the dominant processes for the KREEP enrichment in the finer fractions.

#76

A SPECTRAL REFLECTIVITY STUDY OF THE REINER GAMMA FORMATION

Bell, J.F. and Hawke, B.R.
Hawaii Institute of Geophysics, Honolulu, HI 96822

The Reiner Gamma Formation in western Oceanus Procellarum is a peculiar surficial deposit similar in albedo but not in shape to the rays of recent craters. Recent analyses of Apollo subsatellite data have shown that the 30 x 60 km central portion of this feature appears to be highly magnetic in comparison with returned lunar samples.[1] We are investigating the nature of this almost unique lunar feature by means of telescopic reflection spectra and color ratio images. A 0.3-1.1 μm spectrum of the central region does not match in detail any observed fresh mare or highland region, but might be produced by a mixture of the two. The crater Dawes in the Serenetatis-Tranquilitatus boundary area has a similar spectrum and represents such a mixture.[2]

Color ratio images show that the formation's "tail" which extends north into the Marius Hills has very similar optical properties. This severely constrains models in which the bright areas of Reiner Gamma are preserved by magnetic deflection of the solar wind.[3] Further work will include infrared spectra (to 2.5 μm) of selected regions of the formation and possible source areas.

[1]Hood, L.L, Coleman, P.J., and Wilhelms, D.E., Lunar Nearside Magnetic Amomalies. Proc. Lunar Planet. Sci. Conf. 10th, 2235-2257, (1979).

[2]Pieters, C., Characterization of Lunar Mare Basalt Types - II: Spectral Classification of Fresh Mare Craters. Proc. Lunar Sci. Conf. 8th, 1037-1048, (1977).

[3]Hood, L.L., and Schubert, G., Lunar Magnetic Anomalies and Surface Optical Properties. Science, 208, 49-51, (1980).

FORMATION OF A LUNAR MAGMA OCEAN BY PARTIAL MELTING

Drake, Michael J.
Lunar and Planetary Laboratory, University of Arizona, Tucson, Arizona 85721

The concept of a lunar magma ocean is a widely accepted paradigm for interpreting lunar petrology, geochemistry, and geophysics. Its application has led to disturbing results, however, including apparently nonchondritic ratios of refractory elements such as Ca, Al, and REE in the bulk Moon, in conflict with the predictions of simple theories of nebular condensation, and to the controversy concerning the identification of ferroan anorthosites and the Mg-rich plutonic series as magma ocean products. Partly in consequence some authors question the former existence of a magma ocean, while others invoke complex dynamical processes during its crystallization. It seems possible, however, that chemical fractionations may occur during the formation of a magma ocean.

Unless the Moon melted totally, the magma ocean must have accumulated from increments of partial melt. Partial melting requires by definition that chemical fractionations occur. Recent calculations by other authors suggest that, in a melting system with large physical scale, melt will segregate efficiently from solid at low degrees of melting. In this context it should be noted that the bulk composition of the Moon is sufficiently poorly constrained that the second most refractory phase at depth in the Moon may be orthopyroxene, clinopyroxene, or garnet. In addition phase diagrams appropriate to possible lunar bulk compositions at high pressure are largely schematic. Thus the nature of possible chemical fractionations during partial melting is speculative at best.

Possible consequences of the formation of a lunar magma ocean by accumulation of partial melt increments include:

(i) A magma with fractionated refractory element ratios relative to the bulk Moon. The magma may be chemically stratified.

(ii) A magma depleted in siderophile and chalcophile elements relative to the bulk Moon.

(iii) Complications due to pressure-induced phase transitions as the residual solid compacts beneath the segregating melt or as additional material accretes to the Moon during partial melting.

(iv) A refractory, barren, olivine-rich layer beneath the base of the ocean zoning downwards towards a more fertile bulk lunar composition.

#78

ECCENTRIC LUNAR ANOMALIES: GEOCHEMISTRY CORRELATED WITH LONGITUDE

Paul H. Warren
Department of Geology, Institute of Meteoritics, University of New Mexico, Albuquerque, NM 87131

The Apollo and Luna samples come from locations that may be classified by longitude: (a) western sites: A 12 and 14, 23.4-17.5° W; (b) near-eastern sites: A 11, 15, 16 and 17, 3.7-30.8° E; (c) far-eastern sites: L 16, 20 and 24, 56.3-62.2° E. Wakita et al. (1975) observed that among ANT (i.e., nonmare, nonKREEPy) rocks there is an excellent linear correlation between Sm concentration and Eu anomaly (sample (Eu/Sm) ÷ chondritic (Eu/Sm)). The diagonal line in Fig. 1 is based on lines in figures by Wakita et al., which were based almost exclusively on near-eastern ANT rocks. Fig. 1 shows that even when the data set is restricted to pristine materials only, the correlation is still very good. This may not be too surprising.

However, another phenomenon manifested in Fig. 1 has (to my knowledge) never been observed – or predicted, before: Simply put, a given western sample with a given Sm concentration is likely to have a far greater Eu anomaly than a near-eastern sample with the same Sm concentration. The most extreme case is anorthosite 14160,105 (Warren and Wasson, 1980), which has 7.6 times more Eu than does a typical near-eastern rock with the same Sm concentration. Also, far-eastern (Luna) samples tend to have smaller Eu anomalies than near-eastern samples. Thus, the intermediate longitude sites are also intermediate in terms of Sm-Eu systematics.

Even though western ANT rocks tend to have higher Eu/Sm than eastern ANT rocks, they generally have lower Ti/Sm and Sc/Sm (Warren and Wasson, 1980).

The origins of these geochemical-geographical correlations are still unclear. The proportionality of the plagioclase/liquid distribution coefficient for Eu to the Ab content of the plagioclase (Zielinski, 1975) may have played a role. The sheer size of the area involved (~80° of longitude) suggests that the origins were somehow tied up with differentiation of a magma ocean, as opposed to strictly local magmatic processes.

References

Wakita H., Laul J.C., and Schmitt R.A. (1975) Geochem. Jour. 9, 25-41.

Warren P.H. and Wasson J.T. (1980) Proc. Lunar Planet. Sci. Conf. 11th, in press.

Zielinski R.A. (1975) Geoch. Cosmoch. Acta 39, 713-734.

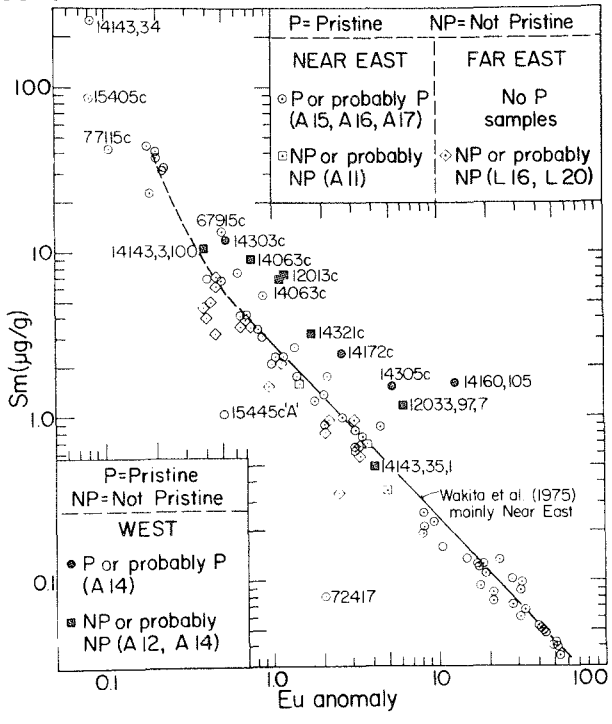

Fig. 1 →

LABORATORY EXPERIMENTS ON THE MOBILITY OF AU AND OTHER SIDEROPHILE ELEMENTS IN LUNAR HIGHLAND MATERIAL.

Wänke H., Dreibus G., Palme H., Rammensee W., and Spettel B.

Max-Planck-Institut für Chemie, 6500 Mainz, W.-Germany

The influence of mobilization effects on the observed distribution of siderophile elements in lunar highland samples was studied in laboratory experiments. In order to model the lunar condition closely, we have used samples from lunar soil 60601. After neutron irradiation (7×10^{11} n/cm^{2}sec for 6 hours) aliquots of about 100 mg of lunar soil were put in a quartz tube together with a Ni, respectively Fe foil (thickness 10μ), which was kept about 10 mm apart from the soil samples. After evacuation the samples were heated to temperatures between 600°C and 1200°C for 1 hour to 50 hours. At the end of each experiment the metal foil was removed from the quartz tube, carefully cleaned from adhering dust and analysed by γ-spectroscopy. Oxygen fugacity was fixed by the FeO-Fe, resp. NiO-Ni buffer system. The results from these experiments as obtained so far can be summarized as follows:

1.) Volatile elements: Cu, Zn, Ga.

Equilibrium between metal foils and soil samples was reached within 50 hours at temperatures below 1000°C. Typical experimental results (50 hours, 1000°C): 92 % of the total amount of Cu (originally present in the soil sample), 74 % of Zn and 21 % of Ga are in the Ni-foil. Replacing the Ni-foil by an Fe-foil, resulted in 20 times lower concentrations of Zn in the Fe-foil, because the activity coefficient of Zn in Ni is much lower than in Fe. In this case significant amounts of Zn were found in the quartz tube.

2.) W, Au, Fe and Co.

After 50 hours at 1000°C: The fractions of these elements in the Ni-foil: W 26 %, Au 25 %, Fe 21 %, Co 12 %. The respective numbers for 800°C (50 hrs): W 2.6 %, Au 4.4 %, Fe 8.4 %, Co 2 %. At 600°C (50 hours) about 0.1 % to 0.4 % of these elements were found in the foil. None of these elements was ever found in the quartz.

3.) Iridium.

After 50 hours at 1000°C: Iridium is below detection limit in Fe and Ni foils, i.e. Ir is at least a factor of 30 less mobile than Au. Even at 1200°C Ir is not mobilized.

4.) Lithophile elements: Na, Sc and La.

At 1000°C for 50 hours: Less than 0.1 % of these elements were found in Fe- and Ni-foils. But some Na and K was found in the quartz tube.

Conclusions:

Already at temperatures of 600°C to 800°C non-refractory siderophile elements will be redistributed in the lunar regolith. Tungsten does not behave as a refractory element under these conditions. However, siderophile elements only redistribute among metal phases.

#80

Evolutionary History of Volatiles During Lunar Regolith Maturation

E. H. Cirlin and R. M. Housley
Rockwell International Science Center
Thousand Oaks, California, 91360

Thermal release profiles of Pb and Zn in immature and mature regolith samples (<1mm) from Apollo 11, 14, and 16 sites were obtained by flameless atomic absorption technique (FLAA). Samples were chosen according to maturity index (1). Most of Pb in immature sample 14141 (I_S = 5.7) and submature samples 63501 (I_S = 46), 67701 (I_S = 39) were released below 1000°C and therefore is surface Pb. On the other hand, mature samples 10084 (I_S = 78) and 65701 (I_S = 106) showed very little surface Pb. Most of Pb in mature samples were released >1100°C when the samples were molten suggesting loss of the surface volatiles and entrapment of volatiles in high temperature sites during brecciation or agglutination processes. Meyer et al. (2) showed that the concentration of volatiles in minerals increased as the size of mineral grains decreased. On the other hand, volatile contrations in agglutinates stayed the same. They suggested that volatiles such as Zn or Cd might have been lost during the maturation processes. Laul et al. (3) also reported that the Zn depth profile of an Apollo 17 drill core sample showed anti-correlation with the maturity index.

We also studied thermal release profiles of Zn in various types of hand-picked individual grains from 150-420 μm size fraction of submature sample 67701 which contains substantial surface Zn. Five clean anorthites showed almost no surface Zn or high temperature Zn. On the other hand, shocked anorthite grains showed both surface and interior Zn. Breccias showed very little surface Zn, but high concentrations of high temperature Zn (4). Agglutinates showed (4) considerable amounts of both surface and interior Zn (less surface Zn than interior Zn).

References

(1) Morris, R. V. (1978), "The Surface Exposure (Maturity) of Lunar Soils: Some Concepts and I_S/FeO Compilation." Proc. Lunar Sci. Conf. 9th (1978), pp. 2287-2297.

(2) Meyer G., von Gunten, H. R., Grütter, A., Jost, D., Krähenbühl, U., and Wegmuler, F., (1979) "Grain Size Distribution and Origin of Trace and Major Elements in Agglutinates and Minerals of Soil 75080" (abstract). In Lunar Science X, pp. 839-841. The Lunar Science Institute, Houston, Tx.

(3) Laul, J. C., Lepel, E. A., Vaniman, D. T., and Papike, J. J., (1979), "The Apollo 17 Drill Core: Chemical Systematics of Grain Size Fractions". Proc. Lunar Sci. Conf. 10th, pp. 1269-1298.

(4) Cirlin, E. H., Housley, R. M., and Grant, R. W., (1978), "Studies of Volatiles in Apollo 17 Samples and Their Implication to Vapor Transport Processes". Proc. Lunar Sci. Conf. 9th, pp. 2049-2063.

SURFACE DEPOSITS OF TRACE ELEMENTS ON LUNAR SAMPLES INVESTIGATED BY HEATING TECHNIQUES

J. Sörensen, F. Wegmüller, U. Krähenbühl and H.R. von Gunten
Anorganisch Chemisches Institut, Freiestrasse 3, CH-3000 Bern 9

The volatilization behaviour of trace elements such as Ag, Br, Cd, Hg, In, Se and Zn is investigated by heating techniques. The samples are activated in a reactor, separated according to their magnetic properties and grain-sizes. The resulting fractions are heated in He or H_2 gas for time intervals of 30 s to 12 hours and temperatures between 130°C and 1000°C. The mobilized volatile elements and compounds are separated from each other in a second step in presence of N_2/Cl_2 gas and are measured by γ-ray spectroscopy.

Tracer experiments with Zn-65 established the possibility to distinguish between surface deposited species and those residing in the interior of the samples.

For lunar samples the following results were obtained: Volatile elements are enriched on the surfaces of minerals and agglutinates. The surface concentrations were determined for a number of elements. The volatilities of the elements under laboratory conditions follow the sequence Hg $\gg$ Cd $>$ Zn $>$ Se $>$ In $>$ Br $\gg$ Ag. Hg is volatilized significantly at $T \leq 130^{o}$. It is therefore volatile during lunar days.

#82

NITROGEN AND SAMARIUM ISOTOPES IN ANCIENT LUNAR MICROBRECCIAS

Thiemens, M.H.[1], Lugmair, G.W.[2], and Clayton, R.N.[1] (1) Enrico Fermi Institute, Univ. of Chicago, Chicago, IL 60637 (2) Dept. of Chemistry, Univ. of California San Diego, La Jolla, CA 92093

The Apollo 11 and 17 soil breccias 10018, 10060, 79135 and 79035 have been shown [1] to be unique in their nitrogen isotopic components in that (1) they contain the lightest, and presumably most ancient, implanted solar wind component and (2) the ^{15}N cosmic ray exposure ages are all in excess of 2.0b.y. Since these exposure ages are at least a factor of four longer than any reported rare gas exposure ages we have analyzed aliquots of these four samples for samarium isotope ratios to determine their neutron fluence Φ, which possibly might help to constrain the effective average irradiation depth in the lunar regolith.

The results are given in Table I along with the bulk nitrogen isotopic ratios. For fluence calculations we have tentatively assumed an effective neutron capture cross section of 5×10^4 barns for ^{149}Sm. There is, of course, at least a 10% uncertainty in these calculations since, for instance, no attempt has been made as yet to account for effects of soil chemistry on $\langle\sigma_{149}\rangle$.

There are several remarkable features to be noted in Table I; in particular are the neutron fluences for the pairs 10018, 10060, and 79135, 79035. Within experimental error the fluences are identical. In addition, the total implanted solar wind nitrogen in all four samples is very similar, all containing components in their stepwise heating release which are less than -170‰ ($\delta^{15}N$). The ^{15}N exposure ages for the four samples are all quite similar, 2.5 ± .3 b.y. based on surface production rates, which suggests very similar regolith histories since these parameters measure different exposure indices. The close resemblance of the Apollo 11 and 17 soil breccias implies that the constituent soils must be derived from very similar layers which are completely unlike any soil that has been sampled in either the Apollo 15 or 17 drive tubes. These layers must be at least several meters deep and perhaps reside at the very bottom of the regolith and are possibly compacted against the bedrock during their compaction.

The neutron fluxes given in Table I are calculated using the ^{15}N exposure ages (which assumes surface production rates). The fluxes imply that the samples received their spallogenic and neutron exposure records either very shallow (<10 cm) or at a depth between 1 and 2 meters.

[1] Thiemens, M.H. and R.N. Clayton (1980) Earth Planet. Sci. Lett. 47, 34-42.

TABLE I

	ε(1)	Φ(10^{16} n cm^{-2})	$\delta^{15}N$ (‰)	Flux (n cm^{-2}sec^{-1}
Standard	≡ 0	≡ 0	---	≡ 0
10060	53.2 ± .9	3.70 ± .09	-134	0.42
10018	52.5 ± .9	3.64 ± .06	-136	0.50
79135	82.3 ± 1.3	5.71 ± .09	-138	0.85
79035	84.1 ± .6	5.84 ± .04	-171	0.70

(1) $\varepsilon = 10^4 \times [(^{150}Sm/^{149}Sm)_{sample}/(^{150}Sm/^{149}Sm)_{terr.\ std.} - 1]$

LONG TERM AVERAGE, 2 m.y., OF He AND Ne ISOTOPIC RATIOS IN SOLAR FLARES.

Yaniv, A.[1,2] and Marti, K.[3]
[1]Dept. of Phys.&Astronomy,Tel Aviv Univ., Ramat-Aviv, Israel; [2]Present address: Max-Planck-Inst.f. Kernphysik, Heidelberg, F.R. Germany
[3]Chemistry Dept., Univ. of California, La Jolla, Calif., USA.

Stopped solar flare He and Ne were found in the top few mm-layers of lunar rock 68815 whose exposure age on the lunar surface is 2 m.y. The concentration profiles agree well with the expected ranges for stopped solar flare particles. The long term average, 2 m.y., of the solar flare ratio $He^3/He^4 \approx 10^{-1}$ compares to $He^3/He^4 \approx 3 \cdot 10^{-4}$ observed in the solar wind, but agrees with some satellite observations of solar flare events. Ne^{20}/Ne^{21}; Ne^{20}/Ne^{22} ratios in solar flares were found to be smaller than those observed in solar wind, which is in agreement with recently reported ratios from satellite observations. More work on several other moon rocks is in progress. The possibility that the observed variations may be due to nuclear reactions during solar flare particle propagation will be discussed. In addition, implications for the possible introduction of isotopic anomalies into solar system material are considered.

#84

INVESTIGATION OF HEAVY ION INDUCED SPUTTERING: IMPLICATIONS FOR THE SOLAR WIND EROSION OF EXTRATERRESTRIAL SAMPLES.*

Thiel, K., Külzer, H. and Herr, W.
Institute of Nuclear Chemistry, University of Cologne,
D 5000 Koeln-1, Federal Republic of Germany

Silicate, phosphate and borate glasses as well as selected silicate minerals (orthoclase, plagioclase) were chosen to study Ar^+-, Fe^+- and Xe^+-induced sputtering in the energy range of 50 to 130 keV at different angles of incidence (0^o, 45^o, 60^o).Total sputter yields were determined using particle track and interferometric methods. The determination of differential angular distributions of the sputtered particles was achieved by means of a specially developed technique of particle track autoradiography. Dose and energy dependence of the total sputter yield as well as the emission of "chunks" in the given dose and energy range were studied. No indications of preferential sputtering were observed after the erosion of surface layers having thicknesses in the order of the incident ion range. Total sputter yields of the glasses for vertical ion incidence were found to vary from 1.2 atoms/ion (borate glass) to 9.9 atoms/ion (phosphate glass). In the case of feldspars the sputter rate of different crystallographic planes was investigated for vertical incidence of 50 keV Ar^+-ions in the dose range of $6 \cdot 10^{16}$ to 10^{18} cm^{-2}. Calculated values for the solar wind erosion rates of the glasses and crystals investigated are presented.

*This work was financially supported by the Bundesministerium fuer Forschung und Technologie, Bonn.

XENON IN MAGNETIC SEPARATES OF AN ALLENDE INCLUSION

Kirschbaum, C. and Bond, J.K. (Sponsored by J.H. Reynolds)
Department of Physics, University of California, Berkeley, CA 94720

Lumpkin and Zaikowski (1) developed a method for performing magnetic mineral separations of small amounts of fine grained samples. They obtained four fractions of an Allende inclusion, with olivine and clinopyroxene concentrated in the most magnetic fraction, and spinel, grossular, perovskite and anorthite concentrated in the least magnetic fraction. We have measured the xenon released in stepwise heatings of these separates. Trapped $^{132}Xe_t$, radiogenic $^{129}Xe_r$, and fissiogenic $^{136}Xe_f$ amounts are set out in the Table.

There is a strong correlation between trapped xenon and the magnetic property with trapped xenon being concentrated in the most magnetic fraction. For the total sample (as determined by summation) the release of $^{132}Xe_t$ was 10% at 800°C; 57% at 1100°C; 32% at 1300°C and 1% at 1500°C, similar to results obtained by other workers (2,3). These results suggest that the trapped xenon is primarily in clinopyroxene and/or olivine. There is no strong correlation between $^{129}Xe_r$ content and the magnetic property; the middle fractions have slightly more $^{129}Xe_r$ than the most and least magnetic fractions. The release of $^{129}Xe_r$ (again for the total sample) was 4% at 800°C; 86% at 1100°C; 9% at 1300°C and 0.5% at 1500°C, again similar to previous results (2,3). The apparently more random siting of the $^{129}Xe_r$ suggests that it is located in minor phases heterogeneously distributed in the inclusion. Fissiogenic xenon is readily apparent in the least magnetic fraction, but less so in the more magnetic fractions. It is partially masked in those by the large trapped xenon amounts. For the least magnetic fraction three isotope correlation plots show that the fissiogenic gas has a $^{132}Xe/^{136}Xe$ ratio of 1.17 ± 0.25, and a $^{134}Xe/^{132}Xe$ ratio of 0.90 ± 0.15, consistent, within errors, with ^{244}Pu fission (4), but distinct from ^{238}U fission (5) and H-xenon (6). The release of $^{136}Xe_f$ (total sample) was 12% at 800°C, 68% at 1100°C, 20% at 1300°C and less than 1% at 1500°C. Other workers (2,3) have observed ^{244}Pu fission xenon in Allende inclusions. The release patterns we obtain are similar to those obtained by Zaikowski (2) but differ from those by Podosek and Lewis (3). The Table has been prepared assuming ^{244}Pu fission for all fractions. Because of large errors in the results no reasonable conclusions can be drawn regarding which minerals contain the fissiogenic component.

Fraction	Weight (mg)	$^{132}Xe_t$ (10^{-10}cc/g)	$^{129}Xe_r$ (10^{-10}cc/g)	$^{136}Xe_f$ (10^{-10}cc/g)
1 (most magnetic)	13.4	8.77(.65)*	32.4(3.2)	9.0(3.9)
2	36.8	6.90(.51)	41.7(4.7)	3.6(7.0)
3	44.9	3.13(.26)	60.7(6.1)	15.3(4.5)
4 (least magnetic)	12.4	1.00(.12)	22.4(2.8)	5.6(1.4)

*(1σ errors)

(1) Am. Mineral. 65, 390-392 (1980); (2) EPSL 47, 211-222 (1980); (3) EPSL 15, 101-109 (1972); (4) Science 172, 837-840 (1971); (5) J. Inorg. Nucl. Chem. 33, 1509-1513 (1971); (6) Preprint by Pepin and Phinney, submitted to Moon and Planets.

#86

RADIOGENIC ^{129}Xe IN MINERAL SEPARATES FROM THE ALLENDE METEORITE

Jan Hertogen* and Jane Crabb

Department of Chemistry and Enrico Fermi Institute, University of Chicago
Chicago, IL 60637

Xenon has been measured in 23 fractions separated from Allende, in order to investigate the siting of $^{129}Xe_r$. A bulk sample was disaggregated by repeated freezing and thawing, and divided by settling into coarse and fine material. A chondrule fraction was removed from the coarse material, after which it was separated by grain size and by magnetic susceptibility. Sulfides were concentrated by handpicking. Most fractions were analyzed for Fe, Cr, Co, Sc, Ir, and Au by INAA. Data have already been reported for several of the sulfide separates (*1*).

Though 98% of the material and 70% of the trapped Xe were recovered, only some 40% of the $^{129}Xe_r$ remained. This suggests that $^{129}Xe_r$ is either located mainly in a minor, easily lost phase, or that it was leached by water during disaggregation. Separates that are most enriched in a single component--high temperature inclusions, isolated sulfide grains and metal--tend to have particularly low contents of $^{129}Xe_r$ (1 to 4×10^{-10} cc/g; all gas concentrations are given in these units). For the coarse-grained (>100 μ) material, $^{129}Xe_r$ ranged from 1 to 9 and was inversely correlated with Fe content (44 to 17%). This argues against Fe-bearing phases such as sulfides and iron-rich silicates as the host for $^{129}Xe_r$ in these fractions. More than half of the $^{129}Xe_r$ recovered was in the fine-grained (<5 μ and <44μ) matrix fractions (129_r ~7) and another 30% was associated with chondrules (129_r ~7-11).

One component that is often enriched in $^{129}Xe_r$ is sulfide-rimmed chondrules, as previously found by (*2*). A measurement on separated rims shows them to be enriched over whole chondrules, although they still account for only a few percent of the mass and $^{129}Xe_r$ of the meteorite. The sulfide mineralogy, peripheral location, and a high Ir content suggest that the rims formed by relatively low temperature (<700°K) alteration of a refractory metal precursor. An interesting parallel is rims on fine-grained inclusions, which are rich in volatiles and contain a substantial portion of the bulk $^{129}Xe_r$ (*3,4*). These two occurrences suggest that a comparatively late addition of I is responsible for a large part of the $^{129}Xe_r$.

REFERENCES

1. Lewis R.S., Hertogen J., Alaerts L., and Anders E. (1979) *Geochim. Cosmochim. Acta 43*, 1743.
2. Fireman E.L., DeFelice J., and Norton E. (1970) *Geochim. Cosmochim. Acta 34*, 873.
3. Wasserburg G.J. and Huneke J.C. (1979) *Lunar Planet. Sci. Conf. X*, 1307.
4. Zaikowski A. (1980) *Earth Planet. Sci. Lett. 47*, 1743.

*Current Address:
K.U.L., Fysico-chemische geologie
de Croylaan 42
B-3030 LEUVEN-Heverlee, BELGIUM

SEARCH FOR ^{129}Xe BEARING PHASES IN ALLENDE BY LASER MICROPROBE

Rison, W., Zaikowski, A.† and Lumpkin, G.R.
Department of Physics, University of California, Berkeley, CA 94720

A laser microprobe connected to a conventional rare gas mass spectrometer was used to probe various phases of the Allende C3 meteorite for xenon. Minerals in polished sections were identified optically and by SEM/EDAX. The polished sections were placed in a vacuum chamber with a glass window, which was attached to the sample inlet system of the mass spectrometer. A zap from the laser, fired through the window, produces a roughly hemispherical pit approximately 50μ in radius, vaporizing about 1 μg of sample. To obtain sufficient xenon to measure with the conventional system, 50 zaps of the sample were required for each run. ^{129}Xe excesses were measured, and variations were observed in different phases of the meteorite. Preliminary results are described in the Table.

The fine grained inclusion CAI-F6 (nepheline with minor pyroxene) had about 10^4 atoms of $^{129}Xe_r$/zap, or about 3×10^{-10} cc/g, much less than the 10^{-8} cc/g measured in other fine grained inclusions by some other workers (1,2), but comparable to the amounts found in "chondrules" by Fireman et al. (3). Within single inclusions and chondrules different minerals had different $^{129}Xe_r$ contents. For example, melilite had more $^{129}Xe_r$ than pyroxene in coarse grained inclusion CAI-B2. Pyroxene had significantly more $^{129}Xe_r$ than olivine in chondrule C7, and a dark rim surrounding the chondrule had $^{129}Xe_r$ comparable to the pyroxene. The same minerals in different samples had differing $^{129}Xe_r$ contents. Pyroxene in C7 had considerably more $^{129}Xe_r$ than pyroxene in CAI-B2, and olivine in C7 had more than olivine in the chondrule G2.

It appears that the iodine sites in Allende are heterogeneously distributed [cf. Reynolds et al. (4), in a study of individual mineral grains].

Sample	Mineral or (run)	^{129}Xe (10^3 atoms/zap)
Matrix	(1)	3.5(3.2)*
	(2)	8.0(0.8)
C7	pyx	8.0(1.9)
chondrule	olv	2.9(0.6)
	rim (pyx)	7.4(0.8)
C9	(1)	4.5(2.5)
chondrule	(2)	5.7(1.6)
olivine + glass	(3)	1.3(0.8)
CAI-B2	melilite	3.5(1.1)
coarse grained	pyx	1.6(1.0)
inclusion		
CAI-F6	(1)	11.2(1.4)
fine grained	(2)	6.9(1.7)
inclusion		
G2	olv	-1.7(1.5)
chondrule	glass	1.0(0.9)

*(1σ errors)

Results for coexisting minerals are generally consistent with the ability of various mineral structures to accommodate large atoms of ^{129}I, which should follow the order nepheline > melilite > pyroxene > olivine. The main shortcoming of our work is the low precision obtainable with the conventional system. The use of the laser microprobe with a mass spectrometer designed specifically for analyses of very small samples, such as those described by Reynolds et al. (4) and Hohenberg (5), holds great promise as a means to probe meteorites effectively with 50μ resolution.

(1) EPSL 47, 211 (1980); (2) GCA 34, 341 (1970); (3) GCA 34, 873 (1970); (4) Z. Naturforsch. 35a, 257 (1980); (5) Preprint, subm. to Rev. Sci. Instr.

†Present address: Bendix Field Engineering Corporation, P.O. Box 1569, Grand Junction, CO 81502

#88

ALIEN XENON IN ALLENDE INCLUSIONS.

Jordan, J., Jessberger, E.K., Kirsten, T., and El Goresy, A.
Max-Planck-Institut f. Kernphysik, Heidelberg, F.R. Germany

Recent measurements in our laboratory of xenon released by stepwise heating on two Allende inclusions have revealed an unusual isotopic structure. One of these inclusions (no.18 from (1)) has been shown to have an old Ar-Ar age (1); the other (no. 21 from (1) or 3529,29 from (2)), while having a normal age (3), was attractive on the basis of the observation of the presence of Ru and Mo in the oxidized state, indicating condensation under oxidizing conditions (4). The most salient feature of the xenon structure is a tremendous excess of the usually "normal" isotope 132, which was most pronounced for the inclusion in which the presence of oxidized Ru and Mo was observed. In the 1650^{o}C fraction of this inclusion, the ratios of 132 to the next most abundant isotopes 129 and 131 are $\sim$1.5 and $\sim$5, respectively. The origin of this anomalous 132-xenon will be discussed.

References:

(1) Jessberger, E.K. and Dominik, B., 1979: Nature 277, No.5697, p. 554.
(2) Mason, B. and Martin, P.M., 1977: Smith.Cont. Earth Sci., No.19, p. 84.
(3) Jessberger, E.K. et al.,1980, Icarus 41, in press.
(4) El Goresy, A. et al., 1979, Meteoritics 14, p. 390.

NUCLEOSYNTHETIC ORIGIN OF ANOMALOUS KRYPTON : TEST OF A SIMPLE MODEL

Urs Frick

School of Physics and Astronomy, Univ.of Minnesota, Minneapolis MN 55455

So far the large negative anomaly at ^{78}Kr in samples with enhanced light and heavy Xe isotopes has been seen only in a Berkeley mass spectrometer *(1)*. Although it seemed unlikely, an instrumental artifact could not be strictly ruled out until independent confirmation in a different system. We have now analyzed the Kr mobilized during closed -system combustion of an Allende acid residue. The new data accord well with correlations seen earlier; most importantly, the large negative anomaly at ^{78}Kr is fully confirmed in our double-focusing spectrometer which completely resolves Kr from hydrocarbon peaks at mass 78. The most extreme data point (600°C combustion) is depicted in the left panel of the Fig. The solid line connects data corrected for the lowest blank, measured immediately after the experiment; solid squares ■ represent the composition of anomalous Kr from straight line correlations to $^{78}Kr/^{84}Kr = 0$ through all Minneapolis and Berkeley data. We have related this composition to first results of astrophysical modeling utilizing n-capture and photodisintegration within various shells of an evolving star of 25⊙ *(2)*. Plots of M/84 vs. 86/84 show that *the anomalous Kr at most M is consistent with a two component mixture of R and P nuclei,* perhaps with some addition of S-products. Here we present the only "non-conforming"graph, for M=82, in the right panel of the Fig. Xe ratios produced in the synthesis for various values of the neutron dose (R) and the time scale of the P-process are indicated on the Kr-ratio curves. S-Kr is taken from *(3)* with experimental limits for ^{86}Kr *(4)*. Although the anomalous Kr component ■ does not fall right on the mixing line between R- and P-Kr at parameters which produce anomalous Xe ⟶, the nuclear modeling provides to first order a surprisingly consistent roadmap for the environments of simultaneous nucleosynthesis of Kr and Xe components. Thus the proposal of nucleosynthetic origin for the heavy gas anomalies emerges as a most viable alternative to a widely promulgated interpretation based on mass fractionation and fission processes.

Ref.:(1)Frick(1977)Proc.LSC 8th.273;(2) Heymann and Dzcizkaniec(1980) preprint; (3)Clayton and Ward(1978)Ap.J.224,1000;(4)Alaerts et al.(1980)GCA 44,189.

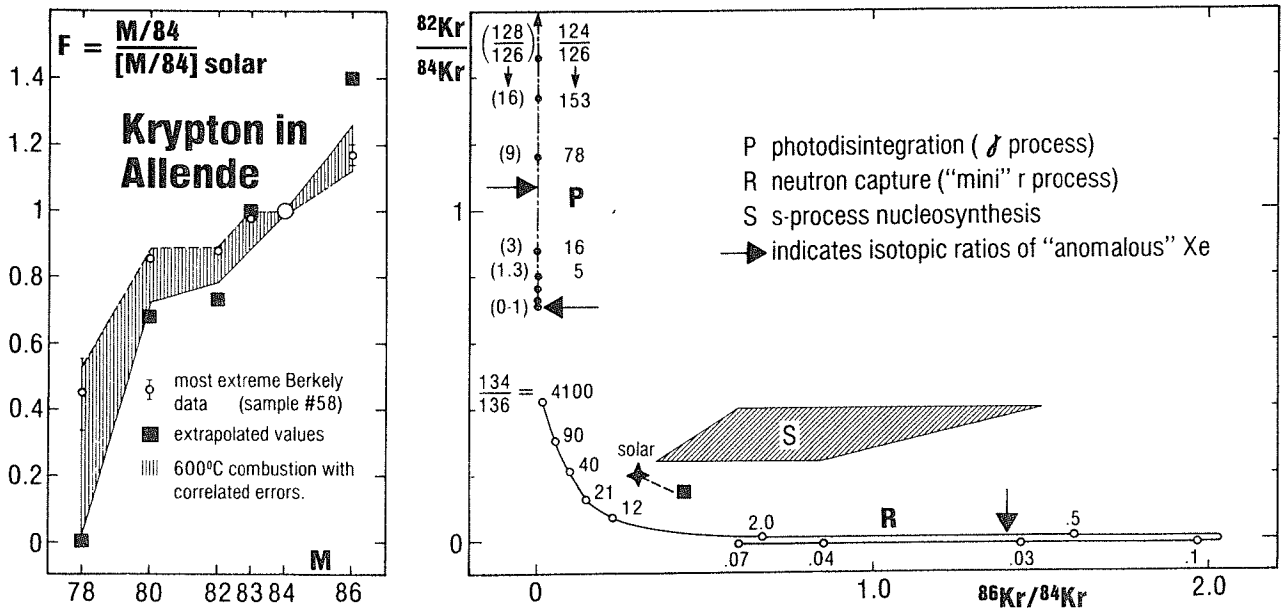

#90

FURTHER STUDIES OF AMINO ACIDS IN THE MURCHISON C2 CHONDRITE

Cronin, J. R., Gandy, W. E., Kjos, K. M., and Pizzarello, S.
Department of Chemistry and Center for Meteorite Studies, Arizona State University, Tempe, AZ 85281

The bulk of the carbon of carbonaceous chondrites has long been recognized as occurring in the form of organic compounds. About ten years ago indigenous amino acids were convincingly shown to account for a part of this carbonaceous matter. An extraterrestrial origin for these amino acids was suggested, in part by the wide range of their structural diversity. Within the two general classes of amino acids found (saturated aliphatic monoamino monocarboxylic aicds and the corresponding dicarboxylic acids) all possible chain and position isomers appear to be present. In order to more rigorously test the concept that chemical evolution of these chondritic amino acids has given rise to all possible isomeric forms, analyses have been carried out for the C_6 α-amino acids. These include seven chain isomers (the amino acids norleucine, 2-methyl norvaline, isoleucine (and alloisoleucine), leucine, 2-amino-2-ethyl butyric acid, 2-amino-2,3-dimethyl butyric acid, and pseudoleucine) comprising a total of 15 possible stereoisomers. Evidence for the presence of these amino acids (except norleucine) in hot-water extracts of powdered Murchison samples has been obtained by combined GC-MS. Quantitative data were obtained by ion exchange chromatography with fluorimetric detection. The results are consistent with the view of chemical synthesis by a qualitatively nonselective process.

Considerable variation is seen in the relative amounts of C_6 α-amino acids found in Murchison. Quantitative comparison was made between these recent Murchison results and the amino acid products of Fischer-Tropsch type (FTT) syntheses and Miller-Urey spark discharge syntheses. The Murchison amino acids are seen to comprise a characteristic suite differing from the amino acids produced by either of these proposed synthetic models. The low level of straight chain forms in Murchison is in marked contrast to the prevalence of these amino acids in FTT products. The relative amounts of the C_6 α-amino acids in Murchison suggest that reactions of radical species may have been a controlling factor in formation of the carbon chain structures of these amino acids. (Supported by NASA grant NSG-7255)

CARBON ISOTOPIC CHANGES PRODUCED BY THERMAL VOLATILIZATION OF THE MURCHISON C2 CHONDRITE

Everett K. Gibson, Jr., and Sherwood Chang
SN7, Geochemistry Branch, NASA Johnson Space Center, Houston, TX 77058, and Chemical Evolution Division, NASA Ames Research Center, Moffett Field, CA 94035

During the past decade, numerous studies have been carried out on the behavior of meteoritic materials during thermal volatilization or vacuum pyrolysis. These studies have concentrated on investigating the role of thermal metamorphism in the evolution of early solar system objects and its effects on the retention of volatile/mobile elements during heating events. Studies of the effects of thermal volatilization on the total carbon and sulfur abundances for the Murchison C2 chondrite have been reported by Gibson (1976) in which samples were heated under vacuum (10^{-6} torr, $P_{O_2} < 10^{-10}$ atms) for 72 hours in 100° intervals between 100°C and 1200°C. Sample residues were analyzed for their volatile element abundances in order to investigate the volatile element fractionations which occur within primitive meteorites when they are subjected to varying degress of thermal metamorphism. Results of that study showed that carbon loss below 800°C was largely related to the pyrolysis of organic compounds and thermal decomposition of carbonate-like phases present in the meteorite, whereas carbon lost above 800°C results from reactions between residual carbon and the silicate matrix.

In order to better understand the nature of the carbon evolution during vacuum pyrolysis, the same sample residues analyzed by Gibson (1976) have been analyzed for their carbon isotopic compositions. Procedures were those of Sakai et al. (1976) in which the carbon remaining in the sample was combusted to CO_2 and analyzed for its isotopic composition. Bulk samples of the Murchison chondrite which were not heated contained carbon with an isotopic composition of -6.6 ‰ ($\delta^{13}C_{PDB}$) which is similar to previously reported values for other C2 chondrites and previously analyzed samples of Murchison. With heating to 300°C and 400°C, the isotopic composition changed from -6.6 ‰ to -7.7 ‰ and -8.6 ‰, respectively, indicating a small change or loss of heavy carbon components. This is consistent with the loss of heavy carbon that was in the form of pyrolyzable organic compounds or trapped heavy CO_2 in the sample or both. For the sample heated to 500°C, the residual carbon was -11.5 ‰. Over this temperature range the bulk of the pyrolyzable organic coupounds are lost and decomposition of isotopically heavy carbonates has begun. For the 600°C, 700°C, and 800°C sample residues, the isotopic compositions were -14.8 ‰, -15.9 ‰, and -16.5 ‰, respectively. Carbon from the carbonate-like phases should be lost over this temperature range. The isotopic composition of the carbon remaining in the heated samples falls within the ranges observed for bulk C3 chondrites (-15 to -19 ‰) and within the wider ranges observed for the acid insoluble carbonaceous material found in C1, C2, and C3 chondrites (-11 to -28 ‰).

References:

E. K. Gibson (1976) Meteoritics 11, 286-287.
H. Sakai et al. (1976) Geochem. J. 10, 85-96.

#92

CARBON, HYDROGEN, AND NITROGEN ISOTOPIC COMPOSITION OF THE RENAZZO AND ORGUEIL ORGANIC COMPONENTS

Robert, F. and Epstein, S.
California Institute of Technology, Pasadena, CA 91125

The concentration and isotopic composition were determined for carbon, nitrogen, and hydrogen extracted from bulk samples and acid (HF-HCl) residues of Orgueil and Renazzo meteorites. The samples were heated step-wise and the measured quantities of gasses given off at each step were analyzed mass spectrometically. The whole rock δD and $\delta^{15}N$ values are +930 ‰ and +190 ‰ for Renazzo and +170 ‰ and +40 ‰ for Orgueil respectively. Hydrogen concentrations from the acid residues, shows a bimodal release pattern at temperatures between 400 and 1300°C and the average δD of hydrogen from the acid residues from Renazzo is +2500 ‰ and from Orgueil is +1100 ‰ . The δD of the hydrogen released at the high temperature release mode is on the average of +1500 ‰ for Orgueil and +3100 ‰ for Renazzo. The low temperature-release-hydrogen has a δD value of +1000 ‰ for Orgueil and +2000 ‰ for Renazzo. These results imply that the hydrogen isotopic composition is not homogeneously distributed among the various compounds of the acid residues. The $\delta^{13}C$ of the carbon in the acid residues measured -20 ‰ for Renazzo and -5 ‰ for Orgueil. With our previous results on δD's acid residues of Murray and Murchison (+600 ‰ and +800 ‰ respectively) we are able to calculate by mass balance an approximate isotopic composition of phyllosilicates in these four meteorites. The δD's of inorganic hydrogen are calculated to be ~-250 ‰ for Murray, Murchison, and Orgueil. The minimum calculated δD values of the Renazzo phyllosilicates is +200 ‰ and thus, the unusual deuterium enrichment of this meteorite occurs both in organic and inorganic hydrogen.

Considering our isotopic measurements on various carbonaceous chondrite acid residues as a whole, it seems that there is no correlation between the isotopic composition of hydrogen and carbon or or hydrogen and nitrogen. Interstellar medium organic molecules (I.M.O.M.) show deuterium enrichment interpreted in terms of chemical fractionations during ion-molecule reactions. During this process it seems that the carbon and nitrogen are not chemically fractionated, and that their isotopic variations are due to heterogeneity of the organic molecule reservoirs. The absence of isotopic correlation in our carbon, hydrogen, and nitrogen results, suggests an analogy of the meteorite polymer with I.M.O.M.

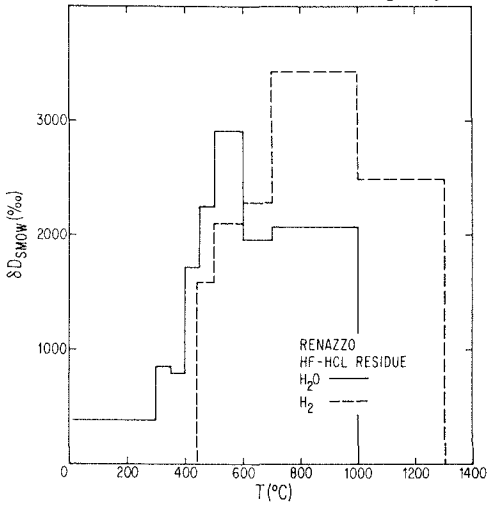

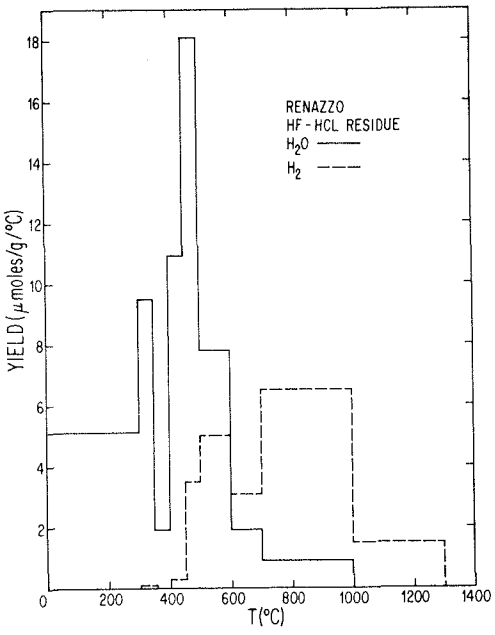

STELLAR OR INTERSTELLAR MOLECULES IN METEORITES.

M. JAVOY and Jérôme HALBOUT.
Univ. Paris VII - Labor. Géochimie Isotopique - 4, Pl. Jussieu 5ème

ROBERT, MERLIVAT and JAVOY (1) had found in the LL3 chondrite CHAINPUR the highest D/H ratios (up to 9 10^{-4}) ever found inside the solar system. In the same meteorite we have found oxygen enriched up to 1% in ^{17}O relative to other LL chondrites. The total range in oxygen isotope variation is 3 to 10.5‰ in $\delta^{18}O$ and 0.9 to 15.3 in $\delta^{17}O$ relative to SMOW. These results have been checked for the possible interferences due to the presence of NF_3 both directly in the mass spectrometer and by analyzing a meteorite of known oxygen isotopic composition rich in nitrogen. The ^{17}O rich samples define a straight line of steep slope (8±1) in the $\delta^{17}O$ $\delta^{18}O$ diagram. The ^{17}O anomaly is apparently removed by heating at moderate (400°C) to high (1200°C) temperatures. It appears to be located in the matrix and the solid rim of chondrules. It does not show up to now any correlation with the deuterium enrichments.

These results cannot be satisfactorily explained by in situ creation within the solar system. They are discussed in terms of the admixing of stellar molecules ^{17}O-enriched by nucleosynthesis or interstellar molecules enriched by nuclear or physico-chemical processes. The first hypothesis is presently favoured.

(1) ROBERT F., MERLIVAT, L. and JAVOY M.
Deuterium concentration in the early Solar System : hydrogen and oxygen isotope study.
Nature, Vol. 282, n° 5741, pp. 785-789 (1979).

#94

A COLD-ACCUMULATION MODEL FOR OXYGEN ISOTOPES

Clayton, D.D.
Rice University, Houston, TX 77001

The meteoritic community commonly assumes that meteoritic matter condensed thermally from a cooling gaseous solar nebula. I go to the opposite extreme in taking the meteoritic parent bodies to be cold accumulates of precondensed matter (1). Exothermic liberation of chemical energy forms large refractory inclusions from cold dust (2) and provides a heat source for thermal metamorphism of small parent bodies. I here illustrate by numerical example how the bulk oxygen isotopic compositions of different bodies can come about in this theory. I assume that the oxygen content is fixed by that of the cold bulk carriers, rather than by exchange with a hot gaseous nebula, in contrast to the more common picture of oxygen fractionation during hot condensation onto a few very refractory carriers of excess ^{16}O (3). Letting superscripts designate differing oxygen isotopic compositions I consider sums of carriers

$$Al_2O_3^{(1)} + MgO^{(2)} + FeO^{(2)} + NaO^{(2)} + SiO_{1.4}^{(3)} + O_2^{(4)}$$

chosen to give the average bulk chemical composition of E, H, L, and C3 chondrites. Then designating $(^{17}O/^{16}O, ^{18}O/^{16}O)$ by the vector $\underset{\sim}{O}$ and the cation abundances by their chemical symbols, the bulk oxygen composition is

$$\underset{\sim}{O} = \frac{1.5\ Al\ \underset{\sim}{O}^{(1)} + (Mg + Fe + Na)\underset{\sim}{O}^{(2)} + 1.4\ Si\ \underset{\sim}{O}^{(3)} + \Delta O\ \underset{\sim}{O}^{(4)}}{1.5\ Al + Mg + Fe + Na + 1.4\ Si + \Delta O}$$

where ΔO is the excess O_2 frozen onto cold grains to give the observed oxygen content of the meteorite (i.e. the excess over that in other carriers).

The $\underset{\sim}{O}^{(j)}$ of each carrier should differ owing to different astrophysical history. The following motivated construction yields the correct differences between E,H,L and C3 chondrites: $\underset{\sim}{O}^{(1)}$ is a linear mix of ^{16}O-pure in SUNOCON half and a smaller ^{18}O excess in STARDUST half; $\underset{\sim}{O}^{(2)}$ is mass fractionated by the process of monoxide formation and recoil ejection from grain surfaces; $\underset{\sim}{O}^{(3)}$ is a linear mix, half deficient by 5% in ^{17}O and half mass fractionated owing to older SiO_2 component; $\underset{\sim}{O}^{(4)}$ is 2% deficient in ^{16}O because that fraction is preferentially locked up in supernova CO. The significance lies not so much in these numerical details, arbitrary but reasonable, as it does in illustrating how the theory works. NASA NSG-7361.

REFERENCES

(1) D. Clayton, Moon and Planets 19, 109.
(2) D. Clayton, Lunar Planet.Sci. XI, 162 and Ap.J. (Letters) 239, July 1,1980.
(3) R.N. Clayton et al., EPSL 30, 10.

THOUGHTS ON CAI'S, OXYGEN ISOTOPES, AND REE

Wood, J.A.
Harvard-Smithsonian Center for Astrophysics, Cambridge, MA 02138

Excepting FUN inclusions:

The anomalies in meteoritic O isotope compositions (1) are not due to an incomplete mixing of several dust or gas-plus-dust components, each with a different nucleosynthetic history and a characteristic O isotope composition. If they were, other elements would display similar anomalies. For the same reason, individual CAI's were not condensed in the envelopes of several or probably even a single supernova.

The O anomalies must therefore stem from differing degrees of exchange between the primordial gas component and the dust component of the nebula, as suggested by (2). Each of these components resulted from a different blend of nucleosynthetic histories, and each had a characteristic O isotope composition. *The unique thing about O is that it is the only element with >2 stable isotopes which would have been present in major amounts in both the gas and solid phases,* allowing the possibility of incomplete exchange. Mg, for example, could not have exchanged in this way because at practically any temperature virtually all of it is either in the gas phase or in the condensed phase.

The larger of the two O reservoirs, namely the gas phase, is more likely to have had an O isotope composition similar to what we consider "normal" solar system O at the outset. The dust component must have been enriched in ^{16}O.

If the dust had been completed vaporized in the nebula, its O would have equilibrated with O in the gas phase, and no O anomalies would be displayed by the condensate. Since CAI's show O isotope anomalies, they are not condensates but must represent the residues of partial volatilization (distillation) of the primordial dust. Some recondensation onto the residues probably occurred, but the condensate should not display significant O isotope anomalies. Presumably most of the volatilized material recondensed as dust, which appears as matrix material in the chondrites.

A critical constraint on CAI formation is Boynton's (3) observation that Er and Lu, which are strongly depleted in Group II fine-grained CAI's, are the most refractory REE. This seems to require that the Group II CAI's, which appear to be the *most abundant* subclass of CAI's, condensed from vapor which had been separated from extra-refractory solids containing the system's Er and Lu. It appears all but impossible to accomplish this in the solar nebula, if the point raised in the preceding paragraph is correct.

It may be that pre-solar system supernova envelopes are a more plausible place for this to have happened. A model is developed in which the most refractory elements (incl. Er and Lu) condense in supernova envelopes into grains that are systematically coarser than other interstellar dust, and are thus readily fractionated from it in the solar nebula, somewhat along the lines of (4). Heating (short of total vaporization) of dispersed dust and aggregation in the nebula produced Group III CAI's in regions where the refractory-rich grains were present, and Group II CAI's where they were absent.

(1) R.N. Clayton et al. (1977) EPSL 34, 209, and elsewhere. (2) G.J. Wasserburg et al. (1979) in Proc. 22nd Liege Int. Astrophys. Sypos. (3) W.V. Boynton (1978) in Protostars and Planets, U. of Ariz. Press, 427. (4) D.D. Clayton (1980) EPSL 47, 199.

#96

ISOTOPE FRACTIONATION IN THE PROTOSOLAR MEDIUM

M. J. Corrigan, R. W. Fitzgerald, D. A. Mendis and G. Arrhenius
University of California, San Diego, CA. 92093

The discovery of enhancement of ^{16}O in refractory crystals in carbonaceous meteorites [1] and in local regions of the space medium [2] and of highly efficient chemical fractionation mechanisms in interstellar clouds [3] have led us to survey the processes likely to cause this fractionation and to attempt experimental modelling. In cases where "anomalous" isotope distributions are observed in a specific molecule, or in a specific atomic position of a molecule, the effect is likely to be due to chemical fractionation. In other cases a nucleosynthetic origin of the anomaly cannot be excluded and may be likely if the effect is associated with a major region in the galaxy, or with a supernova remnant. Laboratory verification is excluded for nucleosynthesis of ^{16}O.

Three types of chemical fractionation processes have been considered as potentially relevant to the excess of ^{16}O. One is resonance excitation in rotational fine structure of a molecule with well-separated isotopic vibrational bands. The excitation, to be important, should be caused by a prominent line in interstellar space, the excited molecule must be reasonably abundant and undergo reaction, and the density, unless ionization takes place, must be high enough for collision to occur within the time of radiative decay. Regions of high density behind shock fronts and in stellar atmospheres may be the loci of such conditions. Selective excitation of ^{18}O and ^{13}C by excitation with a VUV line was first discovered by Harteck and collaborators [4]. In space the coincidence of the intense H Lα line at 1216 Å with the 14th vibrational band of A-X transition in $^{12}C^{16}O$ has been proposed as a potential cause of fractionation [5]; other such isotopic coincidences may also occur between strong stellar emission lines and abundant interstellar molecules. In the laboratory the reaction of CO* with CO forming CO_2 and C_3O_2 is particularly convenient to study as a model system; in the space environment collisions of the excited molecule with hydrogen species will be by far the most important reactions. Another mechanism of interest for single-isotope fractionation is Frank-Condon selection during predissociation [6]. The third mechanism of interest is Teare-Treanor pumping with enhanced reaction of the heavier isotopic species [7,8]. This process is expected to operate in a mass dependent manner but to lead to such large fractionation effects (in excess of 40% observed in ^{15}N and of 50% in ^{18}O) that the reservoir eventually may become sufficiently depleted in the two heavier and less abundant isotopes to place them near or below the detection limit.

References: [1] Clayton, Grossman and Mayeda, (1973) Science 182, 485; Clayton and Mayeda, (1977) Geophys. Res. Lett. 4, 295; [2] Penzias, (1980) Science 208, 663; [3] Watson, (1978) in Gehrels ed. Protostars and Planets. Univ. Arizona Press, Tucson, AZ.; [4] Liuti, Dondes and Harteck, (1966) J. Chem. Phys. 44, 4052; [5] Arrhenius, Corrigan and Fitzgerald, (1980) Lun. Planet. Sci. 11, Lun. Planet. Sci. Inst., Houston, TX., [6] Murrell and Taylor, (1969) Mol. Phys. 16, 609; Schaefer and Miller, (1971) J. Chem. Phys. 8, 4107; Arrhenius, McCrumb and Friedman, (1979) Astrophys. Space Sci. 60, 59; [7] Basov et al., (1974) Soviet. Phys. JETP 19, 190; [8] Arrhenius, (1978) in Dermott ed; The Origin of the Solar System, Wiley, N.Y.

GRIER (b) A NEW "BRECCIATED" L 4-7 CHONDRITE

Nelen, J., P. Brenner and K. Fredriksson
Smithsonian Institution, Washington, D.C. 20560

The Grier (b),* New Mexico, 929gr. chondrite was found in 1969. The bulk composition with ~8 wt% metal and an estimated total iron content of 25 wt% as well as the constant Fe/Mg ratio of olivines ($Fa_{25.5}$) and orthopyroxenes (Fs_{23}) place this chondrite within the L-group. Although original metal content and the iron in the pyroxenes are close to the upper limits for the L-group, the main part meets the criteria for a grey to intermediate hypersthene (L 4-5) chondrite. However, a large (several cm^3) dense and fine-grained fragment (L 6-7) with essentially no metal or chondrules is conspicuous although the composition of its bulk silicates and individual phases is similar to that of the main mass. The contact between fragment and matrix is somewhat diffuse but the olivine-pyroxene compositions must have been established before accretion or any thermal metamorphism of this chondrite breccia. Small differences in chemical composition, to some extent caused by weathering, will be demonstrated and the textural relations illustrated.

*Tentative name submitted to the Committee for Meteorite Nomenclature.

#98

ALLAN HILLS 77216: A PETROLOGIC AND MINERALOGIC DESCRIPTION

Roberta Score, Lunar Curatorial Laboratory, Northrop Services, Inc., P.O. Box 34416, Houston, Texas 77058

Allan Hills 77216 is a brecciated L-group chondrite of petrologic type 4 that contains clasts of other petrologic types. The meteorite contains subrounded to irregular clasts, as large as 3 cm across, set in a light gray matrix. Material finer than 0.02 mm was arbitrarily defined as matrix and constitutes 28% of the sample. Allan Hills 77216 together with 3 other stones (Allan Hills 77215, 77217, 77252) represent a single fall based on macroscopic, microscopic and microprobe data and collectively weigh 3.1 kg.

Microprobe analyses indicate that the meteorite is composed of the following: 43% olivine, 24% clinopyroxene, 15% orthopyroxene, 6% glass, 4% kamacite, 1% taenite, 5% troilite and 2% minor accessory minerals. Olivine composition ranges from Fa_{15-35}, with a mode of Fa_{24} and pyroxene composition ranges from Fs_{14-23}, with a mode of Fs_{20}. The Fa and Fs contents differ from inclusion to inclusion, but are the same within any individual inclusion.

Fluid drop chondrules (7 vol%) range from 0.15 mm to 3.95 mm in diameter. These include several types: barred olivine, excentroradial pyroxene and microporphyritic chondrules. A few of these fluid drop chondrules are totally rimmed with nickle-iron.

Lithic chondrules (10 vol%) range from 0.45 mm to 2.85 mm in diameter. Lithic chondrules exhibit a wide range of textures ranging from equigranular to microbrecciated and they display irregular and ameboid to very regular and rounded margins.

Mineral, lithic and chondrule fragments greater than 0.02 mm make up 47 vol% of this chondrite. Of these 25% are mineral fragments, 16% are lithic fragments and 6% are chondrule fragments. About 50% of the mineral fragments are isolated anhedral to subhedral olivine and pyroxene grains as much as 0.6 mm in maximum dimension. The remaining mineral fragments are metal and opaque mineral complexes which are as much as 1 cm in diameter.

Several large lithic clasts (8 vol%) are contained in the three thin sections studied. Microprobe analyses of the largest clast (3.60 mm x 1.30 mm) show that it consists of radial, poikiolitic, twinned-clinopyroxene (En_{77} Fs_{19} Wo_4). A distinct border (0.65 mm wide) of finner grained, semi-rounded pyroxene, olivine grains and glass, totally encloses the poikiolitic clinopyroxene.

The textural character of this specimen is neither indicative of a lunar regolith, as it lacks the agglutinates and glassy component present in the lunar regolith, nor is it indicative of an impact melt sheet, as the matrix appears to be composed of comminuted mineral grains with a composition similar to the larger inclusions set in the matrix. Allan Hills 77216, however, does appear texturally similar to lunar sample 14318.

CHEMICAL AND PETROLOGIC STUDIES OF THE LEIGHTON CHONDRITE: A PROGRESS REPORT

Biswas, S.[1], McSween, H.Y. Jr.[2] and Lipschutz, M.E.[1]
1-Dept. of Chemistry, Purdue University, West Lafayette, IN 47907
2-Dept. of Geological Sci., University of Tennessee, Knoxville, TN 37916

Leighton, like other light/dark gas-rich meteorites, is a breccia in which the dark gas-containing portions are generally volatile-rich and petrographically unequilibrated. We are systematically studying a number of carefully selected samples of the 600 gram main mass for 12 volatile/mobile trace elements (Ag, Bi, Cd, Cs, Ga, In, Rb, Se, Te, Tl, Zn) and for their petrographic characteristics. Histograms of olivine and pyroxene compositions suggest that the samples are mixtures of various proportions of equilibrated and unequilibrated materials, but all are H chondrite in character. Different samples exhibit variable patterns of volatile elements, precluding simple mixing of more and less equilibrated end members or admixture of a volatile-rich component of constant composition with volatile-depleted material. Volatile elements in some highly unequilibrated dark clasts are enriched over known ranges for H3 chondrites, and some elements have significantly higher concentrations than in C1 chondrites. The olivine and pyroxene PMD values correlate well with concentrations of the most volatile elements (Bi, Tl, In) but not with other less volatile ones. The trends suggest that Leighton represents a mixture of a wide variety of compositions and may constitute a microcosm of H group parent materials. Carbonaceous chondrites, generally considered to have primitive compositions, have many of the distinctive chemical characteristics of H group chondrites and may represent only part of the full compositional range for volatile-rich condensate. Additional analyses of dark material in Leighton, which appears to be less altered than C1 chondrites, may further delineate the spectrum of petrologic and chemical properties inherent in primitive solar system matter.

#100

ON THE ORIGIN OF THE EXCESS OF VOLATILE TRACE ELEMENTS IN THE DARK PORTION OF GAS-RICH CHONDRITES.

Dreibus, G. and Wänke, H.

Max-Planck-Institut für Chemie, 6500 Mainz, W.-Germany

In the dark portion of solar rare gases containing chondrites excess amounts of various trace elements compared to the concentration in the light gas-free portions have been observed by a number of authors. In the case of Br and I Reed et al. (1) found in the dark portion of Pantar with 0.74 ppm, respectively 0.55 ppm, a 3-fold concentration as compared with the light portion. Especially remarkable was the finding of Rieder and Wänke (2) that the dark portions of all gas-rich bronzite chondrites analysed were highly enriched in indium. For Leighton (H5) In concentrations considerably in excess to that of C1 chondrites were found.

Recently, this work was confirmed by Bart and Lipschutz (3) who in addition to In also found for Tl, Bi, Cd and Cs concentrations in excess or comparable to those in C1 chondrites. However, like Rieder and Wänke these authors were also not able to give a definite explanation for these very striking observations.

We recently analysed Cl, Br and I in Pantar and found an enrichment for all three elements in the dark portion. For Leighton, however, we found more Cl in the light phase as compared to the dark phase, whereas the Br concentration of 1.03 ppm in the light and 1.14 ppm in the dark phase showed an equally distribution for these elements. For I we found in the dark portion of Leighton with 0.24 ppm an enrichment factor of 2 compared to a factor of 7 for Pantar.

Unfortunately, we cannot finally distinguish between halogens introduced by contamination and the true indigenous concentrations, as leach experiments revealed a number of new observations but could not decide the question of a possible contamination, especially in the case of Cl.

Bart and Lipschutz speculated that the excess amounts of volatile trace elements in the dark portion of solar rare gases containing chondrites represent material from hitherto unknown nebular fractionations. We do not follow this suggestion but believe that these elements originate as emanations from the metamorphism in the interior of the parent body of these chondrites, which found their way towards the surface where they were deposited and mixed in the very surface layers during their exposure to the solar wind (4).Hence, similar as in the case of earth and moon the volatile elements are also enriched in the surface regions of the chondrite parent body.

1.) Reed, G.W. and Allen, R.O. (1966) Geochim. Cosmochim. Acta 30, 779-800.
2.) Rieder, R. and Wänke, H. (1969) Meteorite Research (ed. P.M. Millman), 75-86.
3.) Bart, G. and Lipschutz, M.E. (1979) Geochim. Cosmochim. Acta 43, 1499-1504.
4.) Wänke, H. (1965) Z. Naturforschg. 20a, 945- 949.

FISSION TRACKS IN FAYETTEVILLE AND WESTON PHOSPHATES: METAMORPHIC OR BRECCIATION AGES?

B.K. Kothari and R.S. Rajan
Dept. of Terrestrial Magnetism, Carnegie Institution of Washington, 5241 Broad Branch Rd., N.W. Washington, D.C. 20015

Gas-rich meteorites are gently compacted breccias, presumably from asteroidal regoliths. The brecciation events have been so mild that it did not reset the radiometric clocks such as Rb-Sr and K-Ar. Since the tracks in phosphates are more easily reset, we have measured the fission track densities in phosphates from two gas-rich meteorites hoping to date the compaction events, and to better understand the nature of brecciation processes.

Our results are shown in Table 1 which also include data on the gas-poor chondrite Bhola for comparison (1). We have taken the $(Pu/U)_{4.55\ Gyr}$ = 0·045 as the best mean for the chondritic whitlockites, though it can vary by as much as a factor of three (2). For both the meteorites the fission track ages are old: 4·1-4·3 Gyr for Weston and 4·26-4·50 Gyr for Fayetteville. Each phosphate is a potential chronometer; it is thus significant that none of the ages are <4·1 Gyr.

What do these ages mean? If the phosphates are reset during compaction then they all should have the same age (or track density after correcting for U and Pu concentrations). Because of the uncertainty in (Pu/U) ratios of our samples it is more useful to compare the data from gas-rich chondrites with that from Bhola. The metal from Bhola is equilibrated and hence its phosphates must have been reset during brecciation (3). After normalizing the track densities for their varying U content, 11 crystals from Fayetteville show a factor of eight variation while the five Bhola crystals differ by only a factor of two. Because of the heterogeneity of these meteorites it is difficult to rule out either of the following two possibilities from our limited data. (i) The phosphates are reset by the brecciation event, the track density spread being due to (Pu/U) variation of individual crystals; it would imply compaction ages of ∿4·2 and ∿4·3 Gyr for the two meteorites. (ii) The phosphates are indeed dating different events. This is consistent with the metal being not equilibrated and our fission track ages being in the same range as that expected from metallographic cooling rates (3). The fission track ages are then upper limits to the times of brecciation. To ensure that occasional young clasts are not preferentially missed, further analyses of phosphates from lithologically distinct phases are needed.

References (1) LPI, XI (1980), p. 573. (2) USGS Survey Rep. (1978), 78-701, p. 215 (3) LPI, XI (1980), p. 1015.

Table. Summary of track data in whitlockite crystals

Meteorite	Wt of the sample (gm)	U content (ppb)[1]	Cosmic ray track density (10^6 cm^{-2})	Measured track densities[1] (10^6 cm^{-2})	Track retention age[2] (Gyr)
Fayetteville (H)	1.3	125-575 (11)	∿2·6	50-88(11)	4·26-4·50
Weston (H)					
-Yale	1.8	-	∿0·5	23-58(8)	4·10-4·24
-NMNH1180	1·3	270-650(4)		25-75(35)	4·15-4·30
Bhola (LL)	0.9	140-560(11)	∿0.5	3·7-6·3(20)	4·01±0·1

[1]Number in parentheses refer to crystals studied.

[2]Assuming $(Pu/U)_{4.55\ Gyr}$ = 0·045

#102

ODD XENOLITHS IN ACHONDRITES: A RADIOCHEMICAL STUDY

Mitusru Ebihara and Rainer Wolf

Enrico Fermi Institute and Department of Chemistry, University of Chicago
Chicago, IL 60637

To expand the range of known meteorite types, we have analyzed xenoliths from 3 achondrites: Haverö (ureilite), Khor Temiki (aubrite), and Kapoeta (howardite). In addition to our usual 20 siderophile and volatile trace elements, we also measured a number of REE.

Haverö. A sample of vein material (B-18-2), obtained through the courtesy of Prof. F. Begemann, was quite similar to its sister sample, B-18-1 (Wänke *et al.*, 1972). But with the additional elements measured, new trends could be recognized. It fits the correlations of Ni, Ge, Au vs. Re, Ir for whole-rock ureilites (Novo Urei, Dyalpur, Haverö, and Goalpara (Higuchi *et al.*, 1976), supporting the view of these authors that ureilites contain an injected component rich in siderophiles, especially refractory siderophiles. The linearity of the correlation suggests that a single component is involved for all 4 ureilites. Yet the cosmochemical history of this component is complex, judging from the simultaneous enrichment (by 0.6x-4x Cl) of elements differing greatly in volatility: Re, Os, Ir, Au, Ge, Ag, Tl, and depletion (0.02-0.03 Cl) of others: Rb, Cs, Zn, and Bi.

Khor Temiki. A dark inclusion from this brecciated aubrite was rather rich in siderophiles, relative to Cl chondrites: Au 0.24, Ir 0.065, Os 0.017. It was low in most volatiles (e.g. Bi, Tl, Cd - 0.002-0.006), but was strongly enriched in Rb (6.0), Cs (1.8), and U (3.2). The very low Re/Ir ratio is unprecedented, surpassing that of an earlier, unpublished analysis of the same meteorite (J. Hertogen, M.-J. Janssens, H. Palme, 1977). The enrichment of alkalis and U is likewise unprecedented among enstatite chondrites and achondrites, and suggests that this xenolith is a more evolved, highly fractionated member of this class. It will be interesting to assess the relative importance of nebular and igneous fractionations in the genesis of this material.

Kapoeta. The 3 samples measured show only minor compositional variations.

REFERENCES

H. Higuchi, J.W. Morgan, R. Ganapathy, and E. Anders (1976) *Geochim. Cosmochim. Acta 40*, 1563-1571.

H. Wänke, H. Baddenhausen, B. Spettel, F. Teschke, M. Quijano-Rico, G. Dreibus, and H. Palme (1972) *Meteoritics 7*, 579-590.

A CHEMICAL STUDY OF INDIVIDUAL ROCK CLASTS FOUND WITHIN THE KAPOETA HOWARDITE

SMITH, M.R., AND SCHMITT, R.A.
DEPARTMENT OF CHEMISTRY AND THE RADIATION CENTER, OREGON STATE UNIVERSITY, CORVALLIS, OREGON 97331

The abundances of major, minor, and trace elements have been determined via instrumental neutron activation analysis in seventeen lithic clasts, as well as two 'dark' and four 'light' matrix fractions extracted from the Kapoeta howardite. The averaged abundances of the 'light' matrix fractions fall within the range of previously reported values. The 'dark' fractions have been found to contain large enrichments of Zn, Co, Ni, Ir, and Au indicative of significant chondritic contributions.

Various investigators have previously interpreted howardites as being mechanical mixtures of eucritic and diogenitic components. Detailed min.-pet. studies have shown that some of the clasts found within howardites have impact melt and metaigneous origins. The chemical data presented in this study confirms these observations as well as offers genetic implications.

The eucritic like clasts which have major, minor, and trace element abundances that are representative of known eucrites have chondritic normalized (C.N.) rare earth element (REE) patterns representing a wide range of igneous differentiates with $(La/Lu)_{C.N.}$ ratios ranging from 1.62 to 0.45 and $(Sm/Eu)_{C.N.}$ values of 1.71 to 0.67. Low abundances of Au and Ir in these eucritic like clasts have been interpreted as representing insignificant amounts of regolith mixing. The diogenitic clasts have very low abundances of REE as well as undetectable amounts of Au and Ir (<9 and <4 ppb, respectively). These clasts are also considered to have been derived from igneous melts unrelated to regolith materials. A third group of clasts analyzed in this study show chemical evidence which is suggestive of metaigneous and impact melt rocks. The genesis of these howarditic like clasts based on chemical data and whole clast observations are either two component mixtures which have undergone metamorphic episodes or igneous accumulations which have fractionated from primary or impact melts with eucritic tendencies. Normalized REE patterns suggest both cumulates and metaigneous mixtures. However, higher siderophile abundances similar to the concentrations found in other howardites and in the Kapoeta matrix fractions suggest that these clasts have only impact melt or metamorphic origins.

One clast with a chemical composition similar to howardites has some important and interesting features. This clast has a Fe/Fe+Mg atomic ratio of 0.27 and chondritic element ratios of Al, Ca, Sr, La, Sm, Eu, Yb, Sc and Hf. It has been shown by Dreibus and Wänke (1980) that a howardite composition exists which may represent primitive elemental abundances. This clast's relative elemental abundances are similar to such a composition except for enrichments of Ti, Cr and V. We argue against the possibility of this assemblege being derived from eucritic and diogenitic mixtures based on chemical trends and low undetectable siderophile abundances. In order to account for such a composition one would have to invoke eucritic and diogenitic end members presently unknown. Even if this possibility exists it seems very unlikely that siderophile concentrations would not be enriched during the mixing process. The limitations of this study precludes further speculations concerning the igneous character of this clast. Nevertheless this clast's chemical composition, when combined with approximately 18% olivine, yields a eucritic parent body composition very similar to previously proposed models (metal and sulfide free). We wish to acknowledge Dr. M.S. Ma for his comments.

Dreibus, G. and Wanke, H. (1980) Z. Naturforsch. 35a, 204-216.

#104

ANTARCTIC POLYMICT EUCRITES

Arch M. Reid[1] and Carol M. Schwarz[2]
[1]Dept. of Geology, University of Cape Town, Rondebosch, South Africa
[2]Northrop Services Inc., P.O. Box 34416, Houston, Texas 77034

The basaltic achondrite meteorites collected in the Allan Hills region of Antarctica (76005, 77302, 78040, 78132, 78158 and 78165) are all petrographically similar and could even be pieces from a single fall. They are breccias with abundant but small (from fine dust to a maximum diameter of approximately 1 cm) angular clasts of rock and mineral fragments. The lithic clasts are basaltic consisting of subequal amounts of pyroxene and feldspar with a range of igneous textures. The diverse clast types correspond to a range of thermal histories and to a limited range of basaltic compositions. Rock and mineral fragments studied to date correspond in texture and in mineral composition to the known range of eucrites, including both unequilibrated and equilibrated types (1-5). The range in pyroxene compositions is wide (Wo_4En_{69} to $Wo_{13}En_{33}$) but pyroxenes with the compositions of those in diogenites are absent or rare.

The Allan Hills basaltic achondrites are unlike previously described eucrites and howardites (with the possible exception of Macibini) in that they contain a series of fragments covering a range of eucrite types and are thus polymict but they do not appear to contain a diogenite component as in typical howardites. The name polymict eucrite (2) seems appropriate. Very similar polymict eucrites are common in the suite of achondrites collected in the Yamato region of Antarctica, almost 3000 km from Allan Hills.

Consortium studies of these meteorites began with the processing of 10 g each of 76005, 77302, 78040 and 78132 plus 2 g of 78156 and 78165 to obtain representative interior samples and to isolate individual lithic clasts. We have separated 5 coarser grained eucritic clasts with a range of igneous clasts (.02 to .9 g), 3 fine grained eucrite clasts with quench textures (.01 to .2 g), and 4 aphanitic black clasts (.02 to .13 g). A combined petrographic/analytical study of these clasts is now being initiated.

References: (1) Reid A.M. and Barnard B.M. (1979) Lunar Planet. Sci. X, 1019-1021. (2) Miyamoto M., Takeda H. and Yanai K. (1979) Lunar Planet. Sci. X, 847-849. (3) Takeda H., Miyamoto M. and Ishii T. (1980) Lunar Planet. Sci. XI, 1116-1118. (4) Labotka T.C. and Papike J.J. (1980) Lunar Planet. Sci. XI, 590-592. (5) Simon S.B. and Haggerty S.E. (1980) Lunar Planet. Sci. XI, 1033-1035.

THE ANTARCTIC ACHONDRITE ALHA 76005: A POLYMICT EUCRITE

Olsen, E.[1], Grossman, L.[2], Davis, A.M.[2] and Tanaka, T.[2]
[1]Field Museum of Natural History, Chicago, IL 60605.
[2]University of Chicago, Chicago, IL 60637.

Olsen *et al.* (1) described the Antarctic achondrite ALHA 76005 and concluded that it is a eucrite on the basis of major elements, but a polymict breccia based on the petrography of its clasts. Because eucrites are not normally described as polymict, we re-examined some of these clasts by petrographic, SEM and EMP techniques and sampled the bulk meteorite and one clast for trace element and oxygen isotopic analysis.

Three basaltic clasts were studied in detail. As a group, they have subophitic to intergranular textures and pyroxene/plagioclase ratios ~2:1. Plagioclase compositions are An_{79-93} and pyroxenes range from $En_{60}Fs_{35}Wo_5$ - $En_{30}Fs_{55}Wo_{15}$ - $En_{30}Fs_{30}Wo_{40}$ in all of them. One clast has much larger plagioclase laths than the others ($\leq$ 2mm *vs* $\leq$ 200μm) and was sampled for trace element and isotopic study. Two anorthositic gabbro clasts were studied. They have cumulate textures and pyroxene/plagioclase ratios of ~1:2. Plagioclase compositions are An_{73-84} in the first clast and An_{77-90} in the second. Both have Ca-rich pyroxenes with compositions around $En_{25}Fs_{30}Wo_{45}$, but the first has Ca-poor ones with higher FeO/MgO ratios ($En_{25}Fs_{55}Wo_{20}$) than the second ($En_{35}Fs_{50}Wo_{15}$). Also studied were four clasts, each several hundred μm in size, consisting of portions of single crystals of plagioclase (An_{88-93}) with regularly-spaced poikilitic pyroxene inclusions. No such crystals were observed in any of the lithic clasts described above. The achondrite is indeed polymict.

INAA data were obtained for 25-30 elements in the bulk meteorite and the coarsest-grained basaltic clast. Abundances of lithophile trace elements in the bulk meteorite fall within the concentration ranges for eucrites and outside those for howardites. Its REE pattern is similar to that of Nuevo Laredo, but with slightly lower REE abundances than the latter. Consolmagno & Drake (2) proposed that the REE pattern of Nuevo Laredo is that of the liquid remaining after 30% fractional crystallization of a melt having the composition of the main eucrite group. This results in a higher atomic FeO/FeO+MgO ratio in Nuevo Laredo than in the main group (0.67 *vs* 0.62). Although the REE pattern of ALHA 76005 could be produced by slightly less fractional crystallization than that of Nuevo Laredo, the fact that ALHA 76005's FeO/FeO+MgO ratio (0.59) is *lower* than 0.62 suggests that its parent liquid was more magnesian than the main group. The basaltic clast has a REE pattern very similar to that of Moore County, but with slightly lower REE abundances and a smaller Eu excess. The REE pattern of Moore County is thought to be that of the crystals forming after 85% fractional crystallization of a melt having the composition of the main eucrite group (2). The slightly lower REE abundances in the clast suggest that it could have formed after slightly less fractional crystallization than Moore County, but the higher FeO/FeO+MgO ratio in the clast (0.57 *vs* 0.50) implies that its parent liquid was more iron-rich than that which formed Moore County. It is doubtful that the same parent liquid could have differentiated to form both the clast and its host.

Oxygen isotopic measurements by Clayton *et al.* (3) underscore both this point and the polymict nature of ALHA 76005. The bulk meteorite and the basaltic clast came from different isotopic reservoirs.

(1) Olsen, E. *et al.* (1978) *Meteoritics* 13, 209. (2) Consolmagno, G.J. & Drake, M.J. (1977) *GCA* 41, 1271. (3) Clayton, R.N. *et al.* (1979) *LPSX*, 221.

#106

HIGHLY DIFFERENTIATED EUCRITIC CLASTS IN POLYMICT BRECCIAS ALLAN HILLS A78040 AND A77302.

Delaney, J.S., Bedell, R., Frishman, S., Klimentidis, R., Harlow, G.E. and Prinz, M.
Dept. Mineral Sciences, Amer. Mus. Nat. Hist., New York, NY 10024

Modal analysis by automated electron microprobe, of lithic clasts from these eucrite polymict breccias, reveal dramatic variations of modal silica and cpx/opx. Bulk compositions of lithic clasts in A78040, define a new trend in the eucrite pseudoternary diagram (ol-qtz-an), away from the peritectic on which most basaltic eucrites plot (Fig. 1). This trend is the result of crystal-liquid separation and liquid evolution toward the minimum in the system. If eucritic magma differentiated down the cotectic B" of Stolper (1977) it would produce the illustrated compositions. Eruption of these liquids produces rapid cooling which is indicated by the presence, in both A78040 and A77302, of 'Pasamonte-type' basaltic clasts with Fe-Mg zoned, uninverted pigeonites (Takeda et al., 1979), while liquid trapped at shallow depth would equilibrate to the more uniform compositioned, granular textured clasts found. The increase in modal silica reflects the trend of magma evolution. This silica occurs petrographically either as dark interstitial devitrified glass containing the assemblage silica±Ca-rich pyroxene±fluorapatite or as large, often slightly altered, tridymite laths (~2mm long) which crystallized simultaneously with the pyx and plag. The more evolved liquids also have higher modal cpx (>cpx/opx) indicating that Ca-enrichment occurs in the later liquids. Two clasts in A78040 contain over 50% silica. These are very fine grained and have compositions like the devitrified glass in A76005 (Olsen et al., 1978). They are also compositionally similar to the interstitial, silica rich areas of some clasts. These clasts therefore probably represent late-stage liquids remaining after much fractionation. Some of these evolved clasts cooled very rapidly (indicated by Pasamonte-type pyroxenes, 'feathery' pyx/plag intergrowths and devitrified glass) but some cooled more slowly or were later equilibrated by a thermal event.

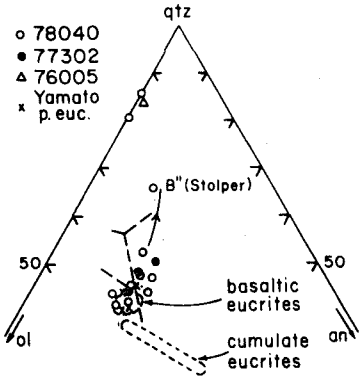

Fig. 1: Bulk compositions of clasts

These polymict breccias are therefore considered to have formed by impact brecciation of a series of near surface intrusions or lavas which are the result of internal evolution of a eucritic parent magma. Impact melting may be responsible for the textures of some of the clasts and perhaps is responsible for the production of some of the high-SiO_2 clasts. It seems unlikely that the regular variation of bulk chemistry (Figure 1) could be produced by impact melting. The eucrite polymict breccias contain relicts of rock types derived from differentiated eucritic melts which have not been recognized in monomict basaltic eucrites, except perhaps Pasamonte which is currently under investigation.

REFERENCES: Olsen E., Noonan A., Fredriksson K., Jarosewich E. and Moreland D. Meteoritics 13, 209-225 (1978); Stolper E., Geochim. Cosmochim. Acta 41, 587-612 (1977): Takeda H., Duke M.B., Ishii T., Haramura H., and Yanai K. Proc. 4th Symp. Antarctic Meteorites, 54-76 (1979)

Textural and Modal Analysis of Apollo 16 and 17 Highland Breccias

Reimold,W.U., Borchardt,R., Ostertag,R., and Stöffler,D.(1)
Institute of Mineralogy, Univ. of Münster, Germany and (1) Lunar and Planetary Institute, Houston, TX 77058.

Thin sections of 20 samples of lunar highland rocks from Apollo 16 and 17 representing all textural types of breccias as defined by (1) have been analyzed by means of a semiautomatic linear analyzer (2): fragmental breccias and different types of crystalline melt breccias with finely granular, subophitic, and poikilitic crystalline matrix. Quantitative textural parameters and statistical parameters of the grain size distribution have been calculated from the line scannings of about 1000 grains per thin section.

Independently of the breccia type the modal composition of the matrix is rather constant for all crystalline melt breccias and is predominated by plagioclase as compared to pyroxene + olivine in all types of breccias. In contrast to this, the grain size distribution of the main matrix minerals varies significantly as a function of the breccia type. Their mean grain size increases in going from granular to poikilitic and subophitic textures. The inner specific surface (3), an important textural parameter, increases for plagioclase and pyroxene in going from subophitic to poikilitic and granular breccia matrix.

The matrix/clast ratio also varies with breccia type. The abundance of mineral and lithic clasts decreases drastically in the sequence granular-poikilitic-subophitic while the mean grain size of the clasts is increasing in the same direction. According to our interpretation the systematic variation of matrix and clast characteristics for breccias with crystalline matrix means that the various types of these breccias are derived from impact melts of different geological setting within the parent craters. Therefore they display different amounts of admixed clasts and consequently different cooling and crystallization histories (4). The observed textural variation at a particular sampling site may be produced by a single cratering event although multiple events cannot be excluded on the basis of textural and compositional arguments alone.

References: (1) Stöffler,D., Knöll,H.D., and Maerz,U. (1980) Terrestrial and lunar impact breccias and the classification of lunar highland rocks. Proc. Lunar Planet. Sci. Conf. 10th, 639-675; (2) Knöll,H.-D. (1978) Mikrochemische und gefügekundliche Untersuchungen an Impaktbreccien der Fra Mauro Formation des Mondes. Ph.D. Thesis, Institut für Mineralogie, Munster, Germany; (3) Blaschke,R. (1970) Spezifische Oberflächen und Grenzflächen der Mineralphasen als Gefügeparameter. Fortschr. Miner. 47, 197-241; (4) Simonds, C.H., Warner,J.L., Phinney,W.C., and McGee,P.E. (1976) Thermal model for impact breccia lithification: Manicouagan and the Moon, Proc. Lunar Sci. Conf. 7th, 2509-2528.

#108

LUNAR SAMPLE AND CRUSTAL MAGNETIZATION AND EARLY HEAT SOURCES IN THE SOLAR SYSTEM. S.K.Runcorn, School of Physics, University of Newcastle upon Tyne, England, W.F.Libby and L.M.Libby, University of California, Los Angeles, USA.

Magnetic stability of many of the Apollo samples suggests that the magnetization was acquired during initial cooling in the presence of an ambient field. Palaeointensity studies suggest that this field has decayed from about 1 Gauss at 4 b.y. to about .022 Gauss at 3 b.y. (1) Various arguments lead to the hypothesis that this field was of internal origin generated by dynamo action in an iron core. Recent interpretations of the direction of this field, inferred from the Apollo 15 and 16 sub-satellite magnetometer data lead to the hypothesis of lunar polar wandering which fits well with the early mechanics of the Moon. (2) The existence of a core is strongly indicated by recent determinations of the moment of inertia factor. (3)

Two fundamental problems emerge: the nature of the heat source which melted the Moon in the first 100 My to produce its differentiation and in particular the core and the nature of the heat source which maintains convection in a molten core at the level necessary to generate these fields. We suggested the speculative hypothesis that siderophile superheavy elements could explain both these observations. (4) The known, very short-lived radioactive isotopes could explain the initial melting but do not fit the later requirement. Conventional heat sources suggested for the Earth's dynamo do not work for quantitative reasons in the Moon. Search for superheavy elements in the solar system has so far proved negative. However, no other solution to these two related problems has yet been suggested.

(1) S.K.Runcorn, D.W.Collinson and A.Stephenson. Intensity and origin of the ancient lunar magnetic field. Phil.Trans.R.Soc.Lond.A285, 241-247, 1977.

(2) S.K.Runcorn. Lunar polar wandering. 11th Lunar Science Conference Proceedings. In press.

(3) A.J.Ferrari, W.S.Sinclair, W.L.Sjogren, J.G.Williams and C.F.Yoda. J.Geophys.Res. 1980. In press.

(4) S.K.Runcorn, L.M.Libby and W.F.Libby, Primaeval melting of the Moon. Nature, 270, 676-681, 1977.

AN UPPER LIMIT ON THE ABUNDANCE OF SUPERHEAVY ELEMENT Z=110 IN THE EARLY SOLAR SYSTEM

Nozette, S. Dept. of Earth and Planetary Sciences, Massachusetts Institute of Technology, Cambridge, Mass. 02139
Boynton, W. V. Dept. of Planetary Sciences and Lunar and Planetary Laboratory, University of Arizona, Tucson, Az. 85721

We report on the determination of the abundance of the rare earth elements (REE) in the Santa Clara IVB iron meteorite. These measurements were performed by radiochemical neutron activation analysis and allow an upper limit to be placed on the abundance of siderophile superheavy elements present in the iron meteorite parent body. Based on nuclear models, nuclide $^{294}110$ is predicted to be the longest-lived of the superheavy elements (1). Element 110 is in the same group of the periodic table as Pt, and, like the other platinum metals, it should be enriched relative to the solar 110/Fe ratio. Nuclide $^{294}110$, or its possible alpha-decay daughter $^{290}108$, will decay by spontaneous fission (1) and its fission yield curve will probably be symmetric around mass 140 (2). (The effect of higher mass in a fissioning nucleus is to move the light mass peak, observed in normal asymmetric fission, to higher values while the heavy mass peak, centered at mass 140, moves only slightly (3).) Because both fragments will contribute to the mass yield curve, we take twice the ^{252}Cm spontaneous fission yield of 2% for ^{152}Sm (3) as an estimate of the yield from $^{294}110$. The observed concentration of ^{152}Sm ($\sim 10^9$ atoms/g) sets an upper limit of about 2.5×10^{10} atoms of 110/g, assuming that all ^{152}Sm atoms are from spontaneous fission of element 110. This sets an upper limit to the solar 110/Fe ratio about 2.5×10^{-12}(atomic), or a 110/U ratio of about 0.0001, at the time Santa Clara formed. The evidence for decay of ^{107}Pd ($t_{\frac{1}{2}} = 7 \times 10^6$y) in Santa Clara (4) indicates that Santa Clara formed very early, although alternate interpretations cannot be ruled out (5). If Santa Clara is indeed a very old rock, then either element 110 was not synthesized in the event that made ^{107}Pd, or its half-life is less than 10^7y. This result lends serious doubt to the possibility that a siderophile superheavy element played a role as a significant heat source in the early solar system.

References

1. Randrup, J., Larsson, S. E., Möller, P., Sobiczewski, A., and Łukasiak, A., Physica Scripta 10A, 60 (1974).
2. Schmitt, H. W., and Mosel, U., Nucl. Phys. A186, 1 (1972).
3. Hyde, E. K., The nuclear properties of the heavy elements. III. Fission phenomena, 519 pp. (Prentice Hall, 1964).
4. Kelly, W. R., and Wasserburg, G. J., Lunar Planet. Sci. X, 652 (1979).
5. Kaiser, T., Kelly, W. R., and Wasserburg, G. J., Lunar Planet Sci. XI, 527 (1980).

#110

HOBA AND TLACOTEPEC: TWO NEW METEORITES WITH ISOTOPICALLY ANOMALOUS Ag. Kaiser, T.*, W. R. Kelly†, and G. J. Wasserburg*, *The Lunatic Asylum, Division of Geological and Planetary Sciences, California Institute of Technology, Pasadena, CA 91125 and †Center for Analytical Chemistry, National Bureau of Standards, Washington, D.C. 20234

Excesses of $^{107}Ag/^{109}Ag$ ($^{107}Ag^*$) of up to 4% relative to terrestrial silver were discovered by Kelly and Wasserburg (1978) in the Santa Clara iron meteorite. Subsequent investigations by Kaiser, Kelly, and Wasserburg (1980) (hereafter KKW) revealed much larger ratios of $^{107}Ag/^{109}Ag$ and showed that the true ^{109}Ag concentration was at a very low level for both the Piñon and Santa Clara iron meteorites. Experiments on other iron meteorites were indicated in order to further clarify the role of extinct ^{107}Pd as the source of the ^{107}Ag excesses compared to other possible sources. We present new results on the Hoba, Tlacotepec, and Canyon Diablo iron meteorites. Using our surface decontamination procedure we find Ag concentration levels in Hoba and Tlacotepec, two IVB iron meteorites, which are smaller by 1-2 orders of magnitude than reported earlier (Kelly, Tera, and Wasserburg, 1977, hereafter KTW). The new ^{109}Ag concentration levels found for Hoba and Tlacotepec ($1.0\pm0.04 \times 10^{11}$ and $2.2\pm0.1 \times 10^{11}$ atoms/g respectively, corrected for blank) are essentially identical with the levels found for Piñon and Santa Clara. At the same time the $^{107}Ag/^{109}Ag$ ratio for Hoba and Tlacotepec was discovered to be distinctly different from normal (2.92 ± 0.09 and 1.113 ± 0.014, respectively, corrected for blank). The large decrease in Ag concentration found for IVB meteorites compelled us to check the high levels found for other meteorites by using our surface decontamination procedure. The results for Canyon Diablo, a IA iron meteorite, which were done after strong etching, confirm the earlier high levels of concentration (by Smales et al., 1967, and KTW) and also confirm the normal isotopic composition for this meteorite clan.

From these data it appears that ^{107}Ag excesses are a common feature of the IVB meteorites. Hoba has a $^{107}Ag^*/^{108}Pd$ ratio of 1.7×10^{-5} with a short galactic cosmic ray (GCR) exposure age of 0.3AE (Voshage and Feldmann, 1979). Piñon has approximately the same $^{107}Ag^*/^{108}Pd$ ratio but an exposure age of 0.8AE. Furthermore Tlacotepec shows a small ^{107}Ag excess (2%) with nearly the same Pd/Ag ratio as the other IVB meteorites and with an exposure age comparable to that of Piñon. The analyses of spallation gases on specific samples analyzed here, reported by Villa et al. (1980) show considerable differences in GCR secondary particle fluences for these samples, indicating no correlation between ^{107}Ag excesses and cosmic ray exposure. These observations appear to rule out significant contributions from GCR secondary neutrons on Pd as the cause of the ^{107}Ag excesses. This possibility was discussed earlier by KKW who showed that the multiplicity times the cross section would have to be ~100 barns in order for there to be a dominant contribution of such secondary nuclear reactions. Our recent observations are in accord with the theoretical analysis by Reedy (1980) based on the ^{53}Mn production from iron. From direct observation of Ag anomalies in meteorites with different irradiation ages as well as from the estimated production rates of the ^{107}Ag excesses from GCR, the most plausible explanation of the ^{107}Ag excesses still appears to be the decay of extinct ^{107}Pd in the early solar system.

Kaiser T., W.R. Kelly, and G.J. Wasserburg, 1980. Geophys. Res. Lett. 7, 271. Kelly W.R. and G.J. Wasserburg, 1978. Geophys. Res. Lett. 5, 1079. Kelly W.R., F. Tera, and G.J. Wasserburg, 1978. Anal. Chem. 50, 1279. Reedy R.C., 1980. Proc. 11th Lunar & Planet. Sci. Conf. (preprint). Smales A.A., D. Mapper, and K.F. Fouché, 1967. Geochim.Cosmochim.Acta 31, 673. Villa I.M., J.C. Huneke and G.J. Wasserburg, 1980. Met.Soc.Abs., this volume. Voshage H. and H. Feldmann, 1979. Earth and Planet. Sci. Lett. 45, 293. Div.Contrib.No.3463(356).

SPALLOGENIC RARE GASES IN IRON METEORITES WITH ISOTOPICALLY ANOMALOUS Ag

Villa, I. M., J. C. Huneke, and G. J. Wasserburg, Lunatic Asylum, Division of Geological & Planetary Sciences, Calif. Inst. of Tech., Pasadena, CA 91125

Cosmic-ray produced rare gases have been measured in four meteorites with excess $^{107}Ag^*$ (1,2,3) to determine if $^{107}Ag^*$ is related to cosmic ray exposure. Kaiser et al. (2) considered the possibility that $^{107}Ag^*$ could derive from energetic particle reactions on Pd if the cross section times multiplicity for all reactions were $\sim 10^2$ b. However, they noted that relative $^{107}Ag^*$ were inconsistent with published cosmic ray exposure ages. Reedy (4) estimated the production of ^{107}Ag from Pd and concluded that a cosmic ray bombardment of $\sim 10^9$ yr would probably produce at most 1% of $^{107}Ag^*$ observed in Santa Clara and Piñon. To directly compare $^{107}Ag^*$ with spallogenic rare gases produced at the same shielding depth, He, Ne, and Ar were measured in portions sawn from the same small pieces analyzed for Ag. This comparison is not possible using literature data. Two pieces from different locations in Santa Clara and in Piñon were analyzed. These are the first spallogenic gas measurements on Santa Clara. $^4He/^{38}Ar$ vs. $^3He/^{21}Ne$ in all four meteorites is in accord with the systematics determined by Signer and Nier (5) from the Grant iron meteorite. No sample appears to have had an unusual irradiation.

^4He and $^{21}Ne/^4He$ are plotted versus $^{107}Ag^*/Pd$ in Fig. 1. The content of ^4He is most representative of the total fluence of lower energy particles through the piece analyzed; $^{21}Ne/^4He$ increases with the hardness of the energy spectrum of the particle flux. There is no correlation of $^{107}Ag^*/Pd$ with either the total fluence of energetic particles or the hardness of the particle energy spectrum. The absence of any such correlation is evidence that the $^{107}Ag^*$ in these iron meteorites is not produced by energetic particles capable of producing the spallogenic He and Ne. A quantitative conclusion using published GCR spectral distributions is hampered by the theoretical difficulties in extrapolating from high-ΔA products (Ne, Ar from Fe) to $\Delta A = 3$ (^{107}Ag from ^{110}Pd).

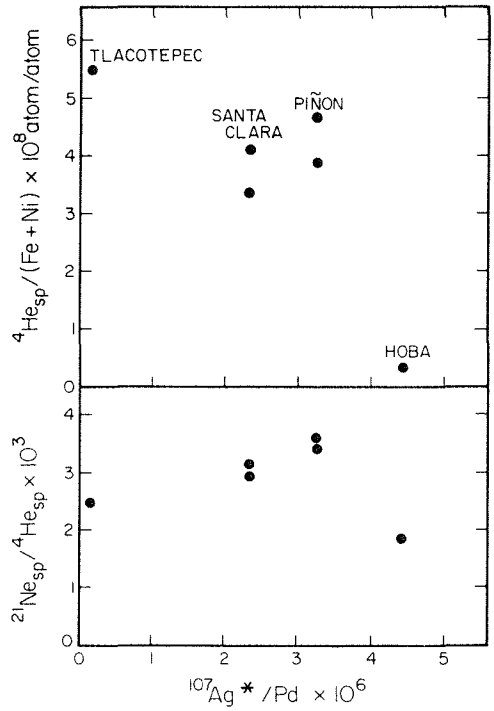

Fig. 1. (top) ^4He vs. $^{107}Ag^*/Pd$. $^{107}Ag^*/Pd$ is not proportional to the fluence of bombarding particles producing ^4He, as shown in the extreme by Hoba and Tlacotepec. (bottom) $^{21}Ne/^4He$ vs. $^{107}Ag^*/Pd$: If $^{107}Ag^*$ derives from cosmic ray bombardment, $^{107}Ag^*/Pd$ should increase monotonically as $^{21}Ne/^4He$ decreases. Piñon is a clear exception to such a trend.

Ref. (1) Kelly W. R. and G. J. Wasserburg, GRL 5 (1978) 1079. (2) Kaiser T., W.R. Kelly, and G. J. Wasserburg, GRL 7 (1980) 271. (3) Kaiser T., W. R. Kelly, and G. J. Wasserburg, Met. Soc. Abs. (1980) this volume. (4) Reedy, R. C., Proc. 11th LPSC (1980) in press. (5) Signer, P. and A. O. Nier, JGR 65 (1960) 2947.
Div. Contrib. No. 3465 (357).

#112

U AND Pb ISOTOPES IN ALLENDE INCLUSIONS AND METEORITIC WHITLOCKITE

Chen, J. H., and Wasserburg, G. J., Lunatic Asylum, Division of Geological and Planetary Sciences, Caltech, Pasadena, CA 91125

We measured the isotopic composition of U and Pb in five Ca-Al rich inclusions from the Allende and in phosphates from the St. Sévérin chondrite and the Angra dos Reis achondrite. The purpose of this study is to test claims of large isotopic anomalies in U from meteoritic materials made by other workers. Many of the Allende inclusions analyzed here show excess $^{26}Mg^*$ in phases with high $^{27}Al/^{26}Mg$ ratios. Samples of Allende inclusions were dissolved in HF, HCl, and HNO_3, leaving an insoluble residue which consisted almost exclusively of spinel. The U isotopic results are shown in Fig. 1 where $\delta^{235}U$ represents fractional deviation of the measured ratio from the nominal ratio $(^{235}U/^{238}U)_{\oplus} = (1/137.88)$ in parts in 10^3. The error bars represent $2\sigma_m$. It is clear that all five samples have U isotopic composition similar to the normal value within limits of error. The $^{206}Pb/^{204}Pb$ ratios measured on the coarse grained inclusions range from 63 to 226. The calculated $^{207}Pb/^{206}Pb$ model ages range from 4.557 to 4.568 AE, which indirectly substantiates the observation of normal U by direct measurements.

The U isotopic compositions on both pure (Wh-1,>99%) and less pure (Wh-3, ~ 95%) whitlockite samples separated from the St. Sévérin chondrite are shown in Fig. 1. These results are also indistinguishable from normal. The observed $^{206}Pb/^{204}Pb$ ratios on St. Sévérin whitlockite range from 144 to 178 and the calculated $^{207}Pb/^{206}Pb$ model ages range from 4.550 to 4.553 AE. The U isotopic composition on a whitlockite separate (99% pure) from Angra dos Reis (Fig. 1) is also normal. The observed $^{206}Pb/^{204}Pb$ ratio is 302 and the $^{207}Pb/^{206}Pb$ model age is 4.553 AE. In summary, the U isotopic composition in Allende inclusions and meteoritic whitlockites either determined by direct measurements or inferred from $^{207}Pb/^{206}Pb$ ratios are indistinguishable from the normal value. The results of this study complement the conclusions of our previous report (Geophys. Res. Lett. 7, 275-278, 1980) that the $^{235}U/^{238}U$ value in meteoritic materials analyzed by us so far is similar to that in lunar and terrestrial materials. These results are in complete disagreement with the reports by Tatsumoto et al. (Lunar Planet. Sci. XI, 1125-1127, 1980) of the existence of large variations in the isotopic abundance of U in meteoritic samples including the St. Sévérin whitlockite. While there may yet be variations in $^{235}U/^{238}U$, they are not present in the materials so far studied at the level of 5‰. We can as yet provide no positive evidence for the existence of ^{247}Cm in the early solar system in large amounts.

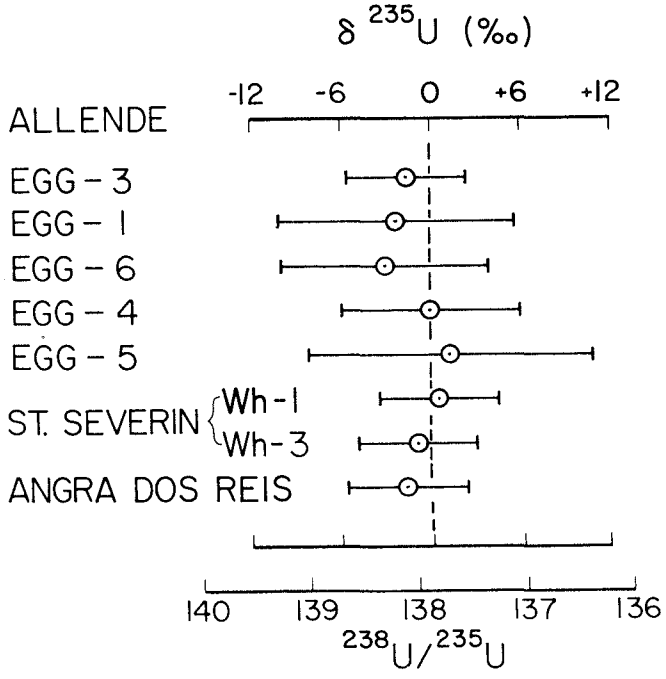

Fig.1

Div. Contrib. No. 3460 (354).

U ISOTOPIC COMPOSITION IN METEORITIC PHOSPHATE

Tatsumoto, M.[1], Nakamura, N.[2], Unruh, D. M.[1], and Pellas, P.[3]
[1]U.S. Geological Survey, MS 963, Box 25046, Denver, CO 80225, U.S.A.
[2]Dept. of Earth Sciences, Kobe University, Nada, Kobe 657, JAPAN
[3]Muséum d'Historire Naturelle, 75005 Paris, FRANCE

Isotopic compositions of uranium in phosphates from ordinary chondrites will be reported as additional evidence for the presence of live ^{247}Cm ($t_{1/2}$ = 1.6 x 10^7 yr) in the early solar system (1).

Small apparent variations in $^{238}U/^{235}U$ ratios in minute samples (< 1 ng of U) can be artifically induced either by spurious background peaks during mass spectrometry or by ^{235}U contamination from previously used spikes. However, these artifacts, if they exist, will always tend to lower the $^{238}U/^{235}U$ ratio. The carbon method for mass spectrometry (2) provided a 3 to 4 times stronger U-signal, but after a half dozen consecutive standard runs, the $^{238}U/^{235}U$ ratio became smaller (~135-136 for NBS 950a Standard). Thus, we currently consider the U_3O_8-triple filament method to be more reliable for isotopic measurements on < 1ng of U.

We have recently reported $^{238}U/^{235}U$ ratios of 129-136 for whitlockite from the St. Sévérin amphoterite (3). A new double-spike ($^{236}U/^{233}U \sim 0.14$) has been prepared in order to test our previous results. The advantage of this spike over the old one ($^{236}U/^{233}U \sim 1$) is that spurious background peaks (at least at mass 236) will be reflected in abnormally low apparent fractionation factors. The new results for St. Sévérin whitlockite are identical to those previously reported (3).

Light REE are slightly depleted in St. Sévérin whitlockite, with Gd/Nd and Sm/Nd ratios enriched 1.1-1.2 times relative to chondrites. If REE fractionation approximates actinide fractionation, $^{238}U/^{235}U$ = 133-136 in the whitlockite can be predicted by assuming that the $^{238}U/^{235}U$ ratio in the spike spinel-rich fraction of Allende residue is free of ^{247}Cm from the last nucleosynthesis (1). The agreement between the observed and predicted values is excellant and provides additional support for the presence of live ^{247}Cm in the early solar system.

Earlier analyses of uranium and fissiogenic ^{136}Xe in whitlockite (4) and in the whole-rock of St. Sévérin chondrite (5) indicated that the $^{244}Pu/^{238}U$ ratio in whitlockite was enriched by a factor of two relative to that in the bulk meteorite. If a similar enrichment occurred in the $^{247}Cm/^{238}U$ ratio in whitlockite, then the predicted modern $^{238}U/^{235}U$ ratio is 119. The present results indicate that the REE enrichment factors may be used to estimate actinide fractionation in meteorites (6). Phosphate fractions from Beaver Creek (H4) and Elenovka (L5) have been separated (~ 95% purity) and the U isotopic compositions of these separates will be used to test this hypothesis.

References: (1) Tatsumoto, M. and Shimamura, T., Nature (in press).
(2) Arden, J. W., Nature 269, 788 (1977).
(3) Tatsumoto, M. et al., Lunar Planet. Sci. XI, 1125 (1980).
(4) Wasserburg, G. J. et al., J. Geophys. Res. 74, 4221 (1969).
(5) Podosek, F. A., Geochim. Cosmochim. Acta 36, 755 (1972).
(6) Lugmair, G. W. et al., Earth Planet. Sci. Lett. 35, 273 (1977).

#114

Search for nickel isotopic anomaly of meteorites

Morand, Ph., Audouze*,J., Allègre, C.J.
Laboratoire Géochimie-Cosmochimie 4 Place Jussieu 75230 Paris 5
* Institut d'Astrophysique, 81 Bld Arago 75013 PAris

Since the discovery of oxygen anomalies in the Allende meteorite (Clayton et al., 1973), the principle of isotopic homogeneity in the early solar system has been overturn.

The study of the theories of nucleosynthesis show the great importance of the temperature and the neutron-proton ratio in the iron equilibrium peak (e.g. Truran, 1973; Arnett, 1973); this dependence can provide a variety of isotopic abundances in the iron peak region.

Thus a chemical separation and precise mass spectrometric measurement of nickel have been developed. The present isotopic composition of Ni is : $^{61}Ni/^{60}Ni = 0.04328 \pm 0.00003$, $^{62}Ni/^{60}Ni = 0.13753 \pm 0.00004$, $^{64}Ni/^{60}Ni = 0.03459 \pm 0.00004$. These values are normalized to the NBS value of $^{58}Ni/^{60}Ni = 2.6164$ and correspond to the mean of 13 runs on the same mass spectrometer. Errors represent the reproducibility of 13 runs.

One C1 - chondrite (Orgueil), one CV3-chondrite (Allende), three H-type chondrites (Kernouvé (H6), Kirin (H4) and Tieschitz (H3)), two E-type chondrites (Hvittis (EII) and Indarch (EI)), one L-type chondrite (Hedjaz(L3)) two LL-type chondrites (Chainpur (LL3) and Olivenza (LL5)), one pallasite (Eagle Station) have been analyzed. In addition we have studied the heavy fraction of Allende (d > 4.0), three Allende chondrules and one Allende white inclusion. Unfortunately no type FUN inclusion could be analyzed.

No significant variation of the Ni isotopic composition has been found. This result indicates that the studied samples of the solar system were formed from an homogeneously mixed reservoir as Ni isotopic composition is concerned. In particular, the nucleosynthetic processes which created the "anomalous" components in the Allende white inclusions, either did not involve any effect in the iron peak region, or occurred in temperature and neutron excess conditions such that the Ni isotopic composition be closed to the mean composition of the solar system.

Chromium isotopes in meteorites and terrestrial samples

Birck, J.L., Ricard, L.P. and Allègre, C.J.
Laboratoire Géochimie Cosmochimie 4 Place Jussieu 75230 Paris 5

Since the discovery of the witnesses of the presence of Al^{26} in the early solar system many authors have suggested to search for the presence of the decay product of Mn^{53} in the same type of materials, the behaviour of the two parent daughter systems (^{26}Al-^{26}Mg and ^{53}Mn-^{53}Cr) in the geochemical processes, being quite similar. ^{53}Mn has the advantage over ^{26}Al of a longer decay period (3.7 m.y. vs 0.7 m.y.). This fact gives more time for geochemical processes to occur (fractionation of the Mn to Cr ratio) before the parent isotope has completely decayed.

The eventual excess of ^{53}Cr in the present samples should be detected by precise chromium isotopic measurements. An experimental technique was devised to handle samples containing down to 50 ng of Cr with negligible blanks. With regard to mass spectrometry the isotopic ratios are normalized to $^{52}Cr/^{50}Cr$ = 19.283 (NBS value). Both $^{54}Cr/^{52}Cr$ and $^{53}Cr/^{52}Cr$ are measured to detect any eventual nucleosynthetic effect on Cr isotopes in addition to extinct ^{53}Mn.

For samples containing around 1 µg of Cr our current precision is in the 10^{-4} range.

Our data on commercial salts and terrestrial rocks are in agreement with the NBS data i.e. $^{53}Cr/^{52}Cr = 0.11344 \pm 0.000015$, $^{54}Cr/^{52}Cr = 0.028203 \pm 0.000007$.

We have analyzed :
- differentiated meteorites : Juvinas and Tatahouine whole rocks
- chondrules from Chainpur
- chondrules and refractory inclusions from Allende
- oldhamite from Indarch which has a very high Mn/Cr ratio.

Taking into account :
- the amount of Fe and Cr present in the silicate samples,
- the production of ^{53}Cr and ^{54}Cr by spallation of the iron,
- and the exposure ages of the meteorites, the spallogenic productions of ^{53}Cr and ^{54}Cr are negligible compared to the initial content of the samples in all cases.

All the data give the values of the terrestrial chromium within the error limits. Several explanations may be asserted :

a) ^{53}Mn was not present or was present in negligible amounts in the analyzed samples.

b) Cr has been homogenized isotopically with solar chromium after complete decay of ^{53}Mn.

Concerning both ^{53}Cr and ^{54}Cr the chromium isotopes have not incorporated significant amounts of any component which would have resulted from nucleosynthetic processes different from those which produced the mean solar Cr.

#116

Lu-Hf ISOTOPE SYSTEMATICS OF THE EUCRITE METEORITES

Patchett, P. J.[1,2] and Tatsumoto, M.[2]
[1]Colorado School of Mines, Golden, CO 80401
[2]Branch of Isotope Geology, U.S.G.S., Denver Federal Center, Box 25046, MS 963, Denver, CO 80225

A method has been developed which allows low-blank separation and precise mass spectrometric analysis (0.001-0.003%) of Hafnium from rock and meteorite samples. This allows (1) cosmochronology using the ^{176}Lu-^{176}Hf decay scheme, and (2) studies of Hf isotopic evolution in the earth's crust and mantle.

The ratio Lu/Hf has a greater variation than the Sm/Nd ratio in eucrites. However, Juvinas has a $^{176}Hf/^{177}Hf$ ratio (0.28285, normalized to $^{179}Hf/^{177}Hf$ = 0.7325) closely similar to terrestrial basalt BCR-1, as is the case for Nd.

Data will be presented for the eucrites Juvinas, Pasamonte, Stannern, Moore County, Nuevo Laredo, Moama, Sioux County, and Bereba. The regression line through these data yields the initial $^{176}Hf/^{177}Hf$ for the eucrites, and assuming that the whole-rock system is undisturbed since 4.55 Ga, as for Rb-Sr (1), a cosmochronological determination of the decay constant $\lambda^{176}Lu$ can be made.

Reference: (1) Papanastassiou, D. A. and Wasserburg, G. J., Earth Planet. Sci. Lett. 5, 361-376 (1969).

RELATIVE AGES OF CHONDRITES BY I-XE AND ^{40}AR-^{39}AR DATING: A CONTINUING STORY

Hohenberg, C. M., Hudson, B., Kennedy M. and Podosek, F. A.
McDonnell Center for the Space Sciences, Washington University, St. Louis, Mo. 63130

In our continuing effort to compare noble gas radiometric chronologies based on the K-Ar, I-Xe, and Pu-Xe techniques, a collection of neutron irradiated meteorites have been analyzed by high precision mass spectroscopy. Samples used in this study include a suite of enstatite chondrites, Kota-Kota, St. Sauveur, Daniel's Kuil, Khairpur, and Blithfield (re-analysis); the anomalous chondrite, Pontlyfni; light and dark lithologies of the LL6 chondrite St. Séverin (re-analysis) and Bjurböle (I-Xe irradiation monitor).

Figure 1 shows the "high-temperature" ^{128}Xe-^{129}Xe correlation for the enstatite chondrite Daniels' Kuil. The value of the correlation slope gives an age difference (relative to Bjurböle) of 3.10 ± .08 my. The statistical error in the slope (derived from a least squares fit) corresponds to an age variation of ± .025 my.

Figure 2 shows the "high-temperature" $^{128}Xe/^{129}Xe$ correlation for a re-analysis of the light fraction of St. Séverin. The line through 1075°C to 1550°C gives an age comparable to that previously reported for the dark lithology (Hudson et al., 1979) but with a much higher $^{129}Xe/^{130}Xe$ trapped value. However, a good linear correlation also exists through 1400°C to 1650°C corresponding to an age difference (relative to Bjurböle) of 8.8 ± .5 my and a trapped $^{129}Xe/^{130}Xe$ ratio of 6.38 ± .12. These values are comparable to the relative age and trapped value previously reported (Hudson et al., 1979) for the light lithology of St. Severin.

These results as well as the results for the other enstatite chondrites and Pontlyfni will be discussed in the context of thermal histories of meteorite parent bodies.

Hudson B., Kennedy B. M., Hohenberg C. M., and Podosek F. A., 1979. Meteoritics 4, 425-426.

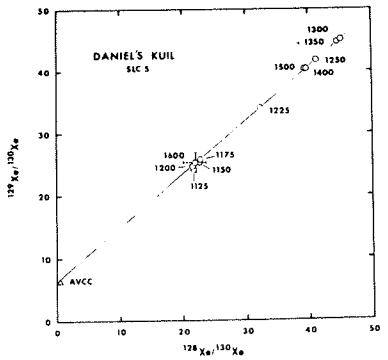

Figure 1

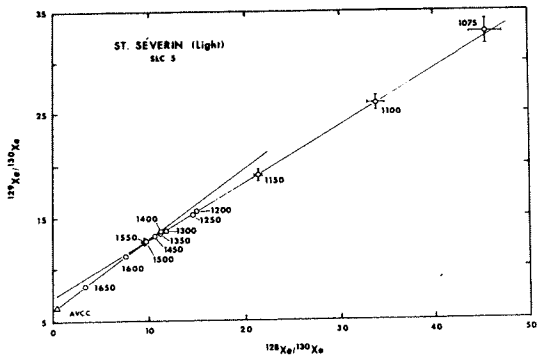

Figure 2

#118

More data on ^{87}Rb-^{87}Sr dating of LL chondrites.

MINSTER J.-F. and ALLEGRE C. J.
Laboratoire de géochimie et cosmochimie 4, Place Jussieu 75230 PARIS

In our systematic survey of ^{87}Rb-^{87}Sr dating of chondrites we obtained a whole rock isochron age for LL chondrites of 4.48 ± 0.04 b.y. and $^{87}Sr/^{86}Sr$ initial ratio $^{87}Sr/^{86}Sr = 0.69899 \pm 0.00020$. These age and initial ratio were respectively slightly younger and higher than those for H or E type chondrites. Since most LL chondrites are polymict breccia, the possibility that something specific affected the Rb-Sr system in these objects had to be studied further.

Samples and clasts from 10 different meteorites have been analyzed. With the exception of Ngawi (LL3) and Ensisheim (LL6), they define an isochron of age 4.493 ± 0.018 b.y. and initial ratio $^{87}Sr/^{86}Sr = 0.69882 \pm 0.00008$. These values are indistinguishable from those for the other chondrite types. Ngawi and same samples Ensisheim have probaly been contaminated by strontium.

Internal studies have been made for Chainpur (LL3), Soko Banja (LL4), Guidder (LL5), Jelica (LL6) and Ensisheim (LL6). Chainpur and Soko Banja appear to be formed of chondrules of very variable composition embedded in an homogeneous matrix of composition close to that of the whole rock. However, the variation of the composition of LL chondrites cannot be due to random repartition of the chondrules. Our further study on Chainpur has destroyed the isochron obtained formerly. This is attributed to leaching or contamination during the alteration which severely affected this meteorite. Chondrule analyzes of two different pieces of Soko Banja yield two parallel isochrons. One of these is very well defined, and gives an age of 4.452 ± 0.020 b.y. and strontium initial ratio $^{87}Sr/^{86}Sr = 0.69959 \pm 0.00024$. Isotopic homogenization did not affected the whole meteorite but rather involved migration of strontium on the mm scale of chondrules. Time scale for metamorphism is of 38 ± 9 My. This will be discussed in relation with the thermal history of the Soko Banja parent body in conjunction with the maximum temperature for metamorphism of type chondrites. This result indicates that the thermal history of LL chondrites has been longer than that for H chondrites, as suggested by fission tracks cooling rates. Alternatively, this can indicate that the parent body for Soko Banja is not an "instantaneously" formed, conductive object, heated by ^{26}Al. No isochron has been obtained for Guidder, Jelica and Ensisheim. The sizes of the scatters indicate that they must have resulted from later perturbations possibly due to shock or brecciation.

Sm-Nd ISOTOPIC SYSTEMATICS OF CHONDRITES AND ACHONDRITES.

Jacobsen, S. B. and G. J. Wasserburg, Lunatic Asylum, Division of Geol. Plan. Sci., CALTECH, Pasadena, CA 91125

The $^{143}Nd/^{144}Nd$ and $^{147}Sm/^{144}Nd$ ratios have been measured in five chondrites and the Juvinas achondrite. The range in $^{143}Nd/^{144}Nd$ for the analyzed meteorite samples is 5.3 ε-units (0.511673 to 0.511944) normalized to $^{150}Nd/^{142}Nd = 0.2096$. This is correlated with the variation of 4.2% in $^{147}Sm/^{144}Nd$ (0.1920 to 0.2000). Much of this spread is due to small scale chemical heterogeneities in the chondrites and does not appear to reflect the large scale volumetric averages. It is shown that all samples lie within 0.5 ε-units of a 4.6 AE reference isochron and define an initial $^{143}Nd/^{144}Nd$ ratio at 4.6 AE of 0.505828±9 (Fig. 1). As there is a range of $^{147}Sm/^{144}Nd$ in chondrites there is no unique way of picking solar or average chondritic values for $^{143}Nd/^{144}Nd$ and $^{147}Sm/^{144}Nd$. From these data we have selected a new set of selfconsistent present-day reference values for CHUR ("chondritic uniform reservoir") of $(^{143}Nd/^{144}Nd)_{CHUR} = 0.511836$ and $(^{147}Sm/^{144}Nd)_{CHUR} = 0.1967$. The new $^{147}Sm/^{144}Nd$ value is 1.6% higher than the previous value assigned to CHUR using the Juvinas data of Lugmair. This results in a small but significant change in the CHUR evolution curve. At 4.6AE ago the new CHUR curve is 1.8 ε-units lower than the old CHUR curve. Some terrestrial samples of Archean age show clear deviations from the new CHUR curve (Fig. 2). If the new CHUR curve is representative of undifferentiated mantle then it demonstrates that depleted sources were also tapped early in the Archean. Such a depleted layer may represent the early evolution of the source of present-day mid-ocean ridge basalts. There exists a variety of discrepancies with most earlier meteorite data which includes determination of all Nd isotopes and Sm/Nd ratios. These discrepancies require clarification in order to permit reliable interlaboratory comparisons. The new CHUR curve implies substantial changes in model ages for lunar rocks and thus also in the interpretation of early lunar chronology. In addition to the total chondrite data isochrons will be presented for St. Severin and Angra dos Reis.

Division Contrib. No. 3464 (358)

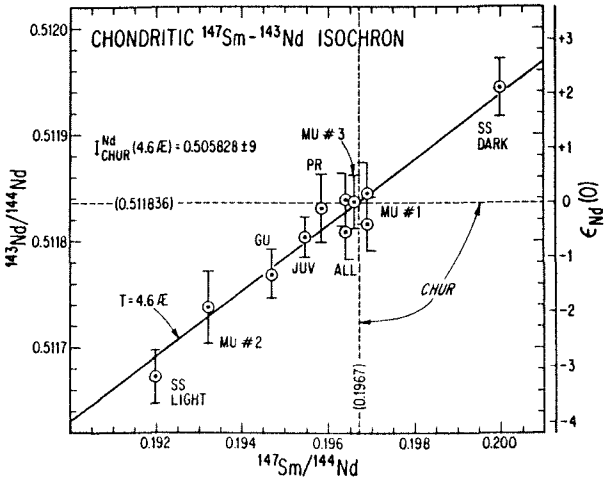

Fig. 1. Sm-Nd evolution diagram for chondrite samples and Juvinas (=JUV). SS = St. Severin, MU = Murchison, GU = Guareña, PR = Peace River, ALL = Allende.

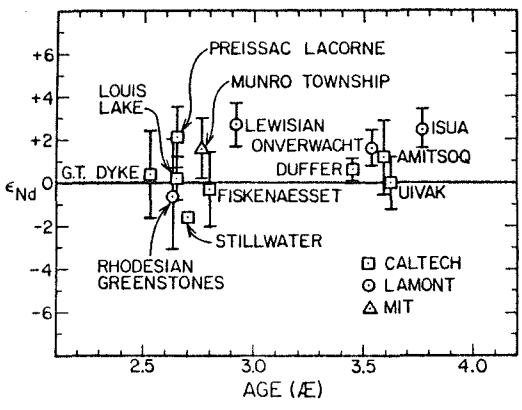

Fig. 2. Fractional deviations in parts in 10^4 of initial $^{143}Nd/^{144}Nd$ of Archean rocks, from evolution in the CHUR reservoir.

#120

A UNIFORM U-Pb AGE FOR L CHONDRITES AND A METHOD FOR CORRECTING FOR TERRESTRIAL Pb CONTAMINATION

Unruh, D.M. and Tatsumoto, M.
U.S. Geological Survey, MS 963, Fed. Ctr., Denver, CO 80225

U-Pb analyses of whole rocks and troilite separates from 9 L-chondrites indicate that the apparent age differences and excess radiogenic Pb commonly found in U-Pb studies of chondrites can both be attributed to terrestrial Pb contamination. Pb-Pb model ages of individual meteorites range from 4500 to 4560 m.y. Furthermore, all of the U-Pb data plot above the concordia curve, showing ∿5-70% apparent excess ^{206}Pb relative to that could have been produced by U-decay (assuming primordial Pb has the isotopic composition of Cañon Diablo troilite). In contrast to iron meteorites, troilite separates from L5 and L6 chondrites contain only ∿6-200 ppb Pb, with terrestrial-like isotopic compositions ($^{206}Pb/^{204}Pb$ ∿16-18). Using the Pb isotopic composition of the troilite to calculate the isotopic composition of the contaminant in the bulk meteorite, the whole-rock data can be accurately corrected for terrestrial Pb contamination. The corrected $^{207}Pb/^{206}Pb$ ages fall in the narrow range of 4548-4560 m.y. and a best-estimate age of 4556 $\pm$ 5 m.y. (95% C.I.) is obtained for the age of equilibration of the L5-6 chondrites. Data for three L3 chondrites corrected in the same manner yield a mean age of 4550 $\pm$ 40 m.y., which is indistinguishable from that of the L5-6 chondrites. The single L4 chondrite analyzed contains 26% excess ^{206}Pb and yields a 4556 $\pm$ 15 m.y. model age when corrected only for primordial Pb, but a 4587 $\pm$ 19 m.y. concordant age when corrected for terrestrial Pb. If the contamination model is valid, then the meteorites analyzed contain ∿3-50 ppb terrestrial Pb. This corresponds to ∿0.1-4% of the ^{204}Pb in the L3 chondrites, but 90-100% of the ^{204}Pb in the L5 and L6 chondrites. U in two L3, one L5 and one L6 chondrites have $^{238}U/^{235}U$ ratios of 137.4 $\pm$ 0.8 - 137.7 $\pm$ 0.4, which are not distinguishable from the terrestrial value of 137.9.

^{187}Re - ^{187}Os chronology of Meteorites.

LUCK J.-M. and ALLEGRE C. J.
Laboratoire de géochimie et cosmochimie, 4, Place Jussieu 75 PARIS

Continuing our approach to dating iron and sulfide phases of meteorites, we have extended our investigations to the different iron meteorite groups. The range for $^{187}Os/^{186}Os$ ratio has been considerably increased and goes from 0.98 to 1.40.

Stony-iron meteorites and samples from the different chondrite classes (L, LL, H, E) have also been studied by this method. All our results confirm the simultaneous formation of the iron phase in all of these planetary objects.

#122

STRONGLY RECRYSTALLIZED METEORITES FROM ANTARCTICA:YAMATO-74160 AND ALHA77081

Takeda, Hiroshi[1,2] and Yanai, Keizo[2].
[1]Mineral. Inst., Fac. of Sci., Univ. of Tokyo, Hongo, Tokyo 113, Japan and
[2]National Inst. of Polar Research, Kaga, Itabashi-ku, Tokyo 173, Japan.

Many meteorites, which show glanoblastic textures indicating extensive recrystallization, have been found and recovered from Antarctica by both Japanese Antarctic Res. Expedition and U.S.-Japan joint teams. On the basis of pyroxene mineralogy and bulk chemistry, eight Yamato meteorites have been identified as recrystallized diogenites of possiblly one fall.

Yamato-74160 weighes 31.4g and has hemisphere-like shape with a black fusion crust except one side, where olive yellow to pale gray interior can be seen. It is brecciated and is composed of subangular recrystallized clasts. It consists of 50% olivine and 30% orthopyroxene with minor augite and plagioclase. Trace amounts of metal associated with chromite and troilite have been detected. Microprobe analyses show olivine Fa_{30}, orthopyroxene $Ca_4Mg_{72}Fe_{24}$, augite $Ca_{43}Mg_{46}Fe_{11}$ of uniform composition. The metal is very rich in nickel (Fe 50.0, Co 2.3, Ni 46.7 wt%). The plagioclase is present as a discrete elongated grain up to 0.2mm and shows a small range in composition with dominant values at An_8 and An_{18}. The clustering of the compositions is so good that one may suspect that they represent the coexisting pair. The bulk chemical composition estimated from the weight percentages of the minerals and their compositions and the texture are in favor of a strongly recrystallized LL chondrite (LL7). The temperature of the last equilibration of the Opx-Aug pair estimated by Ishii's pyroxene geothermometer, 1090°C is considerably higher than about 970°C of ordinary chondrites.

ALHA77081 is coarse-grained and shows recrystallized texture. It is olivine(32%)-pyroxene(36%) rocks, with abundant metal and minor augite and plagioclase(An_{15}). The metal grains acompany troilite and chromite. The chemical composition of olivine(Fa_{10}) is very low in CaO and Cr_2O_3(<0.02) and high in MnO(0.49). The temperature of the last equilibration estimated from the compositions of rare coexisting pair of Opx $Ca_2Mg_{88}Fe_{10}$ and Aug $Ca_{45}Mg_{51}Fe_4$ in contact with each other by the pyroxene geothermometer is between 985°C and 1070°C. The difference is due to the slight Ca-enrichment at the augite rim. A large pale-green augite crystal (0.5mm) gave the X-ray diffraction pattern of the $C2/c$ symmetry, but with minor reflections of $P2_1/c$ pigeonite. The augite is rich in Cr_2O_3 and Na_2O, suggesting an enrichment of the $NaCrSi_2O_6$ component. The MnO content of the orthopyroxene and chromite (up to 2.46 wt.%) is the highest among the chondrites. The chromite is also high in Cr_2O_3 and FeO contents and is close to those of iron meteorites.

Similarity of ALHA77081 to Acapulco(forsterite chondrite), which has mineral compositions intermediate to the E and H chondrite, has been pointed out by Mason (1979). Prinz *et al.*(1980) mentioned that these two meteorites and related meteorites such as Winona and silicate inclusions in IAB irons form a primitive achondrite group. Mayeda and Clayton (1980) showed that these meteorites have come from a similar oxygen reservoir. The MnO/FeO plots of Y-74160 and ALHA77081 are on the extension of the anti-correlation line of chondrites(Takeda *et al.*,1980). Although this trend has some near-chondritic characteristics, the correlation may only indicate that the metal fractionation was involved during the recrystallization episod. The minor element chemistry and crystallography of the ALHA77081 augite are suggestive of a primitive achondrite, which is different from chondrites and the howardite-like achondrites.

PETROGRAPHY OF THE LOUISVILLE METEORITE (L6e)

Basu, Abhijit and Shaffer, Nelson R.
Department of Geology, Indiana University, Bloomington, IN. 47405, U.S.A.
Hunt, Graham
Department of Geology, University of Louisville, Louisville, KY.40207, U.S.A.

Fall, recovery, bulk chemical composition (Jarosewich, analyst) and chondrule-matrix relationship of the Louisville meteorite have been reported earlier (1,2). Study of one polished thin section from the largest fragment (1051 g) and macroscopic observations form the basis of this preliminary petrographic report.

The meteorite contains a few extremely brecciated dark bands which do not seem to cut one another. The bands comprise anastomising veins of troilite and recrystallized glass (with numerous disseminated Fe^{o} metal granules) enclosing clasts of the wall-rock material. The bands appear to represent melt pockets of the sinuous form (3). Undefined barred olivine-plagioclase chondrules as well as those with radiating and equant crystals of pyroxene occur in the light portion. The margins of all the recognizable chondrules are either blurred or are rimmed by recrystallized maskelynite. Many fragments of the chondrules are also intimately mixed with the crystalline matrix. Electronprobe analyses show that olivine (Fa = 24.8 ± 1.0; n=131) followed by plagioclase ($Ab_{11}An_{83}Or_{6}$; n=60) and pyroxene (Fe/Fe+Mg : HY(Wo∿2) = 0.21, PG(Wo∿7) = 0.19; n=91) are severely restricted in composition. Interestingly, one small grain of augite ($Wo_{44}En_{46}Fs_{10}$) was also found. Matrix and chondrule minerals are similar in composition indicating that the meteorite is well equilibrated. Apatite occurs in the vugs of the matrix. Irregular patches of troilite are common along with disseminated Fe^{o} metal.

Extreme fracturing, granulation, and undulose extinction of olivine and pyroxene, maskelynitization of plagioclase (at places even as veins in olivine), and the apparent free flowing forms of troilite attest to a moderately heavy shock event(∿"e" of Dodd and Jarosewich). However, maskelynite is almost totally recrystallized with no change in the major element composition. Mosaicism in plagioclase and rarely in olivine and pyroxene is seen at places and appears to predate and survive later maskelynitization etc. Tabular and rounded olivine is wrapped by a feathery intergrowth of acicular plagioclase and sheaf-like olivine/pyroxene in certain areas of the matrix. If this indicates a rapid cooling from a clast-laden melt, such melting event probably took place prior to the later shock event resulting in the dark bands, etc. In this regard the Louisville meteorite may represent a transition between usual L6 chondrites (4) and Shaw (5,6).

(1) Hunt, G. and Boone, T.E. (1978): Trans. Ky. Acad. Sci., 39 (1-2), 39-53.
(2) Hunt, G. (1978): Geol. Soc. Am., Abs. Prog., 10 (6), 256.
(3) Dodd, R. T. and Jorosewich, E. (1979): EPSL, 44, 335-340.
(4) Van Schmus, W.R. and Wood, J.A. (1967): GC Acta, 31, 747-765.
(5) Dodd, R.T. et al. (1975): GC Acta, 39, 1585-1594.
(6) Taylor, G.J. et al. (1979): GC Acta, 43, 323-337.

#124

MORRO DO ROCIO, AN UNEQUILIBRATED H5 CHONDRITE.

Wlotzka, F. and Fredriksson, K.
Max-Planck-Institut für Chemie, Mainz, and Smithsonian Institution, Washington,D.C.

Chondrites are agglomerates of silicate chondrules and other components. In the case of the so-called equilibrated chondrites the composition of the main mafic silicates is uniform. At a first look this is also the case with Morro do Rocio, S. Catharina, Brazil. It contains olivine with Fa 17.8 ± 0.3, and pyroxene with Fs 16.5 ± 1, which places it in the H group of chondrites. From texture and petrologic features (chondrules not well defined, coarse matrix, absence of clinopyroxene and of clear isotropic glass) it belongs to petrologic type 5.

In a thin section, however, two inclusions were found with higher fayalite content in the olivine. The first is a normal porphyritic olivine chondrule, the olivine has Fa 19.7 ± 0.1. The second is mainly one anhedral olivine grain with Fa 20.8 ± 1 grown together with a high-silica glass (SiO_2 75 %) which is different from the usual feldspathic matrices of the chondrules (SiO_2 about 63 %). Both values fall into the gap between H and L group chondrite olivine compositions.

Another sign of non-equilibration is the variation in the alkali-content of the feldspathic matrices of chondrules. Potassium (average about 1 % K_2O) varies from 0.6 to 6 % (Na stays more or less constant), not including the Si-rich glass mentioned before with 0.3% K_2O. This variation in potassium is especially noteworthy with regard to the formation mechanism of the K-rich glass described from inclusions in some LL chondrites like Bhola (Fredriksson et al., 1975) and Krähenberg (Wlotzka et al.,1979).

Another peculiar feature is the occurrence of pure silica. It is found in spherical shape (diameter about 100 microns), surrounded by a shell of small diopside crystals, inside an otherwise normal radiating pyroxene chondrule. The shape of these silica bodies suggests formation by liquid segregation.

These "anomalies" in an ordinary, otherwise uniform chondrite show that this meteorite is not equilibrated. Such anomalies are only found after the analysis of many grains and chondrules or by chance, and are probably not as rare as it seems. That is, they are not really anomalies and have to be taken into account also for the interpretation of "ordinary" chondrites.

Fredriksson, K., Noonan, A. and Nelen, J. (1975) Meteoritics 10, 87.
Wlotzka, F., Palme, H., Spettel, B., Wänke, H., Fredriksson, K., Noonan, A. (1979) Meteoritics 14, 566.

A HETEROGENEOUS LITHIC FRAGMENT IN THE BOVEDY L3 CHONDRITE: ORIGIN BY IMPACT MELTING OF PORPHYRITIC CHONDRULES

A.E. Rubin, K. Keil and G.J. Taylor, Inst. of Meteoritics, Univ. New Mexico, Albuquerque, NM 87131; M.-S. Ma and R.A. Schmitt, Radiation Center, Oregon State Univ., Corvallis, OR 97331; D.D. Bogard, Geochemistry Branch, NASA JSC, Houston, TX 77058

The Bovedy L3 chondrite contains a light-colored poikilitic lithic fragment with a bulk composition (Table 1) and olivine, orthopyroxene and kamacite compositions characteristic of porphyritic chondrules (PC) from unequilibrated ordinary chondrites. The low Na_2O, K_2O and P_2O_5 content of the fragment, its texture, its compositional similarities to PC and the unusually calcic plagioclase in the fragment and host indicate that the fragment represents a solidified impact-melted area of the Bovedy parent body that was rich in PC. The fragment is heterogeneous, with a progressive increase in the bulk MgO/FeO ratio and the MgO content of olivines (Fig. 1) and orthopyroxenes across its length. The heterogeneities in the fragment were probably caused by an abundance of minute unfused particles in the impact melt, acting as nucleation sites at one end of the fragment and causing crystallization of MgO-rich olivines and orthopyroxenes at low ΔT as the fragment cooled from the liquidus at $<\sim 2^{o}C$/hr. The residual melt was enriched in FeO and crystallized olivines and orthopyroxenes at greater ΔT. Textural evidence supports this: the MgO-rich end of the fragment contains olivines with an equigranular texture (indicative of crystallization at low ΔT, whereas the FeO-rich end (area A) contains elongated olivines (morphologies indicative of crystallization at greater ΔT). Sub-solidus equilibration of area A and the host (indicated by a compositional gradient across area A from the host boundary and the closer mineral compositional similarities of area A to the host than to the other areas of the fragment) must have occurred as the fragment and host cooled together as a single assemblage. The $^{39}Ar/^{40}Ar$ analysis of the fragment as well as the host (G. Turner, unpublished data) indicates that the meteorite experienced extensive degassing of Ar due to reheating of the assemblage. The approximate age of 0.5 - 0.94 Ga dates the reheating event and not the formation of the lithic fragment. This reheating event renders the metallographic cooling rate of 1-10°C/Ma (through 500°C) imprecise. However, the absence of martensite and the presence of kamacite and zoned taenite in the fragment are consistent with such slow cooling through 500°C. This cooling rate must have resulted from burial of the fragment-host assemblage beneath insulating material on the Bovedy parent body. If the thermal diffusivity (κ) of this overburden was comparable to that of the lunar regolith (10^{-5} cm^2/sec) then the fragment was buried at a depth >1.5 km; if $\kappa = 10^{-2}$ cm^2/sec (similar to chondritic material), then the fragment was buried at a depth >45 km.

TABLE 1

	LF	POC
SiO_2	45.6	45.8
TiO_2	0.14	0.15
Al_2O_3	3.7	3.7
Cr_2O_3	0.61	0.55
FeO	13.5	9.8
MgO	33.1	33.1
MnO	0.33	0.28
CaO	2.33	2.4
Na_2O	0.60	1.5
K_2O	0.05	0.15
P_2O_5	0.04	0.10
Total	100.00	97.53

LF = normalized bulk comp. of silicate portion of lithic fragment

POC = average bulk comp. of 25 porphyritic olivine chondrules (after Lux et al., 1980)

Fig. 1

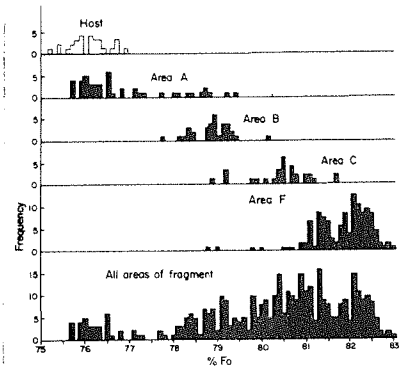

#126

A NEW MEASURE OF THE METAMORPHIC HISTORY OF ORDINARY CHONDRITES

Melcher, C.L.*; Ross, L.M. McDonnell Center, Washington Univ., St. Louis; Mills, A.A., Geology Dept., Leicester Univ., U.K.; Grossman, J.N. and Sears, D.W., Inst. Geophys. & Planetary Phys., U.C.L.A.

In a study of the TL sensitivity** of 29 ordinary chondrites, we have discovered that there is a strong relationship between TL sensitivity and metamorphic history, as predicted by Liener and Geiss in 1968. Our 11 meteorites of Type 5 and 6 cover a range in TL sensitivity of $\lesssim$10 and Type 5 cannot be distinguished from Type 6. Our four Type 4 specimens cover a similar range, but tend to have values of about half that of the higher types. Type 3 sensitivity values cover a range of $\sim$1000, being comparable with Type 4 only at the top end of this range.

The Type 3 meteorites display strong relationships between TL sensitivity and i) PMD of the fayalite content of the olivine, ii) PMD of the Co in the kamacite, iii) percent matrix crystallization and iv) FeO/(FeO+MgO) in matrix normalized to whole rock. Furthermore, their bulk carbon and ^{36}Ar contents show a relationship with TL sensitivity and, like TL sensitivity, display a range of values in Type 3 $\gtrsim$10 times that displayed in the three higher petrologic types put together. It seems, therefore, that there is some justification for sub-dividing Type 3. For various reasons, we propose a decimal-numerical nomenclature; viz., Types 3.2, 3.4 and 3.6 in order of increasing equilibration and TL sensitivity. We reserve Type 3.0 for as yet undiscovered, completely unmetamorphosed, ordinary chondrites and Type 3.8 for some Type 3s more equilibrated than those which we examined (eg. Carraweena).

The mineral normally responsible for producing TL in meteorites is feldspar. From our study, we conclude that the TL sensitivity value is particularly sensitive to the extent of devitrification of feldspathic glass and this is why it shows such a large range in Type 3 chondrites. Our data are consistent with the observations of Van Schmus and Wood, that in Type 4 the glass has largely, though not completely, devitrified, whilst in Types 5 and 6 it is entirely crystalline.

Type 3.6 Meteorite	TL Sens.	Type 3.4 Meteorite	TL Sens.	Type 3.2 Meteorite	TL Sens.
Bremervörde	2.6	Tieschitz	0.17	Bishunpur	0.0054
Mezö-Madaras	1.1	Chainpur	0.078	Semarkona	0.0045
Dhajala	1.0	Sharps	0.071	Krymka	0.0027
Hedjaz	0.82	Manych	0.070		
Khohar	0.44				
Parnallee	0.42				
Ngawi	0.25				

Table:TL sensitivity normalized to Dhajala

*Present address: Kellogg Radiation Lab., Caltech.
**TL emitted by a sample which has had its natural TL removed by heating to 500°C, and then given a standard laboratory test dose of radiation.

CONFIRMATION OF DIFFERING COOLING HISTORIES OF CHONDRITIC ASTEROIDS

P. Pellas
Lab. de Mineralogie du Museum, 61 rue Buffon, 75005 Paris, France.

Cooling rates between fission xenon and track retention temperatures (∿ 950-∿ 350 K) in phosphates from chondritic materials have been recently revised(1, 2). Especially for the H chondrites the new data lead to major revisions of previously published results. In the H case, the last results (∿ 560 - ∿ 370K: ∿ 3/Ma for H6, > 10/Ma for H4) are consistent with an onion-shell structure of the parent asteroid in which petrologic type 6 materials resided near the central region, and types 5, 4, and 3 in the outer shells. The very fast cooling of H4 materials (> 44/Ma for 870-670 K) seems to preclude the existence of an insulating regolithic layer at the time when the early cooling took place (i.e. in the first hundred million years after the H object was formed). In any case, the size of the H object is restrained to a radius of 50-70 km.

More data recently obtained for Bjurbole (L4), Ausson and Elenovska (L5),and Tillaberi (L6) confirm our revised cooling rates for the L chondrites. The picture that emerges for the L object, although similar, differs in many respects from that of the H object. In particular, the cooling rate of Bjurbole is very close to that of H6 materials. Such a low cooling rate for a surficial sample would require either an insulating regolithic layer or a large size parent object (R_o > 100 km), or both. The reason why, in the first hundred million years, a regolith could have been present on the L (and LL) and not on the H object is still a subject of speculation. Moreover, the differences in cooling rates between L5 and L6 (Tillaberi) materials (∿ 2.4 versus ∿ 1.8/Ma for 560-370 K) are much less clear-cut than for the corresponding H materials.That could indicate that Tillaberi, classified as L6 (3), might well be a L5-L6 chondrite like Barwell (4). If so, it would be important to study a typical L6 meteorite like Tatlith.

St. Séverin (LL6) shows a low cooling rate (1.6/Ma for 560-370 K) indicating a rather large parent object (R_o : 110-150 km). This large size seems to be confirmed by both the high abundance (65 %) of xenolithic breccias among the LL chondrites and the low ^{40}Ar-^{39}Ar age of St. Séverin (4.38-4.42 Ga) (5). Work still in progress on Uden (LL7), which should come from a deeper location inside the LL object, will hopefully be reported at the conference.

Among all chondritic materials the lowest cooling rates were found for silicate inclusions from I A irons (Copiapo and Landes : 1.2/Ma for 600-300K) (6), if the anomalous case of Shaw is discarded (2,7). For these two irons, however, the ^{40}Ar-^{39}Ar plateau ages (4.48 and 4.50 ± 0.03 Ga respectively) (8) do not reflect a later Ar closure temperature than for St. Séverin.

1) Pellas and Storzer, 1979. Meteoritics 14, 513.
2) Pellas and Storzer, 1980. Phil. Trans. Roy. Soc. Lond. A, in press.
3) Christophe and Malezieux, 1976. Meteoritics 11, 217.
4) Hutchison et al., 1979. Appendix,Catalogue Meteorites, B.M.N.H., London.
6) Benkheiri et al., 1979. Icarus 40, 497.
7) Scott and Rajan, 1979. Proc. Lunar Planet. Sci. Conf., 10th, 1301.
8) Niemeyer, 1979. Geochim.Cosmochim. Acta 43, 1829.

#128

THERMAL HISTORY OF CHONDRITES CONTAINING RAPIDLY SOLIDIFIED METAL-TROILITE INCLUSIONS

Scott, E.R.D.
Department of Geology, Institute of Meteoritics, University of New Mexico, Albuquerque, NM 87131

Rare metal-troilite inclusions (0.2 to 4 mm in size) which have a dendritic or cellular texture indicative of fast cooling during solidification were studied in 10 ordinary chondrites. In Weston*, Dimmitt*, Tell and San Emigdio, the inclusions were embedded in normal chondritic material, whereas in Pulsora[1], Tysnes Island*[2] and Mezö-Madaras the inclusions were inside or attached to metal-poor clasts from which they had been derived by partial or complete melting (* = gas-rich). From the spacing of secondary dendrite arms or the widths of cells (10-100 μm), cooling rates of 1-300°C/sec during solidification can be derived using laboratory data (see ref. 3). Three spherules in San Emigdio had cooled at 10,60 and 100°C/sec.

The absence of heating effects in the hosts of the Weston group shows that their inclusions were not produced in situ by shock melting, but were probably derived from melted clasts, as in Pulsora. Except in Mezö-Madaras, the inclusions cooled through 500°C very much faster then host metal grains, which had normal textures indicative of cooling at 1-1000°C/Myr. Thus metal grains and inclusions cooled at these rates in different locations before compaction of the meteorites, as in gas-rich chondrites.[4] In Mezö-Madaras, normal kamacite-taenite textures were superimposed on the metal dendrites implying that whole meteorite cooled through 500°C at 1°C/Myr after compaction.

To cool through 1000°C at 1-300°C/sec, the dendritic inclusions could not have been in contact with hot silicate masses larger then ∿ 40 mm in size. At least one of the inclusions cooled next to cold silicate, others may have cooled by radiation only. This is quantitative evidence that these inclusions and the attached clasts with igneous textures were melted on the surface of a parent body (by impact), and were not formed at depth from an internally derived melt.

In Ramsdorf[5], Rose City and Shaw[6] where the hosts have been heated above 1000°C, larger dendrite dimensions imply slower cooling rates during solidification viz., 10^{-1} to 10^{-4} °C/sec. Thus the dimensions of the surrounding hot material were ∿ 30-50 cm for Ramsdorf and Rose City and ∿ 6 m for Shaw. The mixture of melted and unmelted material in Shaw[6] and Rose City implies that they were part of a melt-breccia mixture of larger dimensions and did not necessarily cool through 1000°C within a few m of the surface.

References: 1, Fredriksson et al. (1975) Smithsonian Contrib. Earth Sci. 14, 41-53; 2, Wilkening (1978) Meteoritics 13, 1-9; 3, Blau and Goldstein (1975) GCA 39, 305-24; 4, Scott and Rajan (1980) GCA submitted; 5, Begemann and Wlotzka (1969) GCA 33, 1351-70; 6, Taylor et al. (1979) GCA 43, 323-37.

OCCURRENCE AND ORIGIN OF TETRATAENITE, ORDERED FeNi, IN METEORITES

Clarke, R.S.[1] and Scott, E.R.D.[2]
[1]Mineral Sciences, Smithsonian Institution, Washington D.C. 20560. [2]Inst. of Meteoritics, Univ. of New Mexico, Albuquerque, NM 87131.

Tetrataenite is a tetragonal mineral with ideal formula FeNi, which forms by ordering of Fe and Ni atoms in taenite. The name and the mineral have been approved by the Commission on New Minerals of the I.M.A. It has the CuAu or $L1_0$ structure[1], contains 48-57 wt.% Ni and has been observed in over 60 chondrites, mesosiderites, irons and pallasites.[2,3] It typically occurs as 1-20 μm wide rims on zoned taenite, 10-50 μm grains ('clear taenite') and ≤ 1 μm grains in "cloudy taenite". We describe new occurrences of larger grains and their implications for the origin of tetrataenite.

Metal in LL chondrites contains ∿ 25-50% Ni. In Appley Bridge which has the highest Ni concentration, all the metal is tetrataenite, the largest grain being 1.2 mm in size; tetrataenite grains contain 52.9% Ni, 2.0% Co and 0.18% Cu. Metal in Manbhoom has a slightly lower bulk concentration of Ni and consists of tetrataenite with minor kamacite, but no taenite. Most LL chondrites, like Bhola, have metal with 25-40% Ni which contains kamacite, "cloudy taenite" and tetrataenite. Thus the relative abundances of these phases reflect the bulk compositions.

Tetrataenite also forms large grains in a 4 x 2.5 cm sample (USNM 3256, mislabelled Copiapo), which displays a fine octahedral pattern in what was once polycrystalline taenite (crystal size 5-10 mm). Troilite nodules are aligned along former taenite grain boundaries and contain silicates. Silicate and schreibersite compositions and the texture of the metal suggest that this sample may be a metallic nodule from a mesosiderite (Vaca Muerta?) although the bulk Ni (∿ 10%) and fine octahedral pattern are not typical. Tetrataenite grains up to 400 μm wide coat the grain-boundary troilites and form 5-80 μm wide plates and blebs between the oriented kamacite crystals. Only a few large tetrataenite grains contain tiny residual blebs of cloudy taenite. Thus the Widmanstätten pattern is composed almost entirely of tetrataenite pseudomorphing taenite, and kamacite.

Large tetrataenite grains in LL chondrites and USNM 3256 have the optical properties common to other occurrences. Crossed polars reveal three different orientations of intergrown crystals displaying polarization colors of orange-brown, bluish-green and khaki, each of which is decorated with magnetic domain patterns. We see no evidence for fine mixtures of taenite and tetrataenite as proposed by Mehta et al[4]. We suggest that they misidentified tetrataenite crystals with [101] and [011] parallel to the electron beam (orientations which do not show superlattice spots) as taenite.

We propose that tetrataenite (or its precursor γ) forms on preexisting taenite below 350°C by inward and outward growth of Ni-rich rims when Ni is rejected from kamacite. The former requires Ni diffusion through tetrataenite (or Ni-rich taenite), the latter only through kamacite. In many occurrences outward growth aided by rapid diffusion along kamacite grain boundaries may dominate, but in others, especially in USNM 3256, Ni must have diffused through 40 μm of tetrataenite (or Ni-rich taenite). Since the maximum calculated diffusion distance in taenite below 400°C is <5 μm, calculated diffusion rates in taenite, and consequently metallographically derived cooling rates, may be too low.

References: 1, Albertsen et al. (1978), Nature 273, 453; 2, Scott and Clarke (1979) Nature 281, 360; 3. Clarke and Scott (1980) Am. Mineral. in press; 4, Mehta et al. (1980) Nature 284, 151.

#130

K-U STUDIES OF SILICA-RICH INCLUSIONS IN THE SHAW CHONDRITE

W.R. Heuser, D.S. Burnett and J.W. Larimer*
Div. of Geol. & Planet. Sci., Calif. Inst. of Technology, Pasadena, CA 91125
*Dept. of Geol., Ariz. St. U., Tempe, Ariz. 85281

The K/U can be regarded as a "planetary constant" which is invariant during magmatic processes but which differs for cosmochemical reasons between planets. This assumption is universal in all thermal history calculations for planets. K-SiO_2-rich inclusions are found in Shaw which many authors believe is a chondrite which has been subjected to partial melting (1,2). Although the origin of these inclusions is not well understood, it is possible that they represent the first melts or magmatic fluids produced in the formation of planets. Thus it is of interest to see if U and Th have followed K into these liquids. For the case of Shaw some evidence of K/REE fractionation already exists (2). Six polished sections of Shaw with affixed mica fission track detectors were irradiated with ~$2x10^{18}/cm^2$ thermal neutrons. Excellent fission track images were obtained with no evidence for any significant contamination. (Random scans on our most-studied section give 6 ppb U). The fission track distributions show a high degree of localization. In one section, mapped in great detail, 20-30 large (>50 micron) fission track localizations, can all be accounted for by whitlockite and chloroapatite. The whitlockite U concentrations (300-700 ppb) are variable, but typical for chondrites. The phosphate grains serve as fiducial points, allowing accurate location of the melt inclusions on the mica track detector (maximum position error=20 microns). In many cases no localizations of tracks are found (U contents <10 ppb) corresponding to the K-Si-rich inclusions, but in 7/25 cases localizations are found with U concentrations up to ~300 ppb. The inclusions are small (usually <20μ), and there are many other small track localizations in this size range which have no obvious sources, thus some of these 7 cases may be accidental. However, track mapping at 13 random fields of view showed only 2 localizations (track density 3-4 times surroundings) within 20 microns. The small track localizations of unknown origin can be explained by a combination of buried sources (within 10 microns of surface), local contamination (which can never be ruled out) or localization of U on grain boundaries or cleavage planes in major phases. There is no correlation of U content with inclusion chemistry (K), size, opaque mineralogy, or petrographic location. Many of the inclusions are within large (hundreds of microns) olivine grains, including some that seem U-rich. In two of these cases the track localizations stand out from an almost blank background and match the location and size of the inclusion. It seems inescapable that the tracks do arise from the inclusions in these cases. It may be that these inclusions were a preferential site of contamination during sample preparation or by terrestrial weathering, but it is also possible that U-bearing phases only occasionally participated in the partial melting process. It may be significant that the inclusions contain no P, thus this U reservoir has not participated. Regardless, the important result is that in most cases K was mobilized to a much higher degree than U in the Shaw partial melting event. (The inclusion K/U is at least 10X bulk chondrites). Although the inclusions are relatively Fe-rich, the concentration of K and Si and the exclusion of U and rare-earths follows the chemical systematics of immiscible silicate melts (3,4). To the extent that Shaw is representative of very small degrees of partial melting in planets, K and U appear to be frationated.

References: (1) Taylor et al., GCA, 43, 323, 1979; (2) Rambaldi and Lamimer, EPSL, 33, 61, 1976; (3) Watson, Cont. Min. Pet. 56, 119, 1976; (4) Ryerson and Hess, GCA, 42, 921, 1978.

SOME STUDIES ON THE METAL OF UNEQUILIBRATED ORDINARY CHONDRITES

Sears, D.W. and Marshall C. Institute of Geophysics and Planetary Physics, University of California, Los Angeles.

Metal grains from a suite of 12 unequilibrated ordinary chondrites have been examined by X ray diffraction, electron microprobe and metallographic techniques. XRD patterns of U.O.C. differ markedly from equilibrated chondrites. The XRD patterns of equilibrated chondrites are dominated by peaks produced by α and γ nickel-iron, whose relative intensity varies between H, L and LL chondrites in the expected manner. In contrast, peaks due to α and γ are very weak or missing from the XRD patterns of the highly unequilibrated Semarkona and Krymka, although weak α reflections are present in the data for equally unequilibrated Bishunpur. A small proportion of the Bishunpur and Semarkona metal contains Si and is believed to have equilibrated at high temperatures and in the γ state, but evidently much was still equilibrating when it cooled into the $\alpha+\gamma$ field of the Ni-Fe phase diagram. In these three highly U.O.C., the XRD patterns of the magnetic material are dominated by one or two peaks which we tentatively identify as due to trevorite and magnetite. These are also present in more equilibrated Type 3s, but α and γ metal are more prominent than before, suggesting the possibility that XRD patterns are showing a trend which reflects the degree of equilibration within the petrologic type.

Sulfide textures which can be interpreted as the result of mobilization, have frequently been reported in UOC. In the present study, silicates which appear to have been soaked in sulfide have been observed in Bishunpur, Krymka, Semarkona, Manych and Khohar. We have also found various forms of recrystallized Kamacite. Jagged α_2, formed by massive transformation of γ, occurs in Bishunpur, , Hedjaz, Manych, Sharps and, possibly, Tieschitz. Polycrystalline α (formed by annealing deformed α) occurs in Tieschitz, Sharps and Mezö-Madaras. The metal in several UOC contains regions of pearlite, suggesting the presence of carbon and fairly slow cooling from $\gtrsim 500^{\circ}C$. These regions are also P-rich and some α regions contain small precipitates, presumably of phosphide. The presence of pearlite and recrystallized α suggests that the sulfide mobilization was due to reheating, probably after agglomeration of the chondrites. Only three of our 12 UOC (Parnallee, Dhajala and Chainpur) contain no evidence of reheating. Most ordinary chondrites which have been studied for their reheating effects, have K-Ar ages $\sim$ 500 My, whilst these UOC have ages $\sim$ 4.6 Gy. It seems that either the event which caused the reheating was too mild to cause appreciable gas-loss or, more likely, occurred very early in solar system history. Maybe it was part of the agglomeration process.

#132

Ar DIFFUSION PROPERTIES AND ^{40}Ar-^{39}Ar DATING OF METEORITES

Donald D. Bogard
NASA Johnson Space Center, Houston, Texas 77058

We have measured the Ar isotopic composition (including ^{37}Ar and ^{39}Ar) from stepwise heating of neutron-irradiated samples of approximately 20 shock-heated and unshocked ordinary chondrites, individual clasts from the Abee E4 chondrite, remelted clasts from brecciated chondrites, and mineral separates of achondrites. Many whole-rock samples of chondrites exhibit releases of ^{39}Ar (from K) and ^{37}Ar (from Ca) from two phases with distinct K/Ca ratios and with average laboratory degassing temperatures which differ by several hundred degrees. Values of the diffusion parameter, D/a^2, for ^{39}Ar have been calculated from these data. When values of D/a^2 are plotted versus reciprocal temperature in Arrhenius plots, the resulting curves commonly deviate substantially from linear trends. When values of D/a^2 are calculated separately for the two K-bearing phases, however, two distinct and linear Arrhenius plots result, which apparently correspond to the degassing of different mineral phases with appreciably different Ar retention properties. Activation energies for these two phases are $\sim$ 35 kcal/mole and $\sim$ 70 kcal/mole, and values of D/a^2 at 800°C are $\sim 10^{-5}$ sec^{-1} and $\sim 10^{-8}$ sec^{-1}. The wide variation in literature values of activation energies for Ar diffusion in chondrites may be due in part to variable mixtures of two K-bearing phases. Two K phases with quite different Ar diffusion properties appear to exist for neutron-irradiated and unirradiated chondrites, highly shock-heated and unshocked chondrites, and clasts from Abee. However, the distinction between these phases is much less apparent in remelted clasts from the Bovedy (L3) and Dimmitt (H3) chondrites and from the Shaw chondrite, apparently because of the recrystallization experienced by these materials. The ability to resolve Arrhenius plots for Ar into linear components for a variety of meteorites lends support to the use of such data in modeling the thermal histories of these meteorites from Ar data.

^{40}Ar-^{39}Ar ages calculated from these data commonly show differences between the two K-bearing phases, especially for meteorites which have been partially degassed, such as shocked or brecciated chondrites. Previous explanations for such age differences have included a range of grain sizes, reactor recoil effects, chronological information on more than one event, etc. The existence of two (or more) phases with distinct Ar diffusion properties must also be considered in interpretations of such ages. For example, a heating event which would only partially degas ^{40}Ar from the high-temperature phase can be expected to completely degas ^{40}Ar from the low-temperature phase. This can result in two apparent plateaus in the ^{40}Ar-^{39}Ar age profile for which only the lower age may have significance. We attribute the older apparent ^{40}Ar-^{39}Ar ages in the high-temperature phase of severely shock-heated chondrites to incomplete Ar loss due to the very high activation energy for Ar diffusion, even though reheating temperatures in some cases apparently reached 1200°C. Thermal models suggest cooling from these temperatures was rapid. Recrystallized clasts from the Bovedy and Dimmitt chondrites suggest ^{40}Ar-^{39}Ar degassing ages of $\sim$ 1 Gy, with only partial degassing of K phases. Unlike the situation for a clast from Plainview, these clasts may have been heated after incorporation into the meteorite.

A 4.0 B.Y. IMPACT METAMORPHISM AGE OF THE MODOC L6 CHONDRITE DETERMINED BY THE Sm-Nd METHOD

Nakamura, N.* and Tatsumoto, M.†
*Dept. of Earth Sciences, Kobe University, Kobe 657, Japan; †U.S. Geological Survey, MS 963, Box 25046, Denver, Colorado, 80225

In order to evaluate the age and history of the L-chondrites, we have examined the Sm-Nd systematics of the Modoc (L6), Bruderheim (L6) and Barwell (L5) chondrites. The Modoc whole-rock analyses yield $^{147}Sm/^{144}Nd$ and $^{143}Nd/^{144}Nd$ ratios of 0.1948 and 0.512581 ± 0.000025 (2 δm) (normalized to $^{150}Nd/^{144}Nd$ = 0.236433), respectively. The model age of the whole rock relative to the initial $^{143}Nd/^{144}Nd$ ratio of the Moore County eucrite (Nakamura et al., 1977; corrected) of 4.52 ± 0.03 b.y. is not resolvable from the meteorite formation age of 4.55 b.y. The whole-rock analyses of Bruderheim and Barwell yield similar results. As we previously stated at the 42nd Annual Meeting of the Meteoritical Society (Nakamura et al., 1979), there was a small error in our Sm-Nd tracer calibration so that the Sm-Nd ages of Pasamonte, Moore County, and Moama should be reduced by ~0.03 b.y. This problem was restated by Jacobsen and Wasserburg (1980).

Mineral separates from the Modoc chondrite show variations of 50% in $^{147}Sm/^{144}Nd$ and 0.27% in $^{143}Nd/^{144}Nd$, with apatite having the lowest ratios and clinopyroxene the highest. Four of the five separates analyzed define a linear array on a $^{147}Sm/^{144}Nd$ vs. $^{143}Nd/^{144}Nd$ plot with a slope corresponding to an age of 4.03 ± .04 b.y. (2σ) and an initial $^{143}Nd/^{144}Nd$ ratio of 0.50739 + .00005 (2σ). The data for the 3.32-3.4 g/cm^3 density separate do not lie on the line.

Because the Sm-Nd age and the initial $^{143}Nd/^{144}Nd$ ratio obtained for Modoc are consistent with two-stage, closed system evolution from the initial ratio of Moore County, and possible two-component mixing effects have not been found, the 4.03 b.y. age may be real. If so, this is the first evidence by the Sm-Nd method for a strong thermal event in chondrites at significantly later time than the initial meteorite formation. However, because one point deviates from the line a shock event rather than thermal metamorphism (Minster and Allegre, 1979) may be indicated. If this is the case, then the 4.03 b.y. "age" may only represent an upper limit to the age of the disturbance. The Sm-Nd results for Modoc suggest that the Sm-Nd method can potentially determine the precise time of late heavy meteorite bombardments or thermal metamorphism in the chondrite parent bodies.

References

Nakamura, N., Masuda, A., Coffrant, D., and Tatsumoto, M. (1979), Oral Presentation, 42nd Meeting of Meteoritical Society, Heidelberg, W.G.

Nakamura, N., Unruh, D. M., Gensho, R. and Tatsumoto, M. (1977), Lunar Science, VIII, 712-713.

Minster, J-F. and Allegre, C. J. (1979), Earth Planet. Sci. Lett., 42, 333-347,

Jacobsen, S. B. and Wasserburg, G. J. (1980), Lunar Planet. Sci. XI, 502-504.

#134

OXYGEN ISOTOPIC COMPOSITIONS OF PETROLOGICALLY CHARACTERIZED CHONDRULES FROM UNEQUILIBRATED CHONDRITES

Gooding, J.L.[1,2], Keil, K.[1], Mayeda, T.K.[3], Clayton, R.N.[3], Fukuoka, T.[4,5], and Schmitt, R.A.[4] (1) Dept. of Geology and Institute of Meteoritics, Univ. of New Mexico, Albuquerque, NM 87131 (2) Jet Propulsion Laboratory, Pasadena, CA 91103 (3) Enrico Fermi Institute, Univ. of Chicago, Chicago, IL 60637 (4) Dept. of Chemistry and Radiation Center, Oregon State Univ., Corvallis, OR 97331 (5) Dept. of Chemistry, Gakushuin Univ., Tokyo 171, Japan

Whole chondrules separated from the Dhajala (H3/4; 2 chondrules), Hallingeberg (L3; 4 ch.), and Semarkona (LL3; 4 ch.) chondrites were individually analyzed for bulk elemental composition by instrumental neutron activation with half of each chondrule subsequently sacrificed for oxygen isotopic analysis and half retained for petrographic and electron microprobe analysis. A three-isotope plot shows that chondrule δ O-17 and δ O-18 are positively correlated although the chondrule data do not form clusters corresponding to their respective host-chondrite chemical groups but rather form a single stream of points which lie along a mixing line between the previously determined (1) H- and L/LL-group whole-rock three-isotope compositions. However, the chondrule trend continues toward greater O-16 depletion (δ O-17$\simeq$ 4.8 ^{o}/oo, δ O-18$\simeq$ 5.8 ^{o}/oo, rel. SMOW) in a manner similar to that previously observed for the LL3 chondrites ALHA 76004 (2) and Chainpur (3). At least one chondrule (from Semarkona), though, lies significantly away from the mixing line and may be related to ordinary chondrite material by fractionation. The O-isotopic heterogeneities among chondrules are similar in magnitude to their bulk elemental and phase compositional heterogeneities and strengthen the proposition that chondrules in unequilibrated H-, L-, and LL-chondrites were formed from the same or similar populations of materials (4). Weak inverse correlations between chondrule δ O-18 and total Fe, and between δ O-18 and molar Fe/(Fe + Mg) in olivine and pyroxene, contrast with positive correlation between the latter parameters in average whole-rock ordinary chondrites and supports the notion of an independent, pre-chondrite history for chondrules in unequilibrated chondrites. Furthermore, 7 of the 10 isotopically analyzed chondrules show a positive correlation between δ O-18 and bulk weight ratio $(CaO + Al_2O_3)/MgO$, suggesting that at least some chondrule compositions might be explained by mixing of mafic and felsic components as might be expected if chondrules formed by melting of pre-existing, heterogeneous materials (4).

References: (1) R. N. Clayton, N. Onuma, and T. K. Mayeda (1976) Earth Planet. Sci. Lett., 30, 10-18.
(2) R. N. Clayton, T. K. Mayeda, and N. Onuma (1979) Lunar Planet. Sci. X, Houston, Texas, 221-223.
(3) F. Robert, L. Merlivat, and M. Javoy (1979) Nature, 282, 785-789.
(4) J. L. Gooding, K. Keil, T. Fukuoka, and R. A. Schmitt (1980) Earth Planet. Sci. Lett., in press.

OXYGEN ISOTOPIC ANOMALIES IN AN ORDINARY CHONDRITE

Mayeda, T.K.[1], Olsen, E.J.[2] and Clayton, R.N.[1]
1. University of Chicago, Chicago, Il 60637
2. Field Museum of Natural History, Chicago, Il 60605

Antarctic meteorite 76004 is an LL3 chondrite containing a variety of clasts and irregularly-shaped inclusions which appear to be chondrule fragments. Oxygen isotope analysis of four of these inclusions yields a linear array on a three isotope plot, with a slope of unity, indicating ^{16}O additions and depletions relative to the bulk composition. The data fall precisely along the ^{16}O-mixing line which passes through the bulk compositions of H-chondrites and of L and LL-chondrites (Clayton and Mayeda, 1978). The range of observed variation in $\delta^{18}O$ and $\delta^{17}O$ is 10‰, which is far greater than has previously been reported for unequilibrated ordinary chondrites (Clayton et al., 1979; Robert et al., 1979). The most ^{16}O-rich sample ($\delta^{18}O$ = -1.9‰, $\delta^{17}O$ = -3.2‰) is a medium gray fine-grained inclusion containing iron-rich olivine (Fa_{34-51}), magnesian pyroxene (Fs_{3-10}), metal, troilite and an iron-rich glass. The most ^{16}O-poor sample ($\delta^{18}O$ = +6.1‰, $\delta^{17}O$ = +4.7‰) is a large dunitic clast, consisting of olivine (Fa_{15-25}), a high-silica, high-alumina glass, metal and sulfides. A low-temperature fluorination of this sample produced oxygen primarily from the glass, with $\delta^{18}O$ = +8.3‰, $\delta^{17}O$ = +6.8‰. The other two inclusions had $\delta^{18}O$ of 4.5‰, and $\delta^{17}O$ of 2.9‰. These are richer in ^{16}O than the bulk meteorite, for which $\delta^{18}O$ is +5.9‰ and $\delta^{17}O$ is +4.3‰ (Clayton et al., 1979). These results confirm the observation of Gooding et al. (1980) that chondrules in unequilibrated ordinary chondrites fall along the ^{16}O-mixing line defined by the bulk compositions of the ordinary chondrites and show that isotopic heterogeneities of presumed nucleosynthetic origin are preserved in these meteorites. They are therefore prime candidates for a search for radiogenic ^{26}Mg and for isotopic effects in other elements.

References:

Clayton, R.N. et al. (1979) Lunar Science X, 221-223.

Robert, F. et al. (1979) Nature 282, 785-789.

Olsen, E.J. et al. (1978) Meteoritics 13, 209-225.

Clayton, R.N. and Mayeda, T.K. (1978) E.P.S.L. 40, 168-174.

Gooding, J. et al. (1980) Abstracts 43rd Meteoritical Society Meeting.

#136

INTERRELATIONSHIPS OF PETROGRAPHY, MINERALOGY, AND CHEMISTRY IN CHAINPUR CHONDRULES.

Grossman, J.N.
Institute of Geophysics and Planetary Physics, University of California, Los Angeles, CA 90024.

Chemical, mineralogical, and petrographic data on a suite of 36 separated chondrules from the Chainpur (LL3.4)(see Melcher, et al., this volume) chondrite have been the subject of a multivariate analysis. The data comprise: elemental concentrations of Na, Mg, Al, K, Sc, V, Cr, Mn, Fe, Co, Ni, Zn, Ga, Ge, As, Se, Sm, Ir, and Au, modal abundances of olivine, pyroxene, glass, metal, and sulphide, as well as individual chondrule weights and the Fe/(Fe+Mg) ratios in the ferromagnesian silicates.

Factor analysis reveals the following groups of elements: 1) Co, Ni, Zn, Ge, As, Se, and Au (siderophile and chalcophile elements); 2) Mg, Al, Sc, V, and Sm (non-volatile and refractory lithophiles); 3) Na, K, and Ga (moderately volatile lithophiles). Ir and Fe mainly behave as group 1 elements, although they also display some affinity for group 2; Fe anticorrelates with other group 2 elements. Mn and Cr are weakly associated with both groups 1 and 2, being anticorrelated with the elements in those groups.

The assignment of modal amounts of minerals to these groups by factor analysis helps in the interpretation of elemental data. Metal and sulphide belong to group 1, showing that the variance in group 1 elements is due to varying amounts of those phases. The modal amount of glass belongs to group 3, so Na, K, and Ga must be associated with any glass that is present. Modal olivine and pyroxene anticorrelate, and are essentially independent of other variables, although the pyroxene rich chondrules tend to be enriched in Mn and Cr, and the olivine rich chondrules contain more refractories. The fayalite content of olivine and mass also anticorrelate with the group 2 elements.

The three main groupings of variables extracted by the factor analysis are linearly independent. If these groups represent the only components of chondrules then they would have to be mutually dependent. Therefore chondrules must be composed of more than three components. The lack of strong Mn and Cr associations with other groups, combined with their restricted ranges of concentration compared to other elements suggests that they mainly reside in a fourth component. This component may be a Si- and O-bearing group that was not analyzed in this study.

The analysis implies that chondrules are composed of random mixtures of a low-temperature metal/sulphide component, a high-temperature lithophile component enriched in forsteritic olivine, and a low-temperature lithophile component; these groups together will display a negative correlation with a fourth Mn- and Cr-bearing, Si and O component. Despite significant variations in chondrule chemistry, factor score plots revealed no clear relationships between chondrule compositions and internal textures. It seems that chondrule textures are determined independently of the precursor material.

THE ORIGIN OF CHONDRULE RIMS IN THE BISHUNPUR (L3) CHONDRITE

Rambaldi, E.R. and Wasson, J.T.
Institute of Geophysics and Planetary Physics
University of California, Los Angeles, CA 90024

Chemical and textural studies of chondrule rims (1,2) have indicated that they might be accretional features, acquired after chondrule formation, but before accretion and metamorphism. Two distinct rim types have been identified in these studies: sulfide-poor and sulfide-rich.

We have carried out a detailed study of metal and sulfide compositions in chondrule interiors, surfaces and matrix of the Bishunpur (L3) chondrite which, as indicated by recent studies (3,4) is a highly unequilibrated chondrite preserving a relatively unaltered record of solar nebular processes.

A comparison of Co contents of kamacite from chondrule interiors, surfaces, and nearby matrix indicates that the surface kamacite is compositionally different from that in the interior: it has a higher Co content and is always Si and Cr-free. While the surrounding matrix metal shows a wide compositional range, often as great as in the entire section, the metal in the chondrule rims tends to cluster around specific Co values. In the thin sulfide-poor rims Co concentrations are lower than in the surrounding matrix. In thick sulfide-rich rims kamacite Co contents are well above those found in the surrounding matrix and, in some cases, abundant taenite is also present. Thus, chondrule surface metal is not identical with matrix metal.

After chondrule formation, chondrule interiors became chemically isolated from the surrounding nebular gas, but the material on the surface probably continued reacting while chondrules were slowly settling toward the middle plane of the nebula, where accretion occurred.

Sulfide-rich rims were probably acquired by partial sulfuration of preexisting metal grains on chondrule surfaces, with a complementary increase in kamacite Co content and in the amount of coexisting taenite. Chondrules with sulfide-poor rims probably settled before substantial sulfuration could take place.

Our textural and chemical study of chondrules in Bishunpur seems to indicate that chondrule formation processes were continuously active throughout most of the pre-accretional history of chondrites, following condensation of the major mineral species.

1) Allen J.S. et al. (1979): Lunar Science X, p. 27-29.
2) King T.V.V. and E.A. King (1980): Lunar Science XI, p. 557-559
3) Afiattalab F. and J.T. Wasson (1980): Geochim. Cosmochim. Acta 44, p. 431-446.
4) Rambaldi E.R. and J.T. Wasson (1980): Geochim. Cosmochim. Acta, in press.

#138

MULTI-ZONED CHONDRULES: A NEWLY RECOGNIZED PARTICLE TYPE FROM ORDINARY CHONDRITES.

Elbert A. King
Department of Geology, University of Houston, Houston, Texas 77004

Abstract - Multi-zoned chondrules are common minor constituent particles of many ordinary chondrites of low petrologic type, but they are particularly abundant in the Inman (L3) chondrite. They consist of a central clast, crystal or chondrule that is completely or partially surrounded by more or less concentric zones of silicates, metal and sulfide in any order, ranging to an overall diameter of as much as 3 mm. Many concentric mineral zones are only partially continuous about the central particle giving the appearance in thin sections of festoons of alternating transparent and opaque minerals. The overall dimensions of multi-zoned chondrules may be as much as several times that of the central particle. The dominant minerals of the zones surrounding the central particle are olivine, orthopyroxene, nickel-iron and troilite of virtually uniform major element composition within each individual multi-zoned chondrule. The globular to droplet and spherical shapes of much of the nickel-iron and troilite indicates that these minerals probably were accreted to the surface of the growing multi-zoned chondrule as fluid droplets or that the metal and sulfide has been molten within and immiscible with surrounding silicate melt. The central particles generally appear to be recrystallized, probably from the heat carried by the accreting droplets. The general history of the multi-zoned chondrules seems to be that of a central particle that accretes fluid droplets of silicates, metal and sulfide in some unspecified, organized, chemically alternating mode. The production of multi-zoned chondrules either in the Solar Nebula or in the environments associated with hypervelocity impacts requires rather fanciful scenarios.

This research was supported by NASA Grant NSG-7617.

CHONDRULES IN THE KAPOETA AND BUNUNU HOWARDITES

Noonan, A.F., Rockwell Hanford Operations, Richland, Washington 99352
Rajan, S., Department of Terrestrial Magnetism, Washington, D.C. 20015
Fredriksson, K. and Nelen, J., Smithsonian Institution, Wash., D.C. 20560

The presence of impact generated glass spherules in howardites and lunar breccias has been well documented. Our search for spherules in the Kapoeta and Bununu breccias has produced glass balls and objects which display classic porphyritic and radiating pyroxene chondrule textures. The degree to which these objects are crystalline seems to be a function of both cooling history and composition. Therefore, for all similar impact produced objects we extend the traditional definition of chondrules to include both glass spherules (glass chondrules) and partly or wholly crystalline spherules (crystalline chondrules).

Broad beam electron microprobe analyses of glass in Kapoeta and Bununu chondrules are presented below. The relevant major oxides reported in the bulk analyses are recast for direct comparison with the glass composition. The glass analyses are similar to the respective normalized bulk analyses providing indisputable evidence that these spherules represent indigenous impact produced melt droplets. The Bununu chondrules, which frequently contain partially resorbed mineral and rock fragments of the parent material, appear to be relatively low-temperature homogenized melt droplets with no alkali loss. Kapoeta chondrules, however, are free of unaltered host rock, depleted in sodium and somewhat variable in composition suggesting more selective, higher-temperature melts.

A variety of crystalline and glass chondrules will be described. The implications of our findings is that at least some fraction of chondrules in chondrites (impact breccias) must have been formed by impact processes.

Composition of Glass in Chondrules from the Kapoeta and Bununu Howardites

	K-1	K-2	K-3	K-4	Kapoeta Bulk*	B-1	B-2	B-3	B-4	Bununu Bulk+
SiO_2	51.75	48.53	50.76	44.76	49.89	50.76	50.83	50.70	50.85	50.65
Al_2O_3	8.36	7.98	7.25	7.48	9.74	9.53	8.40	9.89	9.01	9.23
FeO	17.15	17.36	16.10	22.68	17.66	17.12	16.68	16.91	16.95	16.69
MgO	14.52	17.64	17.09	16.86	12.35	12.97	15.67	12.59	13.88	14.78
CaO	6.83	6.67	6.07	5.97	8.32	8.10	7.05	8.34	7.72	7.05
Na_2O	0.28	0.10	0.24	0.38	0.47	0.40	0.28	0.38	0.34	0.35
MnO	0.54	0.54	0.56	0.47	0.55	0.56	0.51	0.55	0.56	0.55
TiO_2	0.44	0.39	0.39	0.38	0.38	0.52	0.43	0.49	0.49	0.51
Cr_2O_3	0.83	0.70	0.81	0.61	0.65	0.60	0.69	0.63	0.68	0.58
	100.70	99.91	99.27	99.59	100.01	100.56	100.54	100.48	100.48	100.39

* Reported oxides normalized to 100%; analysis by Wiik (Mason & Wiik, 1966).

\+ Reported oxides normalized to 100%; analysis by Jarosewich (Mason, 1967), TiO_2 recent determination by Jarosewich.

#140

COOLING HISTORIES OF CHONDRULES IN THE MANYCH (L-3) CHRONDRITE

Roger H. Hewins* and Lisa C. Klein**
*Geological Sciences, **Ceramics, Rutgers University, New Brunswick, N.J.08903

The Manych L3 chondrite contains two principal droplet chondrule types, barred olivine (41% SiO_2, 31% MgO) and excentroradial pyroxene (55% SiO_2, 26% MgO), plus abundant lithic clast chondrules (olivine microporphyry) with similar compositions to barred olivine chondrules (1). Liquidus and glass transition temperatures were determined in controlled cooling experiments on ten-component analogues to the droplet chondrules. These temperatures are 1400°C and 600°C for the SiO_2-poor melt, and 1280°C and 710°C for the SiO_2-rich melt. Calculations using these data plus viscosity determinations yield critical cooling rates for forming glass of 3000° min^{-1} for the SiO_2-poor melt and 1° min^{-1} for the SiO_2-rich melt (2).

The majority of excentroradial pyroxene chondrules contain little glass and therefore cooled more slowly than 1° min^{-1}. Rare silica-poor chondrules composed of glass plus extremely fine sub-parallel spherulitic olivine cooled at rates approaching 3000° min^{-1}. SiO_2-poor glass occurs as a coating on a crystalline lithic chondrule, indicating that objects in Manych cooled at different times as well as at differing rates. The cooling history of olivine microporphyry has not been defined, but the growth of faceted crystals rather than dendritic olivine from such highly olivine-normative melts requires very little undercooling and very low cooling rates (3). The range of cooling histories of objects in Manych is more easily explained by impact processes than nebular condensation, because an impact of small objects or impact on a regolith generates liquid that can experience a range of cooling rates.

(1) Dodd R.T. (1978) Earth Planet. Sci. Lett. 39. 52-66; 40, 71-82.
(2) Klein L.C. et al. (1980) Proc. Lunar Planet. Sci. Conf. 11th.
(3) Donaldson C.H. (1975) Ph.D. thesis, St. Andrews University.

CHONDRULE-SIZED SPHERULES FROM AN EXPLOSION CRATER

William K. Hartmann and Laurel L. Wilkening*
Planetary Science Institute, Tucson, AZ 85719
*Lunar and Planetary Laboratory, Univ. of Arizona, Tucson, AZ 85721

Through peripheral involvement with a sample collection program from explosion cratering tests one of us (W.K.H.) obtained samples of crater ejecta collected a few hundred meters from Dial Pack crater, an 86-m diameter, 5-m deep crater formed by explosion of 500 T of TNT. Many of the samples were richly laden with glassy spherules that superficially resemble chondrules. Among the similarities to chondrules were (a) spherical shapes; (b) glassy appearance; (c) sizes mostly in the range 0.5 to 3 mm diameter; (d) cases of fusion where one or more small spherules accreted onto larger ones (probably much more common in these samples than in meteoritic chondrules).

We found the spherules to be siliceous glass of highly vesicular texture. Many larger spherules were hollow "bubbles" with thin, frothy, glass shells. In many cases these larger spherules had many tiny spherules adhering to their surfaces. The vesicularity of the spherules departs significantly from meteoritic chondrules, although a few lunar glassy spherules have such a texture. The Dial Pack spherules have been described previously and specifically compared with lunar spherules by Heiken and Lofgren (1971).

The Dial Pack explosion site was a sandy lake bed, once glaciated, in Alberta Canada. Some 69 m of glacio-lacustrine deposits overlie bedrock. The water table was estimated at about 7 m below the surface, and water partially filled up the crater to a level 14 feet below the original surface within hours after the explosion. Soils penetrated by the crater were silt, sand, and wet clay.

These samples show that glassy spherules can be ejected from explosion craters, consistent with the idea that chondrules are products ejected from planetesimal impacts among meteorite parent bodies. We suggest that the vescularity of the spherules is associated with the high free liquid water content of the cratered soil. These spherules might thus be "wet" end-members of a chondrule spectrum with meteoritic chondrules at the dry end. However, the association of fused material with terrestrial explosion craters is erratic and not well-understood (Roddy, private communication). Spherules such as those described here are very rare. These observations may mean it is difficult to make non-vesicular chondrules from initially volatile-rich primitive materials such as carbonaceous chondrites.

Ref. Heiken, Grant, and Gary Lofgren (1971) Terrestrial Glass Spheres, Geol. Soc. Am. Bull., 82, 1045-1050.

#142

CHONDRULE FORMATION BY IMPACT: THE COOLING RATE.

Kluger, F. and Weinke, H. H.
Institute of Analytical Chemistry, University, A-1090 Vienna

A multitude of time/temperature depending aspects are related to chondrules and precursor material. The differing mineralogy, bulk and isotope chemistry (e.g. variations of FeO content and volatiles, especially water) of target and/or projectile is converted to homogeneous melts. Although distinct variations of bulk chemistry between individual chondrules exist, the oxygen isotope compositions remain within a narrow range. The valuation of cooling rates is of special interest considering diffusion controlled effects.

A set of initial temperatures and involved masses had been computed for cooling times of chondrules. Some simplified input parameters are:

- impact produced ratio of gas/liquid+solid = 4/3 = const.
- geometry is the sector of an expanding sphere; expansion speed remains constant and depends on initial temperature only
- the gas is in radiative thermal equilibrium; energy loss occurs on the surface only (Stefan-Boltzmann)
- 1500 K is assumed to be the temperature where cooling of chondrules begins leading to radiative heating of the gas.

The cooling times are shorter than 60 seconds for masses up to 10^{13} grams and initial temperatures up to a presumed degeneracy limit of 150000 K.

The results of the calculations indicate a short cooling period which is not compatible with diffusion controlled complete homogenization. In addition the impact products are not retained on meteorite parent bodies or even on asteroids, if the transfer of a minute fraction of momentum is considered. Thus the origin of chondrules by impact on meteorite parent bodies is restricted to objects with radius greater than 400 kilometres, the corresponding diameter of projectiles has to exceed 100 metres.

A NEW IMPACT MODEL FOR THE GENERATION OF ORDINARY CHONDRITES

Herbert A. Zook, NASA-Johnson Space Center, Houston, Texas 77058

Wood (1979) has demonstrated that it is theoretically feasible that ^{26}Al decay could have caused major amounts of interior melting in planetary bodies with diameters as small as 20 Km. If the solid sintered layer that is postulated by Wood to surround the liquid interior of these bodies is heavily vesiculated, the thermal heat conductivity of the sintered layer may be significantly less than the solid rock values that he used. Thus largely molten bodies even smaller than 20 Km in diameter can be envisioned. The prospect of great numbers of small, largely molten, bodies orbiting about the early sun gives rise to the following potential scenario: The collision rate between these objects in the early solar system is high; indeed, gravitational perturbations by the still-growing proto-Jupiter may be important in putting many objects on collision trajectories. When collisions between objects not too dissimilar in size occur, the resulting "splash ejecta" will create large numbers of liquid droplets, as well as some fragmental material. The now isolated droplets rapidly solidify and become proto-chondrules. Then - perhaps with the aid of the remaining nebular gas - they again re-accrete into, and are buried inside of, solid small planetary bodies (asteroids?). By this time, most of the ^{26}Al is presumed to have decayed away, so that remelting does not occur. However, longer-lived radioisotopes may help raise the temperature just high enough to permit slow nickle-iron kamacite-taenite growth and other metamorphic processes. Later impact fragmentation gives rise to the ordinary chondrite meteorites now observed. The advantages of this model for creating "droplet chondrules" over other impact models are the following: 1. Plenty of liquid is already available for droplet formation; thus the extremely high impact velocities needed in previous models for impact shock melting are not required; 2. Large amounts of fragmental debris need not be created; thus chondrites with very high volume fractions of chondrules can be generated; 3. The large number of constructional particles, such as agglutinates, normally generated during hypervelocity impacts into planetary regoliths may be much reduced in the new model. The re-accretion part of this model is, of course, similar to the requirements of previous models.

Wood, J. A. (1979) In: Asteroids (Ed. Tom Gehrels), Univ. Arizona Press, Tucson, Ariz.

#144

BORON ABUNDANCES IN METEORITES: A NEW PERSPECTIVE

David B. Curtis
Los Alamos Scientific Laboratory

Boron has been quantitatively measured in chondritic meteorites by the detection of the 473 keV prompt gamma ray induced by neutron capture of ^{10}B i.e. $^{10}B(n,\alpha)^{7}Li^{*} \longrightarrow {}^{7}Li + \gamma\text{-ray}$ ($t_{1/2} \approx 10^{-13}$sec). The boron abundances in 0.5 to 1 gram samples of the interiors of carbonaceous chondrites are significantly less than have been measured in other portions of the same meteorites. Interior portions of Murchison contain five times less boron than previously measured in this meteorite (Weller et al. 1978). Similarly internal portions of Allende contain three times less boron than samples from unknown portions of this chondrite. The median abundance in eight interior samples of these two meteorites is four times less than the median boron concentration determined from all other analyses of carbonaceous chondrites. Even more dramatically, the most boron rich interior sample contains less of the element than 80% of the previously analyzed meteorites of this type. It is probable that many of the previously reported results from carbonaceous chondrites reflect the analysis of boron contaminated samples.

The distinction between boron abundances in interiors and those in samples from unspecified regions of ordinary chondrites is not as well defined as it is in the carbonaceous types. The median abundance of boron in interior pieces is 30% less than it is in all other samples of ordinary chondrites. If meteorites are susceptible to contamination by boron, ordinary chondrites are less adversely affected than the carbonaceous types.

The median silicon normalized boron abundance in interior pieces of ordinary chondrites is 22% less than it is in similar portions of carbonaceous chondrites. However, the ranges of values obtained from the analysis of eight interior specimens of each type of chondrite are very similar. No chondritic type offers an obvious choice for estimating a meteorite based value of the cosmic abundance of boron. Consequently, this value has been calculated from the simple average of the boron concentration as determined from the analysis of interior samples of ten chondrites of different types. This meteorite based cosmic abundance of boron is 8 ± 5 atoms of boron per 10^{6} atoms of silicon. The uncertainty represents one standard deviation of the ten results. Assuming $(Si/H)_{meteorites} = (Si/H)_{solar} = 4.5 \times 10^{-5}$ (Ross and Aller, 1976), the newly measured value corresponds to 3.6 ± 2.3 atoms of boron per 10^{10} atoms of hydrogen. This is in excellent agreement with spectroscopic determinations of (B/H) in the solar photosphere (Kohl et al, 1977; Engvöld, 1970).

References:

1. Engvöld O. (1970) Solar Physics 11 183-197.
2. Kohl J. L., Parkinson W. H. and Withbroe G. L. (1977), Astrophys J. (Letters) 212 L101-L104.
3. Ross J. E. and Aller L. H. (1976) Science 191 1223-1230.
4. Weller M. R., Furst M., Tombrello T. A. and Burnett D. C. (1978) Geochim. Cosmchim. Acta 42 999-1010.

CHLORINE IN CHONDRITES

J.G. Tarter, K. L. Evans and C. B. Moore
Arizona State University, Tempe, AZ 85281

A new analytical technique, combustion ion chromatography, has been used to determine the chlorine content of a suite of chondrites.

Carbonaceous chondrites have higher chlorine contents than ordinary chondrites. Typical values (ppm) are: Orgueil, 540; Murchison, 180; Murray, 325, 360, 420; Mokoia, 302; and Allende, 230. The enstatite chondrites contained: Indarch, 790, 860; St. Marks, 160, 180; Abee, 510. Thirteen ordinary chondrites ranged from 9 to 345 ppm. Finds showed no significant increase of chlorine over falls. Individual chondrites were found to be both heterogeneous and homogeneous with respect to Cl. Three samples of Leedy contained 41, 73 and 104 ppm Cl. Noticeably low values of 9 and 14 ppm in Allegan confirmed similar values obtained earlier by others.

A study of ten separate Allende samples gave 209 to 318 ppm Cl with an average of 250 ppm. Water soluble Cl varied from 15 to 79% of the total indicating the presence of a soluble Cl bearing phase which in some cases accounts for the majority of the Cl present.

#146

SULFUR AND CHLORINE CONTENTS OF ACHONDRITES

C.B. Moore, C.F. Lewis, K.L. Evans and J.G. Tarter
Arizona State University, Tempe, AZ 85281

Sulfur and chlorine contents have been measured on one gram samples of achondrites. At this sample level the samples are often heterogeneous.

Five individual samples of Stannern contained from 170 to 9000 ppm S. Three from Pasamonte ranged from 480 to 1300 ppm S and three from Sioux Co. from 1200 to 2900 ppm S. Single samples from individual eucrites gave: Béréba, 2050; Haraiya, 1050; Juvinas, 1140; Moore County, 3390; Nobleborough, 1500; Padvarninkai, 1660 ppm S. Shergotty contained 360 ppm S.

Sulfur in the howardites contained: Petersburg, 1980; Bialystok, 3130; Pavlovka, 2700, Washougal, 2360; Yurtuk, 2370 and Kapoeta, 3270 ppm S. The hypersthene achondrites included: Johnstown, 3190; Shalka, 1290; Ibbenbüren, 110; and Tatahouine, 640 ppm S.

Eleven enstatite achondrites ranged from a low of 2220 ppm S in Peña Blanca Spring to 11,000 ppm S in Cumberland Falls.

Chlorine contents measured were 39 ppm Cl in Juvinas, 15 ppm Cl in Pasamonte, 13 ppm in Johnstown and 2 ppm in Norton County.

GENETIC RELATIONSHIP BETWEEN ALLAN HILLS (ALHA) 77005 AND SHERGOTTITES--A GEOCHEMICAL STUDY. Ma, M.-S.[1], Laul, J.C.[2] and Schmitt, R.A.[1], [1]Dept. of Chem. and the Radiation Center, Oregon State University, Corvallis, OR 97331; [2]Phys. Sci. Dept., Battelle Pacific Northwest Laboratories, Richland, WA 99352

Petrological and selected trace element chemical studies of shergottites and ALHA 77005 have indicated significant similarities among these achondrites (1-3). It has been suggested that ALHA 77005 may represent either a cumulate that crystallized from a liquid parental to those from which the shergottites crystallized or a peridotitic source material from which the shergottite parent liquid was derived by partial melting (2,3). On the other hand, Rb-Sr and Sm-Nd isotopic data indicate that these achondrites cannot be comagmatic and that their isotopic characteristics are inherited from distinct sources which were established early in the parent body's history (4).

The major, minor, and trace element abundances in ALHA 77005 were measured via INAA at OSU and 12 REE, Ba, Sr, and U were measured via RNAA at BNWL. The normative mineralogy indicates that the sample contains ∿36% ol, 48% low-Ca pyx, 8% high-Ca pyx and 8% plag. The REE abundances measured by INAA and RNAA on different aliquants are nearly identical, indicating the analyzed samples are representative of the whole rock. The REE data exhibit a unique chondritic normalized pattern; i.e., REE's are nearly unfractionated from La to Pr at 1.0X chondrites, monotonically increased from Pr(1X) to Gd(3.4X) with no Eu anomaly, nearly unfractionated from Gd to Ho(3.4X) and monotonically decreased from Ho to Lu(2.2X). The REE abundances are lower in ALHA 77005 and its REE pattern is quite different than those of shergottites. It is also noted that ALHA 77005 has similar chond. norm. abundances at 2.8±0.4X for the heavy REE, Yb and Lu, and Hf, Sc, Ti and V.

The genetic relationship between ALHA 77005 and the shergottites via fractional crystallization of a common parent magma can be examined if the composition of the ALHA 77005 parental liquid is known. To obtain this, the following assumptions and calculations were made. (a) We established the Fe and Mg distribution coefficients for pigeonite and augite (1). (b) We applied these distribution coefficients to the pyx and ol data. (c) We calculated the required degree of fractional crystallization (17-18%) of ol and low-Ca pyx. (d) We calculated the REE and Sc abundances in the ALHA 77005 liquid. (e) We estimated the maximum amount of intercumulus liquid (<15%) in ALHA 77005 by the K_2O abundances in these achondrites. From the calculated REE and Sc in ALHA 77005 parent liquid, the norm. mineralogy of ALHA 77005, and assuming various amounts of intercumulus liquids, it is difficult (if not impossible) to reproduce the observed REE and Sc pattern for an assumed cumulate like ALHA 77005. If we adopt another model that the pyroxenes were zoned prior to crystallization of intercumulus liquid in shergottites (see 2), the conclusion remains the same because the light REE in the shergottite parent liquid are estimated to be enriched relative to the heavy REE, contrary to what is required to produce the observed liquid REE depleted pattern in the cumulate ALHA 77005.

The other hypothesis, which suggests that ALHA 77005 may represent a source peridotite from which the shergottites were derived, is invalid because there are drastic differences in the REE patterns for these achondrites and these patterns cannot be reproduced by reasonable partial melting calculations.

It is concluded that ALHA 77005 and the shergottites are not simply related as has been proposed (2,3) and that the unique REE and Sc pattern of ALHA 77005 suggests a complex history for its derivation if it evolved from a source material with chondritic like trace element abundances. The genesis of ALHA 77005 will be interpreted in the context of other models.

(1) GCA 43, 1475; (2) EPSL 45, 275; (3) Science 204, 1201; (4) Meteoritics 14,502.

#148

U-Th-Pb systematics of the Juvinas achondrite.

MANHES G. and ALLEGRE C.J.
Laboratoire de géochimie et cosmochimie, 4, Place Jussieu-75 PARIS

Juvinas eucrite is one of the two analyzed achondrites (with Ibitira) which shows a non perturbed postformation history: Rb/Sr analyses yield an internal isochron with a cristallisation age of 4.60 $\pm$ 0.14 G.y. (Allègre et al., 1974).

For this reason, we have investigated the U-Th-Pb system in this meteorite. The Pb isotopic composition and U, Th, Pb concentrations were determined on carefully sampled fragments and handpicked mineral separates of plagioclase and pyroxene. The U concentrations ranged from 6 to 100 ppb and Pb concentrations ranged from 60 to 280 ppb. The observed $^{206}Pb/^{204}Pb$ ratios, blank corrected, are in the range of 17.0 to 180.

The data, plotted in a $^{206}Pb/^{204}Pb$ vs. $^{238}U/^{204}Pb$ diagram yield an internal isochron age of 4.54 $\pm$ 0.01 G.y. which is in agreement with the age of 4,544 $\pm$ 0.005 G.Y. obtained from the internal isochron in the $^{207}Pb/^{204}Pb$ vs. $^{206}Pb/^{204}Pb$ diagram.

These U-Pb internal isochrons show for the first time in an achondrite the closed and unperturbed character of the U-Pb system, they justify the use of the high analytical accuracy of the ^{207}Pb-^{206}Pb age.

The Pb initial isotopic composition at the time of cristallization of Juvinas is obtained from the U-Th-Pb internal isochron $(^{206}Pb/^{204}Pb)_o$ = 11.3 ; $(^{207}Pb/^{204}Pb)_o$ = 12.5 ; $(^{208}Pb/^{204}Pb)_o$ = 31.8. The significant difference with the Pb isotopic composition measured in Canyon Diablo troïlite will be discussed.

THE BOUVANTE EUCRITE.

Christophe Michel-Levy M.[1], Palme H.[2], Spettel B.[2], and Wänke H.[2]
1. Laboratoire de Minéralogie-Cristallographie, Université Pierre et Marie Curie, Paris, France.
2. Max-Planck-Institut für Chemie, 65 Mainz, W.-Germany

On the 30th of July 1978 a stony meteorite (8kg) was found at Bouvante near Grenoble, probably a short time after its fall.It is the third fall of an eucrite (a rather rare class of meteorites) in France.

Few thin veins pass through the meteorite. Crystals have been broken rather than being deformed by shock. Some rare fine grained clasts were observed in the otherwise ophitic matrix. The mineralogy consists of about equal amounts of plagioclase and pyroxene. Minor minerals are chromite, ilmenite and quartz. Traces of metal, troilite, whitlockite and zircon have been detected. The plagioclases are zoned and are slightly more alkali-rich (an. 70-90) than usually in eucrites. Pyroxenes have rather constant Mg-concentrations (10-11 % MgO), while Ca and Fe contents show considerable variations. Very thin exsolution lamellae are observed in the pyroxenes. The SiO_2 excess is partly visible as quartz between pyroxene and feldspar laths, together with fine-grained iron-rich pyroxene, and small blebs of iron and troilite. A few zircon crystals, associated with ilmenite, have been detected. Whitlockite is sometimes found to be included feldspar.

Preliminary data on the chemistry of Bouvante indicate that concentrations of major, minor and trace elements are in the range of other eucrites. With 15.1 % Fe Bouvante belongs to the Fe-rich variety of eucrites, possibly representing partial melts from the interior of the eucrite parent body (1). The light REE are higher in Bouvante than in any eucrite analysed so far (6.1 ppm La in Bouvante; 5.5 ppm in Stannern and 3.0 ppm in Juvinas). There is also a marked negative Eu anomaly, similar to that observed in Stannern or Nuevo Laredo. Light REE are slightly enriched relative to heavy REE. Therefore Bouvante may represent an even smaller degree of partial melting than Stannern (4 % of partial melting (2)). The low Co content (around 5 ppm) is also typical for eucritic melts, having equilibrated with a metal phase.

1.) Stolper E. (1977) Geochim. Cosmochim. Acta 41, 587.
2.) Consolmagno G.J. and Drake M.J. (1977) Geochim. Cosmochim. Acta 41, 1271.

#150

MESOSIDERITE BASALTS AND THE EUCRITES.

Nehru, C.E.[1,2], Delaney, J.S.[2], Harlow, G.E.[2] and Prinz, M.[2]
1. Dept. Geology, Brooklyn College, CUNY, Brooklyn, NY 11210
2. Dept. Min. Sci., Amer. Mus. Mat. Hist., New York, NY 10024

Mesosiderite gabbros and basalts (MGBs) were described by Nehru et al. (1980a) and were shown to be unique in comparison with other meteoritic basalts. They are highly enriched in tridymite and phosphate, and some were initially two-pyroxene basalts, whereas eucrites (EUCs) were initially one-pyroxene basalts. MGB clasts were incorporated into a metal-silicate regolith which was heated to temperatures of about 900°C. This resulted in redox reactions (Harlow et al. 1980), coronas around olivine clasts (Nehru et al. 1980b), pyroxene overgrowths (Delaney et al. 1980), and other related phenomena. EUCs were also subjected to a thermal event as evidenced by homogeneous pyroxene compositions, clouding of pyroxene and plagioclase (Harlow and Klimentidis, 1980), and other features. Comparison of these two basaltic groups, which were metamorphosed under somewhat different conditions, is necessary in order to determine their respective origins, the parent bodies from which they were derived and the thermal events at or near their surface(s). Some features of MGBs and EUCs are compared in the table given below.

	Mesosiderite Gabbro-Basalts(MGB)		Eucrites (EUC)	
	Gabbro	Basalt	Cum. EUC	Bas. EUC
Texture	Granular	Ophitic-suboph.	Granular	Ophitic-suboph.
Grain size	Medium	Medium	Medium	Fine-medium
Pyroxenes				
Types(initial)	Pig ± aug	Pig ± aug	Pig	Pig
Exsolved	(Opx and/or pig)+aug	Pig+aug	Opx+aug; pig+aug	Pig+aug
Fe/(Fe+Mg)	Mostly 0.3-0.5	Mostly 0.3-0.5	0.4 - 0.5	0.6 - 0.7
Homogeneity	Inhomogeneous	Inhomogeneous	Homogeneous	Homogeneous
Plag An(Rng)	92 (89-96)	91 (89-92)	95 (93-97)	88 (80-96)
Modes Avg(Rng)				
Tridymite	6.2 (0.9-13.5)	11.4 (5.4-14.0)	1.8 (0-4.1)	6.0 (3.6-8.9)
Phosphate	1.2 (tr - 2.4)	0.3 (tr - 0.7)	tr	0.2 (0.1-0.4)
Cm/Ilm	Cm>Ilm	Cm>Ilm	Cm<Ilm	Cm<Ilm

There are three hypotheses as to their origin:(1) MGBs and EUCs formed on separate bodies with no direct relationship;(2) MGBs and EUCs formed in different parts of the same parent body, but have no direct relationship;(3) MGBs and EUCs are portions of the same larger suite of gabbros and basalts formed on the same parent body and have a direct relationship; the differences are caused by metamorphic events that affected them. Because of complexity of the variety of processes that may have been operative, definitive answers are difficult. However, we conclude that hypothesis (3) is least likely. Reasons for this include:(a) MGBs have more cm than ilm and EUCs have more ilm; this difference could not be explained by metamorphism; (b) More cm than ilm in MGBs correlates with higher initial Mg, as reflected in pyroxenes; (c) The MGBs have two initial pyroxenes and are not the metamorphic equivalents of pigeonite in the eucrites; (d) Bulk compositions of MGBs are higher in Mg, Ca, Al and Cr, which could not be the result of metamorphic processes. Thus, MGBs were originally different from EUCs, but it is not yet possible to choose between hypotheses (1) and (2). The MGBs were probably not originally enriched in phosphate, and P was added to Ca within the clasts. There is no plausible way for enrichment of P by fractionation. Therefore MGBs were derived from sources more Mg-rich than EUCs.

THERMAL HISTORY OF MESOSIDERITES

Crozaz, Ghislaine and Tasker, Douglas R.
Department of Earth and Planetary Sciences and the McDonnell Center for the Space Sciences, Washington University, St. Louis, MO 63130

Our study of the thermal histories of mesosiderites using fission track measurements of U-rich whitlockites has been extended to 11 of the 21 known mesosiderites. Representatives of all the metamorphic groups have been included to determine whether or not there were systematic variations in thermal regimes between the different groups. Exceedingly low cooling rates of only $\sim 0.1^{\circ}C$/m.y., in the temperature range of 500 to $350^{\circ}C$ have previously been inferred from metallographic studies (Powell, 1969). This would imply that the mesosiderites were once buried very deeply (hundreds of kilometers) in their parent body(ies) although their texture suggests that most are regolith breccias and some impact melt deposits.

Although our work is still in progress, it appears that the cooling rate of some of these objects was faster than previously inferred. However, a number of mesosiderites cannot be used to determine cooling rates as they experienced, during their cosmic ray exposure, significant elevations of temperature which led to partial annealing of the tracks in the whitlockite. As recognized earlier by Begemann et al. (1976), Veramin is an extreme case. If, as concluded by these authors, Veramin was heated during an episodic event which occurred less than 0.5 m.y. ago, such an event might manifest itself in thermoluminescence measurements, which are currently in progress.

Powell B.N., 1969. Geochim. Cosmochim. Acta 33, 789-810.
Begemann F., Weber H.W., Vilcsek E. and Hintenberger H., 1976. Geochim. Cosmochim. Acta 40, 353-368.

#152

THE TROUBLES WITH TRIDYMITE AND PHOSPHATE IN MESOSIDERITES: FEASIBILITY OF POSSIBLE REACTIONS.

Harlow, G.E.[1], Delaney, J.S.[1], Nehru, C.E.[1,2] and Prinz, M.[1]
1 - Dept. Mineral Sciences, Amer. Mus. Nat. Hist., New York, NY 10024
2 - Dept. Geology, Brooklyn College, CUNY, Brooklyn, NY 11210

The conspicuous abundances of tridymite and phosphate [merrillite, $Ca_3(PO_4)_2$] in the mesosiderites (up to 9.8 and 3.7 wt%, respectively, of the "silicate" portion; Prinz et al., 1980] relative to all other achondrites has raised the question of their origin. Nehru et al. (1978) discussed petrologic evidence and the possibilities of production by igneous fractionation and by redox reactions between P-bearing metal and calcic pyroxene. Agosto et al. (1980) suggested a specific redox reaction of the form:

$$3CaMgSi_2O_{6_{px}} + 5FeSiO_{3_{px}} + 2P_{Fe} \rightarrow Ca_3(PO_4)_2 + 3MgSiO_{3_{px}} + 8SiO_2 + 5Fe \quad .....[1]$$

In order to evaluate the possible reactions and stability fields, we have examined the system Fe-P-O-CaO-SiO_2 using thermodynamic equilibrium equations for the following set of phases: I-metallic Fe in solid solution; P-dissolved in metallic Fe-Ni; Wo-as $CaSiO_3$ in cpx solid solution; Fs-as $FeSiO_3$ in opx solid solution; M-merrillite; T-tridymite. The following univariant reactions result:

P + O + Wo = M + T .....[2]
P + I + O + Wo = M + Fs .....[3]
I + O + T = Fs .....[4]
P + Fs + Wo = M + T + I .....[5]

While there are many problems with the equilibrium calculations due to lack of data (i.e.-activities of Wo in cpx), solid solution complexities, and variabilities in the mesosiderite phase compositions, some useful schematic relationships and T-fO_2 limits are possible: (1) Reaction [5], which is equivalent to [1] of Agosto et al. (1980) is not applicable to mesosiderites; calculated temperatures are impossibly high (>2000K) or Fe activities have to be vanishingly small. (2) Changing $[P]^{Fe}$ to Fe_3P (schreibersite) does not significantly change the reaction curve topology in T-fO_2 space, but the exact T-fO_2 values are sensitive to the total amount of reduced P "dissolved in metal". The atomic % of $[P]^{Fe}$ varies from the measured value of about 0.02 to a calculated value of about 2.0 if all PO_4^{-3} is recalculated as $[P]^{Fe}$. (3) The region of T-fO_2 space where T and M are both produced is at the intersection of the univariant curves defined by equations [2] and [4]. The region ranges from ~1000°C, log $fO_2 \cong$ -17 at high Fs and $[P]^{Fe}$ to ~850°C, log $fO_2 \cong$ -20 at low Fs and $[P]^{Fe}$(P=1 atm). An important implication is that the ratio of M and T production in mesosiderites would not be fixed as in equation [1] but would vary with changes in local compositions and fO_2, since two separate reactions are operative. (4) The role of igneous fractionation in mesosiderite source rocks can still be a factor in producing M and especially T; however, as the phase compositions and abundances may have been changed by fO_2 "buffering" reactions, evaluation of the role of fractionation must take into account these possible changes. Finally, while the conditions for phosphate-tridymite production from reactions [2] and [4] are reasonable, $[P]^{Fe}$ concentrations needed to produce high M abundances are very high for meteoritic metallic Fe-Ni. The problem is not the state of oxidation of phosphorous but the source of phosphorous.

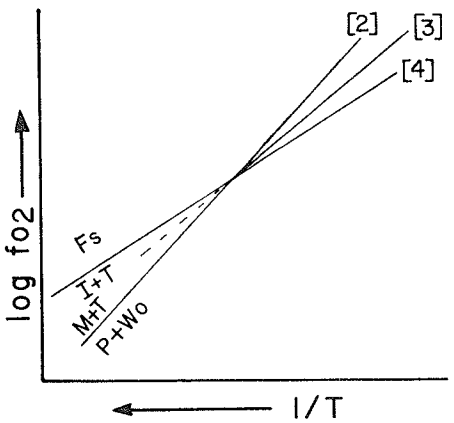

UREILITES REVISITED: PETROLOGIC EVIDENCE FOR A CUMULATE ORIGIN

Berkley*, J. L. and Keil**, K.
*Lunar and Planetary Laboratory, Univ. of Arizona, Tucson, AZ 85721
**Institute of Meteoritics, Univ. of New Mexico, Albuquerque, NM 87131

Based on detailed petrographic analyses, Berkley et al. (1976, 1978, 1980) described ureilites (carbonaceous olivine-pigeonite achondrites) as igneous, ultramafic cumulates. However, this hypothesis was challenged by Wasson et al. (1976), Boynton et al. (1976), and Higuchi et al. (1976), all of whom favored an origin as metamorphic, partial melt residues to explain characteristic trace element abundances (siderophiles, REE etc.). We present petrologic data on eight ureilites (Kenna, Novo Urei, Goalpara, Haverö, Dingo Pup Donga, ALHA77257, Dyalpur, and North Haig) that supports a cumulate origin for ureilites. The following observations are essential to this argument: (1) Abundant subhedral - euhedral silicate crystals occur especially in Dingo Pup Donga, but also in other ureilites, (2) petrofabric analyses on five ureilites show a characteristic mineral elongation lineation lying within a foliation typical of cumulate rocks, and (3) intercrystalline textural relations among silicate crystals are similar to those observed in adcumulates, a special type of cumulate rock (Wager et al., 1960).

Furthermore, the homogeneous (thin section scale), intergranular distribution of carbon (mainly graphite, also diamond, lonsdaleite) suggests an origin as trapped, intercumulus material. Carbon-silicate textural relations are inconsistent with late-stage carbon injection into solid, ultramafic rocks.

Ureilites display evidence for relatively low formational oxygen fugacities, including high Si and Cr in metal and low D's (D=Cr(px)/Cr(ol)) relative to lunar rocks. We suggest these relationships result from carbon - melt reactions that caused progressive reduction of the ureilite parent magma (e.g. Sato, 1978). In terrestrial cumulate systems, late-stage cumulates are enriched in modal px/ol (ol eventually reacts out), are less voluminous than early cumulates, and show progressive increase in FeO/MgO in mafic silicates. However, in ureilites, samples displaying the lowest FeO/MgO in silicates contain the highest modal px/ol and are relatively rare compared to higher FeO/MgO samples in terrestrial collections. This is the reverse of expected terrestrial trends but is consistent with carbon-induced magmatic reduction during progressive igneous fractionation.

Berkley, J., Brown, H., Keil, K., Carter, N., Mercier J-C., and Huss, G., 1976. Geochim. Cosmochim. Acta 40, 1429.
Berkley, J., Taylor, G., Keil, K., and Prinz, M., 1978. (abstract) In Lunar and Planetary Sci. IX, 73.
Berkley, J., Taylor, G., Keil, K., Harlow, G., and Prinz, M., 1980. Submitted to Geochim. Cosmochim. Acta.
Boynton, W., Starzyk, P., and Schmitt, R., 1976. Geochim. Cosmochim. Acta 40, 1439.
Higuchi, H., Morgan, J., Ganapathy, R., and Anders, E., 1976. Geochim. Cosmochim. Acta 40, 1563
Sato, M., 1978. Geophys. Res. Lett. 5, 447.
Wager, L., Brown, G., and Wadsworth, W., 1960. J. Petrol. 1, 73.
Wasson, J., Chou, C., Bild, R., and Baedecker, P., 1976. Geochim. Cosmochim. Acta 40, 1449.

#154

SUESSITE, Fe_3Si, A NEW MINERAL IN THE NORTH HAIG UREILITE.

Keil, K., Berkley J.L., and Fuchs L.H.[1]
Department of Geology, Institute of Meteoritics, University of New Mexico, Albuquerque, NM 87131; [1]Argonne National Laboratory, Argonne, IL. 60439.

The North Haig olivine pigeonite achondrite (ureilite) is a polymict breccia consisting of major olivine, low-Ca pyroxene and an intergranular carbonaceous matrix. Olivine and low-Ca pyroxene vary widely in composition, covering the ranges observed in all known ureilites. Minor granular enstatite clasts with diopside exsolution blebs, akin to enstatite achondrites, were also observed. Native metal in ureilites is normally kamacite of variable Ni content, in some cases with up to 2% Si in solid solution (Berkley et al., in press). However, in North Haig, kamacite with trace amounts of Si is extremely rare (only a few 1-2 μm grains within silicates were observed). Instead, the common metallic phase is (simplified) Fe_3Si, a new mineral which we have named suessite in honor of Hans E. Suess (name and mineral have been approved by the Commission on New Minerals and Mineral Names of the IMA). Suessite occurs as minor anhedral vein fillings in interstitial cracks in silicates and in the intergranular carbonaceous material and ranges in size from 1 μm blebs to elongated grains about 30 x 150 μm in size. Suessite is cream white in reflected light, isotropic, ferromagnetic, and shows no cleavage. Reflectance in % (determined by G.A. Desborough) at the 4 standard wavelengths of 470, 546, 589 and 650 nm for 2 grains is 48.5 (5), 51.6 (3), 53.5 (7), 50 (2), and 49.7 (5), 53.4 (4), 54.5 (6), 52 (1), respectively. Analysis (by EMX, in wt.%) of 67 grains vary somewhat (mean in parentheses): Fe 81.7-87.0 (83.9), Ni 0.4-6.4 (2.18), Co 0.16-0.40 (0.33), Cr < 0.02-0.25 (0.11), Si 12.8-16.4 (14.6), P < 0.01-0.25 (0.19). Thus, suessite is $(\underline{Fe}, Ni, Co, Cr)_{2.6-3.6}$ $(\underline{Si}, P)_{1.0}$ or, simplified mean, $(\underline{Fe}, Ni)_{2.94}$ Si, very close to Fe_3Si. X-ray powder diffraction shows that suessite possesses a similar structure to alpha-Fe (kamacite) and the solid solution alloy $(Fe_3Si)_{SS}$ in displaying three lines (relative intensities in parentheses) as follows: 2.005 (10), 1.42 (1), 1.160 (3) (in Å). The calculated cell size is 2.84 ± 0.002 Å (v= 22.93 Å^3). Silicates, particularly olivine, in ureilites have core compositions of Fo_{76-92} and thin (≳ 100 μm) rims of essentially Fo_{100} formed by reduction and reaction with the carbonaceous matrix material (e.g., Berkley et al., 1976, 1978, in press). We suggest that Si and Fe liberated in this reduction process formed suessite, possibly also by reaction with preexisting kamacite.

References: J.L. Berkley, H.G. Brown, K. Keil, N.L. Carter, J-C.C. Mercier and G. Huss, Geochim. Cosmochim. Acta 40, 1429-1437, 1976; J.L. Berkley, G.J. Taylor and K. Keil, Lunar and Planet. Sci. IX, LPI, Houston, 73-75, 1978; J.L. Berkley, G.J. Taylor, K. Keil, G.E. Harlow and M. Prinz, Geochim. Cosmochim. Acta, in press.

A NEW LOOK AT THE NEAR-EARTH ASTEROID POPULATION AND ITS RELATION TO METEORITES: A REEXAMINATION OF THEIR SURFACE CHARACTERISTICS AS DETERMINED FROM EXISTING AND NEW SPECTRAL REFLECTANCE (0.33-1.0 μm) measurements.

Lucy A. McFadden,University of Hawaii, Honolulu, HI 96822

The spectral reflectance measurements (0.33-1.0μm) of seven previously measured spectra (Chapman and Gaffey,1979) of near-earth asteroids have been reexamined along with two new spectral measurements of 1979 XA and 1980 AA, in order to characterize their surface properities and compare them with meteorites. Among the observed Apollo and Amor asteroids, none of them have surfaces analgous to eucrites, howardites, diogenites, stony irons or nickel irons. Some of the existing spectra show features characteristic of shocked, black chondrites, others show no evidence of a 1.0μm pyroxene band (although these data are noisy). Some near-earth asteroids measured to date show pronounced reddening which must be interpreted in consideration with other spectral properties such as the presence or absence of narrow, weak absorptions in the visible and ultra-violet and the shape of the visible continuum. Of the asteroids observed on more than one night, all of them (3) show spectral variations from night to night. Spectral characteristics will be related to the mineralogy and evolution of these bodies.

Chapman, C.R. and Gaffey, M.J.(1979)."Reflectance spectra for 277 asteroids." in Asteroids (T. Gehrels, ed.). Univ. Ariz. Press, Tucson, 655-687.

#156

1979 VA, A POSSIBLE CARBONACEOUS ASTEROID

Helin, E.F., and Gaffey, M.J.
California Institute of Technology, Pasadena, CA 91125
University of Hawaii at Manoa, Honolulu, Hawaii 96822

Apollo asteroid 1979 VA was discovered in November of 1979 at Palomar Observatory using the 46-cm Schmidt during a dedicated planet-crossing asteroid search program. 1979 VA is an important Apollo discovery for the following reasons — it was bright on discovery, moving with prograde motion allowing 5 months of observations; its unusual orbit takes it out close to Jupiter (closer approach to Jupiter than any known Apollo); its 0.3 - 2.0μ spectrum is suggestive of carbonaceous chondrites; its orbit and composition suggest a link between short period comets and Apollo asteroids.

As a result of the discovery circumstances, a comprehensive set of spectrophotometric observations were obtained, making 1979 VA the most thoroughly observed and examined Apollo during a discovery apparition. Unfortunately, no polarimetric or radiometric albedo was obtained.

There are similarities between the spectral reflectance of 1979 VA and certain carbonaceous chondrites but not with the most common types. The following alternative cases are considered: 1) a typical C1/C2 type iron-rich phyllosilicate with a very spectrally abundant opaque (magnetite and/or graphite) phase - albedo is very low, certainly less than 2%, 2) a typical mafic silicate (olivine or pyroxene with a moderate - 10-40 mole % - iron content) with the spectrally abundant opaques - albedo is low, about 5%, and 3) a low-iron (1 mole %) phyllosilicate with a moderate opaque component - albedo is low, about 8-10% although it could be higher if the iron content is lower.

ASTEROID TAXONOMY USING KIVIAT FIGURES

Charles J. Hostetler and Ann E. Burton Hostetler
Planetary Science Institute, 2030 E. Speedway, Tucson, AZ 85719

In the field of planetary sciences, classification schemes are usually based on a number of readily measurable properties. Divisions, which must be arbitrary to some degree, are made in each of the observables, and if the divisions are well chosen, the objects fall into several distinct groups. Traditional classification tools are two-dimensional graphs and tables of data. Kiviat diagrams are a new classificational tool, in which circular graphs are used to present multidimensional data on one set of axes. (1) The advantage of Kiviat diagrams is, if the axes are well chosen, easily recognizable visual patterns emerge which correspond to normal classifications of data using more traditional methods. These patterns, called Kiviat figures allow presentation of multivariate data in an extremely visual manner. The classification process is much more oriented towards pattern recognition using Kiviat figures, rather than a study of individual pieces of data.

We have followed the conventions in (2) in testing the applicability of Kiviat diagrams to asteroid taxonomy. The observables we used are: 1) geometric visual albedo, 2) maximum depth of the negative polarization branch, 3) R/B, 4) BEND, 5) DEPTH, 6) B-V, and 7) U-B, which are the observables used in the classification scheme of Bowell et al. (3). All data were obtained from the TRIAD file (4). We plotted Kiviat figures for all the asteroids for which all the observables were available, choosing type C as the standard type (30 type S, 10 type C, 3 type M, 3 type E, two type R, and 10 U). The Kiviat figures for each type were found to be very distinct from each other, indicating that the observables were indeed useful in classification, and that the Kiviat technique was a useful one. The Kiviat figures also have the advantage of showing the approximate degree of difference for each asteroid from the standard, as well as providing a very visual display of asteroidal types.

Heretofore, Kiviat diagrams have been used only in evaluating the performance of large computer systems. We feel that due to their extremely visual nature Kiviat diagrams could be employed extensively in the field of planetary sciences as a classificational tool. We have presented results for asteroid taxonomy and are working in the area of iron meteorite classification, but the Kiviat technique is certainly not limited to these areas.

References: (1) Kolence K. and Kiviat P. (1973) Performance Evaluation Review, 2, p. 2. (2) Morris M.F. (1974) Performance Evaluation Review 3, p. 2-9. (3) Bowell E. et al. (1978) Icarus 35, p. 313-335. (4) Bender et al. (1976) Icarus 33, p. 630-631.

This work was supported by NASA Grant NSG 7576.

#158

UNUSUAL MINERALS AND OTHER MATERIALS IN ENSTATITE CHONDRITES

Larimer, J. W., Ganapathy, R.*, Trivedi, B. M. P.
Department of Geology, Arizona State University, Tempe, AZ 85281
*J. T. Baker, Phillipsburg, NJ 08865

Enstatite chondrites contain a variety of minor and trace phases which are unique to these meteorites. We have begun a systematic study of these phases with the aim of understanding their chemistry, petrology and ultimately their origin. The phases are being studied in section with analysis by microprobe and as separates with the SEM and INAA. To date we have concentrated on an unusual volatile-rich material discovered accidently (1), a refractory rich material that appears to be a Ti-rich pyroxene (or perhaps two or more phases) and CaS.

In our search for additional volatile-rich material, which consists largely of carbon (a carbyne?), we have so far only discovered a variety of contaminents: strands of paper, cloth, etc., that are more common than expected. Owing to the observed enrichments in some elements, the material must comprise no more than a part per thousand or so of the meteorite. Hence, it will not be easy to isolate. The refractory rich material has been isolated and analyzed in bulk. It is enriched in all refractory lithophiles (x2 to 50) depleted in siderophiles ($x10^{-1}$ to 10^{-3}) and displays a positive Eu anomaly.

Our study of CaS has progressed part way through the stages of microscopic and microprobe study and samples are now being prepared for INAA. It appears in a least two forms: large euhedral grains enclosed in enstatite and as subhedral to anhedral grains that occur interstially in both the matrix and in chondrule rims. The major and minor element compositions are rather similar; trace element data will be available soon.

From the textural relations it appears that at least some of the CaS formed prior to $MgSiO_3$. This implies an origin in a gas with $C/O \lesssim 0{\cdot}9$, where CaS is predicted to form at higher temperatures than $MgSiO_3$.

(1) R. Ganapathy and J. W. Larimer 1980 Science 209, p. 57.

RARE-EARTH ELEMENT ABUNDANCES IN SEPARATES FROM THE ENSTATITE CHONDRITE ABEE.

Frazier, R. M. and Boynton, W. V.
Department of Planetary Sciences and Lunar and Planetary Laboratory, University of Arizona, Tucson, Az 85721.

We have analyzed four samples from three clasts in the Abee enstatite chondrite. Measurements of major, minor and trace elements were made by INAA, but the major emphasis was on rare-earth elements determined via RNAA. In addition, magnetic and non-magnetic separates of a crushed whole rock sample have been analyzed.

The chondrite normalized REE patterns were generally chondritic in relative abundances (within ± 10%). The irregularities, which significantly exceed our uncertainties of 1 to 2 percent, are similar to those found by Nakamura and Masuda (1973) in one of two chips analyzed by them. None of our samples, however, had the large Yb anomaly which they observed. The anomalies which we observed tend to be correlated, i.e., those samples that have significant anomalies tend to have the anomalies in the same elements and to the same degree. These results and the results of Nakamura and Masuda suggest that at least two REE components are present, and that these components are sampled in different amounts by our fragments.

Both the magnetic and the non-magnetic separates had REE concentrations which were less than those in the crushed whole rock sample. A partially magnetic sample of intermediate purity had concentrations which exceeded the values in the magnetic and non-magnetic separates by a factor of about 4 (final value may differ pending chemical yield determination). The REE containing mineral(s) in this sample have not yet been identified, but accessory phases such as sulfides or phosphides are suspected. It is hoped that more specific mineral separates will soon be analyzed.

Nakamura, N. and Masuda, A. (1973) Earth Planet. Sci. Lett. 19, 429.

#160

A CHEMICAL STUDY OF THE ABEE CONSORTIUM SLICE

Kallemeyn, G.W., Sears, D.W. and Wasson, J.T.
Institute of Geophysics and Planetary Physics, U.C.L.A.
Los Angeles, California CA 90024

We have measured the abundance of 28 elements by instrumental and radiochemical neutron activation analysis in four splits from three clasts from the Abee meteorite. In clasts 1.1.3, 2.1.2 and 2.2.4, Ca/Mg has typical E chondrite values although Al/Mg in all clasts is more typical of C chondrites. Ca/Mg in the remaining clast (3.3.2) is much higher than even CV values. The other refractory lithophiles scatter too much for any conclusions concerning their classification, presumably any element trends are completely obscured by sample inhomogeneity. It is frequently possible to identify the mineral responsible for the scatter by plots like those in the figure. (1) Fe, Co, Ni, Au, Ga, Ge, As and Sb have very similar distribution patterns and reflect metal abundances. Ir and Os are the only siderophiles which do not conform precisely, being depleted x2 in clast 2.1.2.(2) Zn, Mn and Sc show identical variations between the clasts; Cd is similar but drops more in 3.3.2. This probably reflects variations in sulfide abundance, so that we need to propose that Sc is located largely in CaS. (3) Na, Se, K, Al, Cr, Mg and Ca are a combination we do not understand, although the presence of Na, Ca, K and Al suggest feldspar may be involved. (4) Lu, Yb, Sm, La, V and Ti are probably all located in fairly refractory lithophile phases which condense ahead of metal. It is not unlikely that they would be located in a common assemblage, although this has not been observed petologically.

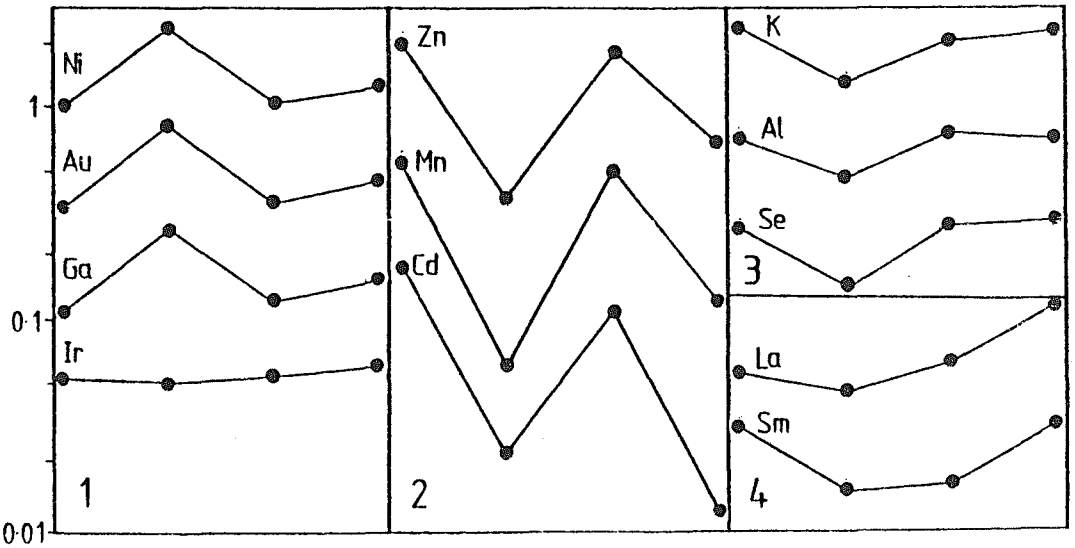

Elemental abundances normalized to clast 1.1.3. From left to right, the clasts are 1.1.3, 2.1.2, 2.2.4 and 3.3.2. The vertical scale is the same for all data, but only the scale for Ni is shown.

MINERALOGY AND PETROLOGY OF THE ABEE ENSTATITE CHONDRITE

A.E. Rubin and K. Keil, Institute of Meteoritics, University of New Mexico Albuquerque, NM 87131

The Abee enstatite chondrite is a monomict breccia with similar mineral compositions (enstatite, silica, plagioclase, oldhamite, niningerite, troilite, kamacite and schreibersite) in the clasts and the meteorite matrix. The abundances of the individual mineral phases, however, differ significantly from one area of the meteorite to the next (Table 1). "Dark" inclusions from the matrix (9,11) and from the interior of a clast (9,12) have the same mineral compositions as the clasts (clast 1, sections 1,1,07 and 1,1,12; clast 2, sections 2,2,01 and 2,1,3; and clast 3, sections 3,3,01 and 3,3,05), but differ primarily in their relatively high abundance of pyroxene chondrules (which compose 25% to 28% of the dark inclusions and only 1% to 4% of the clasts). Round globules of kamacite (0.1 to 1 mm across) with interior enstatite laths (up to 0.3 mm in length) occur in most of the sections. Schreibersite occurs exclusively along margins of kamacite grains and may have exsolved from the kamacite.

Modal analysis indicates that approximately 73% of the silicates undergo parallel extinction under crossed-polarizers. Because enstatite is the most abundant silicate, most of the enstatite grains in Abee are orthorhombic. Although Abee is classified an an E4 chondrite, its abundance of ortho-enstatites, uniformity of mineral composition, apparently-recrystallized silicate areas, low MnO content of enstatites and low Si content of kamacites (Table 2), indicate that Abee shares many of the characteristics of the more equilibrated E5 chondrites.

The euhedral enstatite laths in the kamacite-rich areas suggest that these pyroxenes were the first crystals to form from a silicate-kamacite melt on the meteorite parent body. Abee's sulfide phases may have crystallized subsequently from an immiscible melt that separated from the primary silicate-kamacite liquid. Impact-induced mixing of the Abee parent body regolith caused the varying abundances of mineral phases in different areas; subsequent metamorphic equilibration is responsible for the E5 characteristics of the meteorite.

TABLE 1

MINERAL ABUNDANCES (WT.%)

	c1	c2	c3	9,11	9,12
Enstatite	40.6	31.8	26.7	49.8	42.4
Silica	9.0	7.8	16.2	9.4	13.7
Plagioclase	7.1	5.7	4.2	10.8	11.6
Oldhamite	0.42	0.40	1.7	0.1	0.1
Niningerite	13.2	6.7	3.7	7.1	15.2
Troilite	6.5	6.4	12.9	7.2	4.8
Kamacite	22.1	40.5	34.4	15.4	11.8
Schreibersite	1.1	0.78	0.19	0.2	0.4
Total	100.02	100.08	99.99	100.0	100.0

TABLE 2

MINERAL COMPOSITIONS (WT.%)

Mineral	Enstatite	Silica	Plagioclase
No. of grains	222	51	113
SiO_2	59.8	98.9	70.5
TiO_2	<0.02	<0.02	
Al_2O_3	<0.02	0.31	17.4
Cr_2O_3	<0.02		
FeO	0.78	0.37	0.54
MnO	<0.02	<0.02	
MgO	39.1	0.17	
CaO	0.10	0.04	0.53
Na_2O	<0.02	0.17	10.5
K_2O		0.05	0.67
Total	99.78	100.01	100.14
End member	$En_{98.7}$		$An_{4.6}$

Mineral	Oldhamite	Niningerite	Troilite	Kamacite	Schreibersite
No. of grains	23	151	122	182	80
Mg	1.67	11.3			
S	43.8	41.5	37.0		
Ca	52.2	2.86			
Ti			0.34		
Cr	0.06	1.89	2.03		
Mn	0.48	4.4	0.22		
Zn			0.20		
Fe	1.58	37.9	59.4	88.9	78.2
Si				2.73	0.71
P				0.40	13.8
Co				0.51	0.46
Ni				7.1	6.9
Total	99.79	99.85	99.19	99.64	100.07

#162

U-Pb STUDY OF ABEE CONSORTIUM SAMPLES

Tatsumoto, M. and Unruh, D. M.
U.S. Geological Survey, Fed. Ctr., Denver, CO 80225

Uranium and lead abundances and isotopic compositions have been determined in subsamples 1,01; 2,02; and 3,03 from the Abee consortium sample. The $^{238}U/^{235}U$ ratio of 138.1 ± 0.5 (2σ, 1 determination, sample 1,01) obtained is indistinguishable from the terrestrial value of 137.9. U abundances range from ∿7-11 ppb, whereas Pb abundances range from ∿2.3 to 4.0 ppm. Consequently, the Pb isotopic data are very non-radiogenic ($^{206}Pb/^{204}Pb$ ∿9.44-9.47). The data are too tightly-grouped on a $^{207}Pb/^{204}Pb$ vs $^{206}Pb/^{204}Pb$ plot to yield an isochron. However, the data plot on or very near the 4577 ± 4 m.y. whole-rock isochron for other E-chondrites determined by Manhes and Allegre (1978). The slight deviations observed could be real, but could also reflect a ≲0.1% interlaboratory bias, or small amounts (≲20 ppb) of terrestrial Pb contamination induced during storage or sawing of the Abee sample for allocation.

U-Pb data for sample 2,02 plotted on a U-Pb concordia diagram (assuming Cañon Diablo troilite Pb as the initial Pb isotopic composition) are, within error, concordant at 4700 ± 117 m.y. The large uncertainty results from the propagation of errors due to the extremely large initial Pb correction (∿98% of the ^{206}Pb). U-Pb data for the other splits are somewhat discordant in the Pb-excess direction, but yield more "normal"-looking $^{207}Pb/^{206}Pb$ model ages of 4560-4600 m.y. The discordancy of these samples and/or the somewhat older model age for 2,02 could reflect either terrestrial Pb contamination or a slightly different initial Pb isotopic composition from that in Cañon Diablo troilite.

The calculated differences in initial Pb required to make sample 3,03 concordant are ∿0.4% in the $^{206}Pb/^{204}Pb$ and ∿0.24% in the $^{207}Pb/^{204}Pb$ ratio. Such small differences cannot be resolved from small amounts of terrestrial Pb contamination.

Reference: Manhes, G., and Allègre, C. J. (1978) Meteoritics 13, 543-548.

^{40}Ar-^{39}Ar AGES OF ABEE CLASTS

Bogard, D.D.
Code SN7, NASA Johnson Space Center, Houston, Texas 77058

Samples of three Abee clasts, 1,1,04, 2,2,05, and 3,3,06, were neutron irradiated and the Ar isotopes measured during stepwise temperature extractions. Calculated ^{40}Ar-^{39}Ar ages show complex release curves. All three clasts show a decrease in ages for fractional $^{39}Ar \gtrsim 0.8$, presumably as a result of reactor recoil effects. Clast 3 shows significant loss of ^{40}Ar at low extraction temperatures. The K/Ca ratios of clasts 1 and 2 decrease by a factor of X10 and clast 3 by a factor of X4 throughout the extraction. Below are summarized the maximum, average, and plateau ages.

Clast	Plateau Age	Maximum Age	Average Age
1,1,04	4.5 Gy	4.50 Gy	4.36 Gy
2,2,05	4.5 Gy	4.52 Gy	4.42 Gy
3,3,06	--	4.49 Gy	4.19 (4.38) Gy

The maximum ages of all three clasts have the same value of 4.5 Gy within uncertainties. The average age of all three clasts (when clast 3 is corrected for low temperature ^{40}Ar loss) have the value of 4.4 Gy within uncertainties. Our favored interpretation is that ^{40}Ar retention began $\sim$ 4.4 Gy ago, but we cannot rule out the possibility that the clast ages are as old as 4.5 Gy. Within the range of 4.4 - 4.5 Gy these data do not resolve any possible age differences among the three clasts.

Values of the diffusion parameter, D/a^2, for Ar were calculated from the data and permit us to place some restrictions on the thermal history experienced by the clasts and the Abee meteorite. Clast 1 could not have been heated to 500°C longer than $\sim$ 4 minutes or to 300°C longer than $\sim$ 16 hours. Clast 3, by contrast, shows diffusion loss of $\sim$ 15% of its low temperature ^{40}Ar, consistent with heating to 500°C for $\sim$ 5 days, to 300°C for $\sim$ 1 year, or to $\sim$ 100°C for $\sim 16^6$ years. The Ar loss from clast 3 presumably occurred before incorporation into the Abee meteorite.

#164

NUCLEAR TRACK RECORDS IN THE ABEE CHONDRITE

Goswami, J. N.[1,2], Lal, D.[2] and Sinha, N.[2]

1) Geological Research Division, Scripps Institute of Oceanography, La Jolla, California - 92093; 2) Physical Research Laboratory, Ahmedabad - 380009, India.

Records of cosmic ray heavy nuclei tracks have been studied in fourteen samples taken from different locations of a cut-slab of the Abee meteorite to determine its pre-atmospheric mass and to understand its cosmic ray irradiation history. The measured track densities in different samples range from a few times 10^4 cm^{-2} to $\sim 10^6$ cm^{-2}. No significant variation in track densities for individual grains from a given location has been observed, except for the sample Abee -9-03, taken from the near central region of the slab. Further studies of this anomalous sample are in progress and the results will be presented at the meeting. Based on an exposure age of 9 m.y. (K. Marti, personal communication), we estimate atmospheric ablation of 6 to 15 cm for different locations along the perimeter of the cut slab, representing the mid-plane of the recovered (post-atmospheric) Abee meteorite (Dawson, K. R. et al. Geochim. Cosmochim. Acta. 21, 127, 1960). Measured track density gradients along different directions of the cut-slab indicate its proximity to the radial plane of the original (pre-atmospheric) meteorite. The distribution of the ablation values and the iso-track density contours on the plane of the slab imply asymmetric ablation of the Abee chondrite during its atmospheric transit. The track data are consistent with a spherical pre-atmospheric shape for the meteorite with radius 28±2 cm, corresponding to a mass of 320±70 Kg. The mass loss due to atmospheric ablation (for a recovered mass of 107 Kg; Dawson et al., GCA, 21, 1960) is thus $\sim$66% of the initial mass of the Abee meteorite.

NOBLE GASES IN ABEE

Wacker, J.F.*+ and Marti, K.*
*Dept. of Chemistry, Univ. of California, San Diego, CA
+Lunar and Planetary Lab, Univ. of Arizona, Tucson, AZ 85721

The noble gases have been measured in five samples from the Abee (E-4) meteorite as a part of The Abee Consortium. The five samples are a suite of whole rock chips from four clasts representing a variety of morphological textures and degrees of metal/silicate fractionation. An attempt has been made to sample regions of varying metal to silicate abundance (~10% to ~80%) in order to examine any correlation between rare-gas and metal contents. Temperature step analysis was employed for all but one sample.

The light gases (He, Ne) are due mostly to spallation, the heavy gases are of planetary composition. The rare-gas concentrations tend to be anti-correlated with metal content. There are two exceptions to this trend: first, a small spallation component is present in argon in which the $^{36}Ar_{sp}$ (spallation) is correlated with the metal content, ranging from .05 to 0.37 x 10^{-8} ccSTP/g whereas the $^{36}Ar_{p}$ (planetary) for these samples is 77 and 21 x 10^{-8} ccSTP/g respectively (errors for concentrations are typically 10%); second, the 4He concentrations show a somewhat less defined correlation with metal content. A set of samples from the same clast, one metal-rich (~60%), one metal-poor (~15%), shows the above effect for 4 but also has an average 4 concentration of 2000 whereas the three other samples cluster around 650 x 10^{-8} ccSTP/g. Helium-3 concentrations tend to be between 15 and 20 x 10^{-8} ccSTP/g. Xenon-129, which shows significant excesses due to decay of 129 I, has excesses ranging from 3800 to 5400 x 10^{-12} ccSTP/g as compared to 132, which ranges from 300 to 890 x 10^{-12}ccSTP/g. Bulk 129/132 ratios range from 6 to 14; individual temperature steps range up to 20. This suggests that the iodine host phase is distinct from the trapped xenon host phase(s) and is somewhat more uniformly distributed in the stone.

The isotopes 80 and 82, 83, and 128 also show considerable excesses. The 80 and 82 excesses closely correlate, the 128 and 129 excesses show significant correlation as well. Excesses for 80 and 82 range from 26 to 42 and 15-20 x 10^{-12} ccSTP/g, the 83 excesses (which are quite small) are about 3 x 10^{-12}ccSTP/g, and the 128 excesses range from 5 to 12 x 10^{-12}ccSTP/g. The correlations between 80 and 82, and 128 and 129 suggest that they are due to neutron capture; to former from bromine, the latter from iodine (128 only). Release at similar temperatures (700-900°C) indicates that bromine and iodine are similarly sited. Because of the constancy of the 84/86 ratios the slight excess in 83 (released from 900-1000°C) may be due to neutron capture on 82Se. Variations in the argon 38/36 ratio show no corresponding effect from neutron capture on chlorine indicating that non-thermal neutrons caused the above anomalies (1). The neutrons were most likely produced as secondary products of exposure to galactic cosmic-rays in the recent irradiation history of Abee.

(1) Marti, K., Eberhardt, P., Geiss, J. (1966) Z. Naturforsch 21a, 398.

#166

NITROGEN ISOTOPES IN ABEE CLASTS

Thiemens, M.H. and Clayton, R.N.
University of Chicago, Chicago, IL 60637

Four clasts from the enstatite chondrite Abee have been analyzed for their nitrogen content and isotopic ratios by stepwise heating. The clasts show a wide variation in nitrogen concentrations, ranging from 254 to 848 ppm, whereas the nitrogen isotopic composition is almost constant, ranging from a $\delta^{15}N_{AIR}$ of -28 to -29.8‰. These amounts and isotopic compositions are within the ranges reported for enstatite chondrites (1).

The data for three of the clasts are shown in Fig. 1. There appear to be at least two components present. Most of the nitrogen (>80%) is released between 1000° and 1500°, and has a uniform isotopic composition. The relatively high temperature release for the largest proportion of nitrogen is consistent with the binding of this nitrogen in refractory inorganic phases. There also appears to be a second component present in all of the clasts which is released at temperatures below 1000°C and is isotopically heavier. While some surface-adsorbed terrestrial nitrogen may be present in the low temperature fractions, the amount observed in the analysis of lunar soils, which have been stored in a nitrogen atmosphere, is generally on the order of 1 ppm, rather than 10-20 ppm which is observed in the clasts. The relatively low release temperature is suggestive of a carbonaceous phase. We have shown that in Allende the isotopically distinct component which is observed in the 800 and 900° fractions is also most likely associated with a carbonaceous phase (2). Release temperature alone is insufficient to identify the component and further chemistry is required before the chemical siting for the low temperature nitrogen can be identified.

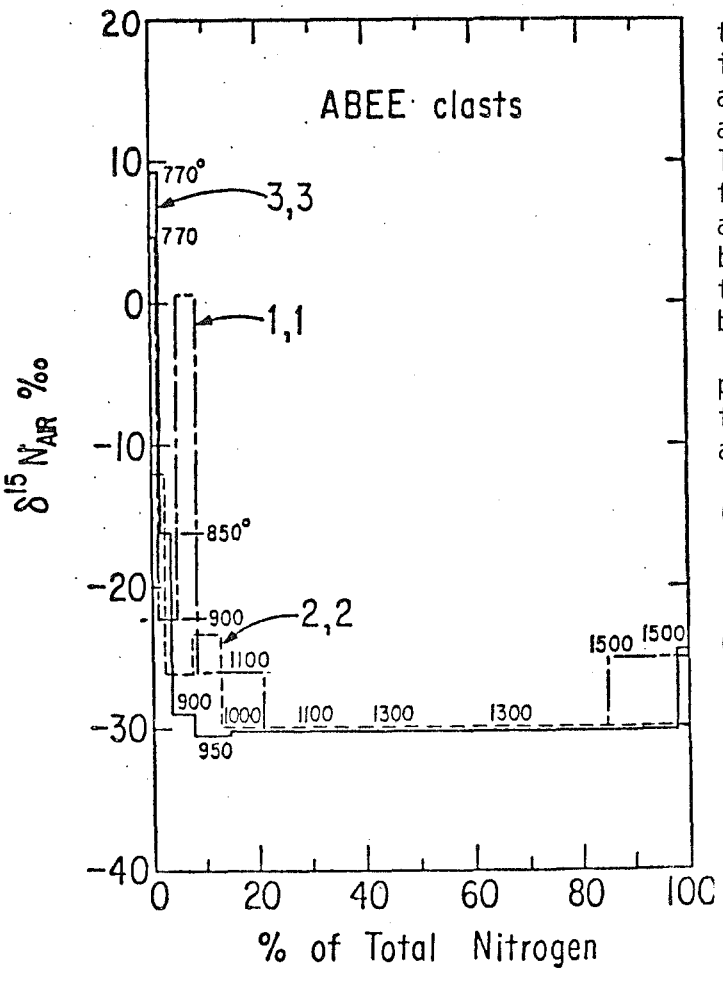

The high temperature (1500°) peak in Fig. 1 may be a mass-fractionated residue or possibly a third component.

(1) Kung, C.C. and R.N. Clayton (1978) Earth Planet. Sci. Lett. 38, 421-435.

(2) Thiemens, M.H. and R.N. Clayton (1980) Lunar and Planetary Science XI, pp. 1137-1139. The Lunar and Planetary Institute, Houston.

THE THERMAL HISTORY OF ABEE

Rudee, M. L. and Herndon, J. M.
University of California, San Diego, La Jolla, CA 92093

Specimens from the center and the outer surface of Abee exhibit identical microstructures within their metal phase--platelets of an iron carbide. Thus the entire body must have cooled at a nearly uniform rate. The density, heat capacity, and thermal conductivity have been measured and used in a theoretical heat flow analysis. From these calculations and observations it is concluded that Abee cooled from 700°C to 200°C in about two hours.

#168

MECHANICAL AGGREGATION OF ENSTATITE CHONDRITES FROM AN INHOMOGENEOUS DEBRIS CLOUD

Leitch, C. A. and Smith, J. V.
U. of Chicago, Dept. of Geophysical Sciences, Chicago, IL 60637

Kota-Kota contains four types of clinoenstatite-rich chondrules: porphyritic > fine-grained > barred > radiating. A luminescence microscope revealed distinct red and blue clinoenstatite grains, as well as orange and blue olivine grains. Porphyritic chondrules are extremely complex and a single chondrule may contain all four phases. Red clinoenstatite grains may enclose blue clinoenstatite, orange olivine and/or blue olivine. Red clinoenstatite was not observed inside blue clinoenstatite. Fine-grained chondrules contain blue clinoenstatite and rare blue olivine. Both barred and radiating chondrules are composed predominantly of lamellae of either red or blue clinoenstatite. All chondrule types are surrounded by a shell composed of a fine-grained mixture of all minerals found in the meteorite.

Minor element contents correlate with luminescence color but not with chondrule type. The observed ranges in minor element contents for both olivine and clinoenstatite are shown below. Red clinoenstatites have higher concentrations of Ti, Al, Cr, Mn and Ca while blue ones have higher concentrations of Na. Orange olivines contain more Cr and Mn than blue ones.

The observed textures and bimodal chemistries of the olivines and clinoenstatites rule out formation of these meteorites by direct condensation from the solar nebula. Mechanical aggregation of material from at least two source regions is needed to explain the red and blue varieties and the observed textures indicate a complex sequence of events. Enclosure of rounded olivine grains by pyroxene grains suggest that olivine formed earlier than clinoenstatite in agreement with condensation calculations. The simplest scheme to be considered for the Kota-Kota meteorite involves (a) progressive condensation of two separate regions of the nebula to give minor forsterite and dominant enstatite, and (b) mechanical mixing of the condensates. We suggest that enstatite chondrites result from mechanical and chemical processes during aerodynamic sorting and gravitational settling of debris from a hot cloud of dust, liquid and gas produced during collision of planetesimals.

NASA NGL 14-001-171.

	Orange Olivine	Blue Olivine	Red Pyroxene	Blue Pyroxene
P_2O_5	0.003-0.008	0.002-0.009	0.000-0.010	0.001-0.009
TiO_2	0.000-0.022	0.002-0.031	0.025-0.120	0.001-0.012
Al_2O_3	0.016-0.100	0.041-0.116	0.151-0.451	0.015-0.195
Cr_2O_3	0.115-0.290	0.029-0.095	0.126-0.568	0.002-0.107
MnO	0.090-0.188	0.014-0.046	0.091-0.418	0.000-0.090
NiO	0.000-0.005	0.001-0.004	0.000-0.010	0.000-0.013
CaO	0.090-0.252	0.082-0.188	0.124-0.472	0.015-0.157
Na_2O	0.000	0.000	0.002-0.093	0.040-0.248

PRIMORDIAL NOBLE GASES IN E-CHONDRITES

Jane Crabb

Department of Chemistry and Enrico Fermi Institute, University of Chicago
Chicago, IL 60637

Mineral separates and bulk samples of 6 E-chondrites have been analyzed for noble gases, to investigate the components and carriers of trapped gases and $^{129}Xe_r$.

The new data extend the range of $^{36}Ar_p/^{132}Xe$ up to 3100 for South Oman (E4), which has the very high ^{36}Ar content of 8.8×10^{-6} cc/g. 36/132 varied by more than a factor of 7 in stepwise heating on a separate of North West Forrest (E6). This result complements previous work showing a large range in 36/132 within this class. It suggests that at least 2 gas-carriers are present, one with planetary elemental ratios similar to carbonaceous chondrites, and another with a less fractionated composition relative to solar.

Mineral separates on Indarch (E4) rule out major minerals as the primary hosts for the trapped gases. Resistance to HCl treatment and enrichment in a low density fraction suggest that some form of carbon may be the host of the planetary component dominant in Indarch. There is a precedent for a carbonaceous phase with high 36/132 ratios in ureilites, so perhaps the less fractionated component is also sited in some type of carbon. It is becoming apparent in recent work from this laboratory that there is a progression to higher 36/132 ratios with increasing degree of reduction along the sequence from C3Vox to to C3Vred to C30 to E-chondrites. This may be pointing to a reduced mineral as the carrier of the component with high 36/132.

Currently 6 out of 7 E4's and E5's have detectable primordial Ne, in contrast to the other chondrites where it is found only in some meteorites of type 3 or lower. This Ne is not clearly associated with either the planetary or less fractionated component. There is a trend of decreasing $^{20}Ne_p$ with increasing petrologic type, and so a metamorphic effect may be obscuring the original elemental pattern. Alternatively, Ne may be located in a different mineral from the heavier gases. The isotopic composition is consistent with planetary Ne (20/22 ~8).

The Xe isotopic composition is variable for the heavier isotopes, with $^{136}Xe/^{132}Xe$ ranging from .309 ±.003, similar to the lowest value observed in meteorites (e.g. Kenna ureilite), to .320 ±.002. The excesses at the heavier isotopes can reasonably be attributed to fission products from known sources. A single measurement on South Oman suggests an enrichment of the light isotopes of Ar, Kr, and Xe relative to Kenna, a trend parallel to its high Ar/Xe and Kr/Xe ratios. However, the observation needs to be confirmed.

This work highlights the diversity of E-chondrites: in contrast to other chondrite classes, gas concentrations fail to correlate with petrologic type or trace element content. Yet 4 E4's for which $^{36}Ar_p$ varies by >2 orders of magnitude show clustering of their exposure ages, implying that they came from a common parent body. Perhaps conditions were more variable over their formation region than for the ordinary chondrites.

#170

THE NORTON COUNTY ENSTATITE ACHONDRITE: A BRECCIATED, PLUTONIC IGNEOUS ROCK

Okada, A., Keil, K., and Taylor, G.J.
Department of Geology, Institute of Meteoritics, University of New Mexico, Albuquerque, NM 87131

The Norton County enstatite achondrite consists of brecciated pyroxenitic material that contains areas of unbrecciated pyroxenite and clasts with microporphyritic textures. The unbrecciated pyroxenitic areas range up to 8 cm across and consist of xenomorphic, granular enstatite crystals ($En_{99}Wo_1$) up to 3 cm in size. Grain boundaries result from mutual interference, as if the crystals grew simultaneously from a melt of pyroxenitic composition; Norton County does not appear to be a cumulate. Diopside ($En_{55}Wo_{45}$) is also present, both as individual grains and as exsolution within enstatite crystals. The exsolved diopside constitutes up to 25 vol. % of the host enstatite and displays blebby, septal, platy and irregularly curved shapes. Although groups of exsolved crystals have the same optical orientation, there does not seem to be a specific crystallographic relationship between the host enstatite and exsolved diopsides. The pyroxene pair gives an apparent equilibration temperature of $\sim$ 1000°C (using the 1-atm phase diagram). The pyroxenitic areas also contain grains of zoned taenite in contact with kamacite. Taenite contains 48.3 wt.% Ni at the phase boundary with kamacite, suggesting a cooling rate of $\sim$ 1°C/m.y. This clearly indicates cooling at considerable depth. This depth is difficult to estimate, but we can place constraints on it: if the tridymite that occurs in the brecciated areas of the meteorite crystallized under similar conditions as the minerals in the pyroxenitic clasts then the pressure must have been < 3 kb.

The microporphyritic clasts are composed mainly of ortho-and clino-enstatite ($Fs_{0.6}$), olivine ($Fa_{0.7}$) and a fine-grained mesostasis. Some enstatite grains are angular and significantly larger than the microphenocrysts; these large enstatites contain less FeO than do the microphenocrysts. Many pyroxenes enclose tiny olivine grains. Minute spherules of troilite and intergrowths of troilite with nickel-iron are present in the interstices between phenocrysts. The bulk composition of one clast (determined by broad-beam microprobe analysis) shows that it contains more Na_2O (0.5 wt.%) than does bulk Norton County (0.1 wt.%). The presence of clasts of enstatite embedded in a rapidly cooled melt suggests that the microporphyritic clasts in Norton County are impact melts.

We propose the following history for the Norton County enstatite achondrite: The rock crystallized at depth in its parent body; its texture indicates simultaneous crystallization of enstatite and diopside, which implies that the melt was pyroxenitic in composition. The melt was probably derived initially by melting or partial melting of an enstatite-rich condensate from the solar nebula. The rock cooled slowly after crystallization as shown by the presence of exsolution within diopside and of zoned taenite and kamacite. One or more impact events then excavated the rock, brecciated it, and mixed it with impact-melted material, represented by the microporphyritic clasts. Differences in bulk chemical composition between microporphyritic clasts and the rest of the meteorite, however, demonstrate that the target material for these impact melts was not the plutonic pyroxenites.

ALHA 78113, MT. EGERTON AND THE AUBRITE PARENT BODY

T.R. Watters[1], M. Prinz[2], E.R. Rambaldi*, and J.T. Wasson*
[1]Dept. of Terrestrial Magnetism, Carnegie Institution of Washington, Washington, D.C. 20015; [2]Am. Mus. Natu. Hist., New York, N.Y. 10024; *Inst. of Geophys. and Planet. Phys., UCLA, Los Angeles, CA 90024

ALHA 78113 is the first Antarctic meteorite to be classified as an aubrite. Enstatite comprises 96% of the silicate phases in 78113. This is within the range observed in aubrites (75-98%). The composition of the enstatite is Wo 0.60, En 99.37, Fs 0.04, similar to Mt. Egerton (En 99.1). Both are inside the range observed in aubrites (En 98.8-99.5). Olivine comprises 0.8% of the silicate phases and also falls in the modal range observed in aubrite (0.3-10.0%). The composition of olivine is nearly pure forsterite (Fo 99.99) and is at the upper limit of the compositional range observed in aubrites (Fo 99.79-99.99). The modal content of plagioclase (0.6%) falls outside the range observed in aubrites (1-16%). Plagioclase occurs both as compositionally homogeneous grains and as fine-grained aggregates. The homogeneous grains have an average composition of An 3.9. This is within the range observed for aubrites (An 1.8-8.2). However, the range in composition found in the fine-grained aggregates (An 1.5-30.5) is much greater than that in aubrites (except for Khor Temiki which has a few grains of composition An 23.8). Diopside comprises 0.3% of the silicates in 78113, inside the modal range observed in aubrites (0.3-8.1%). The composition of diopside is Wo 43.89, En 56.09, Fs 0.02. This is similar in composition to diopside in Mt. Egerton (Wo 44.7), and both are within the range in aubrites (Wo 40.1-46.1). The modal occurrence of kamacite in 78113 is 2.2%, in the range observed in aubrites (<0.1-3.7%). The Ni content of kamacite (4.3%) is also within the range in aubrites (3.7-6.8%) and is more similar to that found in host metal of Mt. Egerton (6.25%) than in inclusions in enstatite (8.25%). Si content in metal (0.1%) is on the lower limit of the range observed in aubrites (0.1-2.4%). Si content in metal of Mt. Egerton is similar for both the included and host phase (2.06%). Modal content of Ti-bearing troilite in 78113 (0.3%) falls inside the range in aubrites (<0.1-7.1%). The Ti content in the troilite (1.84%) is very similar to that found in Mt. Egerton (2.12%), and both are in the range observed in aubrites (1.5-5.7%). Oldhamite, ferro-magnesian alabandite and daubreelite occur in trace amounts in 78113. Both oldhamite and daubreelite are very similar in composition to those in aubrites. Mg content of alabandite in 78113 (2.9%) is just outside the range found in aubrites (1.06-2.2%), but is much less than that found in Mt. Egerton (avg. 7.9%). Schreibersite also occurs in trace amounts in 78113. Ni content in the schreibersite varies from 25.3 to 48.1%, spanning the range observed in Mt. Egerton and the aubrites.

The abundance trends of 12 siderophile elements, relative to Cl, in the metallic portions of Mt. Egerton, Horse Creek (Si-bearing iron) and Hvittis (E6) (if we exclude Cu and Sb) indicates a very close genetic relationship between the three meteorites. Cu in Mt. Egerton and Horse Creek is depleted by a factor of 3.5 relative to Hvittis metal and Sb by a factor of 1.5. These depletions probably indicate that Cu and Sb were partly present in a non-magnetic mineral phase (sulfide and or silicate).

If the aubrite parent body formed by melting and differentiation of E6 chondrites (Watters & Prinz, 1979, 1980), then 78113 and the other aubrites, Mt. Egerton and Horse Creek, all represent parts of the differentiation sequence.

#172

COSMOGENIC ^{53}Mn AND ^{26}Al: DEPTH AND SIZE EFFECTS ON THE PRODUCTION RATES IN ST.SEVERIN, KEYES, KIRIN AND OTHER CHONDRITES.

Englert, P. and Herr, W.
Institute of Nuclear Chemistry, University of Cologne,
D 5000 Koeln-1, Federal Republic of Germany

^{53}Mn and ^{26}Al, the light spallogenic noble gases, as well as the cosmic ray tracks are valuable to get informations on the irradiation history of chondrites. For stony meteorites within the recovered mass-range of St.Severin (~273 kg) and Keyes (~140 kg) supposed relations were investigated between the production rates of cosmogenic ^{53}Mn and/or ^{26}Al,on the one hand,and the spallogenic ^{22}Ne/^{21}Ne- or ^{3}He/^{21}Ne ratios and the respective cosmic ray track production,on the other hand. Slight differences between the St.Severin and the Keyes "trend lines" might result from the different shapes of their preatmospheric bodies. Certain "depth corrections" for ^{53}Mn and ^{26}Al, based on these trend lines, were derived and their use for the evaluation of effective preatmospheric radii is discussed. Measured ^{53}Mn-activities of very large falls,such as Kirin and Norton County,and of rather small ones, as Kiel, Tromoy and Cannakkale (≈ 1 kg),are compared with other cosmogenic nuclides. The aim is to study shielding effects and their influence on the ^{53}Mn production in very small and in larger bodies, for which, up to now, there exists a lack of information.

COSMOGENIC NUCLIDES IN 13 CHONDRITE FINDS: IMPLICATIONS FOR EXPOSURE AGE SYSTEMATICS.

Kirsten, T.[1], Englert, P.[2], Herr, W.[2], and Ries, D.[1]
[1]Max-Planck-Inst.f. Kernphysik, Heidelberg, F.R. Germany
[2]Institut f. Kernchemie, Univ. Köln, Köln, F.R. Germany.

Various attempts have been made to estimate cosmogenic production rates of stable and radioactive nuclides in chondrites in order to develop concordant exposure age scales. In particular, a generalized growth curve for 3.7 m.y. ^{53}Mn constructed with the help of stable ^{21}Ne may serve both, to use ^{53}Mn-$^{53}Mn_0$ as an independent exposure age chronometer for unsaturated (<14 m.y.) meteorites, and to improve the ^{21}Ne exposure age scale by more reliable ^{21}Ne production rates (1,2).

Here we report on "same sample"-measurements of ^{53}Mn and light stable rare gases for 13 chondrites, most of which are unsaturated finds not previously analyzed. With the previously inferred values of $^{53}Mn_0$=434±28 dpm/kg Fe and ^{21}P=0.39±0.03x10^{-8}ccSTP/g m.y. for L-chondrites and applying appropriate corrections for chemical composition (3) and shielding based on measured $^{22}Ne/^{21}Ne$ (^{53}Mn:(4); ^{21}Ne:(3)), seven out of ten unsaturated finds show ^{21}Ne deficit, accompanied by low $^{3}He/^{21}Ne$ ratios (Wellman ## 3; Ashmore, Etter, Portales, Bledsoe, Floyd, Isna). This indicates substantial cosmogenic Ne-losses probably promoted by preferential wheathering of silicates. It stresses the necessity to strictly reject chondrites with $^{3}He/^{21}Ne$<3.5 in generalizing regression analyses of cosmogenic growth curves. Currently suggested reductions of ^{21}P down to 0.30x10^{-8}ccSTP/g, m.y. are probably caused by including such meteorites in the statistical analyses.

Calliham and Achilles are in ^{53}Mn saturation, Hardtner shows evidence for a two-stage irradiation, Isna (CO 3) has an extremely short exposure age (T_{21}=80,000 yrs).

Where applicable, we will also discuss gas retention ages, trapped gases (e.g., Roosevelt, Isna) and ^{26}Al data.

References

(1) P. Englert and W. Herr, Abstract 42nd Met.Soc., Heidelberg, 1979.
(2) O. Müller, W. Hampel and T. Kirsten, submitted to Geochim.Cosmochim.Acta, 1980.
(3) P. Cressy and D. Bogard, Geochim.Cosmochim. Acta 40, 749, 1976.
(4) P. Englert and W. Herr, accepted for publication in Earth Planet.Sci.Lett., 1980.

#174

Irradiation History of Kirin Meteorite.

M.Honda, K.Horie, M.Imamura*1, K.Nishiizumi*2, N.Takaoka*3 and K.Komura*4
Institute for Solid State Physics, Univ. of Tokyo, Minato-ku Tokyo, Japan
*1: Institute for Nuclear Study, Univ. of Tokyo, Tanashi-shi Tokyo, Japan
*2: Dept. of Chem., Univ. of California, San Diego, La Jolla,CA 92093, U.S.A.
*3: Dept. of Earth Sciences, Yamagata Univ., Yamagata, Japan
*4: Lowlevel Radioactivity Lab., Kanazawa Univ., Tatsunokuchi,Ishikawa,Japan

Cosmogenic nuclides, radio-active and stable, have been studied in the Kirin chondrite (H5). Som experimental results obtained in samples sent to us (Nos. 1, 4 and other fragments) and in aliquots of other samples, which were available to us, are described and compared with other data obtained in many laboratories. In our laboratories, the gamma rays of ^{54}Mn, ^{60}Co, ^{26}Al, ^{22}Na and ^{40}K (natural) were measured using Ge(Li) detector systems. ^{53}Mn was determined by an activation method based in ^{53}Mn (n,γ) ^{54}Mn reaction. The light rare gases were measured by a massspectrometer.

After all, we found that it is possible to read out the fossil records of the complex irradiation history and interpret them by, 1) Multi-exposure history and 2) Depths effects in the production of cosmogenic nuclides in different geometries at different stages.

The depth effect seems to be predominant for the production of ^{60}Co, by an (n, gamma) reaction, in the latest stage just before the fall. On the other hand, the depth effects in the earlier stage are recorded predominantly in the production of stable and long-lived isotopes. In contrast to ^{54}Mn and ^{22}Na which show saturation with no significant variation among the samples, the long-lived nuclides, ^{26}Al and ^{53}Mn, are undersaturated by different exposure doses. Based on ^{26}Al data, ca. 0.5 My is reasonable for the 2nd stage irradiation. The contents of light rare gases in bulk samples are not useful to extend our discussion, because of possible loss from the surface samples, perhaps except in the central portion. Based on ^{53}Mn data, and possibly ^{21}Ne contents in the central regions, we may assume 2π geometry for the 1st stage. That is, the body of Kirin was originally located at the surface of an infinitly large object. The irradiation to the surface of this mother body seems to have been started effectively about 10^7y before present.

The importance of the documentation of the individual samples and a future sampling method has been realized through these measurements.

DETERMINATION OF PREATMOSPHERIC MASSES OF METEORITES USING PARTICLE TRACKS AND NEON ISOTOPIC RATIOS. Goswami, J.N., Lal,D., Nautiyal,C.M., Padia,J.T., Rao,M.N., Venkatesan,T.R. Physical Research Laboratory, Ahmedabad 380009, India AND Wasson,J.T., U.C.L.A., Los Angeles, California,USA.

We have determined Ne and He isotopic ratios and particle track densities in the same aliquot samples of 14 chondrites. Using the cosmic ray exposure ages determined by Ne-21 method, we have estimated the parameter TPM (tracks per sq.cm per m.y.). The TPM and $(Ne\text{-}22/Ne\text{-}21)_{sp}$ values are plotted in Fig.1.

Bhandari et al (1) carried out an exhaustive study of these two parameters in about 75 stony meteorites of various sizes and were able to impose limits on the range of variation of $(22/21)_{sp}$ and TPM values in most of the known cases. All the data points obtained in our study fall within the limits set by Bhandari et al(1) indicating that the preatmospheric radii of the meteorites studied here fall within the range of R_o = 10-50 cm. In addition, we calculate the preatmospheric masses (M_o) of these meteorites using the measured $(Ne\text{-}22/Ne\text{-}21)_{sp}$ (NeR) and the relation $M_o(kg) = 1.1 \times 10^{10}$ exp. (-17 NeR) given in ref.(1). The preatmospheric masses estimated in this study vary from about 10 kg to 180 kg. Basing on the measured He-3/Ne-21 and Ne-22/Ne-21 ratios as well as track densities, we deduced the limits on the preatmospheric masses by a suitable combination of the methods described by Nyquist et al (2) and Bhattacharya et al (3). The preatmospheric masses estimated by the method of Nyquist et al are seen to be consistently higher than those by method of Bhandari et al (1). The discrepancy owes itself presumably to the nucleonic cascade model adopted by Nyquist et al (2).

References :(1) Bhandari et al (1980) NTD (in press). (2) Nyquist et al(1973) GCA 37, p.1655. (3) Bhattacharya et al (1973) JGR 78, p.8356.

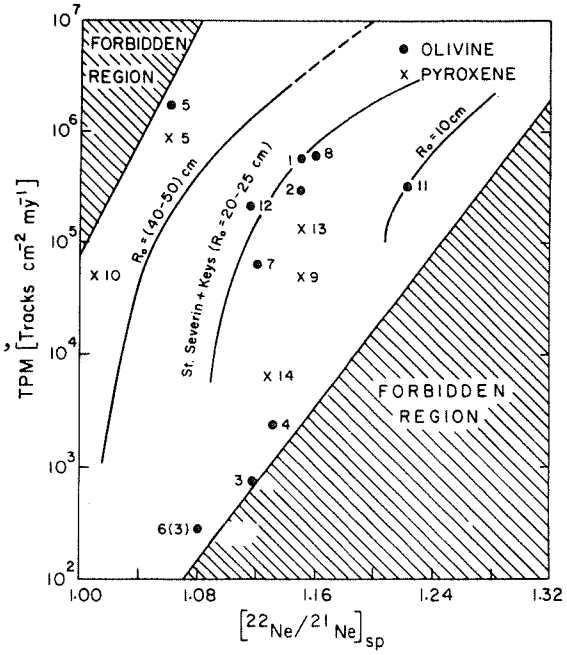

Fig:1. $(Ne\text{-}22/Ne\text{-}21)_{sp}$ v/s TPM plot for chondrites. The hatched portions indicate the forbidden regions. Numeral near each data point in the figure corresponds to the meteorite in the following list. The values in brackets refer to the tentative Ne-21 exposure age (m.y) and the estimated preatmospheric mass (kg) respectively.

1.Allred (4.2,36.4), 2.Densmore (7.9,35.8), 3.Dhajala (6.0,59.2), 4.Frankline(13.8, 53.3), 5.Harrisonville (4.1,169.4), 6.Innisfree (26,117), 7.Lost City (6.3, 64.2), 8.Ogi (12.1,31.3), 9.Patora (5.3, 31.6), 10.Seoni (2.6,78.2), 11.Siena (10.1,10.6), 12.St.Lawrence (21.5,9.8), 13.Madhipura (14.9,35.7), 14.Bansur B-14-2 (14.9,52.3)

#176

MULTIPLE COSMIC-RAY EXPOSURE AGES OF METEORITES

G.W. Wetherill
DTM, Carnegie Institution of Washington, Washington, D.C. 20015

Inferences based on the accumulated record of meteoritic exposure to galactic cosmic radiation are central to our views regarding mechanisms for derivation of meteorites from their parent bodies, the collisional history of meteorites, and the degree of their atmospheric ablation. The possibility that meteorites experienced a multiple exposure history as a result of fragmentation of a previously irradiated object is sometimes invoked to explain discrepancies between exposure data obtained by different techniques. In the absence of such discrepancies it is usually assumed that only a single exposure has occurred, even when the data are inadequate to establish this.

A theoretical investigation of the statistical expectation of multiple exposure has been made. It is assumed that meteorites result from collisional fragmentation of chemically similar larger objects, and that all material within a given "shielding depth" of the surface of these larger objects has been pre-irradiated. Production of meteoritic fragments both by cratering and catastrophic disruption has been calculated. The dependence of the resulting meteorite size distribution and mass yield on fragmentation parameters and mass of the fragmented body has been explicitly evaluated.

It is found that for all fragment sizes the ratio of the rate of production by total disruption (I_D) to that of cratering (I_c) is

$$(I_D/I_C) = (\Gamma_D f_D/\Gamma_C f_C)$$

where Γ_D is the target/projectile mass ratio at the threshold of catastrophic disruption, Γ_C the mass ratio for cratering, and f_D and f_C are calculable functions of similar magnitude and only weakly dependent on plausible collision parameters. For the Dohnanyi (1969) steady-state mass power law exponent $\alpha = -11/6$, and experimental values of the Γ's, $(I_D/I_C) \simeq 2$. This differs from the frequent assumption that cratering is negligible.

The same theory gives the fraction of meteorite fragments derived from objects small enough to be entirely pre-irradiated as well as the fraction obtained by surficial cratering of larger objects. For a 2 meter shielding depth and experimental values of the parameters of fragmentation, the calculated incidence of multiple exposure, for both modes of fragmentation, is

pre-atmospheric meteorite mass (g)	multiple exposures (per cent)	
	catastrophic	cratering
10^6	27	25
10^5	50	44
10^4	67	57
10^3	79	68
10^2	87	77

Although the exact percentages will change when different parameters are used, the general result that multiple exposure should be a common phenomenon is very insensitive to plausible variations in the fragmentation parameters, as well as to the meteorite mass distribution, and is essentially independent of the size distribution of bodies $\gtrsim$ 100m diameter. It is concluded that if conventional ideas regarding origin of meteorites are correct, then multiple exposure history should be a common occurrence and must be explicitly recognized when interpreting exposure data.

DATING THE INITIATION OF COSMIC RAYS IN OUR GALAXY

L. M. Libby, Environmental Science and Engineering
W. F. Libby, Department of Chemistry
University of California, Los Angeles, California 90024

The formation ages of iron meteorites are about 4.6×10^9 years whereas the length of time that they have been exposed to cosmic rays is less than 1×10^9 years. Cosmic rays are accelerated in our galaxy by collision with moving magnetic mirrors. Measurements of red and blue shifts of the 21 cm galactic emissions show that our galaxy is winding up, increasingly strengthening the magnetic fields in its arms, thus causing them to move outward along the arms. These mirrors were of insufficient strength to produce energetic cosmic rays in the first billion years and have grown stronger with time. Thus the cosmic ray flux that is observed in our galaxy built up slowly, both in energy and flux, so that only in the last several hundred million years was it able to produce the spallation products in the interiors of meteorites from which the cosmic ray exposure times are estimated. (We wish to distinguish clearly between the age of individual cosmic rays, which is a few million years, and the time of several hundred million years at which cosmic rays began to be accelerated to high energies.) If our theory is true, then there is no need for the hypothesis that iron meteorites were sequestered for 3.5 billion years and then were released by breakup of a parent body. Of course the cosmic ray exposure history of non-metallic meteorites must parallel that of the irons except that break-up may be more probable. Thus we may expect that the spallation products may be more abundant in the non-metallic meteorites.

#178

METEORITES AS PROBES OF GALACTIC STRUCTURE

Trivedi, B.M.P. and Larimer, J.W.
Department of Geology, Arizona State University, Tempe, USA

Meteorites, along with other members of the solar system, move in closed orbit about the galactic center. During this motion, two significant events occur: 1) encounter with the dense interstellar clouds and 2) the passage through the galactic arms. Both of these events are expected to leave some impression on the solar system objects; e.g. possibility of ice ages and heavy element accretion are already discussed in the literature. Here we discuss how meteorites would be affected by these events and how they can be utilized to deduce information about the interstellar clouds and the spiral structure.

From the UV spectra of the interstellar clouds it is inferred that most of the refractory elements are locked up into grains while the volatile elements are in the gas phase. The passage of the meteorites through these clouds would result into the accretion of the dust grains and adsorption of the free elements on their surface. The grain collision rate ($\dot{N}$) will be given by, $\dot{N} = \pi R^2 V(r) n(r)$ where R is the radius of the meteorite, V(r) is the velocity relative to the cloud at solar distance and n(r) is the grain density of the cloud at solar distances. The following values of the parameters are fairly representative: $V(r) \sim 15$ km sec^{-1}, grain size $\sim 0{\cdot}01\mu$, grain density $n(r) \sim 5 \times 10^{-5}$ cm^{-3}, crossing period of a cloud $\sim 10^5$y, sticking coefficient $\sim 0{\cdot}1$. With these parameters, a meteorite of 100 cm radius would accrete $\sim 7{\cdot}6 \times 10^{17}$ grains or roughly 10 gm of interstellar dust. Although most of this material would be evaporated during fall, there is a good possibility of a small fraction remaining on the surface and be available for study. Such samples will be almost impossible to collect by any human endeavour and might provide valuable clues about the chemical composition of the interstellar clouds. Some of these grains might be unique messengers of the nucleosynthetic activity in stellar ejecta.

During the passage through the galactic arms, meteorites are expected to experience an enhanced cosmic-ray flux, because type II supernovae which presumably generate cosmic-rays are mostly observed in the spiral arms. Suggestions have been made that the solar system entered the orion arm only recently, $\sim$ 1-2 m.y. ago. In that case only short lived cosmogenic nuclides would show saturation. The longer lived nuclides (> 10 m.y.) would indicate any variation in intensity from the interarm region to the arm region of the galaxy. A useful nuclide for such studies will be I^{129} (17 m.y. half life). It will give a direct test of the density wave theory of the galactic structure.

SYSTEMATICS OF NUCLEAR REACTIONS IN METEORITES

Robert C. Reedy
Los Alamos Scientific Laboratory, Los Alamos NM 87545

The cosmic-ray bombardment of meteoroids produces many radioactive and stable nuclides which can be used to study the history of the meteorites and of the cosmic rays. The transport of primary and secondary cosmic-ray particles through matter is complex and results in particle fluxes which vary with the preatmospheric size and shape of the meteorite and the location of the sample. The model developed by Reedy et al. (1979) for galactic-cosmic-ray particle fluxes in the St. Séverin chondrite was used to explore nuclear reaction systematics in a meteorite with a preatmospheric radius of 70 g/cm^2 (about 20 cm). This flux model is similar to one developed for the Keyes chondrite (Reedy et al., 1978) and reproduced well the shape of the ^{21}Ne and ^{22}Ne/^{21}Ne data as a function of depth in St. Séverin.

Production rates for isotopes of He, Ne, and Ar and for several radionuclides were calculated as a function of depth. Large changes in production rates versus depth occurred near the surface, with about one half of the total production-rate variations occurring within 10 g/cm^2 of the preatmospheric surface (the part usually removed by ablation). The changes in production rates between depths of 10 and 20 g/cm^2 were about the same as those between 20 and 70 g/cm^2. Products made mainly by low-energy reactions had the largest variations in production rates with depth (e.g., ^{55}Fe and ^{21}Ne rates increasing by 45 and 34%, respectively, between 10 and 70 g/cm^2), while high-energy products only increased slightly with greater depths (e.g., ^{10}Be and ^{3}He up 6 and 7%, respectively, between these depths). The production rates of ^{36}Ar and ^{38}Ar increased 25% between 10 and 70 g/cm^2, showing that, in calculating ^{38}Ar exposure ages, some shielding corrections should be applied (as they are for ^{21}Ne) if production rates are not inferred from ^{39}Ar activities.

The calculated changes in production rates of cosmogenic nuclides with depth correlated very well ($r \geq 0.994$) with depth variations in the ^{22}Ne/^{21}Ne ratios, as did the ratios ^{3}He/^{4}He, ^{3}He/^{21}Ne, and ^{38}Ar/^{21}Ne ($r > 0.999$). The experimental ^{53}Mn activities (Englert, 1979) and He and Ne data (Schultz and Signer, 1976) for St. Séverin showed similar trends, but with more scatter. However, the calculated depth variations of ^{20}Ne/^{21}Ne and ^{22}Ne/^{21}Ne did not correlate as well ($r \cong 0.95$).

P. Englert (1979). thesis, Univ. zu Köln.
R. Reedy, G. Herzog and E. Jessberger (1978). Lunar and Planetary Science IX, pp. 940-942.
R. Reedy, G. Herzog and E. Jessberger (1979). Earth Planet. Sci. Lett. 44, 341-348.
L. Schultz and P. Signer (1976). Earth Planet. Sci. Lett. 30, 191-199.

#180

DEPTH DEPENDENCE OF COSMOGENIC NUCLIDES IN SPHERICAL METEOROIDS.

Spergel, M. S.,[a,c] Reedy, R. C.,[b] Lazareth, O. W.,[c] and Levy, P. W.[c]
[a]York College of CUNY. [b]Los Alamos Scientific Laboratory. [c]Brookhaven National Laboratory.

The cosmic-ray induced neutron production in meteoroids creates an equilibrium neutron distribution which, in turn, controls the generation of stable and radioactive nuclides. The size and depth dependences, particularly for the thermalized neutrons with high interaction cross sections, determine the formation rates of the cosmogenic isotopes. Distributions of cosmogenic nuclides in planetary and lunar surfaces have been calculated using nuclear reaction production models by various authors [1-6]. Most calculations [1-3] of nuclide production in meteoroids only consider spallation reactions induced by energetic ($E \gtrsim 1$ MeV) particles. Eberhardt et al. [4] used a slowing-down model to estimate rates for neutron-capture reactions in meteoroids. Lingenfelter et al. [5] and Kornblum and Fireman [6] have utilized multigroup transport techniques to calculate the equilibrium neutron distribution and the induced nuclide distribution within the lunar soil.

To be described is a new calculation that utilizes multigroup neutron transport techniques to obtain the depth and energy dependence for both the equilibrium neutron and cosmogenic isotope distributions in spherical meteoroids of various radii. The calculational procedures were similar to those of Lapides et al. [7]. The calculation assumes that the incident cosmic rays are isotropically incident on the spherical meteoroids. The equilibrium neutron distribution computation utilizes recently compiled neutron cross section data [8]. The neutron distribution, particularly at low energy, will depend on the temperature and on chemical composition, especially hydrogen [7]. Also the neutron distribution depends on the radius, except for large or very small meteoroids.

[1] J. R. Arnold, M. Honda and D. Lal (1961), J. Geophys. Res. 66, 3519-3531.
[2] T. P. Kohman and M. Bender (1967), in High Energy Nuclear Reactions in Astrophysics, B. S. P. Shen, ed., p. 169.
[3] R. C. Reedy, G. F. Herzog and E. K. Jessberger (1979), Earth Planet. Sci. Lett. 44, 341-348.
[4] P. Eberhardt, J. Geiss and H. Lutz (1963), in Earth Science and Meteoritics, J. Geiss and E. D. Goldberg, ed., p. 143.
[5] R. E. Lingenfelter, E. H. Canfield and V. E. Hampel (1972), Earth Planet. Sci. Lett. 16, 355-369.
[6] J. J. Kornblum and E. L. Fireman (1974), Center for Astrophysics, Smithsonian Astrophysical Observatory, Preprint Series No. 51.
[7] J. R. Lapides, M. S. Spergel, O. W. Lazareth, P. W. Levy, R. C. Reedy and J. I. Trombka (1980), Lunar and Planetary Science XI, 605-607.
[8] M. S. Spergel, O. W. Lazareth, L. A. Slatest and P. W. Levy (1980), Lunar and Planetary Science XI, 1069.

Research supported by NASA NSG-7434, NASA W-14084, and by DOE under contract DE-AC02-76CH00016.

Magnesium-Calcium-Potassium isotopic variations in iron meteorites: A method for studying cosmic rays

Birck, J.L., Morand, Ph.and Allègre C.J.
Laboratoire Géochimie Cosmochimie 4 Place Jussieu 75230 Paris 5

Very soon iron meteorites have drawn the attention of the authors interested in the study of the cosmic rays. Almost exclusively constituted of iron and nickel their content in lighter elements is very low and allows the measurement of the tiny (ppb range) amounts of nuclide produced by the interaction of cosmic rays with the iron nickel matrix even for irradiation times as short as a few million years.

Numerous data have been reported on light rare gases. Potassium isotopes have been used by Voshage and Hintenberger to determine the exposure age of numerous iron meteorites. Stauffer and Honda, Shima and Honda analyzed several other elements (Cr, V, Ti, Ca) closer to the target nuclei to get data on the role of secondary particles.

It seemed interesting to us to re-investigate K and Ca isotopes with present day experimental techniques, and to get data for the as yet unstudied Mg isotopes. Our experimental method allows us to analyze the isotopes of these elements with a precision better than 10^{-3} (with the exception of ^{46}Ca) on samples containing down to 20 ng. Experimental blanks are presently at the 10 ng level. This permits us to perform analyses on less than 0.5 g of iron meteorite.

Relatively to terrestrial Ca and K, clear excesses of ^{42}Ca, ^{43}Ca, ^{44}Ca, ^{46}Ca and ^{40}K and ^{41}K have been detected in the iron meteorites Grant and Canyon Diablo. Mg isotopic composition is also anomalous in that it presents excesses of ^{26}Mg. Further data will be presented at the meeting.

#182

Li^6/Li^7 variations in meteorites

BIRCK J-L, ZANDA B. and ALLEGRE C.J.

Laboratoire de géochimie et cosmochimie, 4, Place Jussieu 75 PARIS

The Li isotopic composition is an extremely important parameter for the investigation of nucleosynthesis as well as radiation effects in meteorites.

We developed an experimental technique which allows to analyze samples containing down to 1 ng Li with a precision of 1 % in the isotopic composition and with blanks lowered down to a few percents of this value.

Terrestrial materials have been analyzed and display variations of the Li isotopic ratio up to 3 %. For example the analytical grade reagent has a $^7Li/^6Li$ ratio of 12.62 whereas it is of 12.26 in basalts.

Several stone meteorites have been investigated : Allende chondrules, Eagle station, Orgueil, Juvinas. These samples show no significant variation as compared to terrestrial basalts. Chondrules of Chainpur give the same result although they have tremendous variations in the D/H ratio and in the ^{17}O abundance (Robert et al., 1979). Among the several possible models for these last results, an intense early irradiation of the solar system must be discarded in view of our Li data.

Another field of interest is constituted by the iron meteorites. In the later Signer and Nier , Voshage and Hintenberger, Honda et al. clearly detected numerous products of spallation of iron by galatic cosmic rays. In Grant, our measurements show large ^6Li excesses relative to terrestrial lithium ($^7Li/^6Li$ = 5.30). Such large variations in the isotopic composition of Li will yield new strong constraints for the studies of irradiation age and preatmospheric shape of iron meteorites, as well as the interaction of cosmic rays with an iron target.

ALUMINUM-26 SURVEY OF ANTARCTIC METEORITES

Evans, J. C., Jr. and Reeves, J. H.
Battelle Northwest Laboratories, Richland, Washington 99352

For the past two years our laboratory has been conducting a survey of the Antarctic meteorite collection for ^{26}Al content. The eventual goal of this work has been to establish the distribution of terrestrial ages of these objects. All measurements have been by a fully nondestructive multidimensional gamma ray analysis technique. To date we have surveyed a total of 97 meteorites. We show data for 67 of these in the frequency distribution in Figure 1. A normalization factor of 1.09 has been included in the figure to correct for target chemistry effects. The data exhibits a definite shift to lower ^{26}Al values on the average when compared to data on contemporary samples (see Figure 2). This suggests that relatively old ages (>500,000 y.) may be common in the collection. Several such cases have in fact been reported by Nishiizumi and Arnold[1] using accelerator spectrometry measurements. The relative frequency of such objects is still unclear, however, since several of the meteorites with low ^{26}Al have been reported to be petrologically associated and thus may be part of a shower component.

---

[1]Nishiizumi, K. and Arnold, J. R. "Ages of Antarctic Meteorites," Lunar and Planetary Science XI Abstract, p. 815-817, 1980.

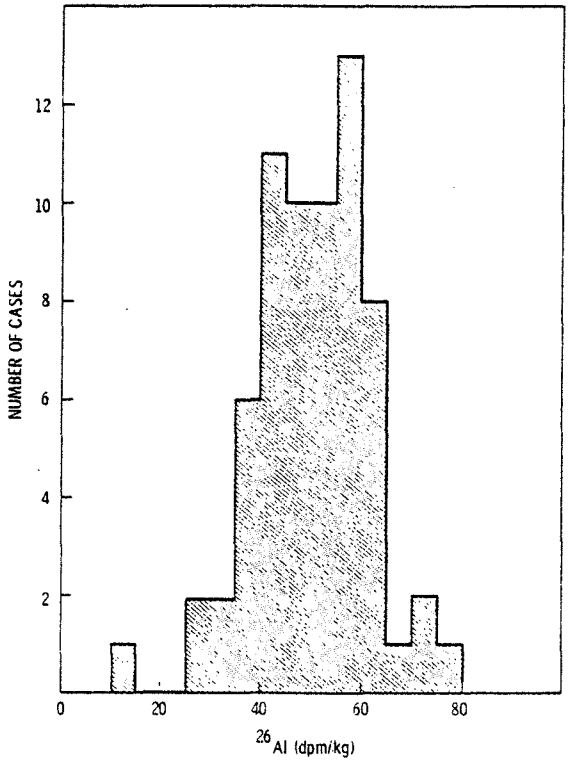

FIGURE 1.

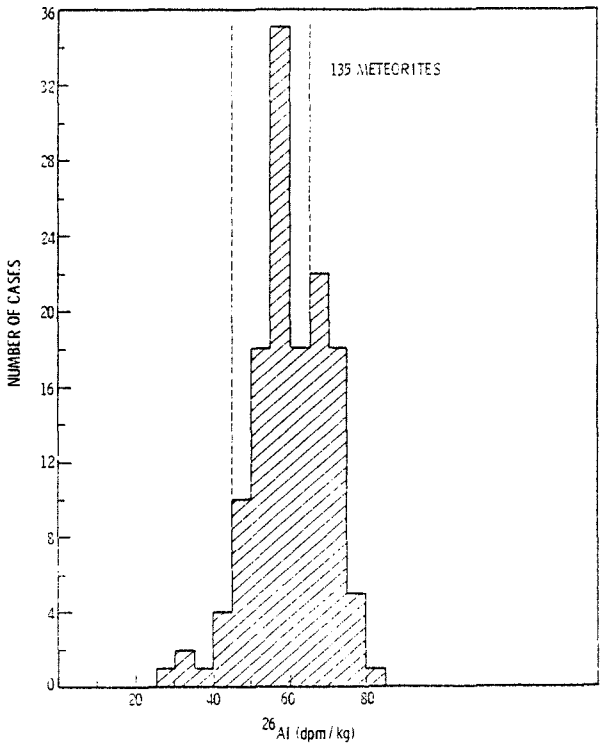

FIGURE 2.

#184

Cosmogenic ^{40}K and ^{53}Mn in Antarctic Meteorites.

O.Nitoh, K.Nishiizumi*1, M.Imamura*2, M.Honda and J.R.Arnold*1
Institute for Solid State Physics, Univ. of Tokyo, Minato-ku Tokyo, Japan,
*1: Dept. of Chem., Univ. of California, San Diego, La Jolla, California,U.S.A.
*2: Institute for Nuclear Study, Univ. of Tokyo, Tanashi-shi, Tokyo, Japan.

As part of a program to compile statistical information of the cosmic ray exposure history of meteorites, cosmogenic ^{40}K ($t_{1/2}$= 1.3×10^{9}y) and ^{53}Mn (3.7×10^{6}y) were determined in many antarctic and other meteorites. The measurements of cosmogenic ^{40}K by massspectrometry were performed in the metal phase separated from chondrites and others. According to our current techniques, starting from 10mg size metal samples cleaned by washing with HF, we are able to measure the exposure ages of higher than one million years at a contamination level of 10^{-9}gK. The production of ^{40}K was compared with the light rare gas contents appeared in literatures, ^{21}Ne in bulk and ^{36}Ar in metal phases. ^{53}Mn was determined by neutron activation analysis using 0.5-0.8g of meteorites. The experimental precedures were essentially the same as in our previous work.

In most of the samples, the contents of ^{40}K, ^{53}Mn activity levels, and other data are found to be consistent each other assuming a single irradiation history. This is partly due to the fact that the terrestrial ages of antarctic meteorites are generally short in comparison to the ^{53}Mn half-life. Some samples are indicating their near surface irradiation histories ; that is, relatively low (<400 dpm/kgFe+Ni/3) saturation values of ^{53}Mn were found in Yamato-74080, -74418, -74663 and ALHA-76007. With a small but not negligible probability,multi-stage irradiation histories were detected with Y-7301, Y-74116 and ALHA-76008. In these samples very low (22-101 dpm/KgFe + Ni/3) contents of ^{53}Mn were found,whereas the contents of ^{40}K and Ne were relatively high. Perhaps relatively low ^{40}K comparing Ne might be reflecting a heavy shielding in the earlier irradiation stages. So far we could not detect any positive signal concerning"early irradiation history"in the samples.

USE OF THERMOLUMINESCENCE FOR METEORITE DATING

Durrani, S.A.
Department of Physics, Birmingham University, Birmingham B15 2TT, U.K.

Since natural thermoluminescence (TL) in most geological materials reaches 'dynamic equilibrium' after time periods of $\sim 10^5$-10^6 yr, the method cannot, in general, be used for determining the total (or even the cosmic-ray exposure) ages of meteorites. Additional factors that need to be taken into account in the case of meteorites include the effect of temperature of irradiation[1] in space, and the uncertainties in the natural dose-rates as a function of pre-ablation sample depth. Additionally, the effects of calibration conditions employed in the laboratory must be considered, especially dose-rate and total-dose dependence[2,3].

TL can, however, be used for making some estimates of the terrestrial ages of meteorites. The property used in such studies is the decay of the natural TL after their fall: the dose-rate regime having diminished by a factor of ~ 10 on Earth as against in space. A particularly useful parameter in this context is the ratio of the heights of the 'low-temperature' and the 'high-temperature' peaks in the glow-structure of a meteorite at a given time after fall. The paper examines the potentialities as well as the problems involved in such an approach. The latter include the question of the 'order of kinetics' obeyed by the TL decay, the uncertainty of the initial value of the peak-height ratios (which are dose-rate dependent), etc. It is possible, however, to place upper or lower limits on the terrestrial ages of meteorites. Some recent results in this field, obtained in our laboratory, will be reported.

References

1. S.A. Durrani *et al.*, J. Phys. D. 10; 1351 (1977).
2. P.J. Groom *et al.*, Council of Europe PACT J., 2, 200 (1978).
3. S.W.S. McKeever *et al.*, paper presented at the 6th Int. Conf. Sol. St. Dos., Toulouse, April 1980 (and to be published in Nuclear Instruments and Methods).

AUTHOR INDEX

Author Index

Author Index

Author Index

SPEAKER INDEX